Dissertation zur Erlangung des Doktorgrades

der Fakultät für Chemie und Pharmazie

der Ludwig-Maximilians-Universität München

Formulation of therapeutic proteins: Protein unfolding, refolding, aggregation and long-term storage stability

Hristo Lyubomirov Svilenov

aus

Sofia, Bulgarien

2019

Erklärung

Diese Dissertation wurde im Sinne von §7 der Promotionsordnung vom 28. November 2011 von Herrn Prof. Dr. Gerhard Winter betreut

Eidesstattliche Versicherung

Diese Dissertation wurde selbstständig und ohne unerlaubte Hilfe erarbeitet.

München, 13.05.2019

_____

(Hristo Lyubomirov Svilenov)

Dissertation eingereicht am: 13.05.2019

1.Gutachter: Prof. Dr. Gerhard Winter

2.Gutachter: Prof. Dr. Wolfgang Frieß

Münchliche Prüfung am: 26.06.2019

To my parents and my sister.

Acknowledgements

I would like to express my sincere gratitude to my supervisor Professor Dr. Gerhard Winter. Thank you for accepting me in your group, giving me the opportunity to work on an exciting project and encouraging me to pursue my ideas. I am very thankful for the numerous opportunities to present my work at conferences around the world. I also very much enjoyed the excellent atmosphere that you have created in your team. Finally, your support and guidance helped me to stay on track in difficult moments during the last several years. Thank you for that!

Second, I would like to thank all supervisors in the Marie Skłodowska-Curie project PIPPI. Everything that happened during the last years would not have been possible without them. I want to express my gratitude especially to Dr. Pernille Harris who did an excellent job as a project head. I would also like to thank Dr. Robin Curtis and Dr. Sasha Golovanov for hosting me during my research stay at the Manchester Institute of Biotechnology and for all the inspiring research discussions. I am very grateful to Dr. Dierk Roessner, Dr. Nuska Tschammer and Dr. Philipp Baaske for the excellent technical support with devices used in the making of this thesis. I would also like to thank the PhD students in the PIPPI project. Mainly, I want to highlight Andreas Tosstorff and Matja Zalar for our rousing scientific and personal discussions. I would also like to warmly thank Lorenzo Gentiluomo for being the heart and the soul of the group during our social events. I will miss that time!

I am also grateful to the advisory board of the PIPPI project, especially Professor Dr. Christopher J. Roberts, Dr. Jens Thostrup Bukrinski and Dr. Fritz Richter, for their eye-opening input and coaching about professional development.

I want to thank Professor Dr. Wolfgang Frieß for interesting scientific discussions and pleasant personal conversations. Also, thank you for being a co-referee of my thesis.

I am thankful to my colleagues from AK Winter, AK Frieß and AK Merkel at the LMU for a good time together and for the numerous social activities. I particularly enjoyed the time with my lab mate and a good friend Julian Gitter who was always the perfect "partner in crime" in and outside the University.

Finally, I want to thank my father Lyubomir Svilenov, my mother Lyusi Svilenova and my sister Emilia Svilenova for their endless patience and support.

Funding acknowledgement:

x

Table of Content

Chapter 1 **General Introduction**

1.1   Aim and outline of the thesis

Protein formulation is a crucial part of the therapeutic protein development process. One primary aim during protein formulation is to find solution conditions that impede protein instability during long-term storage. This instability can be a result of various degradation pathways which can be challenging to predict. This is the case with protein aggregation which has been a subject of intensive research by both academia and industry.

In the context of developing a new therapeutic protein, particularly interesting is the application of predictive methods that can rank protein formulations in order of their effect on protein aggregation during long-term storage. The use of such predictive methods before the start of the stability studies can substantially reduce the effort, costs and risk of failure during therapeutic protein development.

Many techniques for protein characterisation have been developed over the years. In recent times, there was also a significant improvement in the instrumentation with a focus on sample volume reduction, increased throughput and automation. Although the portfolio of stability-indicating techniques for protein formulation studies is continuously expanding, the predictions from these techniques are rarely validated with published peer-reviewed long-term stability data. The lack of such publicly available information continues to raise questions whether the rankings from these techniques are accurate and what would be the best approach to select protein formulations for long-term stability studies. Our aim when we started this thesis was to, at least partially, answer these questions.

The topic was approached from three directions. First, I applied some of the widely-used contemporary stability-indicating techniques to characterise different liquid formulations of several therapeutic proteins. Second, I developed some new concepts for assays that can be used for the selection of stable protein formulations. Third, I performed real-time long-term stability studies on the above-mentioned protein formulations. In the end, the predictions from the established and newly-developed techniques were compared to the long-term stability data. The outcome and conclusions of this work are summarised in several consecutive and logically connected thesis chapters.

In Chapter I, I give a brief introduction to different aspects of therapeutic protein stability, some techniques for biophysical protein characterisation and discuss several considerations during protein formulation development.

In Chapter II, I apply some contemporary techniques to study the stability of interferon alpha2a as a function of pH and ionic strength. Using these techniques, I found a new interferon alpha2a formulation that is very stable during long-term storage at 4 ºC and 25 ºC.

In Chapter III, I discuss some of the disadvantages of stability-indicating techniques that require sample heating during measurements. In this context, I explore the application of isothermal chemical denaturation as an orthogonal technique for protein formulation studies.

In Chapter IV, I present a new approach to study the stability of monoclonal antibody formulations by assessing the aggregates formed after the protein is diluted from different concentrations of a denaturant. I discuss how the latter technique can complement isothermal chemical denaturation experiments during protein formulation development.

In Chapter V, I study the effect of different denaturants and incubation time on the unfolding and aggregation of a monoclonal antibody in several formulation conditions. I show that the formulation pH influences in a similar way the aggregation of the partially unfolded antibody in the presence of a denaturant and the aggregation of the antibody during refolding from a denaturant.

In Chapter VI, a new microdialysis-based isothermal assay, named ReFOLD, is presented. The approach assumes that formulation conditions that suppress the aggregation of multiple partially unfolded protein species are good conditions for long-term storage of the protein. The ReFOLD assay accurately ranks the formulations of two antibodies in order of their effect on the protein aggregation during long-term storage at 4 ºC and 25 ºC.

In Chapter VII, several orthogonal techniques, including the newly-developed ReFOLD assay, are used to probe the effect of additives, i.e. sucrose and two arginine salts, on the unfolding and aggregation of a monoclonal antibody. There is a good agreement between the predictions from these techniques and the long-term stability of the formulations.

In Chapter VIII, the thesis is concluded with a summary and suggestions for a rational approach and use of stability-indicating techniques to select formulation conditions where protein aggregation will be suppressed during long-term storage.

1.2 Protein stability

Protein stability is a very general term that can have a different meaning for scientists with diverse research and educational background. In the world of therapeutic proteins and protein drugs, protein stability is generally related to four stability "types" – the protein conformational stability, the colloidal protein stability, the protein chemical stability and the interfacial protein stability[1]. Each of the aforementioned is important and should be high enough to obtain a therapeutic protein formulation that is stable during storage for several months or years.

1.2.1 Conformational stability

At ambient conditions, most therapeutic proteins exist predominantly in a folded conformation which is required for them to attain their specific biological activity[2]. In solution, the folded protein is usually in equilibrium with a fraction of unfolded protein. This equilibrium can be described by an equilibrium constant, K_{eq} (Fig 1A). The equilibrium constant is related to the fraction of unfolded protein in the solution and to the Gibbs free energy of protein unfolding, dG (Fig 1B).

A — Folded protein ⇌ (K_{eq}) Unfolded protein

B — $dG = -RT\ln(K_{eq})$

K_{eq}	dG (kJ/mol)	% Unfolded protein
1	0	50
0.01	11	1
0.0001	23	0.01
0.000001	34	0.0001
0.0000001	40	0.00001

C — Energy vs Reaction coordinate; Unfolded protein, Folded protein, dG
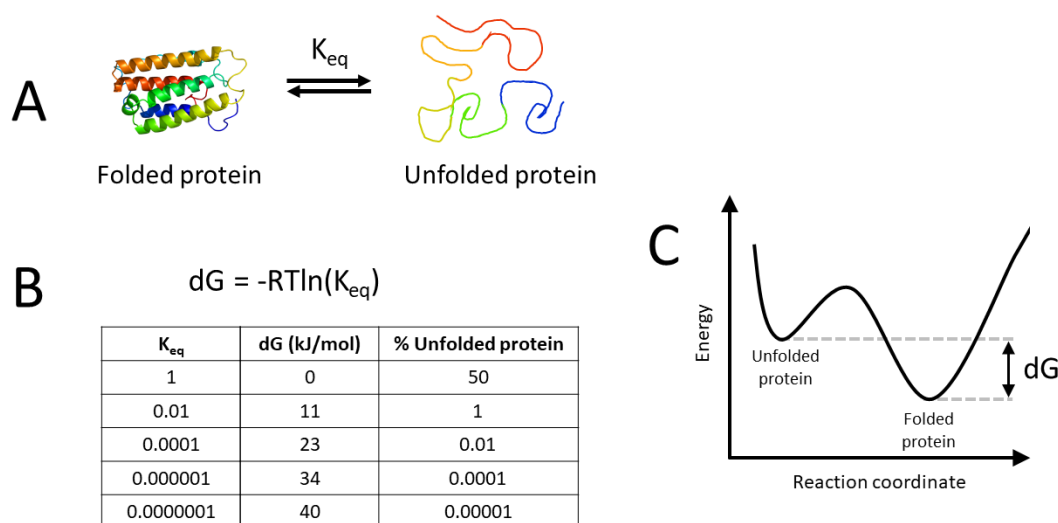
Figure 1. (**A**) Schematic representation of an equilibrium between a folded and unfolded protein with the corresponding equilibrium constant, K_{eq}; (**B**) The connection between the Gibbs free energy of protein unfolding, the equilibrium constant of protein unfolding and fraction of unfolded protein in solution. In the equation, R is the universal gas constant, and T is the temperature (293 K in these calculations); (**C**) Energy landscape representing the Gibbs free energy of protein unfolding as the difference between the unfolded and folded protein state;

The dG is a direct measure of the conformational stability of a protein and represents the difference in the energy of the folded protein conformation and the unfolded polypeptide chain[3] (Fig 1C). Important to note, the Gibbs free energy of protein unfolding differs not only between protein molecules, but also depends on parameters like solution pH and temperature[4]. In the context of protein formulation development, a high Gibbs free energy of protein unfolding is essential since this will indicate the presence of only a small fraction of unfolded protein species which are often prone to form aggregates[5,6].

1.2.2 Colloidal stability

The colloidal protein stability is related to the weak net interactions between the protein molecules in solution[1]. Such net protein-protein interactions can be either attractive or repulsive and arise from the sum of long-range electrostatic, short-range attractive and hard-sphere interactions[5]. The contribution of the different protein interactions can be graphically presented and explained with the DLVO (Deryagin-Landau-Verwey-Overbeek) theory for the stability of colloids[7] (Fig. 2). The weak protein-protein interactions are of high importance during formulation development of therapeutic proteins as they have an impact on the protein aggregation, solubility, viscosity, phase separation and crystallisation behaviour[1,8–13].
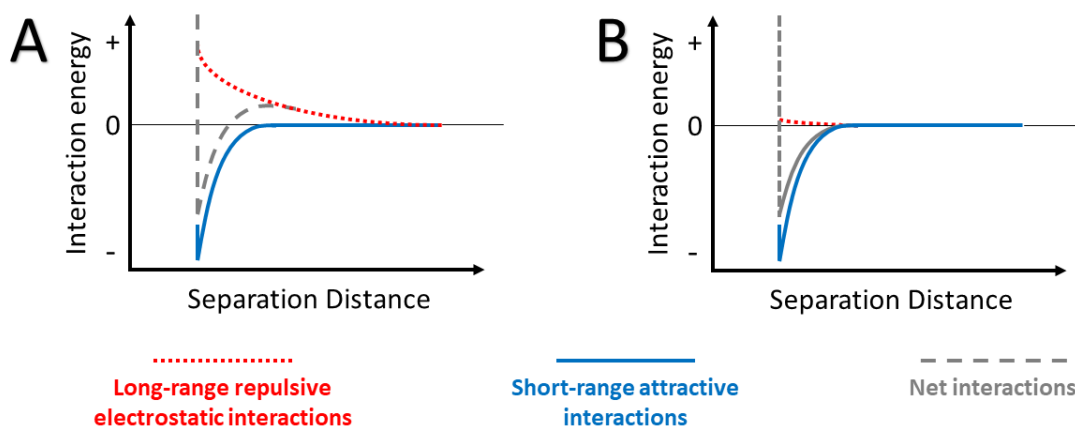
Figure 2. Schematic representation of the DLVO theory for the contribution of long-range repulsive electrostatic interactions and attractive short-range interactions to the net protein-protein interactions. (**A**) and (**B**) present a case with net repulsive and net attractive interactions respectively.

Several parameters can be used to assess the colloidal protein stability. For example, the second virial coefficient, B_{22}, is a measure of the net protein-protein interactions in solution[14].

In general, a large positive B_{22} indicates repulsion between the protein molecules which has been connected to lower protein aggregation rates for a range of protein formulations[5,15–17].

1.2.3 Chemical stability

The chemical protein stability is related to chemical degradation. The latter can occur via various mechanisms like oxidation, deamination and proteolysis[1,18].

Protein *oxidation* can be defined as the covalent alteration of the polypeptide chain by direct interaction with reactive oxygen species[19]. In general, amino acids that contain a sulfur atom or aromatic rings are more prone to oxidation[20]. In the context of therapeutic proteins, the oxidation of methionine, tryptophan, histidine, phenylalanine and tyrosine has been identified as most relevant[21]. Various factors can accelerate oxidation, the most critical being the presence of metal ions, oxygen exposure, light exposure and high temperature[1,18,21]. Oxidation is less affected by solution properties like pH, and the main strategies to suppress this degradation pathway are the addition of antioxidants and chelating agents, the reduction of the oxygen and light exposure in the primary package, and storage at refrigerated temperature[1].

Deamination is another chemical degradation pathway typical for therapeutic proteins[18]. Deamination usually occurs via hydrolysis of amide side chains of asparagine and glutamine residues[22]. The rate of this hydrolysis is pH-dependent and exhibits a minimum between pH 3 and 6[1]. In neutral and slightly acidic solutions, the deamination rate of asparagine is higher than the deamination rate of glutamine residues[18]. Moreover, the process is faster for asparagine residues followed by small amino acids in the primary protein structure[18]. Also, similar to other chemical degradation pathways, deamination rate depends on temperature and typically follows Arrhenius behaviour[23]. Knowing some of the factors that accelerate deamination, the most important strategies to reduce this degradation pathway are to select an optimal solution pH and to store the protein at lower temperature[1].

Proteolysis, also often named hydrolysis, is a chemical degradation pathway which is related to the nonenzymatic cleavage of amide bonds[24]. That degradation mechanism is often observed for monoclonal antibodies where hydrolysis in the solvent-exposed hinge region leads to fragmentation of the protein and formation of free Fab domains, free Fc domains and one arm antibodies. The proteolysis rate of antibodies is pH-dependent and shows a V-shape profile

with a minimum at around pH 6[25]. Accordingly, the most often used approaches to suppress hydrolysis are the selection of optimal solution pH and storage at refrigerated temperature[1]. There are many other chemical degradation pathways besides the three that were shortly discussed above. Examples are asparagine isomerization[26], asparagine hydrolysis[27], tryptophan hydrolysis[28], diketopiperazine formation[29], glycation[30] and disulphide scrambling[31]. However, these degradation pathways typically occur at relevant rates only in certain conditions, e.g. extreme pH or presence of reducing sugars. Moreover, similar to other chemical reactions these processes usually follow Arrhenius behaviour and their rate is diminished by storage at cold temperatures[18].

1.2.4 Interfacial stability

The interfacial stability of a protein is related to stress that occurs at air-liquid, solid-liquid or liquid-liquid interfaces[1,32]. Such interfaces exist, for example, between the protein solution and the primary packaging material, between the protein solution and the air in the container headspace or at the surface of silicon oil droplets. Moreover, new and larger interfaces can be created when the solution experiences mechanical stress like shaking, agitation or if being dropped[33,34]. Many therapeutic proteins are surface active and tend to accumulate at the interfaces mentioned above[35–37]. Although the phenomena of protein destabilisation at an interface are not fully understood, there are several proposed mechanisms which are outside the scope of this thesis[32,35]. Relevant in the context of protein formulation is that in most cases interfacial instability is mitigated by the addition of a suitable amount of non-ionic surfactants like polysorbates which are nowadays present in most protein drugs on the market[38,39].

1.3 Biophysical techniques for protein characterisation

There are many ways to classify the techniques used for biophysical characterisation of proteins. In the context of this thesis, I summarised some of the latter into four big groups depending on their application to study the four aspects of protein stability discussed earlier.

1.3.1 Techniques and parameters used to assess protein conformational stability

The conformational stability of a protein can be assessed by non-isothermal and isothermal methods. The *non-isothermal methods* usually apply a linear temperature gradient to cause

protein unfolding. The unfolding of the protein is detected by a change in a physical observable that depends on the technique (Table 1).

Table 1. Techniques employing thermal denaturation to assess protein conformational stability

Techniques	Physical observable
Differential scanning calorimetry[40]	Change in heat capacity
Circular dichroism spectroscopy[41]	Change in ellipticity
Ultraviolet spectroscopy[42]	Change in the molar absorptivity or the peak maximum of the ultraviolet absorption protein spectra
Fourier-transform infrared spectroscopy[43]	Change in the position and the intensity of the Amide I band in the protein Fourier-transform infrared spectra
Fluorescence spectroscopy (extrinsic fluorescence)[44]	Change in the fluorescence intensity of a fluorescence dye upon interactions with hydrophobic patches exposed during protein unfolding
Fluorescence spectroscopy (intrinsic fluorescence)[45]	Change in the intrinsic protein fluorescence intensity or peak maximum due to change in the environment of fluorescent amino acids upon unfolding

In cases where the protein does not aggregate during the measurement and the thermal unfolding is reversible, these techniques can provide thermodynamic data describing the protein conformational stability and the protein unfolding process[40]. This includes the Gibbs free energy of protein unfolding, the enthalpy of the unfolding process, the change in the heat capacity upon unfolding and the true protein melting temperature. The true protein melting temperature is the temperature at which the ratio of unfolded to folded protein is one, i.e. the Gibbs free energy equals zero (Figure 3A).

The reality is that most therapeutic proteins aggregate during thermal unfolding and the process is not reversible[4]. The latter obstructs the thermodynamic data analysis and extrapolation using the Gibbs-Helmholtz equation (Figure 3B) which resolves the entire protein stability curve that depicts the protein conformational stability as a function of temperature (Figure 3A). As a result of that, the thermal denaturation techniques are usually used to provide only a so-called apparent protein melting temperature which is just an approximation of the true protein melting temperature in Fig. 3A. Still, the apparent protein melting temperatures have

been widely used in industry and academia as a parameter to compare the conformational stability of therapeutic proteins in different formulation conditions[46–49].
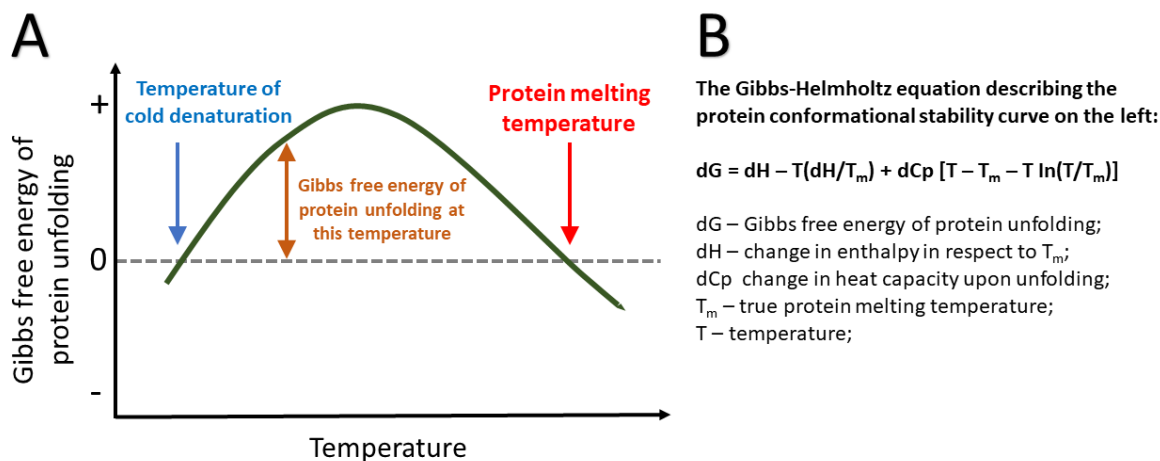
Figure 3. (**A**) The protein stability curve and (**B**) the Gibbs-Helmholtz equation describing what is the protein conformational stability at different temperatures.

The conformational stability of a protein in different formulations can also be measured with an *isothermal method* like isothermal chemical denaturation[3,4]. In this case, the protein in the formulation of interest is mixed with increasing concentrations of a denaturant, i.e. guanidine hydrochloride or urea. Next, the samples are incubated at a constant temperature long enough to reach an equilibrium and a physical observable, e.g. ellipticity or fluorescence, is measured to detect at which denaturant concentrations the protein is partially or fully unfolded (Fig. 4A). Finally, the isothermal chemical denaturation graph is fitted to a suitable model to extract parameters describing the protein conformational stability (Fig. 4B). The fitting models and approaches that can be used for this evaluation have been described in detail elsewhere[4,50,51]. Undoubtedly, isothermal chemical denaturation is a valuable technique since the method can be performed at any temperature of interest and can directly provide the Gibbs free energy of protein unfolding for that temperature without any extrapolations from higher temperatures used in the analysis of thermal denaturation data[4] (Fig 3). However, the accurate thermodynamic analysis of isothermal chemical denaturation data assumes that the protein unfolding in the denaturant is reversible and that the samples are in equilibrium at the time of the measurement. The latter assumptions are not always valid for therapeutic proteins in

different formulations as indicated in some recent publications and discussed later in this thesis[6,52–55].
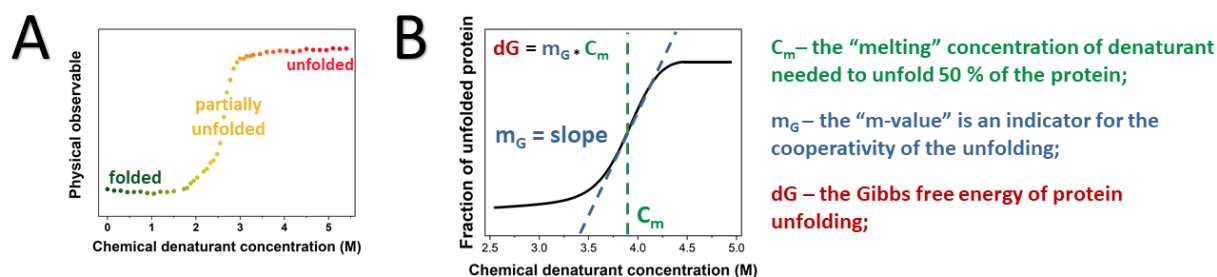
Figure 4. (**A**) Schematic presentation of a protein unfolding curve obtained by isothermal chemical denaturation and (**B**) the protein stability parameters extracted from the analysis of such curve

1.3.2   Techniques and parameters used to assess protein colloidal stability

During formulation development, the colloidal stability of a protein is often assessed with light scattering techniques that can provide information about the net protein-protein interactions in a formulation. For example, static light scattering is used to determine the *second virial coefficient, B_{22},* which describes the net protein-protein interactions in solution. Unfortunately, the accurate determination of the second virial coefficient is tedious regardless of the technique which is used to measure it. Therefore, surrogate parameters for B_{22} more often find application to assess the colloidal stability of a protein during formulation development. One such widely-used parameter is the *interaction parameter k_D* which can be measured in high-throughput fashion in microwell plates. The interaction parameter k_D represents the slope of the concentration dependence of the protein mutual diffusion coefficient determined with dynamic light scattering (Figure 5). Several studies have shown that k_D correlates well with the second virial coefficient $B_{22,}$ and similarly to B_{22}, a high positive k_D will indicate that the protein-protein interactions are repulsive[56,57]. However, k_D and B_{22} can be determined and are valid only in dilute protein solutions[58]. Moreover, measuring k_D in some formulations with low ionic strength can provide an overestimation of the repulsive protein interactions which should be taken into consideration[59]. Defining parameters which more accurately describe the protein-protein interactions in a broader range of conditions is currently a topic of intensive research with both computational and experimental approaches[11,58,60,61].

$$D = D_0(1 + k_D c)$$

k_D – interaction parameter;
D – mutual diffusion coefficient measured with dynamic light scattering;
D_0 – protein diffusion coefficient at infinite dilution;
c – protein concentration;
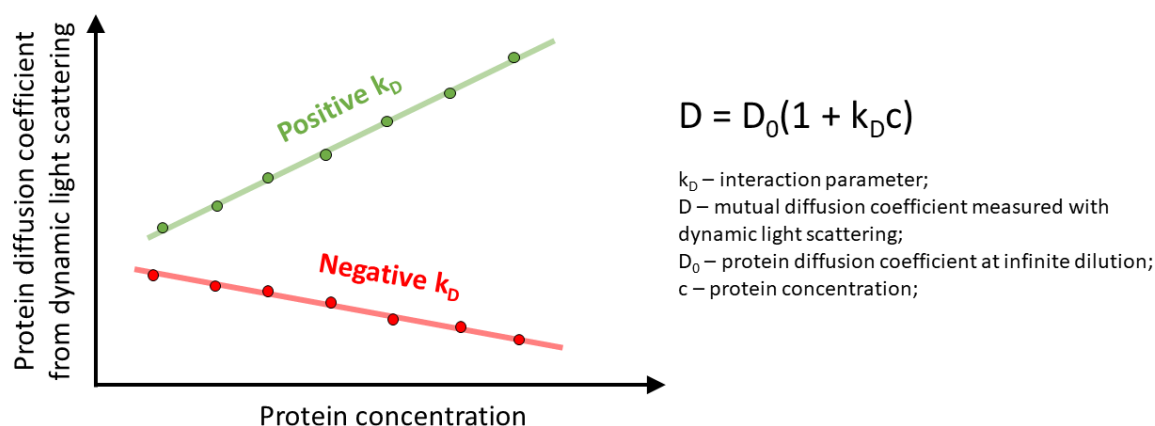
Figure 5. Determination of the interaction parameter k_D from the change of the protein mutual diffusion coefficient determined with dynamic light scattering as a function of the protein concentration

The *aggregation onset temperature* is another parameter which is often measured to compare the colloidal stability of therapeutic proteins in different formulations[47,62,63]. This parameter can be determined with various light scattering or spectroscopic techniques while the temperature of the protein formulation is gradually increased. The aggregation onset temperature is often closely related to the protein melting temperature and does not directly reflect the magnitude of the net protein-protein interactions. However, formulations with higher aggregation onset temperature or formulations that do not aggregate during heating are likely to have high colloidal stability.

Besides the static and dynamic light scattering, there are many more techniques that can be used to assess B_{22} and k_D, or other parameter describing the colloidal protein stability. Such techniques are analytical ultracentrifugation[64], self-interaction chromatography[16], small angle X-ray scattering[65], nuclear magnetic resonance[66], self-interaction nanoparticle spectroscopy[67], precipitation with polyethylene glycol[68] and biolayer interferometry[69]. In the context of protein formulation development, the application of the latter techniques is tedious, not well established or their integration in formulation studies is not straightforward which makes them more rarely used in the early stage therapeutic protein development.

1.3.3 Techniques and parameters used to assess protein chemical stability

The chemical protein stability is usually assessed by a combination of stress or accelerated stability studies and suitable analytical techniques[70,71]. The stress can be, for example, exposure to high temperature, oxidants or light[72]. Such experiments aim to identify what the major chemical degradation pathways of a therapeutic protein are and to compare the rate of chemical degradation between formulations[70,71]. The gold standard analytical method which ultimately provides the exact type and extent of chemical changes is liquid chromatography coupled to mass spectrometry[73]. However, the latter method can be very tedious, and accordingly many other techniques also find application to study the chemical changes of a protein during formulation development (Table 2). Such techniques often do not provide information about the exact type of chemical changes, but their output can be used for comparison between formulations after different stress.

Table 2. Techniques used in the characterisation of protein chemical degradation

Technique	Output
Liquid chromatography coupled to mass spectrometry[74,75]	Amount and exact type* of chemically changed species *Note that peptide mapping[73] is required in some cases.*
Reversed phase chromatography without mass spectrometry[76]	Amount of chemically changed species
Ion exchange chromatography[77]	Amount of acidic and basic variants
Isoelectric focusing	Amount of acidic and basic variants
Protein A chromatography[74]	Amount of antibody species oxidised at the protein A binding site of antibodies
Hydrophobic interaction chromatography[78]	Amount of protein species with changed hydrophobicity
Combination of reducing and non-reducing gel electrophoresis	Qualitative or semi-quantitative information about the presence and type of covalent bond between aggregates

1.3.4 Techniques and parameters used to assess protein interfacial stability

The interfacial stability of a protein is typically assessed after applying mechanical stress. The latter can be shaking, stirring, vibration, freeze-thaw or dropping [1,33,34,79]. Next, the stressed samples are analysed with orthogonal techniques. Ultraviolet-visible spectroscopy and chromatography are typically used to detect a loss of soluble protein which can occur when the protein adsorbs and remains at interfaces, or when insoluble protein aggregates form. Size exclusion chromatography, field-flow fractionation and light scattering find application to study the formation of small soluble aggregates[80]. The presence of larger aggregates is evaluated with techniques like light obscuration, flow imaging microscopy or others[35,81]. The mechanical stress studies aim to investigate the impact of formulation conditions on the interfacial protein stability[82], often with a focus on the effect of different surfactant concentrations[34]. In addition, it is important to also study the stability of the protein formulations in the final primary package as the type of package material, fill volume, headspace, etc., can have a significant impact on protein degradation during mechanical stress[1].

1.4 Considerations for liquid protein formulation development

Finding the optimal formulation for long-term storage of a new therapeutic protein means finding a compromise between multiple variables to ensure that all four types of protein stability are sufficiently high. This concept is presented schematically in Fig. 6 where the change of protein stability is depicted as a function of two imaginary formulation variables. Filled areas represent regions where the respective type of stability is high enough for long-term storage. Although this figure is an oversimplification of the problem, it is important as it illustrates two important things. First, regions, where one type of protein stability is high, can be regions where another kind of stability is low. Second, for some proteins, a "sweet spot" exists where the formulation conditions satisfy all four types of protein stability. In reality, the variables to be considered during formulation development are far more than two and Fig. 6 quickly becomes multidimensional. Moreover, it is very difficult to draw a line defining the threshold between high and low stability. The latter challenges make the development of stable protein formulations a very complex task which must be approached from different directions.
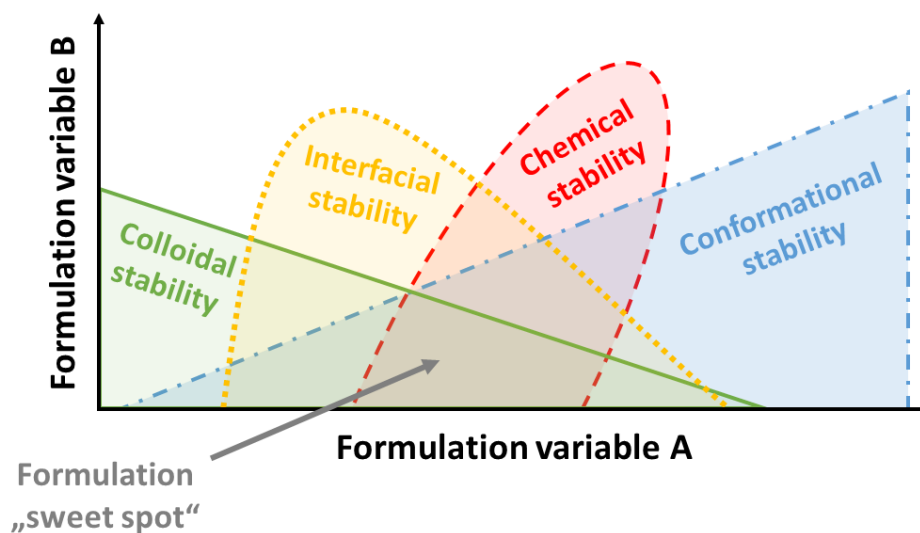
Figure 6. Schematic presentation of the effect of two imaginary formulation variables on the four aspects of protein stability. Filled areas represent conditions where the respective protein stability is high. The area where all four types of stability are sufficiently high is denoted as the formulation conditions "sweet spot".

1.5 Challenges in predicting protein long-term storage stability

The accurate prediction of degradation pathways and their rates during long-term storage can bring immense improvements to the development process of therapeutic proteins. Unfortunately, we are limited by our current knowledge and understanding about the interplay between protein structure, formulation and stability. Therefore, we can make good prognosis only for some degradation pathways. For example, the rates of most protein chemical changes follow Arrhenius behaviour which allows extrapolation and some prediction from data obtained at high temperatures[18,83]. Moreover, the impact of formulation variables on the most common chemical degradation mechanisms for proteins is well studied (See section 1.2.3.).

Other degradation pathways, like *protein aggregation*, are very difficult to predict. The aforementioned can occur via various mechanisms which are extensively discussed elsewhere[84–88]. In general, a protein can aggregate via its native or via its (partially) unfolded state. Especially the partially unfolded protein species have been identified as very aggregation-prone in many studies[89–91]. Aggregation that occurs through the unfolded or partially unfolded protein is often termed non-native aggregation[85]. The latter typically follows non-Arrhenius behaviour which makes the extrapolations from aggregation rates obtained at higher

temperatures very difficult[92]. Moreover, the mechanism and rate of protein aggregation vary between proteins, formulations and can also change with temperature[93–96].

The formation and growth of aggregates can be dictated by low conformational or low colloidal protein stability[8,95,97]. It is, therefore, particularly interesting in the context of protein formulation development to apply stability-indicating biophysical techniques to assess different aspects of protein stability, and by this to predict formulation conditions that will impede protein aggregation during storage. The formulation approaches based on stability-indicating techniques raise two questions. First, which type of protein stability is critical for the protein aggregation in a specific case? And second, which parameters or combination of parameters describing the conformational and colloidal protein stability provide reliable aggregation predictions? Especially the suitability of stability-indicating parameters like the protein melting temperature and the protein aggregation onset temperature has been discussed in multiple studies, and their prediction power has been recently questioned[48,62,63]. Therefore, it remains an open question which techniques or combination of techniques and which stability-indicating parameters should be used to select formulations where the aggregation of a therapeutic protein is suppressed during long-term storage.

Chapter 2 **Rapid sample-saving biophysical characterisation and long-term storage stability of liquid interferon alpha2a formulations: Is there a correlation?**

This chapter is published as:

[*]Department of Pharmacy, Pharmaceutical Technology and Biopharmaceutics, Ludwig-Maximilians-University, Butenandtstrasse 5-13, Munich D-81377, Germany

Author contributions:

H.S. performed the experiments, evaluated the data and wrote the paper. H.S. and G.W. conceived the presented idea and planned the experiments. G.W. supervised the work, provided conceptual guidance and corrected the manuscript.

Note from the authors:

The version included in this thesis is identical with the published article apart from minor changes. The reference, figure and table numbers were changed to fit into the coherent numbering of this document. The text was edited to meet the norms for British English.

The published article can be accessed online via:

2.1 Abstract

The knowledge and tools to characterise proteins have comprehensively developed in the last two decades. Some of these tools are used in formulation development to select formulation conditions suitable for long-term storage. However, there is an ongoing debate whether the predictions obtained with these tools are in good agreement with the outcome from real-time long-term stability studies. In this work, we investigate whether some of the state-of-the-art microscale, microvolume and non-destructive biophysical techniques can be applied to promptly select formulations that minimise the aggregation of interferon alpha2a during storage. Interferon alpha2a was used as a model protein as it is known to form aggregates at concentrations over an order of magnitude higher than used in the commercial product. We apply a systematic formulation approach in which we investigate the effect of pH and ionic strength on protein stability. The predictions from the sample-saving biophysical characterisation are validated by long-term stability studies at 4 ºC and 25 ºC for 12 months on selected formulations. Interferon alpha2a shows minimal aggregation in 10 mM sodium acetate buffer with pH 4 and low ionic strength. The latter is indicated by the rapid sample-saving biophysical characterization and confirmed by the long-term stability data.

Keywords - Protein stability; Protein Formulation; Protein Aggregation; Therapeutic proteins; Protein storage stability; High-throughput protein characterisation;

Abbreviations - ACF – autocorrelation function from dynamic light scattering data evaluation; DLS – dynamic light scattering; HP-SEC – size exclusion chromatography; ICD – isothermal chemical denaturation; IFNα2a – recombinant interferon alpha2a; $IP_{350/330}$ – Inflection point of the protein unfolding transition detected by the integrated intrinsic fluorescence intensity ratio (FI350nm/FI330nm); RP-HPLC – reversed-phase chromatography; T_{agg} – protein aggregation onset temperature from nanoDSF; T_{on} – protein aggregation onset temperature from the increase in the protein hydrodynamic radius measured by dynamic light scattering;
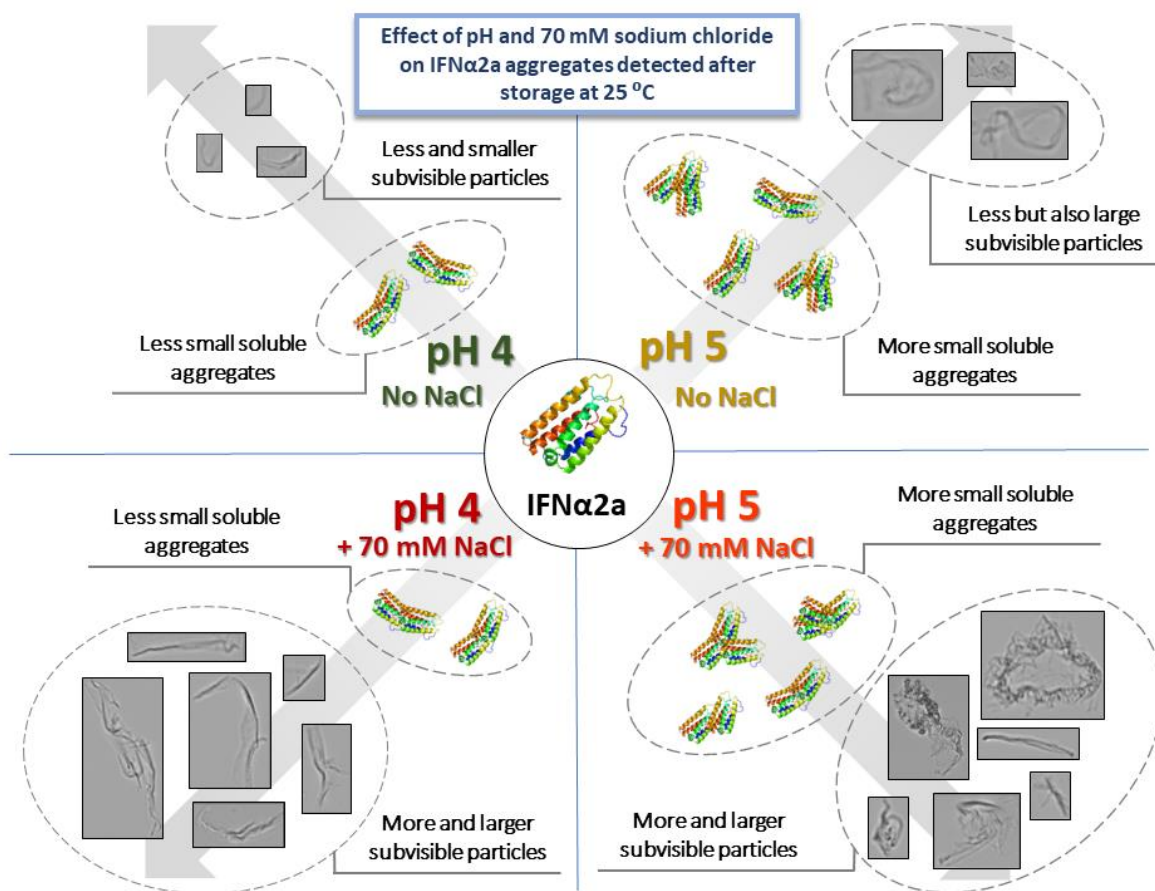
Figure 7. Graphical abstract of Chapter 2 - Effect of pH and ionic strength on the storage stability of IFNα2a

2.2 Introduction

The introduction of the first biologics to the market more than three decades ago has revolutionised the therapy of many severe diseases[98]. Unfortunately, this new type of medicines brought not only benefits to the patients and the pharmaceutical companies but also many new challenges related to their development, production and safety. One common hurdle of biologics, in particular of protein-based drugs, is the tendency of proteins to form aggregates of various sizes and characteristics[85,88,93,99]. On the one hand, the formation of large aggregates during the shelf-life of a medicine can lead to non-compliance with the tight regulatory limits for subvisible and visible particles in parenteral drugs. On the other hand, the protein aggregates are considered degradation products according to the ICH guidelines and their presence has been related to undesired immunogenic reactions in patients[100–103]. The reasons mentioned above require the adoption of different strategies to minimise the presence and

formation of protein aggregates in parenteral drugs. An often-used strategy is the selection of formulation conditions (e.g. pH, ionic strength) that impede aggregate formation and growth during storage[104]. One approach to select the optimal formulation conditions for a protein would be to prepare dozens of different samples and store them at the temperature of interest (e.g. 4 °C) for 1-2 years to see which of them are the most stable. This approach is impractical for both time and sample-consumption reasons. A second approach would be to perform accelerated stability and stress studies (e.g. at 25 °C and 40 °C) for a few weeks/months to select only the most promising formulations that will move on to long-term stability testing. This approach, similar to the first one, is also related to a large sample consumption and a significant analytical effort. A third approach that has been explored by academia and industry for over two decades is to use biophysical techniques that provide data which can facilitate the selection of promising formulation conditions[1,5]. The working principles of the techniques used in the third approach have not changed significantly over the years, and most methods rely on fluorescence or light scattering measurements. Most efforts to improve these methods have been aimed at creating label-free techniques, improving data quality and reproducibility, as well as reducing the sample amounts required for measurements and adapting the methods for automation. Still, there is an ongoing debate if and to what extent the data obtained from these methods is predictive for the stability of the proteins during long-term storage[62,105,106].

Interferon alpha2a (IFNα2a) is a classic example of a protein-based parenteral drug. IFNα2a gained first approval by the FDA in the mid-80s and is used to treat patients suffering from different types of hepatitis, carcinoma, leukaemia, lymphoma and several other conditions[107–110]. The benefit of IFNα2a therapy has been repeatedly proven in various clinical trials. However, IFNα2a is a protein which is prone to form aggregates and the presence of the latter, when formulated with HSA or chemically cross-linked, has been linked to undesired immunogenic reactions in mouse models and human patients[111,112]. Some of these issues led to changes in the formulation, removing HSA, of IFNα2a in the mid-90s[111,113]. More recent work on aggregates and immunogenicity suggests the need for chemical modification, not simply aggregation, to drive immunogenicity to therapeutic proteins[114,115]. Still, the goal during the formulation development is to find conditions that suppress the formation of protein aggregates of any origin. Noteworthy, IFNα2a was developed and characterised in times when the

available techniques for protein formulation and analysis were limited in comparison to the tools we have nowadays.

Our goal in this work is to investigate whether some of the modern rapid sample-saving techniques can be used to promptly obtain stability-indicating data that can be reliably used in formulation development. To do so, we apply a systematic formulation approach, which includes three steps: Step 1 - Screen for optimal pH; Step 2 - Screen for the effect of ionic strength (i.e. sodium chloride) on the protein stability; Step 3 - Advanced structural characterisation; Finally, we study the long-term stability of IFNα2a in different formulations after storage at 4 °C and 25 °C to validate the predictions from the rapid, sample-saving biophysical characterisation. This work shows how the techniques we explore can be integrated into a quick and systematic (pre-)formulation approach which successfully found a liquid interferon alpha2a formulation that is very stable during long-term storage.

2.3   Materials and methods

2.3.1   Materials

Interferon alpha2a was kindly provided by Roche Diagnostics GmbH, Penzberg, Germany. The bulk solution contains 1.35 g/L protein, 25 mM ammonium acetate buffer with pH 5 and 120 mM sodium chloride. The protein concentration was measured spectrophotometrically using the NanoDrop 2000 (Thermo Fisher Scientific, Wilmington, USA) and an $A280_{0,1\%} = 0.972$. All other chemicals were obtained from Sigma-Aldrich. All solutions were prepared with ultrapure water from a Sartorius arium® pro system. All buffers used in this work had a concentration of 10 mM and were prepared by combining the respective amounts of the 10 mM free acid and 10 mM free base stock solutions with no subsequent pH adjustment. The pH after preparation was ±0.1 of the target value. Important to note, the protein concentration 1 g/L that we used is higher than the concentration in the commercially available products with IFNα2a. Our aim was not to compare the stability of our formulations to the commercial products but to use IFNα2a as a model protein for our studies.

2.3.2 Sample dialysis and preparation

2.3.2.1 Screen for the effect of pH (Step 1)

The buffer of interferon alpha2a for the first formulation step was exchanged in the following way – the IFNα2a bulk solution was diluted to 1 g/L, and 100 µL aliquots were filled in Pierce™ microdialysis devices with a membrane having 3.5 kDa MWCO. The samples were dialysed at 25 ⁰C against 1.6 mL of buffer (10 mM sodium acetate with pH 3.5, 4.0, 4.5, 5.0 or 5.5; or 10 mM sodium phosphate with pH 6.0, 6.5, 7.0, 7.5 or 8.0). The buffer was exchanged every two hours (5 exchanges in total) to ensure a constant concentration gradient across the dialysis membrane. After the last change, the samples were left to dialyse overnight. Finally, the samples were collected in microcentrifuge tubes and centrifuged at 10.000 x g for 10 minutes. The following measurements were performed on the supernatant.

2.3.2.2 Screen for the effect of sodium chloride (Step 2)

Few millilitres of IFNα2a bulk solution were filled in Spectra/Por® 6-8 kDa MWCO dialysis tubing (Spectrum Laboratories Inc., Rancho Dominguez, USA) and dialysed at 20 – 25 °C against excess (approximately 1:200) of 10 mM sodium acetate buffer with pH 4 or 5. Two buffer exchanges were performed 3 and 8 hours after the beginning. After the last change, dialysis was continued for another 16 hours. Stock solutions of sodium chloride (10X) were prepared in the respective buffer and spiked into the dialysed IFNα2a to prepare samples containing 1 g/L protein in 10 mM sodium acetate with pH 4 or 5 and varying concentrations of sodium chloride.

2.3.2.3 Advanced Protein Characterisation (Step 3) and Long-Term Stability Study

The IFNα2a buffer was exchanged, and sodium chloride was spiked in the samples to a final concentration of 70 mM as described above. Subsequently, the samples were sterile filtered with 0.22 µm cellulose acetate filter. For the long-term stability study, the solutions were aseptically filled into pre-sterilised DIN2R glass type I vials (2 mL solution in each vial). Finally, the vials were crimped with rubber stoppers and stored at 4 ⁰C and 25 ⁰C. At each time point (i.e. 0, 3, 6, 9 and 12 months for the storage at 25 ⁰C; and 0, 6 and 12 months for the storage at 4 ⁰C), three new vials were opened and used for the analysis of every condition.

2.3.3 High-throughput Fluorimetric Analysis of Thermal Protein Unfolding

nanoDSF® was used to study the protein thermal unfolding and aggregation[116,117]. The IFNα2a solutions were filled into standard glass capillaries (NanoTemper Technologies, Munich, Germany) and placed in the Prometheus® NT.48 (NanoTemper Technologies, Munich, Germany). A temperature ramp of 1 °C/min was applied from 20 to 95°C. All measurements were performed in triplicates. The Prometheus® NT.48 system measures the integrated intrinsic protein fluorescence intensity at 330 and 350 nm after excitation at 280 nm in each capillary. Simultaneously, the system can detect aggregation/precipitation of the samples with a detector which measures the back-reflection intensity of a light beam that passes twice through the capillary[118]. The fluorescence intensity ratio (F350/F330) was plotted against the temperature, and the inflection point ($IP_{350/330}$) of the transition was derived from the maximum of the first derivative of each measurement using the PR.ThermControl V2.1 software (NanoTemper Technologies, Munich, Germany). Also, the aggregation onset temperature (T_{agg}) from the increase in the signal from the aggregation detection optics was determined using the same software.

2.3.4 Dynamic Light Scattering (DLS) in Micro Well Plates

Five µL of IFNα2a solution were filled in 1536 well LoBase plate (Aurora Microplates Inc., Carlsbad, USA) and the plate was centrifuged at 2200 rpm for 2 minutes using a Heraeus Megafuge 40 centrifuge equipped with an M-20 well plate rotor (Thermo Fisher Scientific, Wilmington, USA). Next, each well was sealed with 5 µl of silicon oil and centrifuged again at 2200 rpm for 2 minutes. The well plate was placed in a DynaPro® DLS plate reader (Wyatt Technology Europe, Dernbach, Germany) and 10 acquisitions of 5 seconds at 25 ºC were collected for each sample. The autocorrelation function (ACF) of each sample was calculated from the fluctuation of the light scattering intensity using the Dynamics V7.8 software. Cumulant analysis was performed with the same software to derive the apparent coefficient of self-diffusion (D) and the polydispersity index (PDI). Next, the apparent protein hydrodynamic radius from DLS (R_h) was calculated using the Stokes-Einstein equation using the viscosity of the respective sample. The viscosity of the samples was calculated using the solvent tool of the Zetasizer software (Malvern, Herrenberg, Germany). Additionally, the viscosity of some control samples was measured experimentally with a falling ball viscometer. In all cases, the

viscosity of the solutions was ±2 % of the viscosity of pure water. More data on the viscosity of the solution and its effect on the calculated R_h can be found in Supplementary data of this chapter. For the temperature ramp experiments, 5 acquisitions of 5 seconds were taken while a temperature ramp of 0.1 °C/min was applied from 25 to 80 °C. The aggregation onset temperature (T_{on}) from the increase in the R_h from DLS was determined using the Dynamics V7.8 software. All measurements were performed in triplicates.

2.3.5 Microscale Isothermal Chemical Denaturation (ICD)

Stock solutions of IFNα2a, buffer and 7 M guanidine hydrochloride (GuHCl) in the respective buffer were combined in a non-binding surface 384 well plate (Corning, USA) with the Viaflo Assist system (Integra Biosciences, Konstanz, Germany) as earlier described[54]. Next, the samples are incubated for 1 hour at room temperature, filled into standard nanoDSF® glass capillaries, and the integrated intrinsic protein fluorescence at 330 and 350 nm was measured with the Prometheus® NT.48. The ratio F350/330 was plotted against the denaturant concentration, and the curve was fit to a two-state protein unfolding model using the PR.ChemControl V1.4.2 software (NanoTemper Technologies, Munich, Germany) to obtain the Gibbs free energy of unfolding (ΔG), the melting denaturant concentration (C_m) and the m-value. The experiment was performed in triplicates.

2.3.6 Circular dichroism (CD) spectroscopy

Near- and far-UV circular dichroic spectra of IFNα2a solutions with a concentration of 1 g/L were collected at 25 ºC with a Jasco J-810 spectropolarimeter (JASCO Deutschland GmbH, Pfungstadt, Germany). Quartz cuvettes with 10 mm and 0,1 mm wavelength path were used for the near-UV and the far-UV measurements respectively. 10 accumulations of each sample were taken with a speed of 20 nm/min. The spectrum of the respective buffer was subtracted for each sample, the spectra were smoothed using Savitzky-Golay algorithm with 7 smoothing points[119] and the mean residue ellipticity was calculated as described elsewhere[120].

2.3.7 Fourier-transform Infrared Spectroscopy (FT-IR)

FT-IR spectra of IFNα2a solutions with a concentration of 1 g/L were collected using a Tensor 27 (Bruker Optik GmbH, Ettlingen, Germany) equipped with a BioATR (Attenuated Total Reflectance) cell™ II (Harrick) at 25 °C connected to a thermostat (DC30-K20, Thermo

Haake). 120 scans with a resolution of 4 cm^{-1} were used to obtain each spectrum. The data was further analysed with the Opus 7.5 (Bruker Optik GmbH) software and presented as a vector-normalised second-derivative spectrum. The data was smoothed using a Savitzky-Golay algorithm with 17 smoothing points[119].

2.3.8 Size Exclusion Chromatography (HP-SEC)

A Dionex Summit 2 system (Thermo Fisher, Dreieich, Germany) was used for the size exclusion chromatography. 25 µg of IFNα2a were injected on a TSKgel G3000SWxl, 7,8x300 mm, 5 µm column (Tosoh Bioscience, Tokyo, Japan) and the elution of the protein was detected at 343 nm after excitation at 280 nm with an RF2000 fluorescence detector (Thermo Fisher, Dreieich, Germany). The fluorescence detection to detect IFNα2a aggregates with HP-SEC is already successfully used by other groups[121]. The running buffer consisted of 50 mM sodium acetate pH 5 with 500 mM arginine hydrochloride. The chromatograms were integrated with Chromeleon V7 (Thermo Fisher, Dreieich, Germany) and the relative area of the high molecular species (i.e. small soluble aggregates) was calculated in percentage.

2.3.9 Flow Imaging Microscopy (FlowCAM)

The IFNα2a samples on long-term stability study were analysed for the presence of larger protein aggregates (subvisible particles) with a FlowCAM® 8100 (Fluid Imaging Technologies, Inc., Scarborough, ME, USA). The system was equipped with a 10x magnification cell (81 µm x 700 µm). Before each measurement, the cleanliness of the cell was checked visually. 200 µL of sample were used for the analysis, and the images are collected with a flow rate of 0.15 mL/min, an auto image frame rate of 29 frames/second and a sampling time of 74 seconds. The following settings were used for particle identification - 3 µm distance to the nearest neighbour, particle segmentation thresholds of 13 and 10 for the dark and light pixels respectively. The particle size was reported as the equivalent spherical diameter (ESD). The VisualSpreadsheet® 4.7.6 software was used for data collection and evaluation.

2.3.10 Reversed-Phase High-Performance Liquid Chromatography (RP-HPLC)

A Dionex Summit 2 system (Thermo Fisher, Dreieich, Germany) was used for the reversed-phase high-performance liquid chromatography. The samples were diluted to 0.1 g/L and 20 µL were injected on a BioBasic C18, 250 x 2.1, 5 µm column (Thermo Fisher, Dreieich,

Germany). The sample elution was detected at 214 nm with a UVD170U UV/Vis detector (Thermo Fisher, Dreieich, Germany). A gradient of 32 to 48 % eluent B in A in 30 minutes was used. Eluent A consisted of 10 % w/v acetonitrile and 0.1 % w/v trifluoracetic acid in ultrapure water. Eluent B consisted of 0.1 % w/v trifluoracetic acid in acetonitrile. The flow rate was 0.2 mL/min. The column oven temperature was set at 30 ⁰C. The chromatograms were integrated with Chromeleon V7 (Thermo Fisher, Dreieich, Germany) and the total relative area of all peaks different than the main peak (i.e. impurities) was calculated in percentage.

2.4   Results and discussion

2.4.1   Formulation Step 1 – Studying the effect of solution pH on the thermal unfolding, aggregation and solubility of IFNα2a

In this work, we investigate a systematic sample-saving three-step approach to formulate a model protein. As a model protein, we use interferon alpha2a, a therapeutically-relevant molecule known to form aggregates that can cause clinical complications for the patients. During the first formulation step, we studied the effect of the pH on the solubility, thermal unfolding and aggregation of IFNα2a. To accomplish this, we used commercially available microdialysis devices, which allowed us to dialyse a small solution volume and test a wide range of pH values by consuming only a few micrograms of protein. The IFNα2a content in the supernatant after microdialysis against buffers with different pH was determined by UV spectrophotometry, i.e. with a NanoDrop 2000. The amount of soluble protein is lower at pH 6.0 and 6.5 indicated by the lower protein concentration and fluorescence intensity (Fig 8).
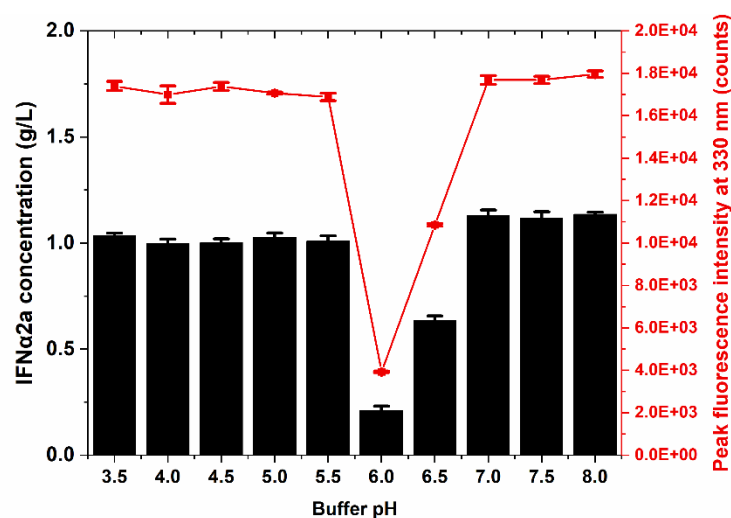
Figure 8. Effect of the pH on the concentration (black bars) and the intrinsic fluorescence of IFNα2a (red circles) in the supernatant after microdialysis. The values are mean of triplicates, the error bar is the standard deviation.

These observations are in good agreement with the results reported by Sharma et al[122]. We also observed that the protein precipitates at pH 5.5 after gentle heating to 35-40 °C (data not shown). The low solubility of the protein in this pH range can be explained with the isoelectric point of IFNα2a which is around 6. It is common knowledge that the aqueous solubility of many proteins is reduced at pH values near the isoelectric point[123]. Based on these observations, we excluded the buffers with pH 5.5-6.5 from further studies.

Next, we used state-of-the-art microscale and microvolume approaches to study the unfolding, aggregation and the apparent hydrodynamic radius R_h of IFNα2a as a function of pH. With an increase of pH from 3.5 to 8.0 the protein unfolding transition becomes more cooperative (Figure 9A). The highest $IP_{350/330}$ is measured at pH 4.0 (Figure 9C). Between pH 4.5 and 8.0 the inflection points ($IP_{350/330}$) are around 66-67 °C. The lowest $IP_{350/330}$ is measured at pH 3.5 (Figure 9C). At pH 3.5 and 4.0 no aggregation during heating is detected with the aggregation detection optics, which indicates high colloidal stability of the protein in these conditions (Figure 9B). At pH 4.5 or higher, the samples start to form aggregates large enough to cause an increase in the signal of the aggregation detector of the Prometheus® NT.48, indicating lower protein colloidal stability (Figure 9B). The lowest aggregation temperature T_{agg} was

measured at pH 5 (Figure 9C). At pH 4.5, 7.0, 7.5 and 8.0 IFNα2a shows similar T_{agg} around 65-66 ⁰C (Figure 9C).
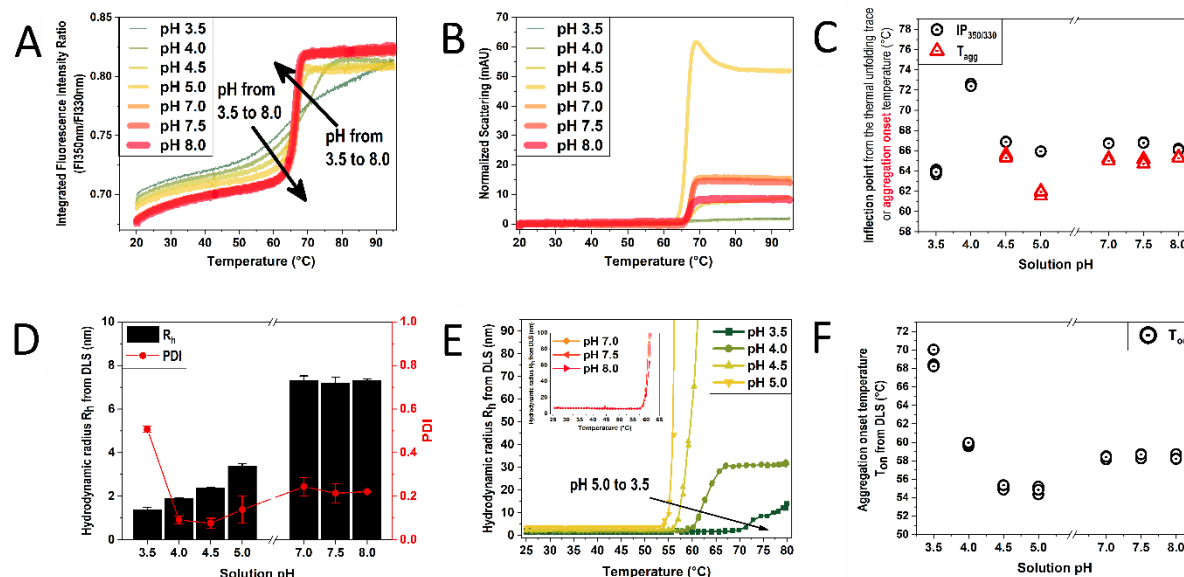
Figure 9. Effect of pH on IFNα2a unfolding and aggregation – **Above**: Thermal unfolding traces (**A**) and scattering traces (**B**) with the corresponding inflection points (IP350/330) and aggregation onset temperatures (T_{agg}) (**C**) measured with nanoDSF®; **Below**: The apparent hydrodynamic radius and PDI (**D**), the temperature dependence of the R_h (**E**) and the calculated aggregation onset temperatures from DLS (**F**). The values in (D) are means of triplicates, and the error bars are the standard deviation. In (C) and (F) each triplicate is shown.

The apparent hydrodynamic radius of IFNα2a and the polydispersity of the samples measured with DLS is highly dependent on the solution pH. The R_h of IFNα2a is lower at pH 4.0 compared to the samples with higher pH (Figure 9D). The highest R_h was measured in the pH range 7 to 8, which indicates that the protein probably forms oligomers in these conditions. Therefore, the pH range 7 to 8 was excluded from further studies. At pH 3.5 the DLS measurements indicated reproducibly that there is a population of larger particles in the samples. The latter is depicted by the high PDI at this pH. The apparent R_h and PDI derived from the cumulant fit for this condition are shown just for informational purpose. The change of the R_h during heating is also dependent on the pH (Figure 9E). At pH 4 the onset of aggregation T_{on} measured by DLS is around 60 ⁰C, and after the aggregates reach an R_h of about 30 nm, the aggregate growth stops (Figure 9E). The small aggregate size explains why

no aggregation is detected with the Prometheus® NT.48 during heating of the IFNα2a samples with pH 4.0 (and pH 3.5). At higher pH (i.e. 4.5 and above) the T_{on} is shifted to a lower temperature or a steep increase in the R_h without a plateau is observed (Figure 9E). The determined T_{on} values of IFNα2a with DLS are lowest at pH 4.5 and 5.0 (Figure 9F), which indicates lower protein colloidal stability in these conditions compared to pH 4.0. Important to note – only 150 µg of protein and less than 15 hours of total instrument measurement time per replicate were required to obtain the data for the entire pH screen presented in Figures 8 and 9. As additional information for the readers we also compared the thermal unfolding of IFNα2a measured by the change of the intrinsic protein fluorescence intensity ratio (from the nanoDSF® measurement) and by the change in the protein ellipticity at 293 nm (from circular dichroism) and found excellent agreement between the two methods (Supplementary data). Further, the inflection point from the change in the intrinsic protein fluorescence ratio during the thermal unfolding of IFNα2a at pH 5.0 corresponds well with the melting temperature of IFNa2a measured with differential scanning calorimetry (DSC) by Sharma et al[124]. Noteworthy is that cuvette-based, DSC and near-UV CD devices do not allow the simultaneous thermal unfolding studies on many samples and require much higher protein amount in comparison to the techniques we used in this study. Both nanoDSF® and DLS in microwell plates can be used to measure dozens of samples simultaneously.

2.4.2 Formulation Step 2 – Studying the effect of sodium chloride on the thermal unfolding and aggregation of IFNα2a

During the second formulation step, we focused on the effect of sodium chloride (i.e. ionic strength) on the stability of IFNα2a at pH 4.0 and pH 5.0. These two pH values were selected since IFNα2a shows very different behaviour – at pH 4.0 IFNα2a undergoes a less cooperative thermal unfolding but has high colloidal stability; at pH 5.0 the protein thermal unfolding is characterised by a sharp transition, but the colloidal protein stability is low.

Increasing the sodium chloride concentration from 0 to 120 mM causes a shift in the unfolding transitions of IFNα2a to a lower temperature (Figure 10A and 10D). This shift is more pronounced at pH 4 (compared to pH 5) where the $IP_{350/330}$ is around 72-73 ºC without sodium chloride and around 61 ºC in the presence of 120 mM NaCl (Figure 10C). This indicates that the addition of sodium chloride has a very unfavourable effect on the protein thermal stability

at pH 4.0. For comparison, at pH 5.0 the difference in the $IP_{350/330}$ with 0 mM or with 120 mM sodium chloride is only 1.5-2 °C (Figure 10F).
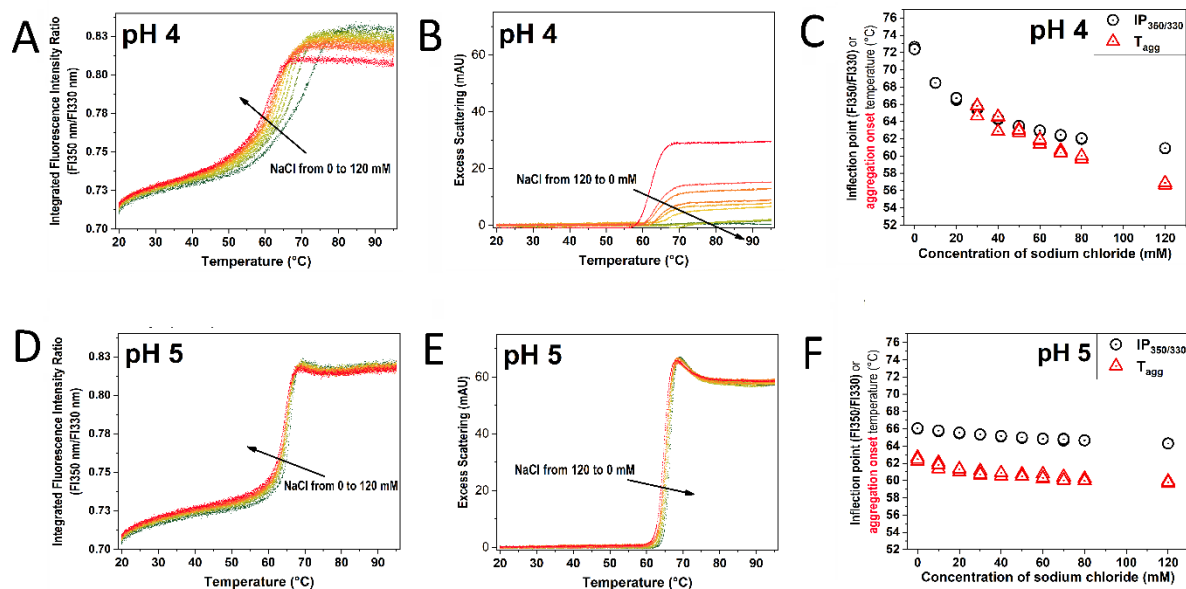
Figure 10. nanoDSF® evaluation of the effect of sodium chloride on IFNα2a – thermal unfolding traces at pH 4 (**A**) and pH 5 (**D**), scattering traces from the aggregation detection optics at pH 4 (**B**) and pH 5 (**E**) and the corresponding inflection points and aggregation temperatures at pH 4 (**C**) and pH 5 (**F**). In (**C**) and (**F**) the value from each triplicate is shown.

The addition of 30 mM or more sodium chloride to the 10 mM sodium acetate buffer with pH 4 results in IFNα2a aggregation (i.e. larger aggregates) during heating, which is detectable by the Prometheus® NT.48 (Figure 10B). An increase in the NaCl concentration from 30 mM to 120 mM shifts the T_{agg} in the samples with pH 4 to lower temperatures (Figure 10C). At pH 5, the sodium chloride has a small influence on the aggregation of IFNα2a during heating, and 120 mM NaCl reduce the T_{agg} with only approximately 2 °C (Figure 10E and 10F). At pH 4.0, the protein R_h from DLS increases with the addition of only 10-20 mM NaCl and does not change when the salt concentration is further increased (Figure 11A). At pH 5.0 the R_h decreases slightly with increasing NaCl concentration (Figure 11A). At pH 4.0 the addition of NaCl greatly shifts the protein T_{on} to lower temperatures (Figure 11B) and causes the formation of larger aggregates during heating (Figure 11C). At pH 5.0 the increasing sodium chloride concentration causes only a moderate decrease in the IFNα2a T_{on} (Figure 11B) and

does not affect the steepness of the increase in the protein R_h during heating (Figure 11D). These observations are in good agreement with the data in Figure 10B and 10E. Once again, it is important to mention that all the data presented in Figures 10 and 11 was obtained with the consumption of 300 µg of protein and less than 15 hours of measurement time per replicate.
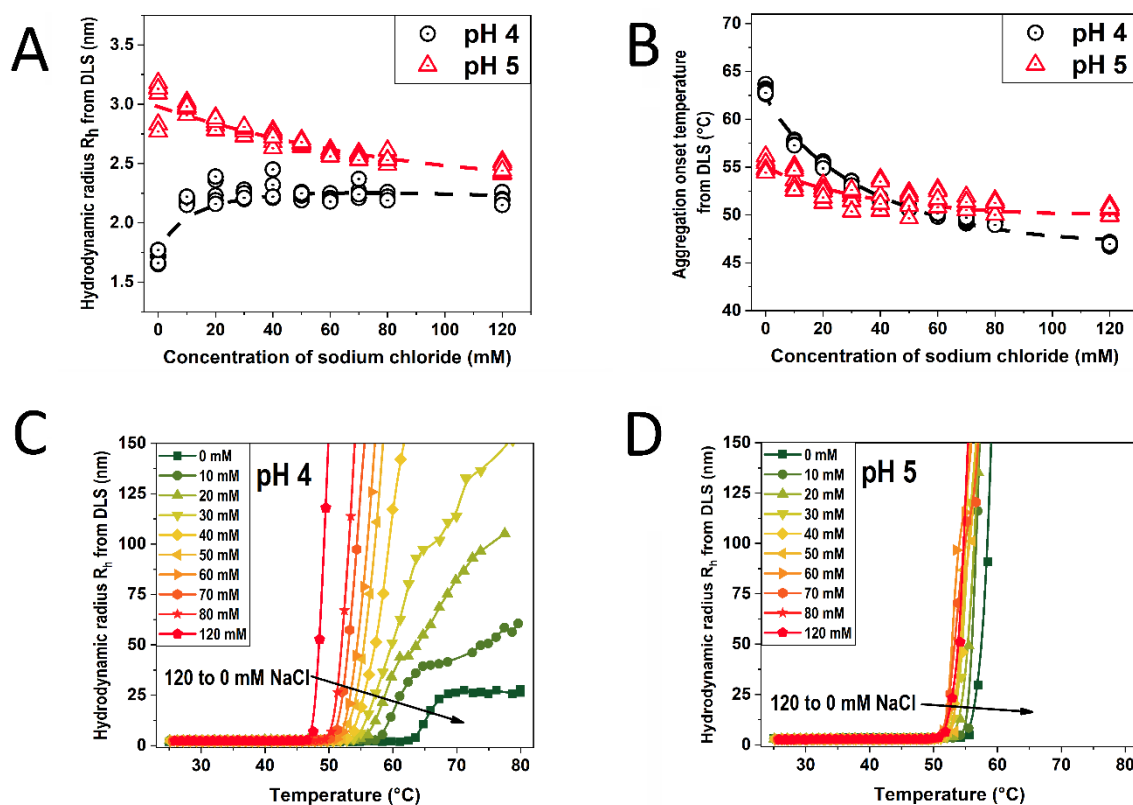
Figure 11. Effect of sodium chloride on the apparent hydrodynamic radius R_h from DLS of IFNα2a at pH 4 and pH 5 (**A**); the aggregation onset temperature of IFNα2a from DLS at pH 4 and pH 5 (**B**); the temperature dependence of the R_h from DLS of IFNα2a at pH 4 (**C**) and pH 5 (**D**). In (A) and (B) each triplicate is shown.

2.4.3 Formulation Step 3 - Advanced structural characterisation of IFNα2a

2.4.3.1 Effect of the pH on the conformational stability of IFNα2a

Interferon alpha2a shows a two-state unfolding behaviour in an isothermal chemical denaturation experiment with guanidine hydrochloride (Figure 12). The calculated Gibbs free energy of unfolding ΔG is lower (mean value of 29.45 kJ/mol) at pH 4 compared to the ΔG at pH 5 (mean value of 40.53 kJ/mol), although the melting denaturant concentration C_m is higher

(mean value of 4.5 M GuHCl) at pH 4 compared to pH 5 (mean value of 4.01 M GuHCl). The reason for the lower ΔG at the lower pH is the lower m-value at pH 4 compared to pH 5, which indicates a less cooperative unfolding of IFNα2a in this condition. According to the ΔG, IFNα2a has lower conformational stability at pH 4.0 compared to pH 5.0. Noteworthy is that the dG, C_m and m-value that were determined at pH 5.0 are in excellent agreement with the values reported by Bis et al.[125]. Another interesting observation is that the unfolding behaviour (regarding cooperativity and the position of the inflection point) of IFNα2a at pH 4 and 5 during heating resembles the unfolding of the protein in guanidine hydrochloride (Figure 9A and Figure 12). Only 240 µg of protein were required to obtain one isothermal chemical denaturation graph containing 24 points like the graphs depicted in Figure 12.
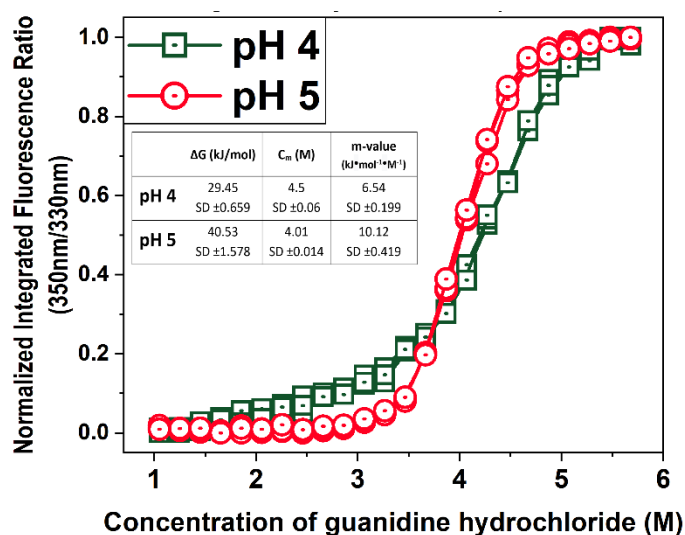
Figure 12. Isothermal chemical denaturation of IFNα2a with guanidine hydrochloride in 10 mM sodium acetate buffer with pH 4 and pH 5. The values for every replicate are shown. The table in the inset shows the calculated means and standard deviations for the ΔG, C_m and m-value from the two-state unfolding fit.

2.4.3.2 Effect of pH and sodium chloride on IFNα2a secondary and tertiary structure

The amide I band of IFNα2a shows a maximum between 1650 and 1655 cm^{-1} at both pH 4 and pH 5 with or without 70 mM sodium chloride (Figure 13A). This corresponds well to alpha-helical secondary protein structure which is expected for this protein and is also consistent with previously published data[122,125,126]. Additionally, the characteristic far-UV CD spectra with two minima at 209 and 222 nm confirm the presence of alpha-helical protein structure in all four

conditions (Figure 13B)[127]. The near-UV CD spectra of IFNα2a in 10 mM Na-acetate pH 4 or 5 with or without 70 mM NaCl show the typical negative peaks at 287 nm and 293 nm which are assigned to the two tryptophan residues of this protein (Figure 13C)[122,124]. This indicates that the tertiary structure of IFNα2a is the same in the four formulation conditions tested. Noteworthy, both CD and FT-IR are non-destructive methods in the way we used them, and the sample was recovered after the measurements.
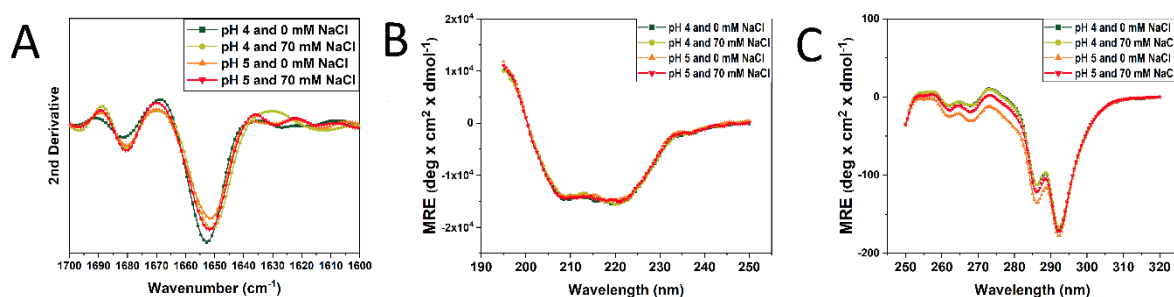
Figure 13. Effect of pH and 70 mM sodium chloride on the IFNα2a secondary structure studied with (**A**) FT-IR and (**B**) far-UV circular dichroism; and the IFNa2a tertiary structure studied with (**C**) near-UV circular dichroism;

2.4.4 Long-term storage stability of IFNα2a

2.4.4.1 Formation of small soluble aggregates detected by HP-SEC

The stock solution of IFNα2a contains approximately 1 % high molecular weight species (i.e. small soluble aggregates) detectable by HP-SEC already after thawing. After dialysis against acetate buffer with pH 5.0 these aggregates remain in the solution, while after dialysis in the buffer with pH 4.0 these aggregates are no longer present (Figure 14). The latter was already observed during formulation/deformulation of IFNα2a[128]. After storage of the samples at 25 ⁰C up to 12 months, the relative area of small soluble aggregates increases more at pH 5.0 compared to the samples with pH 4.0 (Figure 14A). This is in good agreement with the results from the biophysical characterisation which shows that both the thermal and colloidal stability of IFNα2a is higher in 10 mM sodium acetate with pH 4 compared to pH 5. Interestingly, the addition of 70 mM sodium chloride seems to play a small role in the presence of the small soluble aggregates of IFNα2a at both pH 4.0 and pH 5.0 (Figure 14A), although it affected the aggregation behaviour of the protein in the short-term characterisation (Figures 10 and 11). During storage at 4 ⁰C no increase in the amount of small soluble aggregates was observed,

although the samples with pH 5.0 contain more aggregates during the entire stability study compared to the samples with pH 4.0 (Figure 14B). For a sample chromatogram from the HP-SEC method see the Supplementary data to this chapter.
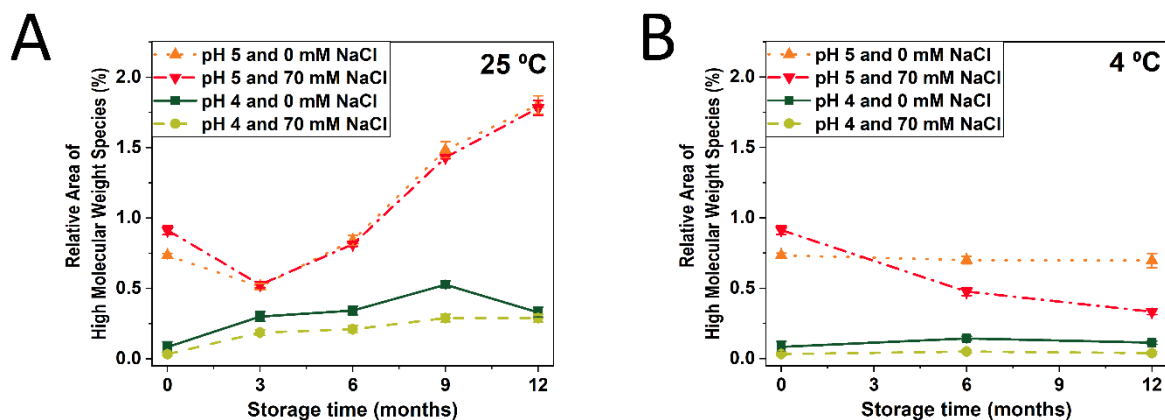
Figure 14. Small soluble aggregates (high molecular weight species) of IFNα2a measured with HP-SEC during long-term storage of the samples at 25 ⁰C (**A**) and 4 ⁰C (**B**). The values are mean of triplicates from three different vials, the bars show the standard deviation.

2.4.4.2 Formation of larger protein aggregates (sub-visible particles)

The highest numbers of particles in all three size ranges were measured in IFNα2a formulations with 70 mM sodium chloride after storage at 25 ⁰C (Figure 15 – Above). This agrees well with the earlier observations that the addition of sodium chloride causes the formation of larger aggregates at pH 4 and reduces the thermal and colloidal protein stability (Figures 10 and 11). Both formulations with only 10 mM sodium acetate and no sodium chloride contain a very low number of particles after storage at 25 ⁰C (Figure 15 – Above). The formulation with pH 4.0 without NaCl contains fewer particles (specifically in the size range 10 to 25 μm and above 25 μm) compared to pH 5.0 without NaCl. During storage at 4 ⁰ C fewer particles are formed compared to storage at 25 ⁰C (Figure 15 - Below). After storage at 4 ⁰C the IFNα2a formulation containing the highest number of particles of any size is with 10 mM sodium acetate pH 5.0 and 70 mM sodium chloride. The formulation containing only 10 mM sodium acetate at pH 4.0 without sodium chloride shows the lowest particle numbers after storage at both 4 and 25 ⁰C (Figure 15). Important to note, this is the condition in which IFNα2a has the highest

$IP_{350/330}$ (Figure 9C), a high T_{on} (Figure 9F), small aggregate size after heating (Figure 9E) and a low R_h and PDI at 25 °C (Figure 9D).
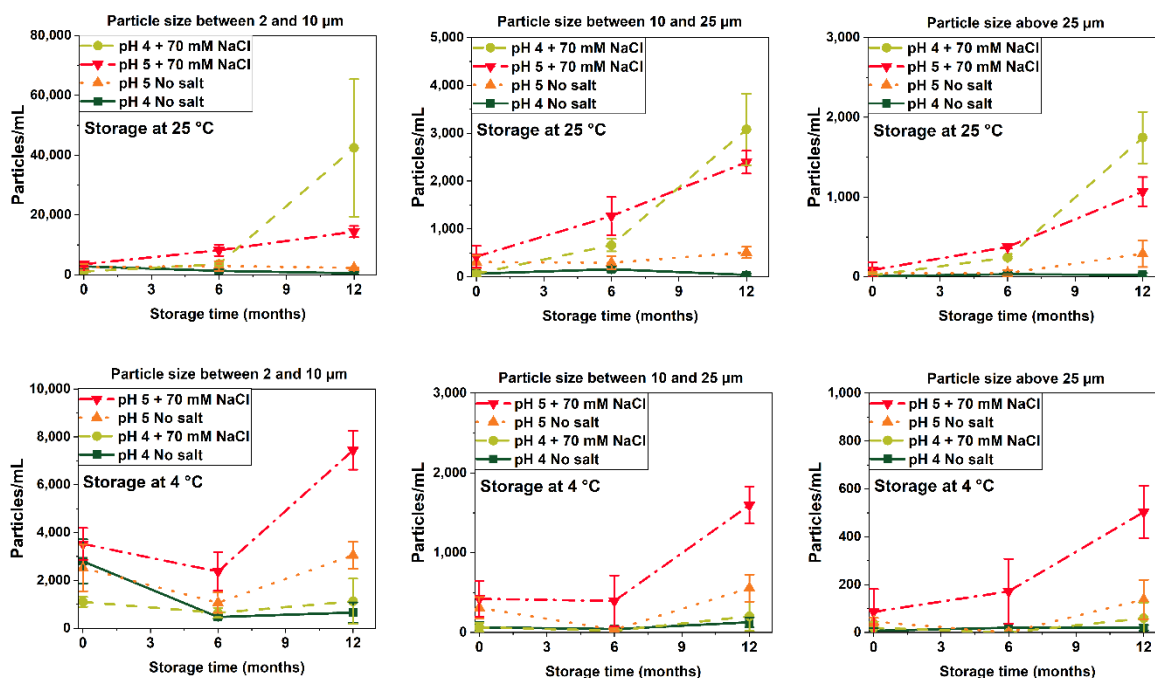
Figure 15. Subvisible particles detected with flow imaging microscopy in IFNα2a solutions during storage at 25 °C (**above**) and 4 °C (**below**). The values are mean of triplicates from three different vials, the error bars are the standard deviation.

2.4.4.3 Formation of impurities detected by RP-HPLC

Although the chemical protein degradation is a topic outside the scope of this article, we wanted to study if there are differences in the chemical degradation of IFNα2a during storage at pH 4 and pH 5 with or without sodium chloride. We selected RP-HPLC as a well-established technique to detect chemically changed species of IFNα2a[122,129,130]. For a sample RP-HPLC chromatogram from the method we used see the supplementary data to this chapter. More chemically changed species (i.e. impurities) detected by RP-HPLC form during storage at 25 °C compared to storage at 4 °C (Figure 16). However, the relative area of impurities formed (and the retention time of the impurity peaks) were the same at both pH 4.0 and pH 5.0, regardless of the presence/absence of 70 mM sodium chloride. These results indicate that the chemical changes of IFNα2a that occur during long-term storage in the four conditions tested in Figure 16 are similar and the differences in the protein degradation in these conditions are

driven by the different conformational and/or colloidal protein stability. Although the chemical changes are not directly assessed by the "1-2-3 Step" protein formulation approach, one could additionally perform short-term stress tests (i.e. high temperature, light exposure) coupled to a suitable analytical technique on the formulations in Step 2 to get complementary data whether a difference in the chemical stability of the lead formulations is expected[1,18].
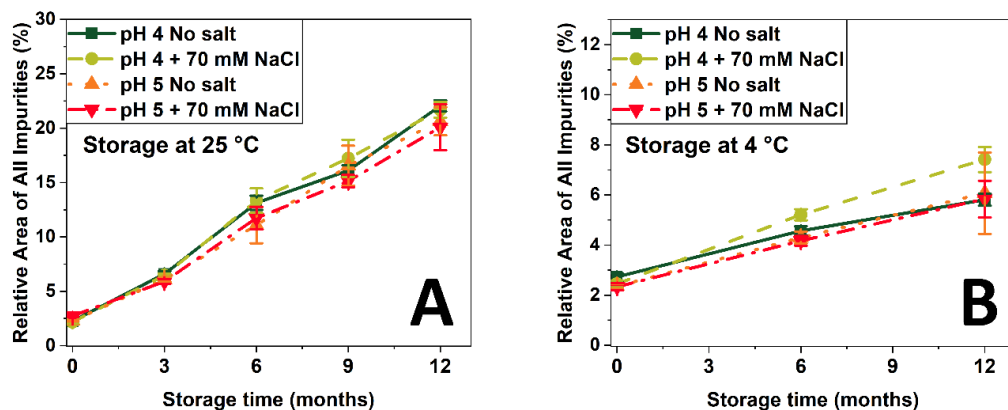
Figure 16. Relative area of all impurities detected by RP-HPLC in IFNα2a solutions during storage at 25 ºC (**A**) and 4 ºC (**B**). The values are mean of triplicates from three different vials, the bars show the standard deviation.

2.4.4.4 Is there a correlation between the rapid sample-saving biophysical characterisation and the long-term stability data?

The aggregation of a protein can be augmented by low conformational or low colloidal protein stability, both of which could be influenced by pH and/or ionic strength[5,8]. Interferon alpha2a has lower conformational stability and shows less cooperative thermal and GuHCl-induced unfolding at pH 4.0 compared to pH 5.0. However, at low ionic strength in 10 mM sodium acetate, the colloidal stability of IFNα2a is higher at pH 4 than at pH 5. This is in excellent agreement with the less small and large protein aggregates formed during storage of IFNα2a at 25 ºC and 4 ºC at pH 4 without sodium chloride, which indicates that the high colloidal stability is crucial to obtain a stable IFNα2a formulation. The addition of sodium chloride (i.e. an increase of ionic strength) has an adverse effect on the protein colloidal stability (depicted by a reduction of the T_{agg}, T_{on} and an increase in the aggregate size formed during heating), which also corresponds well with the formation of large protein aggregates during storage of IFNα2a in solutions containing 70 mM sodium chloride.

2.5 Conclusion

In this work, we demonstrated how some of the contemporary tools for protein characterisation can be used to perform quick and less-sample-demanding formulation studies on interferon alpha2a, studied at protein concentrations significantly higher than used in commercial formulations. We structured these studies in a 3-step formulation approach, including Step 1 - Screen for optimal pH; Step 2 - Screen for the effect of ionic strength (i.e. sodium chloride) on the protein stability; Step 3 - Advanced structural characterisation; We validated the results from the rapid biophysical protein characterisation by performing long-term stability studies at 4 ⁰C and 25 ⁰C during which we studied the formation of small and large aggregates of IFNα2a. Both the rapid sample-saving biophysical characterisation and the long-term stability data indicate that the aggregation of interferon alpha2a is minimal in 10 mM sodium acetate buffer with pH 4. The addition of sodium chloride (i.e. an increase of ionic strength) to IFNα2a solutions has a negative effect on the protein physical stability. The presented work is important in several directions. First, it shows that thanks to technological advancement we can nowadays perform quick systematic formulation studies with miniature samples amounts. Second, it shows that the rapid sample-saving techniques we apply here were indeed able to find an interferon alpha2a formulation that is very stable during long-term storage. Third, the work reveals new insights into the stability of interferon alpha2a in different conditions. Finally, it shows that the proposed combination of sample-saving techniques could significantly and quickly reduce the number of formulations that will move to accelerated or long-term stability studies and therefore reduce development costs and time dramatically.

2.6 Supplementary data
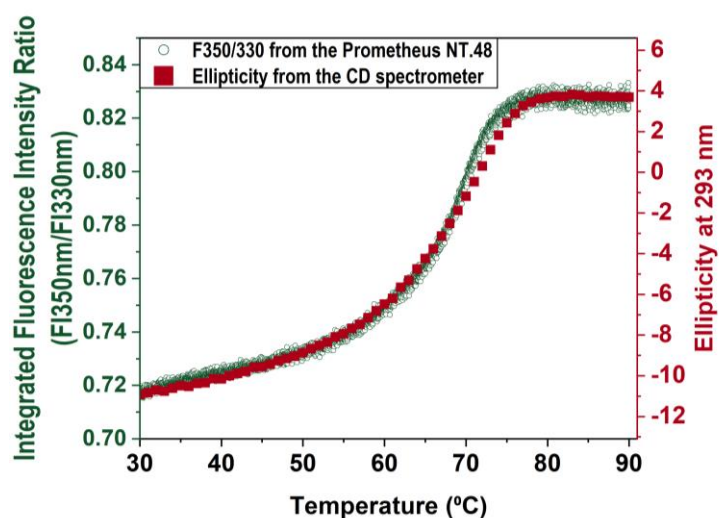
Figure S1. Comparison of the thermal unfolding of IFNα2a measured by the integrated intrinsic protein fluorescence ratio (FI350/FI330) with nanoDSF® (green circles) and the change in the ellipticity at 293 nm with the CD spectrometer (red squares).
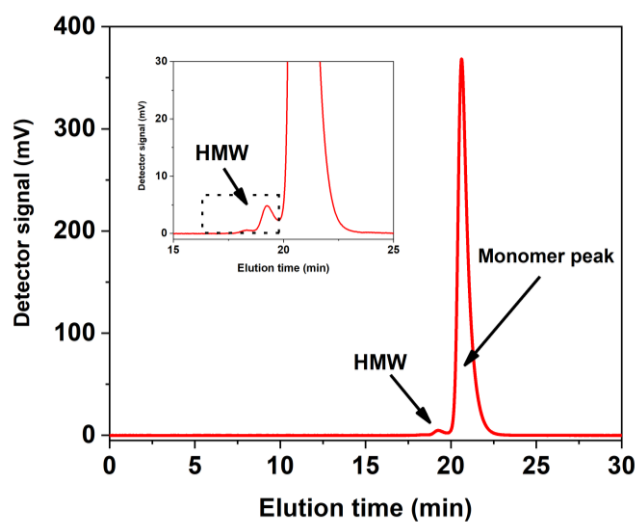
Figure S2. Sample chromatogram showing the monomer peak and the high molecular weight species (HMW) of interferon alpha2a detected with the size exclusion chromatography method.
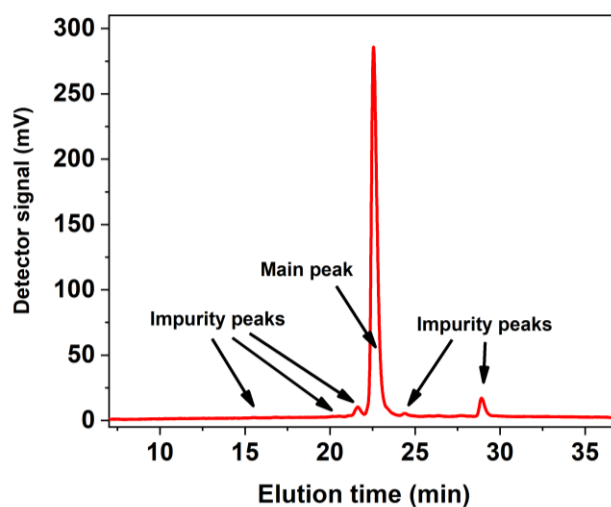
Figure S3. Sample chromatogram showing the main peak and the impurity peaks of interferon alpha2a detected with the reversed-phase HPLC method.

Buffer	Sodium chloride (mM)	Viscosity used for calculating the R_h (cP)
10 mM sodium acetate with pH 4 or 5	10	0.8930
	20	0.8933
	30	0.8944
	40	0.8947
	50	0.8959
	60	0.8961
	70	0.8971
	80	0.8975
	120	0.8983

Table S1. Calculated and measured viscosities of the buffers used in this work. The used viscosity for 10 mM sodium acetate buffer with pH 3.5 to 5.5 and for 10 mM sodium phosphate is 0.889 cP. A control experiment with a falling ball viscometer and subsequently a capillary viscometer provided values for these buffers which were not different than 0.889 cP within the experimental error. The values used calculations of interferon alpha2a R_h in 10 mM sodium acetate buffer including different concentrations of sodium chloride are provided in the table.

Chapter 3 **Isothermal chemical denaturation as a complementary tool to overcome limitations of thermal differential scanning fluorimetry in predicting physical stability of protein formulations**

This chapter is published as:

[*]Department of Pharmacy, Pharmaceutical Technology and Biopharmaceutics, Ludwig-Maximilians-University, Butenandtstrasse 5-13, Munich D-81377, Germany
[+]University of Ljubljana, Faculty of Pharmacy, Aškerčeva 7, 1000 Ljubljana, Slovenia

Author contributions:

H.S. performed most of the experiments, evaluated the data and wrote the paper. U.M performed the accelerated stability studies and contributed with discussions; H.S. and G.W. conceived the presented idea and planned the experiments. G.W. supervised the work, provided conceptual guidance and corrected the manuscript.

Note from the authors:

The version included in this thesis is identical with the published article apart from minor changes. The reference, figure and table numbers were changed to fit into the coherent numbering of this document. The text was edited to meet the norms for British English.

The published article can be accessed online via:

https://doi.org/10.1016/j.ejpb.2018.01.004

3.1 Abstract

Various stability indicating techniques find application in the early stage development of novel therapeutic protein candidates. Some of these techniques are used to select formulation conditions that provide high protein physical stability. Such an approach is highly dependent on the reliability of the stability indicating technique used. In this work, we present a formulation case study in which we evaluate the ability of differential scanning fluorimetry (DSF) and isothermal chemical denaturation (ICD) to predict the physical stability of a model monoclonal antibody during accelerated stability studies. First, we show that a thermal denaturation technique like DSF can provide misleading physical stability rankings due to buffer-specific pH shifts during heating. Next, we demonstrate how isothermal chemical denaturation can be used to tackle the above-mentioned challenge. Subsequently, we show that the concentration dependence of the Gibbs free energy of unfolding determined by ICD provides better predictions for the protein physical stability in comparison to the often-used T_m (melting temperature of the protein determined with DSF) and C_m (concentration of denaturant needed to unfold 50% of the protein determined with ICD). Finally, we suggest a rational approach which includes a combination of DSF and ICD to obtain accurate and reliable protein physical stability ranking in different formulations.

Abbreviations: μDSC - differential scanning microcalorimetry; C_m - concentration (in M) of chemical denaturant needed to unfold 50% of the protein ("melting" concentration of denaturant); dG - Gibbs free energy of unfolding; $H_{ionisation}$ - enthalpy of ionisation; dpH/dT - temperature dependence of pH in pH units per 1 °C; dpKa/dT - temperature dependence of pKa in pH units per 1 °C; DSF - differential scanning fluorimetry; HMW - high molecular weight species; HP-SEC - high-performance size exclusion chromatography; ICD - isothermal chemical denaturation; LMW - low molecular weight species; MWCO - molecular weight cut off; pKa - acid dissociation constant; T_m - protein melting temperature;

3.2 Introduction

3.2.1 Therapeutic protein development and formulation

Therapeutic proteins have been largely successful in the treatment of various severe diseases[131–133]. This success led to the development and market approval of many new biologics over the past two decades. Nowadays, almost every big pharmaceutical company has therapeutic proteins in its R&D program[134]. However, the development process of biologics is often more complicated in comparison to small molecules. Proteins can exhibit various degradation pathways which are intrinsic to their complex structure. One such degradation pathway, which is a major quality and safety issue, is the formation of soluble aggregates. It has been demonstrated that the presence of soluble aggregates can result in reduced biological activity[135,136] or trigger immune response followed by the production of anti-drug antibodies[101,102,137]. Even if the immunogenicity is not an issue for a given protein, the aggregates are product-related impurities according to the ICH guidelines[138], and it is expected that during the shelf life aggregate levels remain within an acceptable range set on a case-by-case study. The formation of aggregates can be reduced by selection of optimal formulation conditions for a new therapeutic protein candidate. Such selection could be based on forced degradation studies followed by accelerated stability testing[70]. However, such studies require a lot of time and a large sample amount (both of which are scarce in the early development stage). For this reason, various high throughput biophysical methods became widespread as tools that can quickly provide data on many formulation conditions with minimal sample consumption. Such high throughput methods are usually used to narrow down the number of promising formulations to a few that will move on to forced degradation studies and accelerated or real-time stability tests[47,49,62,139–141].

3.2.2 Aspects of protein stability

Protein stability has various aspects (i.e. physical stability, chemical stability), each of which can contribute to the formation of aggregates or affect other quality attributes (e.g. biological activity). The connection between protein physical stability and aggregate formation has been described in detail elsewhere[5,38,142]. However, the reader should be aware that conditions (e.g. pH, ionic strength) that maximise the physical stability of a protein might

41

have a detrimental effect on the protein chemical stability (e.g. oxidation, deamination). Therefore, the most stable protein formulation could be a compromise where the physical and chemical stability of the protein is not maximal but sufficient to ensure all aspects of product quality during the shelf life. The stabilisation of proteins against chemical changes is outside the scope of our work, but more information on this topic can be found in the literature[18].

3.2.3   Thermal denaturation techniques to study protein physical stability

A commonly used technique to screen formulations for protein physical stability is differential scanning microcalorimetry (µDSC). Excellent review of the background and applications of µDSC can be found elsewhere[40]. µDSC has been successfully used to measure the melting temperatures (T_m) of various proteins in different formulation conditions. The rankings based on T_m values are in some cases in good agreement with the outcome of the accelerated stability studies[48,105,143,144]. Although µDSC provides stability indicating data much faster than forced degradation studies (or accelerated stability tests), even µDSC devices equipped with an autosampler can measure only several samples over 24 h, and few milligrams of protein are required to screen different formulation conditions.

Differential scanning fluorimetry (DSF) is an alternative to the µDSC technique which provides physical stability-indicating data based on the protein melting temperatures in different formulations[140]. Hundreds of T_m values can be obtained per day with modern DSF methods with as less as few micrograms of protein needed for one measurement. There are two main approaches to perform DSF – the first is based on an increase in the (extrinsic) fluorescence intensity of a fluorescent dye that interacts with hydrophobic protein patches exposed during thermal unfolding[145]. The second approach is label-free and measures the intrinsic tryptophan fluorescence that changes during unfolding due to a change in the tryptophan environment[116]. Excellent agreement was demonstrated between T_m values measured by µDSC and DSF with extrinsic fluorescent dye[47,140,146,147] or DSF based on intrinsic protein fluorescence[148].

Whether µDSC or DSF will be used during protein formulation screening is still a matter of debate and preferences of the formulation scientist. An advantage of µDSC is that this technique will usually provide a better resolution between protein unfolding transitions in comparison to DSF[146]. Also, the detection of protein unfolding by µDSC is independent on the

number of tryptophan residues in the structure or the interaction of the extrinsic fluorescent probe with the (partially unfolded) protein. The benefits of DSF techniques are mostly related to the lower sample consumption and the high throughput compared to μDSC.

Regardless whether heat capacity (μDSC) or extrinsic/intrinsic fluorescence (DSF) is measured as a physical observable to detect protein unfolding during heating, all thermal denaturation methods suffer from the fact that the temperature is increased far above the actual temperature of sample preparation and storage. This requires long error-prone extrapolations to lower temperatures during thermodynamic evaluation of the data[4]. Additionally, thermal protein denaturation is usually a non-reversible process which makes the thermodynamic evaluation of such data invalid and physical stability rankings are based only on apparent T_m values which could represent only a small part of the protein conformational stability curve against temperature[4]. On the other hand, aggregation of the protein at high temperatures will also affect the accuracy of the measured T_m values[149]. These and other challenges to predict protein physical stability from thermal denaturation experiments are extensively discussed in the following papers[4,93].

In addition to the pitfalls of thermal denaturation techniques mentioned above, it is an often-ignored fact that not only protein properties but also excipient properties can change during heating. A typical example of this is the pKa change of many pharmaceutical excipients during heating[150,151]. This includes two of the most frequently used buffers for protein therapeutics – histidine and tris[152].

3.2.4 Isothermal chemical denaturation (ICD) as a tool to study protein physical stability in different formulations

Isothermal chemical denaturation (ICD) was recently proposed as an isothermal method to evaluate protein physical stability in different formulations[4]. A typical ICD experiment includes the preparation of protein samples with an increasing concentration of a denaturant (usually guanidinium hydrochloride or urea). After sufficient incubation time needed to reach an equilibrium, a physical observable is measured (e.g. intrinsic fluorescence) to detect at which denaturant concentrations the protein is (partially) unfolded. The approaches to evaluate ICD data are described in detail elsewhere[4,50,51]. Most evaluation methods can extract several stability-indicating parameters from chemical denaturation graphs, e.g. the amount of

denaturant needed to unfold 50% of the protein (C_m) (sometimes also referred as the "melting" denaturant concentration) and the Gibbs free energy of protein unfolding (dG)[153]. A recently proposed approach would also investigate the variation of dG in samples with different protein concentration (in the same formulation conditions)[154]. It should be noted that in this case, the dG measured is an apparent value. It is suggested that a lower concentration dependence of dG is an indicator for a lower aggregation propensity[6]. Until now, there is some limited data that parameters (i.e. C_m) obtained with ICD can provide reasonable predictions of the outcome of accelerated stability studies[155]. To best of our knowledge, the concentration dependence of dG is not directly related to the physical stability of a protein in a wide range of conditions during accelerated stability studies. Considering also the high sample consumption and the low throughput of ICD, it is still unclear why and how formulation scientists should use ICD to find optimal formulation conditions for new therapeutic proteins in early-stage development.

3.2.5 Problem statement and hypothesis

The reason we stepped into this work is the trend that high throughput thermal denaturation techniques based on T_m measurements are often used on a wide range of formulations to access protein physical stability. We hypothesised that such thermal denaturation techniques are not an appropriate choice for all formulations, especially such containing excipients that change their properties upon heating. We expected that such "inappropriate" use of thermal denaturation techniques could result in misleading physical stability rankings and probably early rejection of stable protein formulations. As identifying the problem is just the first step of the solution, we also wanted to investigate whether isothermal chemical denaturation can find a place as a suitable protein physical stability indicating method in cases where high throughput thermal denaturation might not be an appropriate choice.

To test our hypothesis, we developed a classical formulation case study and investigated the effect of pH and buffer type on the physical stability of a model monoclonal antibody (mAb1). We compared DSF and ICD to see if both methods provide similar physical stability rankings with the different conditions we tested. Finally, we performed accelerated stability studies to validate the predictions.

3.3   Materials and methods

3.3.1   Model protein and sample preparation

The model monoclonal antibody (mAb1) used in this work is a human IgG type 1 with a molecular weight of 145 kDa. The bulk solution has more than 99.5% relative monomer content after thawing (measured by size exclusion chromatography). Further, SDS-PAGE shows only bands corresponding to the monomer and antibody fragments (this data is available on request). mAb1 was selected as a suitable model protein since it shows T_m dependence versus pH which is well described for other IgG type 1 antibodies[140]. Also, our experience shows that the rate of aggregation of mAb1 is highly dependent on the formulation buffer. This behaviour makes it a good model protein to compare the prediction quality of stability indicating techniques when it comes to buffer selection in a narrow pH range. Different formulations of mAb1 were prepared by dialysis at room temperature (20–25 °C) against an excess of the respective buffer using a Spectra/Por® 8000 MWCO dialysis tubing from Spectrum Laboratories Inc. (Rancho Dominguez, USA). The sample to buffer ratio was 1:200 and the buffer was exchanged 3 h and 8 h after the start of the dialysis. The total dialysis time was 24 h. Protein concentration was measured with a Nanodrop 2000 (Thermo Fisher Scientific, Wilmington, USA). Finally, the formulations were sterile filtered with 0.22 µm cellulose acetate filters from VWR International (Darmstadt, Germany). Reagent chemicals were of analytical grade and were purchased from Sigma Aldrich (Steinheim, Germany) or VWR International (Darmstadt, Germany). Highly purified water (Purelab Plus, USF Elga, Germany) was used for the preparation of all buffers.

3.3.2   Differential scanning fluorimetry (DSF) with intrinsic fluorescence and static light scattering detection

Thermal denaturation studies were performed with the Optim® 1000 system (Avacta Analytical, United Kingdom). 9 µL of mAb1 formulations with a protein concentration of 10 g/L were filled in triplicates in microcuvette arrays (Unchained Labs, USA). The samples were excited at 266 nm and fluorescence spectra were collected from 30 to 90 °C with a temperature ramp of 1 °C/min. The obtained intrinsic fluorescence spectra were further processed to create graphs of the fluorescence intensity ratio 350 nm/330 nm (F350/330) versus

temperature. The T_m values were determined from the maximum of the first derivatives of these graphs using the Optim® 1000 software (Avacta Analytical, United Kingdom). T_{m1} was assigned to the first transition (at lower temperature) while T_{m2} was assigned to the second transition (at higher temperature). Simultaneously with the intrinsic fluorescence, static light scattering data at 473 nm was collected by the instrument to evaluate if the protein is aggregating after unfolding.

3.3.3 Isothermal chemical denaturation (ICD) with intrinsic fluorescence detection

8 µL from of each stock solution of mAb1 with concentration 5, 10, 20 or 40 g/L were pipetted in triplicates with a 16-channel 12.5 µL Viaflo pipette (Integra Biosciences, Konstanz, Germany) and the Viaflo Assist (Integra Biosciences, Konstanz, Germany) into non-binding surface 384 well plates (Corning, USA). Next, the respective amount of the formulation buffer and subsequently the denaturant stock solution (same as the formulation buffer regarding concentration and pH but including 6 M guanidine hydrochloride) were pipetted with a 16-channel 125 µL Viaflo pipette (Integra Biosciences) and the Viaflo Assist (Integra Biosciences). Finally, mixing was performed manually with new tips to minimise cross-contamination between the wells. After mixing, the well plate was sealed with an EASYseal™ sealing film (Steinheim, Germany) and incubated for 24 h at room temperature. A FLUOstar Omega microplate reader (BMG Labtech, Ortenberg, Germany) was used to measure the intrinsic fluorescence intensity of mAb1 at 330 and 350 nm after excitation at 280 nm. The measurements for both wavelengths were performed in multichromatic mode using 50 flashes per well and the same gain for each wavelength. The ratio between the fluorescence intensity at 350 and 330 nm (F350/330) was calculated for mAb1 in each denaturant concentration. The data from the triplicates was fitted to a three-state model and evaluated with the CDpal software[50]. Other models available in the software (e.g. two-state, three-state with dimerisation of the intermediates, etc.) were also tested but showed poor fit quality in comparison to the three-state model we used. Different starting parameters for the C_m and m-values were tested, and the different fits were compared with the f-test function of the software. The best fit was used to derive the values for C_{m1}, C_{m2} and dG. The errors for the C_m and dG values are shown as the Jackknife error from the fit. ddG was calculated after the dG value for the lowest protein

concentration was subtracted from the dG determined for the respective higher protein concentration.

3.3.4 pH measurements at different temperatures

The pH measurements were performed with an InLab Expert Pro-ISM pH electrode (Mettler Toledo, Germany) and a SevenEasy pH meter (Mettler Toledo, Germany). 10 mL of each buffer were filled in triplicates in 15 mL Falcon tubes. The Falcon tubes were immersed in a water bath and the temperature was increased in a step of 5 or 10 °C. After each increase, the samples were equilibrated for at least 5 min to reach constant temperature. Before measurement of the samples, the pH electrode was calibrated at each temperature with two calibration buffers pH 2 at 25 °C and pH 7 at 25 °C (Bernd Kraft, Germany) using the pH values provided from the manufacturer for the respective temperature.

3.3.5 Accelerated stability study and size exclusion chromatography (SEC)

mAb1 formulations with a concentration of 10 g/L were sterile filtered with 0.22 μm cellulose acetate filters from VWR International (Darmstadt, Germany). Next, 1 mL of each formulation was aseptically filled in sterilised type one glass vials (DIN 2R) and closed with sterilised rubber stoppers. The samples were incubated for 3 months at 40 °C ± 2 °C. Every four weeks 50 μL were withdrawn from each replicate in a way that sterility of the solution is preserved. The samples were analysed on a Waters Alliance 2695 separation module with a Waters 2487 UV/Vis detector and a Tosoh TSKgel G3000SWXL 7.8 mm ID × 30.0 cm L column (Tokyo, Japan). The flow rate was 1 mL/min, and the protein elution was detected at 280 nm after 25 μg protein were injected on the column. The mobile phase consisted of 25 mM sodium phosphate and 200 mM sodium chloride; the pH was adjusted to 7.0 ± 0.05 with 2 M sodium hydroxide. The chromatograms were integrated with the Chromeleon 6.8 software (Thermo Fisher, Dreieich, Germany) and the relative percentage of high molecular weight (HMW) and low molecular weight (LMW) species was calculated in relation to the total area of all protein peaks. As HMW are evaluated peaks eluting earlier than the monomer, while as LMW are evaluated protein peaks eluting later than the monomer (see the supplementary data to this chapter). Next, the data was fitted linearly to obtain relative aggregation and fragmentation rates. The values

for these rates and the corresponding adj. R^2 from the fits are provided (see the supplementary data to this chapter).

3.4 Results and discussion

3.4.1 Unfolding and aggregation of mAb1 during thermal denaturation

mAb1 shows two unfolding transitions measured by the change of the intrinsic fluorescence ratio F350/330 in the temperature range 30–90 °C in all buffers we tested (Fig. 17A and 17B). Previous work on mAbs shows that the first unfolding transition is assigned to the unfolding of the CH2 domain, while the second transition is assigned to the Fab and the CH3 domains[156]. Also, static light scattering at 473 nm showed that mAb1 aggregates in all conditions with the onset of the second unfolding transition but never during the first transition (see the supplementary data to this chapter).
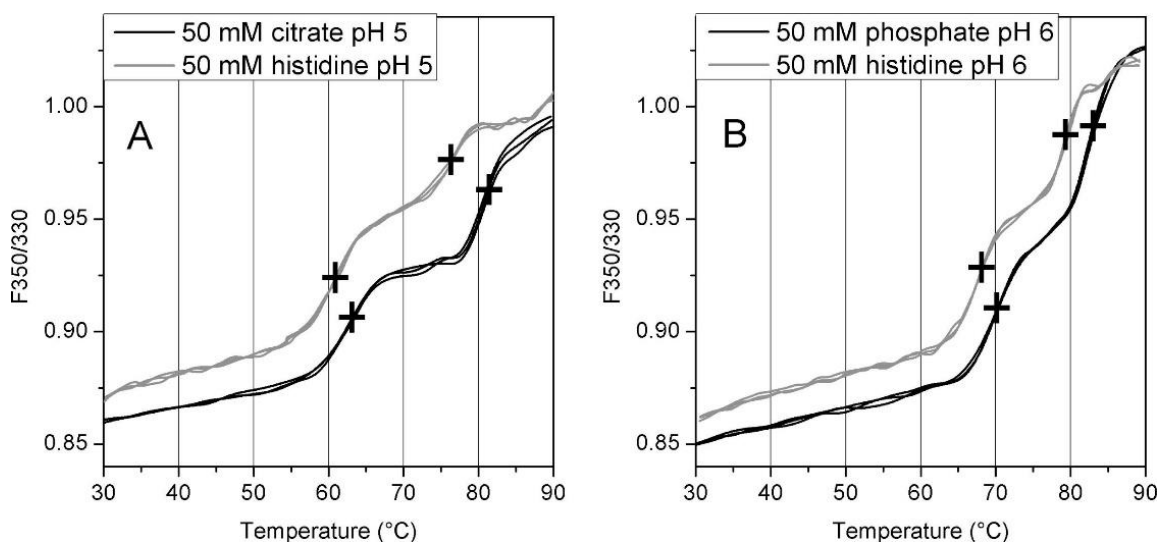
Figure 17. Thermal unfolding of mAb1 detected by intrinsic fluorescence ratio (F350/330) at: (**A**) pH 5 in 50 mM citrate (black) and 50 mM histidine (grey); (**B**) pH 6 in 50 mM phosphate (black) and 50 mM histidine (grey). An overlay of three separate measurements is given for each sample. The place where the T_m values are obtained from the first derivative is marked with a cross.

3.4.2 Melting temperatures of mAb1 in various buffers

The melting temperatures of mAb1 across the pH range from 4.5 to 8.5 was investigated in four different buffers – 50 mM citrate pH 4.5–5.5, 50 mM phosphate pH 6–8.5, 50 mM histidine pH 5–6 and 50 mM tris pH 7.5–8.5 (Fig. 18). The general trend shows a sharp decrease

in both T_{m1} and T_{m2} with a decrease in pH below 6.0 in histidine and citrate. Also, both melting temperatures slightly decrease when the pH is increased above pH 6.5 in phosphate. The highest T_{m1} values were measured in 50 mM phosphate in the pH range 6.5–7 and in all tris formulations. The highest T_{m2} values were measured in 50 mM citrate pH 5.5 and in 50 mM phosphate pH 6 and 6.5 as well as in tris formulations with pH 7.5 and 8 (at 25 °C). Interestingly, mAb1 shows lower T_m values in histidine compared to formulations with citrate or phosphate having the same pH at 25 °C. These differences are more distinct for the second melting temperature. On the other hand, mAb1 shows in general higher T_m values in tris compared to phosphate in the pH range 7.5–8.5.
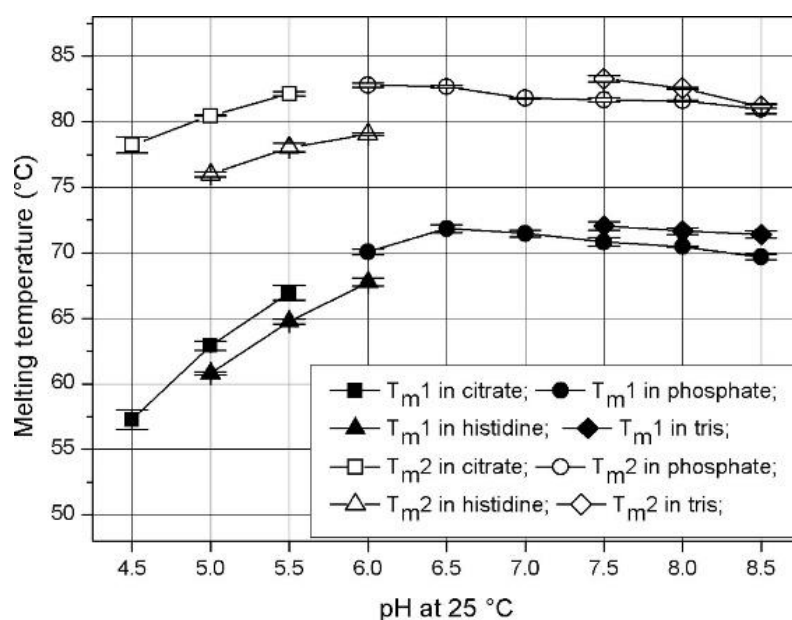
Figure 18. Melting temperatures T_{m1} (filled symbols) and T_{m2} (open symbols) of mAb1 in different buffers measured with thermal denaturation and intrinsic fluorescence – 50 mM citrate (squares), 50 mM phosphate (circles), 50 mM histidine (triangles), 50 mM tris (diamonds). The pH shown on the graph is measured at 25 °C. The provided values are mean of three measurements, and the error is the standard deviation.

Similar observations with thermal denaturation studies of mAbs can be found in the literature. Razinkov et al. reported that the melting temperatures of several mAbs measured by DSC and DSF were lower in histidine buffer in comparison to acetate or phosphate, indicating that "at pH 5.5, the mAbs were more stable in acetate buffer than in the histidine buffer"[140]. Menzen et al. used DSF with two different extrinsic fluorescent dyes to study the melting temperatures of

a model mAb in various formulations[157]. They showed that the T_ms of the mAb were always lower in histidine pH 5 when compared to formulations with phosphate pH 5. This was true for a wide range of protein concentrations from 0.8 to 40 g/L. Interestingly, in the same work from Menzen et al. the melting temperatures of the same antibody were higher in histidine than in phosphate at pH 7.2. Another example is a recent work from Kalonia et. al where μDSC was used to evaluate the thermal stability of a model mAb and reported that "mAb in pH 4.5 and 6.5 citrate solutions had higher onset and melting temperatures compared to the mAb in histidine solution"[95].

Since histidine is a very common buffer for therapeutic proteins, especially for mAbs[152], an explanation with the low physical stability of mAb1 in this buffer is unlikely. Therefore, we hypothesised that such disagreements between histidine and citrate or phosphate buffers might be due to a change in buffer properties, more specifically due to buffer pH shift during heating.

3.4.3 pH temperature dependence of the tested buffers

The pH of 50 mM citrate buffer pH 5 (at 20 °C) was measured over the temperature range 20–80 °C and compared to 50 mM histidine buffer pH 5 (at 20 °C) (Fig. 19A). The pH of histidine decreases linearly and reaches 4.2 at 80 °C, while citrate exhibits a slight increase from pH 5.05 at 20 °C to pH 5.2 at 80 °C. Similar observations were made when we compared 50 mM phosphate buffer pH 6 (at 20 °C) with 50 mM histidine buffer pH 6 (at 20 °C) (Fig. 19B). The slope of pH decrease (dpH/dT) for histidine was −0.014/1 °C and was the same for pH 5 and pH 6 formulations. The pH of citrate and phosphate remained almost unchanged over the investigated temperature range (i.e. dpH/dT was close to zero). This revealed that although having the same starting pH at 20 °C, when the buffers are heated to about 60–65 °C (the approximate temperature of T_{m1} for mAb1) there is a difference of 0.7 pH units between citrate and histidine (Fig. 19A) and a difference of 0.5 pH units between phosphate and histidine (Fig. 19B). This difference becomes even larger at temperatures around 80 °C (where approximately T_{m2} of mAb1 is). Additionally, we also measured the dpH/dT for tris which was −0.022/1 °C for tris buffers with pH 7.5, pH 8.0 and pH 8.5 at 20 °C, indicating that tris formulations will exhibit even larger pH shifts than histidine formulations during heating.
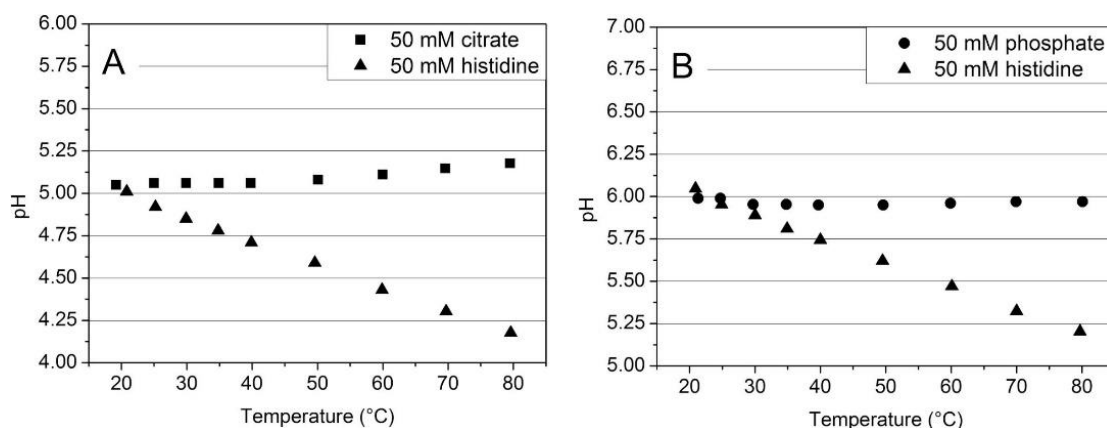
Figure 19. (**A**) pH of 50 mM citrate (squares) and 50 mM histidine (triangles) between 20 and 80 °C, both buffers had pH 5 at 20 °C; (**B**) pH of 50 mM phosphate (circles) and 50 mM histidine (triangles) between 20 and 80 °C, both buffers had pH 6 at 20 °C;

Considering the high pH dependence of the T_ms of mAb1 (Fig. 18), especially at a pH below 6, such pH shifts during heating can significantly affect the protein melting temperatures. This can result in two possible scenarios. In the first case, the pH of the buffer is shifted away from the pH of maximum stability during heating, and the T_m values appear lower. This is the case for the T_ms of mAb1 in histidine in Fig. 18. In the second case, the pH is shifted towards the pH of maximum stability of the protein and the T_m values appear higher. This is the case for the T_ms of mAb1 in tris in Fig. 18.

It is a well-known fact that the behaviour of a particular buffer during heating will be determined mostly by its enthalpy of ionisation dHionisation[158]. High positive or negative $dH_{ionisation}$ will indicate high temperature dependence of the acidic constant pKa, while ionisation enthalpy close to zero will indicate low temperature dependence of the pKa. Subsequently, changes in the pKa will influence the pH of the system according to the Henderson–Hasselbalch equation. A quick comparison between the $dH_{ionisation}$ and the dpH/dT shows that both values are in good agreement for the buffers we tested (for pK$_2$ of histidine $dH_{ionisation} \sim 30$ kJ/mol, for tris $dH_{ionisation} \sim 47$ kJ/mol; for pKa2 and pKa3 of citrate $dH_{ionisation} \sim 2$ kJ/mol and ~ -3 kJ/mol respectively; for pKa2 of phosphate $dH_{ionisation} \sim 4$ kJ/mol [159]). Although, $dH_{ionisation}$ and dpKa/dT will indicate if a large dpH/dT can be expected, a good practice would be to measure the pH of each formulation for thermal

denaturation in the temperature range of interest to determine the exact dpH/dT and avoid mistakes arising from comparison of formulations with different dpH/dT.

Even if the correct pH of a formulation buffer at a given temperature is known, corrections for the pH and melting temperatures should be done with great caution. The reason for this is that the temperature during thermal denaturation studies is increased relatively quickly (typically 0.5–1 °C/min) and this might not allow enough time for the protein to reach equilibrium state at the new pH before it unfolds. We assume that at the temperature and pH of unfolding the protein might be in a state that would not represent its "true" T_m value for a given formulation condition. Therefore, a direct comparison of the physical stability of a protein in buffers with different dpH/dT would be reliable only with suitable isothermal techniques.

3.4.4 Unfolding of mAb1 with isothermal chemical denaturation (ICD)

mAb1 shows a three-state unfolding transition after chemical denaturation with guanidine hydrochloride in all formulations tested (Fig. 20). In another work with a monoclonal antibody, the first transition was assigned to the unfolding of the CH2 domain while the second transition corresponds to the unfolding of the Fab or the CH3 domain[160]. This unfolding behaviour is also in good agreement with the unfolding curves during thermal denaturation. Direct comparison of the denaturation graphs (obtained with ICD) of mAb1 in histidine and citrate or histidine and phosphate reveals that in most cases higher concentrations of guanidinium hydrochloride are needed to unfold the model mAb in histidine which is an indicator for the higher physical stability of mAb1 in histidine.
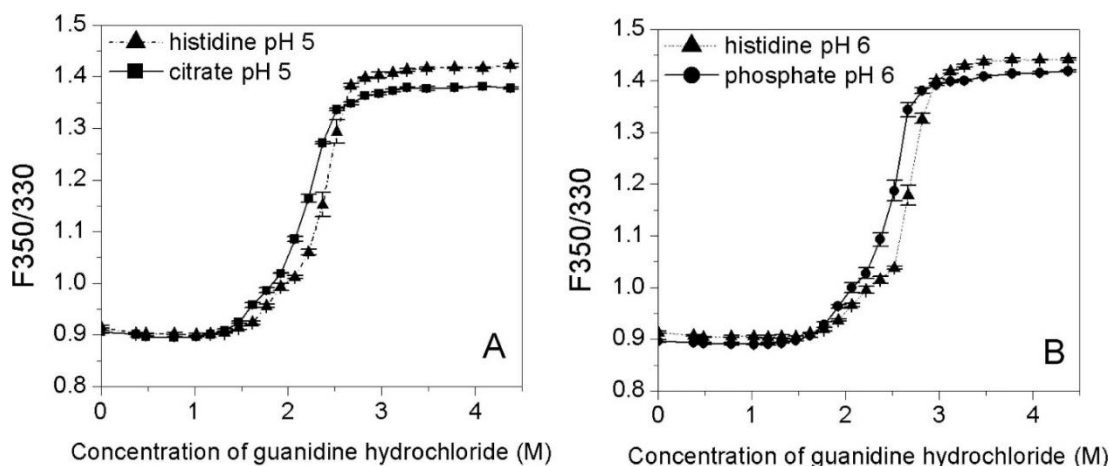
Figure 20. Chemical denaturation of mAb1 detected by intrinsic fluorescence ratio (F350/330) at: (**A**) pH 5 in 50 mM citrate (squares) and 50 mM histidine (triangles); (**B**) pH 6 in 50 mM phosphate (circles) and 50 mM histidine (triangles). The lines on this graph are to guide the eyes and do not represent a fit to a certain model.

The denaturation graphs of mAb1 in different formulations were evaluated with CDpal as described in the materials and methods section. An example fit of a sample denaturation graph can be found in the supplementary data to this chapter. The C_m and dG values obtained from the best fit are used for further comparison of the stability of the formulations. The C_{m1} was derived from the unfolding at the lower denaturant concentration while the C_{m2} is derived from the unfolding at the higher denaturant concentration.

3.4.4.1 C_m values of mAb1 in various buffers

As alkaline pH conditions (pH >7) are known to promote chemical degradation in mAb formulations and are thus not practically relevant, ICD and accelerated stability testing were limited to the pH range 4.5–7 [18]. Both the C_{m1} and the C_{m2} of mAb1 show an increase with the increase of pH in all buffers (Fig. 21) which is in good agreement with the increase of the T_{m1} and the T_{m2} when the pH is increased from pH 4.5 to pH 6.5 (Fig. 18). The C_m values of mAb1 in histidine are similar or higher than the C_m values in the citrate or phosphate formulations with the same pH, while the T_{m1} and T_{m2} values of mAb1 in histidine formulations were lower compared to their citrate and phosphate counterparts. One reason for this is that ICD is an isothermal technique and any pH temperature drift of excipients is avoided.
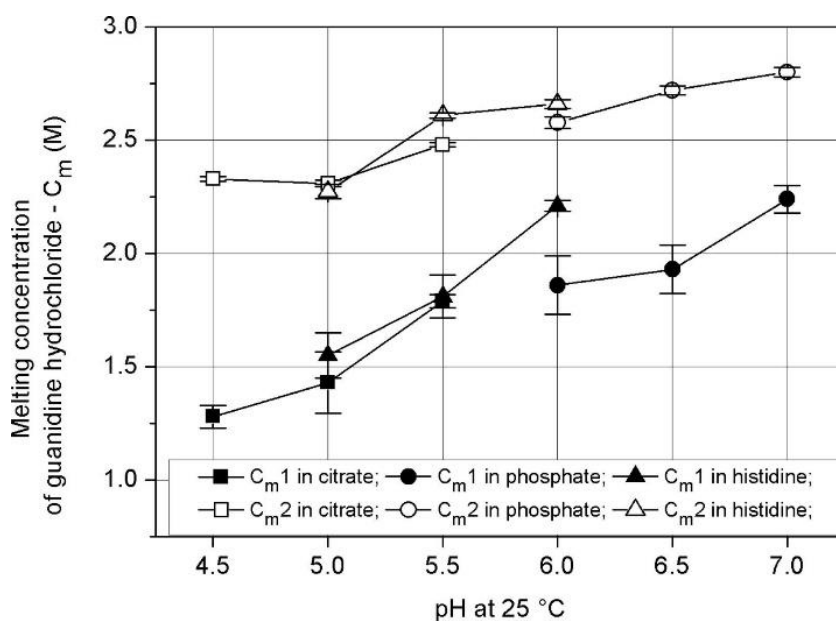
Figure 21. C_m values – C_{m1} (filled symbols) and C_{m2} (open symbols) – of mAb1 in different buffers measured with chemical denaturation and intrinsic fluorescence – 50 mM citrate (squares), 50 mM phosphate (circles), 50 mM histidine (triangles). The pH shown on the graph is measured at 25 °C. The values are obtained from the fit of three denaturation graphs. The error bar represents the Jackknife error from the fit in CDpal.

3.4.4.2 Concentration dependence of the dG of mAb1 in various buffers

The Gibbs free energy of unfolding (dG) can be an indicator of the protein conformational stability[4,153]. However, it has recently been demonstrated that the dG is concentration dependent and this dependence can change in different formulations of the same protein[154]. Therefore, a comparison of different formulations based on a dG value determined at a single protein concentration is rather difficult. On the other hand, the concentration dependence of dG is supposed to give indications whether a protein will be more aggregation prone in certain conditions[154]. High concentration dependence of dG indicates a higher aggregation propensity of the protein while the low concentration dependence of dG is an indicator for a low aggregation propensity of the protein. To evaluate the feasibility of this approach, we investigated the concentration dependence of dG of mAb1 in the range of 0.5–4 g/L for several formulations. In our experiments, we observed that mAb1 shows the lowest concentration dependence (within ±10 kJ/mol) of dG in citrate pH 5.0 and 5.5 (Fig. 22A) and in histidine pH 6.0 (Fig. 22B). The highest concentration dependence (more than ±25 kJ/mol) of dG was

observed in phosphate pH 6 and pH 6.5 (Fig. 22C). This indicates that phosphate is a bad buffer choice for mAb1 despite the high T_m and C_m values of mAb1 measured in it.
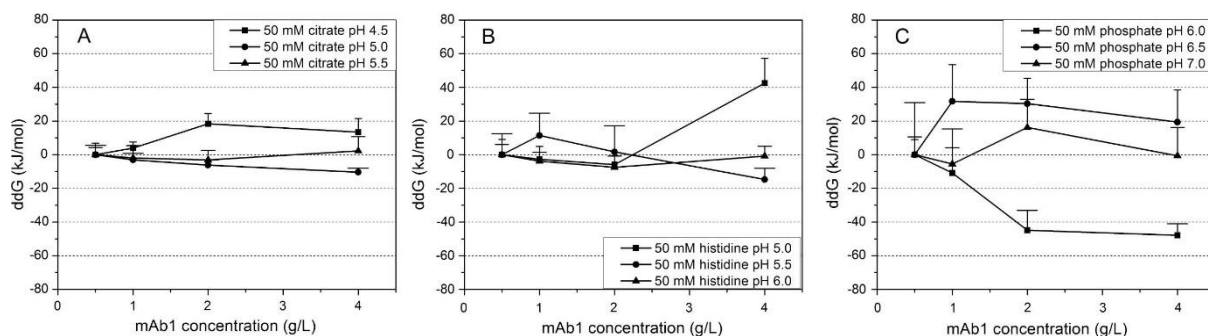
Figure 22. Concentration dependence of dG for mAb1 in various buffers. A. 50 mM citrate with pH 4.5 (squares), pH 5 (circles) and 5.5 (triangles up); B. 50 mM histidine with pH 5 (squares), 5.5 (circles) and 6.0 (triangles up); C. 50 mM phosphate with pH 6 (squares), 6.5 (circles) and 7.0 (triangles up). Each point on the graphs is derived from three chemical denaturation graphs. The errors are the Jackknife error from the fit to a three-state model.

3.4.5 Physical degradation of mAb1 during accelerated stability studies

To validate the predictions made with thermal and chemical denaturation we performed accelerated stability studies for 12 weeks at 40 °C. We observed that not only aggregation but also fragmentation of mAb1 occurred in the samples we tested. Fragmentation was independent of the buffer we used (Fig. 23B) but was highly dependent on the pH showing a minimum at pH 5.5 and 6 which is in good agreement with previously published data with mAbs[18,161]. On the other hand, apparent aggregation rates were dependent not only on the pH but also on the buffer type (Fig. 23A). Minimal aggregation rates of mAb1 were observed in all histidine formulations, followed by citrate formulations with pH 5.0 and 5.5. Highest aggregation rates of mAb1 were observed in phosphate pH 6.5 followed by phosphate pH 7 and 6. At this point, we should underline that the accelerated stability study in our case did not include analytical methods to evaluate chemical degradation (e.g. oxidation, deamination) or changes in the biological activity of the protein (both of which can be observed during storage). As already discussed in the introduction, such changes can also affect product quality and should be studied in parallel with the physical degradation.
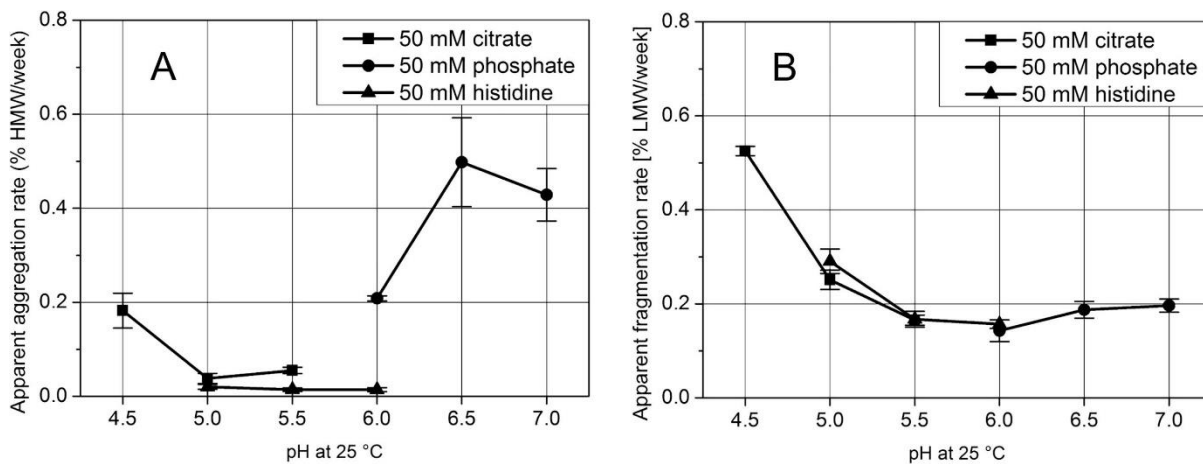
Figure 23. (**A**) Apparent aggregation rates of mAb1 in various buffers determined after 12-weeks storage at 40 °C; (**B**) Apparent fragmentation rates of mAb1 in different buffers determined after 12-weeks storage at 40 °C.

3.4.6 Relationship between stability-indicating parameters and the aggregation rate

Both the T_m and C_m values indicated that mAb1 should have high stability in phosphate buffer. Even worse, due to the pH shift of histidine, it appeared that the physical stability of mAb1 would be lower in histidine than in citrate or phosphate due to the lower T_m values of mAb1 measured in histidine. At this point, the only approach that indicated that phosphate is a bad buffer for mAb1 was the concentration dependence of dG. Also, all formulations showing a minimal concentration dependence of dG in Fig. 22 showed a very low apparent aggregation rate (Fig. 23A), but not vice versa. Still, if the formulations with minimal concentration dependence of dG were selected, this would have resulted in satisfactory results in the accelerated stability studies in this case. However, we should note that the approach to determine the concentration dependence of dG requires more sample in comparison to high throughput methods like DSF.

3.4.7 Rational use of a combination of DSF and ICD to study protein physical stability

Based on our work, we suggest that a combination of DSF and ICD would be feasible to reduce the protein amount required to assess the physical stability in various formulations but still provide a sufficient prediction quality. Such a combination would:

- First – Employ DSF to study the melting temperatures of a new therapeutic protein candidate over a wide pH range in buffers with dpH/dT close to zero to determine the pH range of maximum T_m values;

- Second – Use ICD to determine C_m, dG and the concentration dependence of dG of the therapeutic protein candidate in the pH range of maximum T_m values in various buffers (which can have high dpH/dT e.g. histidine, tris);

- Third – Perform accelerated stability tests on formulations with the highest T_ms, the highest C_ms and the lowest concentration dependence of dG.

3.5 Final words and recommendations

High throughput thermal denaturation is a valuable technique to determine the melting temperatures of therapeutic protein candidates in early stage development when the amount of material is limited. When it comes to formulation studies, thermal denaturation techniques in general are (alongside other pitfalls discussed in the introduction) limited by the fact that the increase in temperature can change critical excipient properties (i.e. pH of the buffer system). Care should be taken when such measurements are conducted. pH screenings based on T_m values should be performed only in buffers with dpH/dT close to zero. After the pH range of maximum thermal stability of a protein is found, further formulation experiments with a wider range of buffers should be performed with isothermal techniques. A suitable isothermal method that can be used at this stage is isothermal chemical denaturation. ICD would allow direct comparison of a variety of formulation buffers regardless of their dpH/dT. Moreover, the concentration dependence of dG seems to be a valuable tool which can allow identification of "bad" conditions where the protein has low physical stability during storage.

3.6   Supplementary data
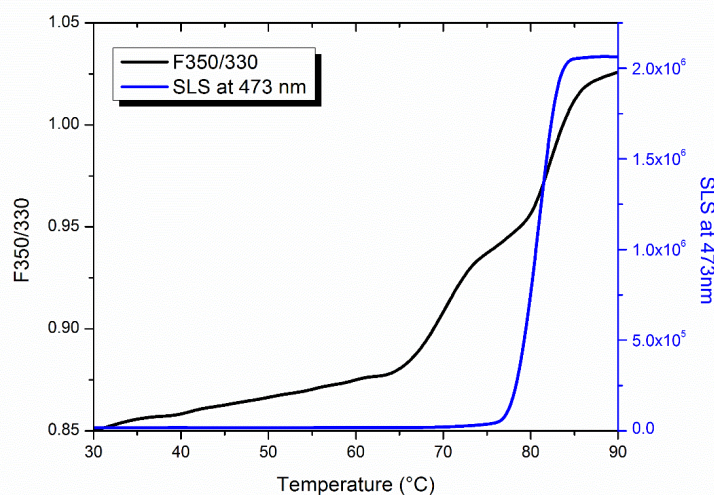
Figure S4. Change in intrinsic fluorescence (F350/330) and static light scattering signal at 473 nm during thermal denaturation of mAb1 in 50 mM phosphate pH 6. A high increase in the scattering is observed with the onset of the second unfolding transition.
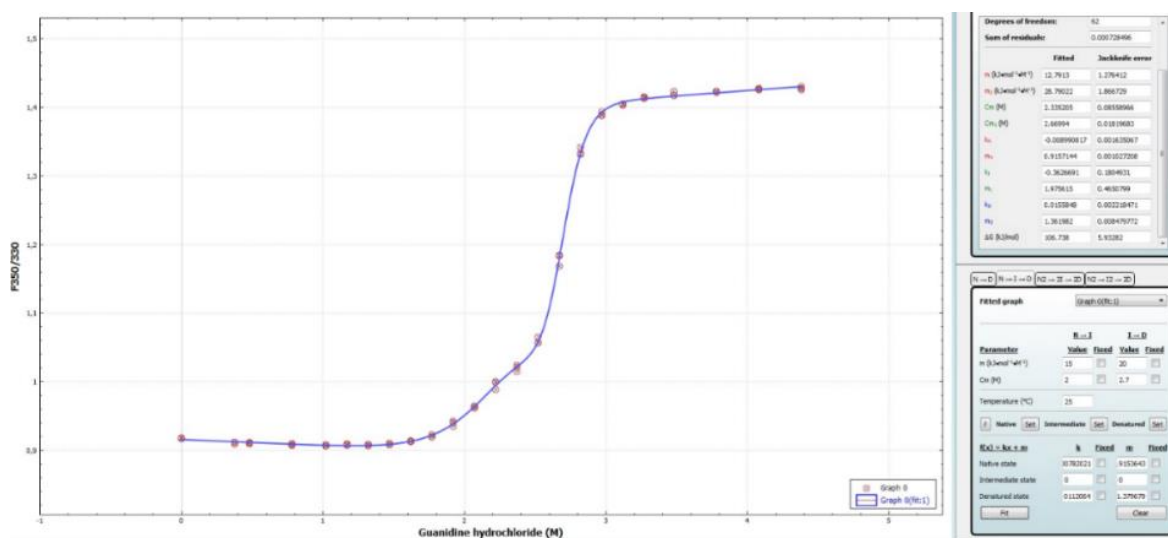
Figure S5. Example fit of chemical denaturation graph in CDpal
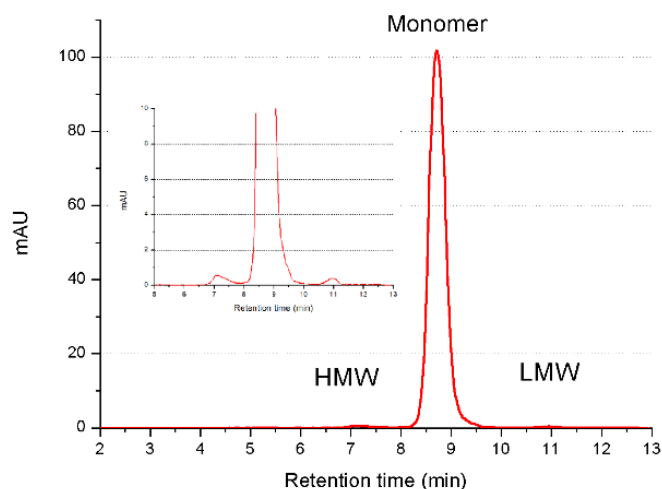
Figure S6. Chromatogram of mAb1 sample from Size Exclusion Chromatography. Integration of the HMW area was done from 5 to 8 minutes elution time. Integration for the LMW area was done from 10,5 to 12 minutes elution time.

Buffer	50 mM citrate			50 mM phosphate			50 mM histidine		
pH	4,5	5,0	5,5	6,0	6,5	7,0	5,0	5,5	6,0
Rate of HMW formation (%/week)	0.18233	0.03808	0.05508	0.20833	0.49792	0.42883	0.02008	0.01425	0.0141
Error from the fit	0.03717	0.01078	0.00691	0.00553	0.09453	0.05566	0.00517	0.0039	0.00422
Adj. R^2	0.8849	0.79273	0.95429	0.99789	0.89914	0.9511	0.82454	0.80482	0.77425
Rate of LMW formation (%/week)	0.52508	0.251	0.16558	0.14308	0.1875	0.19633	0.29067	0.16733	0.157
Error from the fit	0.00976	0.02056	0.01085	0.02287	0.01767	0.01386	0.02596	0.01682	0.00914
Adj. R^2	0.99896	0.98014	0.98724	0.92708	0.97382	0.98519	0.97645	0.97029	0.9899

Table S2. Rate of HMW and LMW formation derived from linear fit of the data in Origin 8.0 with the corresponding adjusted R^2 values. The adjusted R2 values are used as this is a parameter which describes the quality of the regression better than R^2. The adj. R^2 values are always lower than the corresponding R^2 values.

Chapter 4 **A new approach to study the physical stability of monoclonal antibody formulations - Dilution from a denaturant**

This chapter is published as:

Svilenov, H.[*], Gentiluomo, L.[+], Friess, W.[*], Roessner, D.[+] and Winter, G.[*], **2018**. A New Approach to Study the Physical Stability of Monoclonal Antibody Formulations - Dilution from a Denaturant. Journal of pharmaceutical sciences, 107(12), pp.3007-3013.

[*]Department of Pharmacy, Pharmaceutical Technology and Biopharmaceutics, Ludwig-Maximilians-University, Butenandtstrasse 5-13, Munich D-81377, Germany
[+]Wyatt Technology Europe GmbH, Hochstrasse 12a, Dernbach 56307, Germany

Author contributions:

H.S. performed the experiments, evaluated the data and wrote the paper with input from the other authors. L.G., W. F. and D.R. provided guidance on the methodology and data evaluation of the dynamic light scattering and size exclusion chromatography methods. L.G., W. F. and D.R. also contributed with discussions on the work and provided access to equipment. H.S. and G.W. conceived the presented idea and planned the experiments. G.W. supervised the work, provided conceptual guidance and corrected the manuscript.

Note from the authors:

The version included in this thesis is identical with the published article apart from minor changes. The reference, figure and table numbers were changed to fit into the coherent numbering of this document. The text was edited to meet the norms for British English.

The published article can be accessed online via:

https://doi.org/10.1016/j.xphs.2018.08.004

4.1   Abstract

The early-stage assessment of the physical stability of new monoclonal antibodies in different formulations is often based on high-throughput techniques that suffer from various drawbacks. Accordingly, new approaches that facilitate protein formulation development can be of high value to the industry. In this study, a dynamic light scattering plate reader is used to measure the aggregation (by means of the increase in the hydrodynamic radius R_h) of monoclonal antibody samples that were subject to incubation, and subsequent dilution from different concentrations of a denaturing agent, that is, guanidine hydrochloride. The increase in the R_h of the protein samples is dependent not only on the denaturant concentration used but also on the buffer in which the incubation/dilution was performed. We also compare the aggregation after dilution from a denaturant with other high-throughput stability-indicating methods and find good agreement between the techniques. The proposed approach to probe the physical stability of monoclonal antibodies in different formulation conditions offers a unique combination of features - it is isothermal, probes both the resistance to denaturant-induced unfolding and the colloidal protein stability, it is entirely label-free, does not rely on complex data evaluation, and requires very short instrument measurement time on standard equipment.

Keywords: Protein aggregation; Protein formulation; Protein folding/refolding; Light scattering (dynamic); Stability; Fluorescence spectroscopy;

Abbreviations: C_m - concentration of denaturant required to unfold 50% of the protein; dG - the Gibbs free energy of unfolding (apparent values in this work); DLS - dynamic light scattering; GuHCl - guanidine hydrochloride; ICD - isothermal chemical denaturation; mAb - monoclonal antibody; T_m - protein melting temperature;

4.2 Introduction

One of the goals in the (pre-)formulation development of new monoclonal antibodies (mAbs) is to find conditions that provide high protein physical stability. Such studies can be performed with high-throughput techniques that can be classified as isothermal or non-isothermal. Two of the most widely used non-isothermal techniques are differential scanning calorimetry (DSC) and differential scanning fluorimetry (DSF)[40,63,105,140]. In general, non-isothermal techniques suffer from drawbacks related to the heating of the sample. For example, aggregation during temperature ramps often hinders the thermodynamic evaluation of DSC data and affects the accuracy of the determined protein melting temperatures from both DSC and DSF[4,149]. Furthermore, non-isothermal techniques suffer from the fact that the properties of many excipients (e.g., the pH of amine buffers like histidine) change during heating, which can affect the obtained stability rankings based on protein melting temperatures[54].

Isothermal chemical denaturation (ICD) is a valuable technique that avoids the above-mentioned drawbacks of DSC and DSF[4,54]. Historically, ICD was not the method of choice for protein formulation studies mostly due to the tedious sample preparation[162]. These limitations of ICD have recently been overcome by the use of equipment that can (semi-)automatically prepare and measure protein samples containing varying concentrations of a denaturing agent[4,54,162–164]. However, the accurate thermodynamic evaluation of ICD data assumes that the protein unfolding process is fully reversible, the system is in equilibrium, and the denaturation graph fits a known model (e.g., 2-state, 3-state unfolding, etc.)[52,165]. A recent article shows that neither reversibility nor equilibration times in an ICD experiment with mAbs are trivial[52]. In addition, multidomain proteins may also exhibit multiple transitions that can be close to each other or (partially) overlap, which can introduce a large error to the parameters derived from the fit.

Last but not least, high-throughput DSF and ICD methods are usually based on intrinsic protein fluorescence measurements (i.e. observations due to a change in the tryptophan exposure after protein unfolding)[4,105,116]. This creates complications when no tryptophan is present or when the tryptophan in a particular protein domain is already solvent exposed in the native protein conformation.

Considering the issues mentioned above, we saw a demand for novel approaches that can be used in a high-throughput manner to investigate the physical stability of new mAbs in different formulations. The hypothesis we present is that isothermal incubation and dilution of mAbs from guanidine hydrochloride (GuHCl) solutions with a certain concentration will lead to substantial protein aggregation. Furthermore, we propose that the amount and the size of the aggregates formed will depend on the formulation conditions and the physical stability of the mAbs (Fig. 24) and that this aggregation will be in good agreement with other methods used to study the protein physical stability. Previously, dilution from a denaturant was used to probe the molten globule states and the stability during refolding of other proteins (e.g., human growth hormone[4,15], lysozyme[166], recombinant human gamma interferon[167], and others[168–170]). However, previous work focuses mostly on proteins that are expressed as inclusion bodies in bacteria, and the aim of such experiments was usually to achieve higher monomer yields after expression, solubilisation, and subsequent refolding. To the best of our knowledge, we are the first to propose that the assessment of the aggregation after incubation and dilution from different concentrations of a denaturant can be used for high-throughput formulation studies of large proteins (i.e., mAbs that are typically not expressed as inclusion bodies).
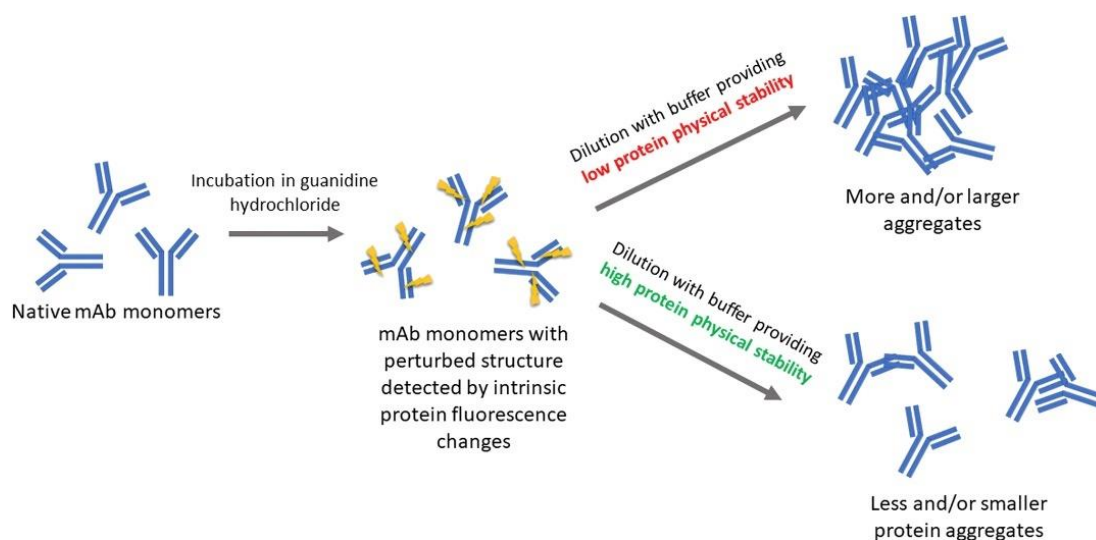
Figure 24. Schematic explanation of the working hypothesis - Impact of the physical stability of a mAb on the protein aggregation after incubation and subsequent dilution from a denaturant.

In this work, we use a dynamic light scattering (DLS) plate reader to assess the aggregation (i.e., the increase in the hydrodynamic radius) of 2 mAbs after dilution from different

concentrations of GuHCl in different buffers. We confirm our hypothesis that conditions that provide higher physical stability of the protein will require higher GuHCl concentrations to induce protein aggregation after dilution of the denaturant. We also show that conditions that provide higher protein colloidal stability will result in a smaller increase of the R_h after dilution from GuHCl. We compare the proposed approach with other established high-throughput methods (e.g. DSF, ICD) to find agreement between the predictions. The method we investigate provides a unique combination of features - it is an isothermal technique that simultaneously probes the resistance to GuHCl-induced unfolding and the colloidal protein stability (i.e. the level of aggregation after dilution from GuHCl). In addition, no complex data evaluation or a fitting to a certain protein unfolding model is required (in contrast to ICD). The approach is label-free and does not rely on intrinsic protein fluorescence measurements (contrary to DSF and ICD). Finally, the proposed approach offers a high potential for scale down and full automation with the existing infrastructure in many protein formulation laboratories.

4.3   Materials and methods

4.3.1   Monoclonal antibodies

Both mAbs (LMU-1 and PPI03) used in this work belong to the IgG1 subclass. Sodium dodecyl sulfate polyacrylamide gel electrophoresis of the protein bulk shows only bands for the mAb monomer and mAb fragments. Relative monomer area of both bulks is >99.5%, measured by size exclusion chromatography.

The mAb buffer was exchanged by dialysis at 20°C-25°C using Spectra/Por® 8000 molecular weight cut-off dialysis tubing (Spectrum Laboratories Inc., Rancho Dominguez, CA). The sample to buffer ratio was 1:200 and 2 buffer exchanges were performed 3 and 8 h after the beginning. After the last change, dialysis was continued for another 16 h. The final buffers of both proteins contained 10 mM citrate or 10 mM histidine with pH 5 or 5.75. In addition, all LMU-1 samples contained 0.05% w/v polysorbate 20, while all PPI03 samples were free of surfactants.

For the experiment where we compare the effect of additives, 2× stock solution of the respective additive (i.e., sucrose, trehalose, arginine hydrochloride or proline) in the respective buffer was mixed with the protein to obtain a final concentration of 200 mM sucrose,

200 mM trehalose, 200 mM arginine hydrochloride, or 200 mM proline. For the final protein concentrations in the different experiments see the Results and Discussion section.

The protein concentration was measured with a Nanodrop 2000 (Thermo Fisher Scientific, Wilmington, DE). Reagent chemicals from the highest grade available were purchased from Sigma Aldrich (Steinheim, Germany) or VWR International (Darmstadt, Germany). Highly purified water was used for the preparation of all buffers.

4.3.2 Sample preparation, incubation, and dilution from different concentration of guanidine hydrochloride

Samples containing protein (LMU-1 or PPI03) and 0, 1, 2, 3, or 4 M GuHCl in buffer were prepared by mixing 25 μL of protein solution in the respective buffer (or in the respective buffer with an additive, i.e., 200 mM sucrose, 200 mM trehalose, 200 mM arginine hydrochloride, or 200 mM proline) with 75 μL of GuHCl solution in the same buffer (or in the same buffer containing an additive - see above). After 24 h of incubation with the denaturant, the samples were diluted 10 times by rapid addition of the respective buffer (or the respective buffer containing an additive - see above) and incubated for another 24 h. For protein concentration in the final samples after the last dilution refer to the Results and Discussion section. The pH of the samples was controlled at each step using an appropriately calibrated InLab™ Nano pH Electrode with a SevenEasy pH meter (Mettler Toledo, Gießen, Germany). The pH reported is the pH of the samples after the final dilution from the denaturant (±0.1 pH units). Finally, the samples were centrifuged at 8200 × g for 10 min and measured with a DLS plate reader (see next sections). All experiments were performed in triplicates.

4.3.3 Isothermal chemical denaturation

Protein in formulation buffer and various amounts of buffer and 6 M GuHCl solution in the respective buffer were combined in a 384-nonbinding-well plate (Corning, Corning, NY) using the Viaflo Assist pipetting station equipped with a 16-channel 12.5 μL and a 125 μL pipette (Integra Biosciences, Konstanz, Germany) as already described[54]. The pH of the samples was controlled after preparation as described in the previous section. Next, the well plate was sealed. After 24 h of incubation at room temperature, the protein fluorescence intensity at 330 nm and 350 nm was measured after excitation at 280 nm with a FLUOstar Omega

microplate reader (BMG Labtech, Ortenberg, Germany). The intrinsic fluorescence intensity ratio F350/330 (the fluorescence intensity at 350 nm divided by the fluorescence intensity at 330 nm) was plotted against the denaturant concentration to obtain ICD graphs. All samples were prepared in triplicates and the best fit to a 3-state model of each replicate in the CDpal software was used to determine the apparent Gibbs free energy of unfolding (dG) and the denaturant concentration needed to unfold 50% of the protein (C_m). Other unfolding models available in the CDpal software (e.g., 2-state, 3-state with dimerisation of the intermediates, etc.) were also investigated but showed worse fit quality than the 3-state model after an f-test comparison. The 3-state model was also used by other groups to evaluate ICD data with mAbs[52,153]. Because all samples were evaluated with the 3-state model, two C_m values were determined—C_{m1} for the transition taking place at lower denaturant concentration and C_{m2} for the other transition.

4.3.4   Dynamic light scattering

Twenty-five microliter of each sample was pipetted in triplicates into a 384-well clear bottom plate (Corning), and the plate was centrifuged at 2000 rpm for 2 min using a Heraeus Megafuge 40 centrifuge equipped with an M-20 well plate rotor (Thermo Fisher Scientific). Next, each well was capped with approximately 5 µL of silicone oil and centrifuged again at 2000 rpm for 2 min. Ten acquisitions of 10 s at 25°C were taken with the DynaPro II DLS plate reader (Wyatt Technology Europe, Dernbach, Germany). The Dynamics V7.8 software was used for all the calculations. The autocorrelation function of each sample was calculated from the fluctuation of the light scattering intensity. Cumulant analysis was used to derive the apparent coefficient of self-diffusion (D) and the polydispersity index (PDI). The viscosity of each sample was measured with a falling ball viscometer, AMVn (Anton Paar GmbH, Ostfildern-Scharnhausen, Germany). The Stokes-Einstein equation was used to calculate the apparent hydrodynamic radius (R_h) at 25°C from the D and the sample viscosity. As an additional part of the data analysis, the sample size distribution was calculated from the regularisation method. Unless otherwise stated, the R_h values reported in this work are derived from the cumulant analysis.

To determine the interaction parameter k_D, different concentrations of LMU-1 (from 1 to 15 g/L) and PPI03 (from approximately 1 to 10 g/L) in each buffer were prepared and measured as described previously.

The interaction parameter was calculated using the expansion of the apparent diffusion coefficient:

$$D=D_0(1+k_Dc)$$

where D_0 denotes the diffusion coefficient of an isolated scattering solute molecule in a solvent and c is the protein concentration. The linear fits of the concentration dependence of D_0 from which k_D was determined can be found in the supplementary data to this chapter.

4.3.5 Differential scanning fluorimetry

All samples were diluted to a protein concentration of 1 g/L with the respective buffer and filled into 9 µL microcuvette arrays (Unchained Labs, Pleasanton, CA). The Optim® 1000 system (Unchained Labs) was used to apply a temperature ramp of 1°C/min starting from 25°C and ending at 100°C. Protein fluorescence spectra were collected during the ramp after excitation at 266 nm. The system software was used to calculate the intrinsic fluorescence intensity ratio from the fluorescence intensity at 350 nm and 330 nm (F350/330) against temperature. The protein melting temperatures (T_m) were determined from the maximum of the first derivatives of these graphs using the Optim® 1000 software (Avacta Analytical, Wetherby, UK). T_{m1} was assigned to the transition at lower temperature, and T_{m2} was assigned to the transition at a higher temperature.

4.3.6 Statistical data analysis and comparison

The mean values, standard deviations, 95% lower confidence interval (LowCI) and 95% upper confidence interval (UpCI) of the means were calculated with Origin 2018. A significant difference between 2 values was considered when the 95% CIs of 2 means were not overlapping. In the case of slightly overlapping confidence intervals, we could not prove a significant difference, although the lack of such cannot be confirmed due to the small samples size and the approach we used[171].

4.4 Results and discussion

4.4.1 Protein aggregation and R_h after dilution from different concentrations of guanidine hydrochloride

The R_h of LMU-1 and PPI03 after incubation with different concentration of GuHCl and subsequent dilution is dependent not only on the denaturant concentration but also on the formulation used (Figs. 25a and 25b). The increase in the R_h is due to the formation of more (and larger) soluble aggregates, which was confirmed with size exclusion chromatography coupled to multiangle light scattering detector (see the supplementary data to this chapter). The differences in the R_h are most pronounced after dilution from 3 M GuHCl for both proteins. A comparison between the different LMU-1 samples diluted from 3 M GuHCl shows that the lowest R_h is measured in 10 mM histidine pH 5.75 with a mean value of 19.43 nm and 95% LowCI and UpCI of 18.81 nm and 20.06 nm, respectively, followed by 10 mM citrate, pH 5.75 (mean = 24 nm with LowCI = 23.1 nm and UpCI = 24.89 nm), 10 mM histidine, pH 5 (mean = 29.6 nm with LowCI = 27.86 nm and UpCI = 31.34 nm), and 10 mM citrate, pH 5 (mean = 43.1 nm LowCI = 40.08 nm and UpCI = 46.11 nm) (Fig. 25a). Similar observations are made for PPI03 (Fig. 25b). In the case of PPI03, the following means and 95% CIs of the hydrodynamic radius after dilution from 3 M GuHCl were measured—in 10 mM histidine, pH 5.75 (mean = 5.37 nm; LowCI = 5.22 nm; UpCI = 5.51 nm), in 10 mM citrate, pH 5.75 (mean = 5.97 nm; LowCI = 5.82 nm; UpCI = 6.11 nm), in 10 mM histidine, pH 5 (mean = 6.87 nm; LowCI = 6.72 nm; UpCI = 7.01 nm), and in 10 mM citrate pH 5 (mean = 7.43 nm; LowCI = 7.29 nm; UpCI = 7.58 nm). The PDI of all samples is between 0.05 and 0.2 when the proteins are diluted from up to 1 M GuHCl, while the PDI of all samples diluted from 3 M or more GuHCl is between 0.2 and 0.4. An example of the autocorrelation functions with the corresponding cumulant fits and the size distribution from the regularisation analysis can be found in the supplementary data to this chapter. Important to mention, none of the samples formed a pellet of insoluble matter after dilution and centrifugation. In addition, the absorption of the protein in the supernatant was measured at 280 nm and no loss of soluble protein was observed (data not shown). Also, the R_h in the samples after 24 h of incubation in GuHCl before dilution is measured and can be found in the supplementary data. Furthermore, we studied

whether the R_h changes during longer incubation time and found no significant differences in the R_h of the samples for up to 1 week after dilution from GuHCl (data not shown).
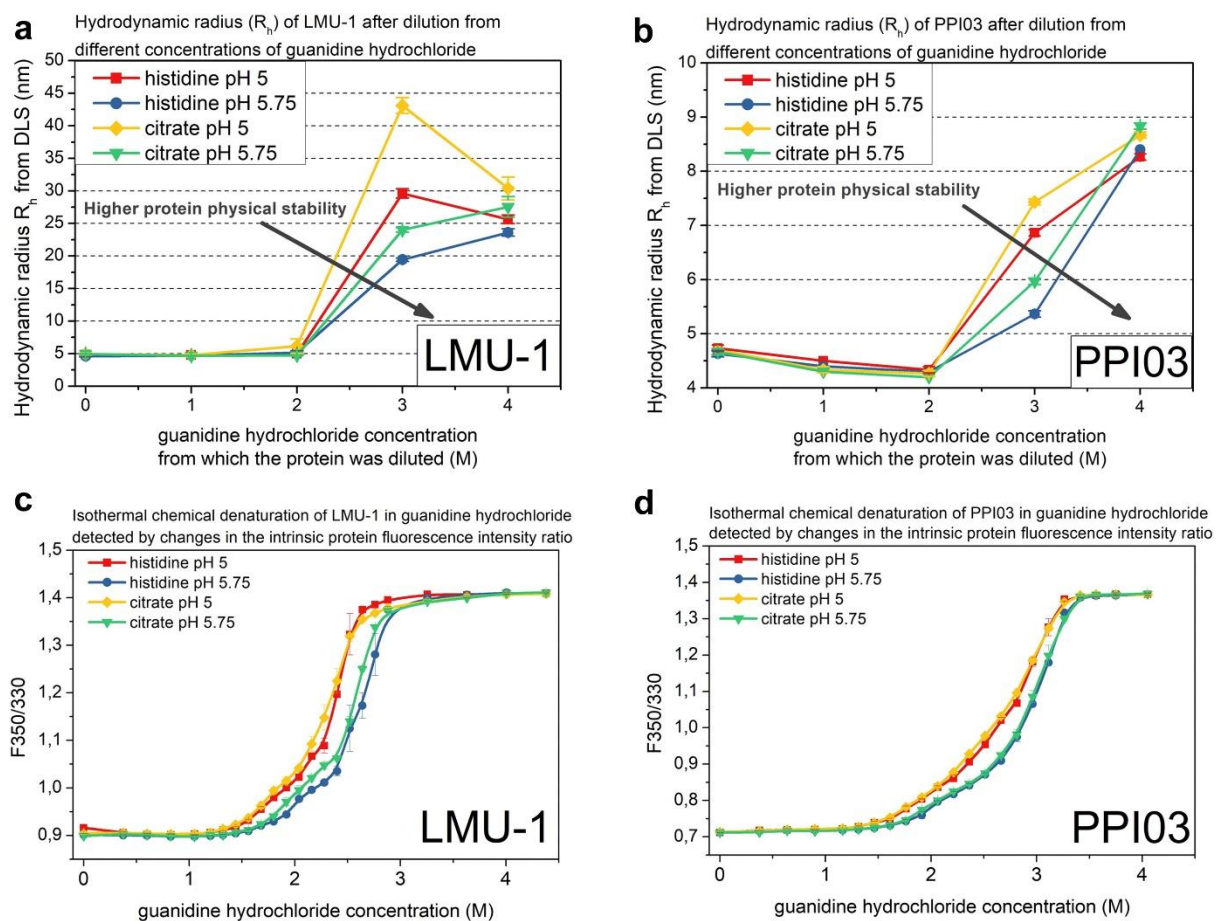
Figure 25. Hydrodynamic radius R_h from dynamic light scattering of LMU-1 (**a**) and PPI03 (**b**) after incubation and dilution from different concentrations of guanidine hydrochloride in 10 mM histidine pH 5 (red squares), 10 mM histidine pH 5.75 (blue circles), 10 mM citrate pH 5 (yellow diamonds), and 10 mM citrate pH 5.75 (green triangles). The protein concentration in the measured samples in (a) and (b) is 1 g/L and 0.2 g/L for LMU-1 and PPI03, respectively; isothermal unfolding of LMU-1 (**c**) and PPI03 (**d**) in presence of different concentrations of guanidine hydrochloride measured by the change in the intrinsic protein fluorescence intensity ratio (F350/330). The protein concentration in the measured samples in (c) and (d) is 1 g/L and 0.5 g/L for LMU-1 and PPI03, respectively.

4.4.2 Isothermal chemical denaturation

The ICD graphs obtained with the intrinsic protein fluorescence intensity ratio (F350/330) show that both mAbs exhibit complex unfolding behaviour, which fits well to a 3-state

transition model (see the supplementary data). Visual observation of the ICD graphs shows that higher concentration of GuHCl is needed to unfold both proteins at pH 5.75 compared to pH 5 (Fig. 25a and Fig. 25b), which indicates higher resistance to the GuHCl-induced unfolding of the mAbs at the higher pH. To further support this statement, in the case of LMU-1, the mean C_{m2} values are significantly higher at pH 5.75 compared to pH 5 with nonoverlapping CIs (Table 3). In the case of PPI03, the difference between the C_{m2} in 10 mM histidine pH 5 and 10 mM histidine pH 5.75 is also significant, although the same statement is difficult to make for the results in 10 mM citrate due to the slightly overlapping CIs (Table 3). Comparing the apparent dG values at different pH values reveals that in the case of LMU-1, there is a significant difference (nonoverlapping CIs) between the dG measured in 10 mM citrate pH 5 and in 10 mM citrate pH 5.75, which indicates higher conformational stability of LMU-1 at the higher pH. In the case of PPI03, although the mean values for the dG differ at pH 5 and pH 5.75, a significant difference cannot be proved due to the overlapping CIs (Table 3). Furthermore, the ICD graphs of the proteins obtained in histidine or citrate with the same pH almost completely overlap (Figs. 25c and 25d). Important to note, when comparing the stability of the 2 mAbs in 10 mM citrate or 10 mM histidine with the same pH, there is not a single case in which a significant difference between ICD data obtained at the same pH can be confirmed due to the overlapping CIs (Table 3).

4.4.3 Colloidal stability of the mAbs in different buffers

The colloidal stability of both mAbs in citrate and histidine buffers was assessed by means of the interaction parameter k_D. It has been shown that k_D describes the interparticle interaction in protein solutions[172]. Highly positive k_D is attributed to repulsive interactions, whereas highly negative is related to attractive interactions[146]. The k_D of both LMU-1 and PPI03 is positive in histidine buffer and negative in citrate buffer (Table 3). This indicates that both proteins have higher colloidal stability in 10 mM histidine buffer compared with 10 mM citrate in the studied pH range. However, the k_D is not a parameter that can assess the conformational stability of the protein, and it is known that both the conformational and colloidal protein stabilities are important for the aggregate formation in solution[8].

Table 3. Physical stability parameters of LMU-1 (**A**) and PPI03 (**B**) in different buffers and pH. The apparent Gibbs free energy of unfolding (dG) and the melting denaturant concentrations for the first and second unfolding (C_{m1} and C_{m2}) are obtained with isothermal chemical denaturation as described in Materials and methods. The melting temperatures of the protein (T_{m1} and T_{m2}) are obtained from the maximum of the first derivative of the protein unfolding measured with differential scanning fluorimetry as described in Materials and methods. All values (except the k_D) are means of triplicates, and the 95 % lower and 95 % upper confidence intervals are reported in the brackets (Lower CI 95 % - Upper CI 95 %) next to each mean.

Table 3A LMU-1	dG, kJ/mol	C_{m1}, M	C_{m2}, M	k_D, mL/g	T_{m1}, °C	T_{m2}, °C
histidine pH 5	94.91 (90.06 - 99.77)	1.76 (1.61 - 1.92)	2.44 (2.40 - 2.49)	37.9	62.20 (61.56 - 62.83)	77.5 (76.90 - 78.20)
citrate pH 5	76.84 (60.35 - 93.34)	1.67 (1.21 - 2.13)	2.38 (2.33 - 2.43)	-1.18	63.52 (62.17 - 64.88)	78.5 (77.41 - 79.58)
histidine pH 5.75	106.10 (98.70 - 113.49)	1.92 (1.74 - 2.10)	2.66 (2.61 - 2.72)	40.2	66.82 (65.09 - 68.55)	79.7 (79.23 - 80.26)
citrate pH 5.75	111.84 (100.98 - 122.7)	1.94 (1.80 - 2.08)	2.60 (2.56 - 2.63)	-8.46	68.29 (66.41 - 70.18)	79.3 (77.45 - 81.15)
Table 3B PPI03	dG, kJ/mol	C_{m1}, M	C_{m2}, M	k_D, mL/g	T_{m1}, °C	T_{m2}, °C
histidine pH 5	75.06 (63.83 - 86.29)	1.86 (1.62 - 2.09)	3.00 (2.99 - 3.01)	42	62.87 (61.48 - 64.25)	76.4 (74.67 - 78.13)
citrate pH 5	74.84 (50.41 - 99.27)	1.99 (1.79 - 2.21)	3.01 (2.81 - 3.20)	-0.58	63.88 (63.31 - 64.44)	77.99 (75.84 - 78.29)
histidine pH 5.75	87.56 (74.70 - 100.42)	2.28 (1.78 - 2.77)	3.09 (3.04 - 3.14)	46	68.26 (68.13 - 68.39)	77.01 (77.68 - 78.30)
citrate pH 5.75	80.03 (68.61 - 91.45)	2.16 (1.66 - 2.67)	3.07 (2.93 - 3.21)	-4.8	69.17 (67.71 - 70.63)	78.66 (77.90 - 79.42)

4.4.4 Thermal stability of the mAbs in different buffers

Both LMU-1 and PPI03 have higher melting temperatures (T_{m1}) at pH 5.75 compared with pH 5 (Table 3). This indicates higher physical stability of both mAbs at pH 5.75 and corresponds well to the higher concentration GuHCl needed to unfold both proteins at higher pH. The mean values of the melting temperatures of both proteins in histidine almost always appear lower compared with citrate counterparts most probably due to the buffer pH shift of histidine during heating[54]. However, a significant difference between the melting temperatures of the mAbs in either 10 mM citrate or 10 mM histidine with the same pH cannot be proved due to the small sample size and the overlapping CIs (Table 3). The thermal denaturation graphs of each mAb sample can be found in the supplementary data to this chapter.

4.4.5 The relation between the R_h after dilution from GuHCl and other parameters

The increase of R_h after dilution from a certain concentration of GuHCl (in our case 3 M) will depend on the degree of protein unfolding at these conditions. In the case of LMU-1 and PPI03 samples with pH 5, the ICD curves are shifted to lower denaturant concentrations compared to samples with pH 5.75, which indicates a lower resistance to the GuHCl-induced unfolding of these proteins at the lower pH (Figs. 25c and 25d). Respectively, a higher R_h (more and larger aggregates formed) is measured after dilution from 3 M GuHCl in buffers with pH 5 compared with dilution in buffers with pH 5.75 (Figs. 25a and 25b).

When the degree of protein unfolding (or structural perturbation) at a given denaturant concentration is the same (e.g., buffers with the same pH or higher denaturant concentrations where the protein is fully unfolded regardless of the pH, i.e., at 4 M GuHCl), the protein aggregation and the measured R_h after dilution will depend mostly on the colloidal stability and the aggregation propensity of the (partially) unfolded protein after dilution in these conditions. For example, the ICD curves of LMU-1 in citrate or histidine buffer with the same pH almost completely overlap (Figs. 25c and 25d). However, the R_h of LMU-1 after dilution from 3 M GuHCl is always lower in histidine buffer compared with citrate counterparts with the same pH (Fig. 25a). Similar observations are also made with the other mAb - PPI03 (Fig. 25b). In addition, at 4 M GuHCl, there is the same degree of unfolding (according to the intrinsic protein fluorescence ratio - Figs. 25c and 25d) for both proteins regardless of the formulation pH and buffer. We assume that in this case, the aggregation after dilution will be driven mostly by differences in the colloidal protein stability and we see that the R_h after dilution of the proteins from 4 M GuHCl is always lower in histidine compared with citrate, regardless of the pH. This behaviour is in good agreement with the high k_D values of both proteins in histidine, which indicates a higher protein colloidal stability in this buffer in comparison with citrate.

4.4.6 Effect of different additives on the change in the R_h after dilution from GuHCl

We further tested if the herein proposed approach could be used to study the effect of different additives (i.e., 200 mM sucrose, 200 mM trehalose, 200 mM arginine hydrochloride, or 200 mM proline) on the increase in R_h (i.e., aggregation) of the mAbs after dilution from GuHCl. To study this, we focused on dilution from 3 M GuHCl because this was the

concentration of denaturant where we observed the largest differences in the earlier experiments. Next, we performed the dilution in a buffer, that is, 10 mM histidine pH 5, in which the physical stability of both mAbs is neither the worst nor the best according to the different techniques we used in this work. We reported the effect of the additives as the difference in the R_h after dilution with the additive compared with dilution without an additive (Fig. 26). We observed that for both LMU-1 and PPI03, all additives tested were significantly better compared with the histidine buffer alone (Fig. 26). However, in the case of LMU-1, 200 mM sucrose and 200 mM arginine chloride caused the largest decrease in the R_h, that is, the highest stabilizing effect (Fig. 26 - left), while in the case of PPI03, 200 mM sucrose and 200 mM trehalose were the most stabilising excipients according to the proposed approach (Fig. 26 - right).
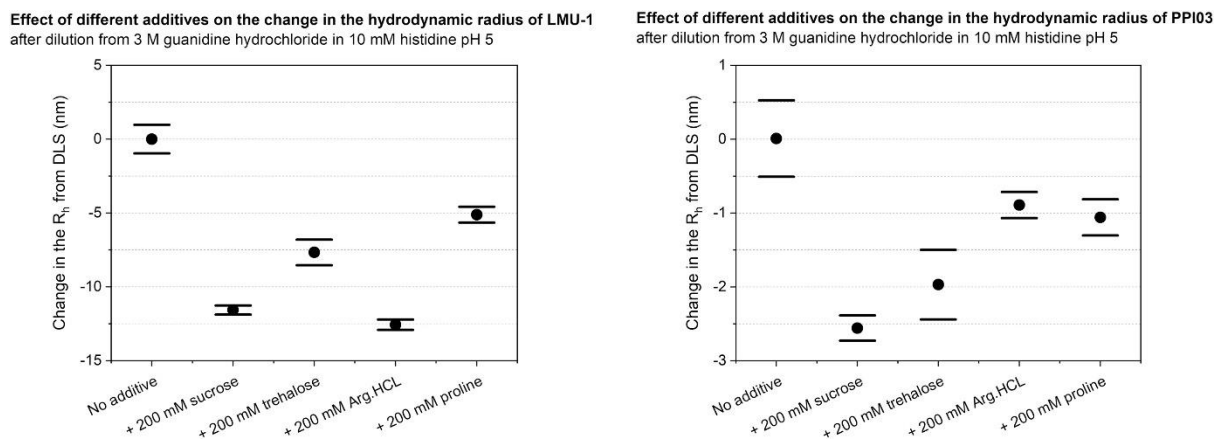
Figure 26. Effect of various additives on the change in the hydrodynamic radius R_h from DLS of LMU-1 (**left**) and PPI03 (**right**) after dilution from 3 M guanidine hydrochloride in 10 mM histidine pH 5. All measurements were corrected for viscosity as described in Materials and Methods. For clarity reasons, the values with additives are represented as a difference from the value without an additive. Negative values indicate that the R_h is lower after dilution with the additive compared with dilution without an additive. The circles represent the mean value of the measurements, and the bars represent the 95% UpCI and LowCI. The final protein concentration after dilution is 1 g/L for both LMU-1 and PPI03.

4.5   Conclusion and outlook

In this work, we demonstrated with 2 mAbs that the DLS assessment of the aggregation (by means of the R_h) after dilution from different concentrations of GuHCl is a promising approach to probe the protein physical stability in different formulations. A formulator would then aim to (1) find buffers and pH that shift the increase in R_h after dilution to higher GuHCl concentrations (i.e., find conditions that provide higher resistance to GuHCl unfolding) and (2) find conditions that minimize R_h after dilution (i.e., find conditions that provide higher colloidal stability and less aggregation during dilution from a denaturant). The proposed method could be used alone or as a complementary technique. If used alone, we suggest that at least several GuHCl concentrations (in a step of 0.5 or 1 M) are tested to find conditions where the increase in the R_h is largest after dilution. Next, this denaturant concentration could be used to test the influence of different buffers and additives on the increase in the R_h. In the case of the antibodies that we tested, such denaturant concentration is usually around 3 M GuHCl.

Alternatively, the method we show could be used as a complementary technique to ICD (e.g., to distinguish if there is a difference in the protein physical stability in conditions that exhibit overlapping curves in an ICD experiment). In such case, we suggest that the concentration of GuHCl that can be used is around the denaturant concentration where the protein is partially unfolded according to the ICD experiment.

The approach we propose offers a unique combination of features: (1) the method is isothermal (problems arising from sample heating are avoided); (2) it can distinguish between overlapping curves in an ICD experiment due to the different colloidal stability and different levels of aggregation after dilution from such samples; (3) the method is label-free and independent of the intrinsic protein fluorescence; (4) very short instrument measurement time for 1 sample is required; (5) there is a high potential for scale-down and automation with the help of already available equipment in many protein formulation laboratories.

4.6 Supplementary data
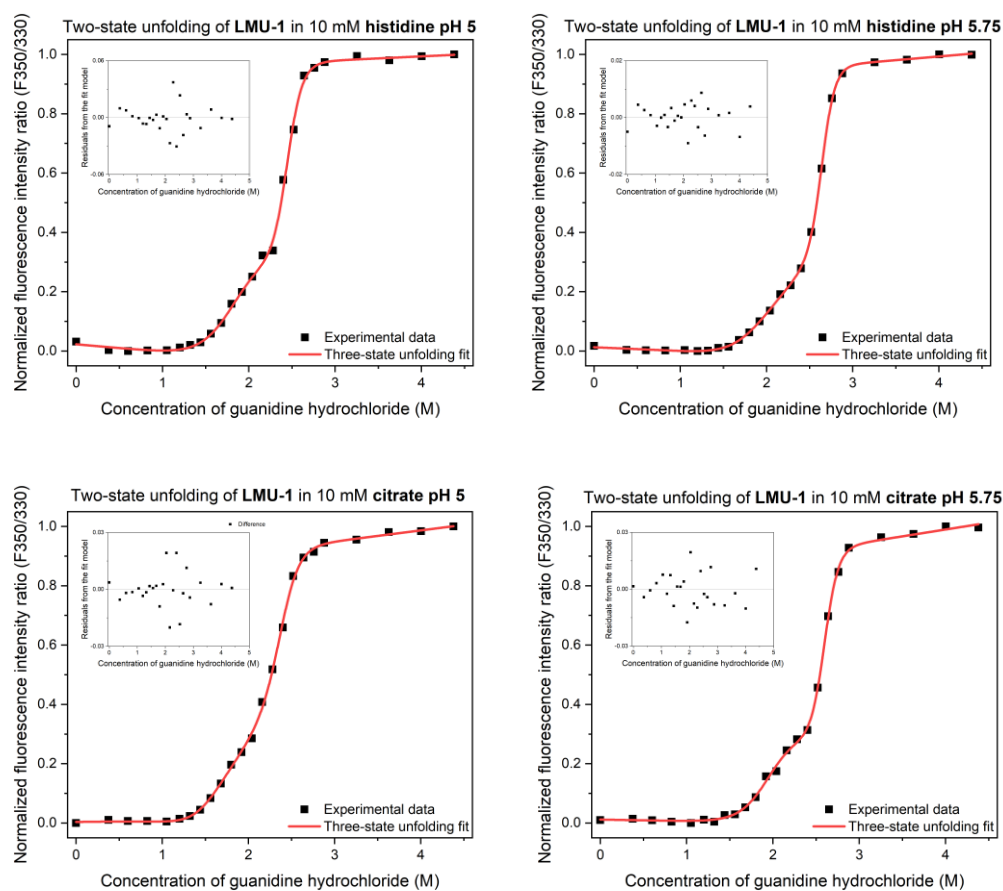
Figure S7. Unfolding of LMU-1 by guanidine hydrochloride in different buffers and pH values. The black points represent the experimentally measured values. The red line is the fit to a three-state unfolding model. The inset shows the corresponding residuals from the fit.
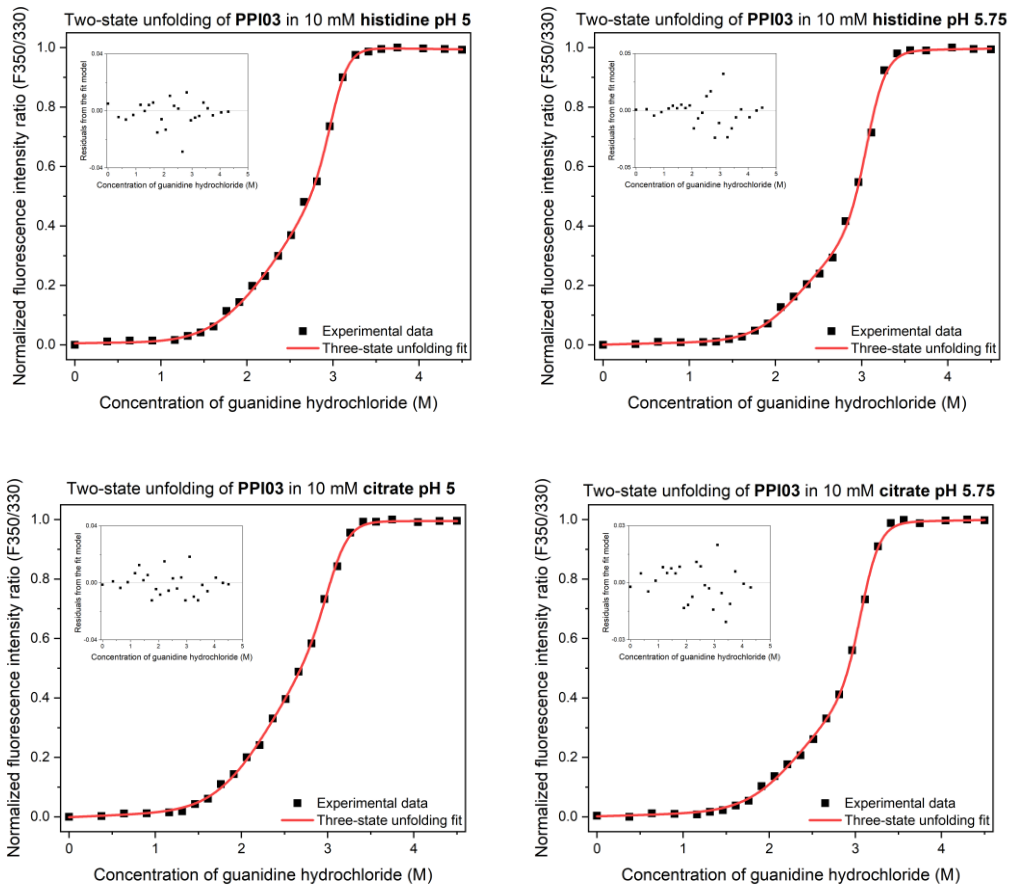
Figure S8. Unfolding of PPI03 by guanidine hydrochloride in different buffers and pH values. The black points represent the experimentally measured values. The red line is the fit to a three-state unfolding model. The inset shows the corresponding residuals from the fit.
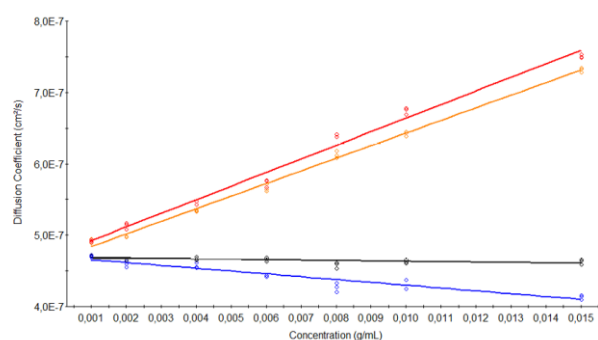
Figure S9. Concentration dependence of the diffusion coefficient of LMU-1 in different buffers and linear fits from which the interaction parameter k_D was derived. In the order top-down the measurements in 10 mM histidine pH 5.75, 10 mM histidine pH 5, 10 mM citrate pH 5, and 10 mM citrate pH 5.75.
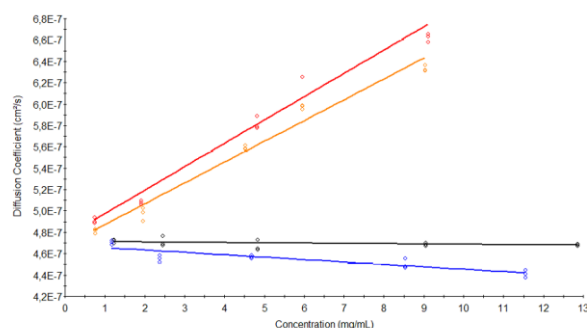
Figure S10. Concentration dependence of the diffusion coefficient of PPI03 in different buffers and linear fits from which the interaction parameter k_D was derived. In the order top-down the measurements in 10 mM histidine pH 5.75, 10 mM histidine pH 5, 10 mM citrate pH 5, and 10 mM citrate pH 5.75.
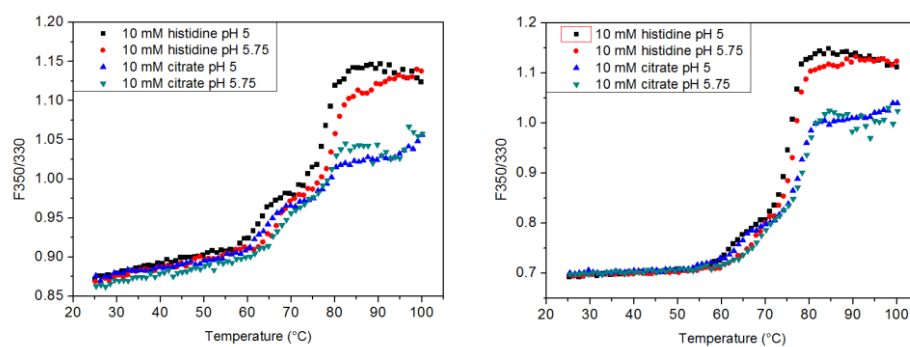
Figure S11. Thermal unfolding curves obtained from the change in the intrinsic protein fluorescence (F350/330) ratio of LMU-1 (**left**) and PPI03 (**right**) during heating in different buffers – 10 mM histidine pH 5 (black squares), 10 mM histidine pH 5.75 (red circles), 10 mM citrate pH 5 (blue triangles up), 10 mM citrate pH 5.75 (green triangles down).
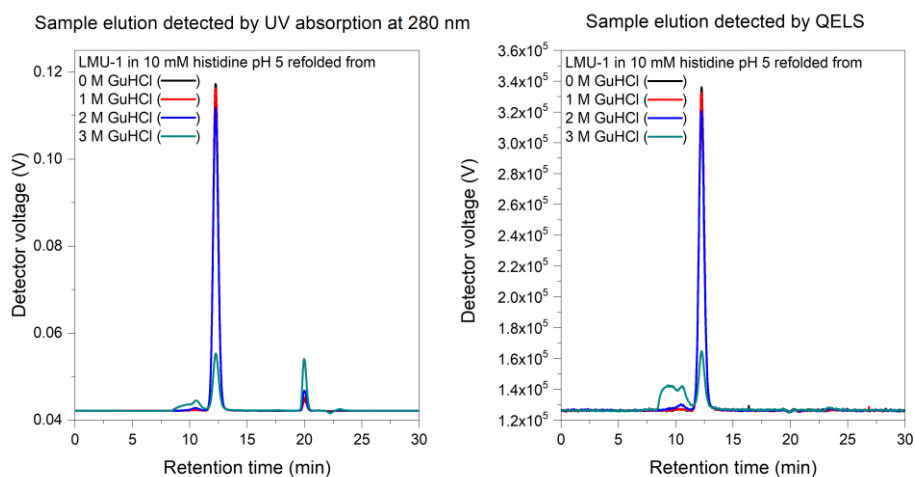
Figure S12. Chromatograms of LMU-1 in 10 mM histidine pH 5 after dilution from 0 M (black), 1 M (red), 2 M (blue) and 3 M (green) guanidine hydrochloride – UV detection at 280 nm (left) and QELS signal (right). The aggregate peak and the light scattering from the aggregate peak increases when LMU-1 is diluted from higher guanidine hydrochloride concentration, which corresponds well to the increase in the Rh measured by DLS.
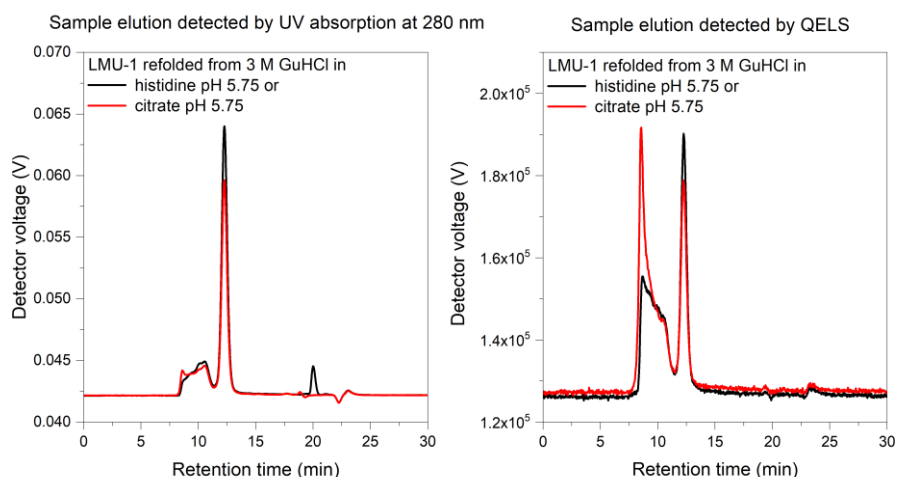
Figure S13. Chromatograms of LMU-1 in 10 mM histidine pH 5.75 (black) or 10 mM citrate pH 5.75 (red) after dilution from 3 M guanidine hydrochloride - UV detection at 280 nm (left) and QELS signal (right). The relative area of the aggregate peak after LMU-1 diluted from either citrate or histidine is similar, but the light scattering from the aggregate peak is higher when LMU-1 is diluted in citrate in comparison to histidine buffer, which indicates that the aggregates formed after dilution in citrate are larger. This corresponds well with the lower R_h measured by DLS after protein dilution in histidine compared to the Rh after dilution in citrate.

Description of the SEC–MALS-DLS method used in this chapter.:

The system consisted of Agilent 1260 infinity II pump (Agilent G7111B, Santa Clara, CA, USA) with an online degasser (Agilent G7111B), and a temperature controlled autosampler (Agilent G7129A) at 4°C. The separation was performed with a SUPERDEX 200 INCREASE 10/30 GL column. A TREOS II MALS detector (Wyatt Technology, Santa Barbara, USA) was connected to the system. The MALS detector measured the intensity of the scattered light at 4 scattering angles, 3 angles were used for the static light scattering while the fourth one was used to measure the dynamic light scattering. In addition, a variable wavelength detector (Agilent G7114A) operated at 280 nm and a differential refractive index detector (Optilab T-rEX,Wyatt Technology Corp.) were connected to the system. Data collection and processing were performed using the ASTRA software, Version 7.1 (Wyatt Technology, Santa Barbara, USA). The aqueous mobile phase consisted of PBS buffer in HPLC-grade water with 200 ppm of sodium azide (Sigma–Aldrich, St. Louis, USA). The reagent was purum grade and the mobile phase was filtered through Durapore VVPP 0.1 m membrane filters (Millipore Corporation, Billerica, MA, USA).
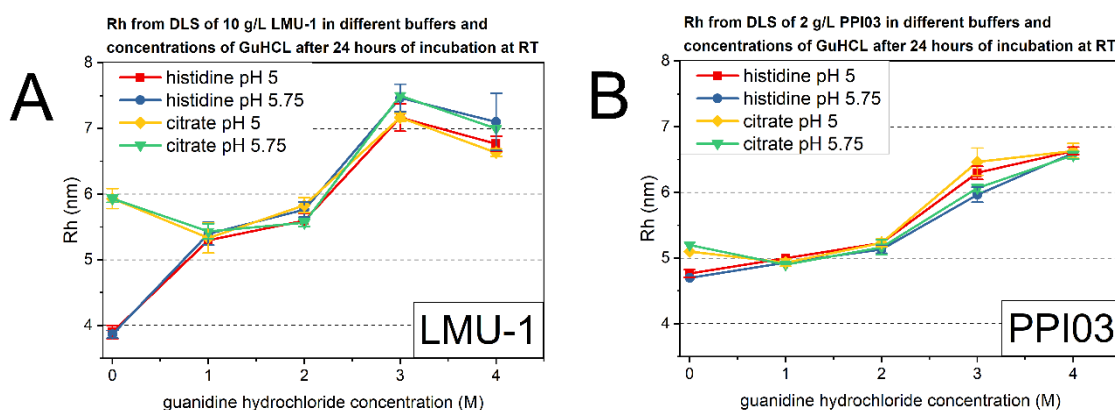
Figure S14. Hydrodynamic radii of LMU-1 (**A**) and PPI03 (**B**) measured with DLS after 24 hours of incubation in different concentrations of GuHCL and different buffers – 10 mM histidine pH 5 (red), 10 mM histidine pH 5.75 (blue), 10 mM citrate pH 5 (yellow) and 10 mM citrate pH 5.75 (green). The protein concentration is 10 g/L in all LMU-1 samples and 2 g/L in all PPI03 samples. The viscosity of the respective GuHCL concentration was measured as described in Materials and methods and used in the calculations of the R_h. The large differences between the Rh of the proteins in the absence of GuHCL are due to effects from the k_D (see Table 3).
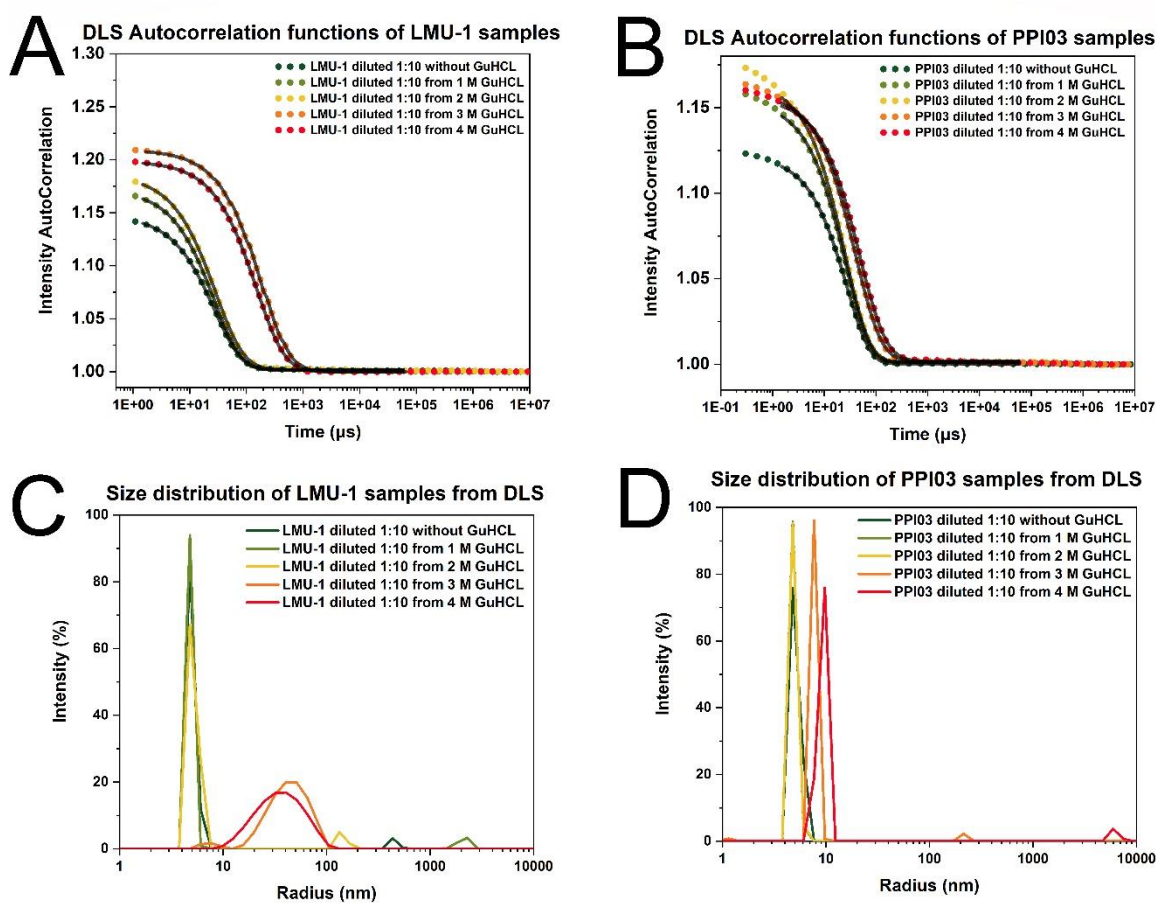
Figure S15. Example of autocorrelation functions and the corresponding cumulant fit (black line) from DLS measurements of LMU-1 (**A**) and PPI03 (**B**) samples after dilution from different GuHCL concentrations. Size distributions from the regularisation analysis of the LMU-1 (**C**) and PPI03 (**D**) samples after dilution from different GuHCL concentrations. All experiments for this figure were performed in 10 mM histidine pH 5. The concentration of LMU-1 and PPI03 are 1 g/L and 0.2 g/L respectively.

Chapter 5 **A study on some variables that affect the isothermal denaturant-induced unfolding and aggregation of a monoclonal antibody in different formulations**

Parts of this chapter are used for the preparation of a manuscript that will be submitted for peer-review and publication.

5.1 Abstract

In this chapter, I investigate several variables in isothermal chemical denaturation (ICD) experiments that affect the unfolding and aggregation of a monoclonal antibody in different formulations. First, I explore if different denaturants can be used to obtain isothermal chemical denaturation curves of an antibody in different formulations. I find that guanidine hydrochloride and urea are most suitable for such studies. The use of other denaturants, in this case, is obstructed due to various reasons like protein precipitation or low denaturant solubility. Second, I study the effect of incubation time on the denaturant-induced unfolding of the antibody in two formulations with different pH. I observe that the isothermal chemical denaturation curves continuously shift during sample incubation. Third, I investigate more in detail how guanidine hydrochloride and urea unfold the antibody in formulations with different pH and briefly comment on the differences between these two denaturants. Fourth, I look for the reasons behind the shifting protein unfolding curves during incubation and use dynamic light scattering and size exclusion chromatography to find that the partially unfolded antibody aggregates in the presence of the denaturants. The aggregation of the partially unfolded antibody is more pronounced in a formulation with pH 6.5 compared to a formulation with pH 5. Finally, I hypothesise that the formulation conditions will affect in the same way (1) the aggregation of the partially unfolded antibody in the presence of a denaturant and (2) the aggregation of the fully unfolded antibody during refolding from a denaturant. In this context, I explore the application of a microdialysis-based unfolding/refolding assay to compare the effect of formulation conditions on the aggregation of an antibody.

5.2   Introduction

Isothermal chemical denaturation (ICD) is a technique that employs denaturants to study protein conformational stability[3,173]. In an ICD experiment, increasing denaturant concentrations are added to a solution to cause protein unfolding at a constant temperature. After some incubation time, the degree of unfolding is assessed by measuring a physical observable like protein fluorescence. The data is plotted to obtain isothermal chemical denaturation curves which show at which denaturant concentrations the protein is (partially) unfolded. Provided that the samples reach an equilibrium and the denaturation is reversible, an ICD experiment can give the Gibbs free energy (dG) of protein unfolding which is a direct measure for conformational protein stability[3,51,174]. Most published work using ICD to assess conformational stability is on small single-domain proteins. However, there is an increasing interest in performing ICD experiments on larger multi-domain proteins like antibodies because ICD recently received more attention as a technique for formulation studies of therapeutic proteins[4,54,165]. When using ICD for formulation studies, one must consider different questions regarding the experimental variables – Which denaturant should be used? How long to incubate the samples with the denaturant? Does the denaturant type affect the information obtained for different protein formulations? Are the denaturant-induced partially unfolded protein species aggregating and, if yes, does this aggregation depend on the formulation conditions?

Regarding the *denaturant selection*, most ICD studies on large therapeutic proteins like monoclonal antibodies are performed with guanidine hydrochloride or urea. Both have drawbacks – for example, guanidine hydrochloride immensely increases the ionic strength of the solution, while urea is considered a weaker denaturant than GuHCl and can sometimes cause only partial unfolding[52,165]. Therefore, investigating the application of alternative denaturants is important to provide more options to the formulation scientists. Particularly interesting are the alkylureas or other guanidine salts which have been successfully used for ICD experiments with small model proteins[175–179].

Besides the denaturant choice, the *incubation time* of the samples is also a variable that is not trivial to optimise[52]. Published work with monoclonal antibodies states incubation times of 15

84

minutes[155], 1-3 hours[52,154], 8 hours[52], 18-30 hours[4,154] or even up to several weeks[153]. Therefore, there is a need for a better understanding of how the incubation time affects the protein unfolding in different formulation conditions.

A further important consideration for ICD experiments is *whether the partially unfolded proteins aggregate* in the presence of the denaturant. In this context, ICD was recently used to study non-reversibility effects due to the aggregation of the native or unfolded protein[154]. Such experiments look at the protein concentration dependence of dG rather than measuring the protein aggregation directly. However, suitable analytical techniques can be used to measure this aggregation as earlier reported for small model proteins and recently for an antibody[180,181]. For the purpose of protein formulation studies, the effect of the formulation on the aggregation of the partially unfolded proteins is particularly interesting.

5.3   Materials and methods

5.3.1   Monoclonal antibodies and chemicals

The monoclonal antibody (LMU-1) used in this work is a human IgG1. The protein bulk contains >99.5% monomer, and the purity of the substance is studied as earlier described[55]. The protein buffer was exchanged to 50 mM histidine/histidine hydrochloride with pH 5 and pH 6.5 by extensive dialysis employing materials and steps described in our previous work[182]. The concentration of the protein was determined at 280 nm with a Nanodrop 2000 UV spectrophotometer (Thermo Fisher Scientific, Wilmington, DE) using the protein extinction coefficient. Reagent chemicals were purchased from Sigma Aldrich (Steinheim, Germany), VWR International (Darmstadt, Germany) or Fisher Scientific (Schwerte, Germany). Highly purified water was used for the preparation of all solutions. The denaturant concentration was confirmed by measuring the solution refractive index and calculating the concentration with the denaturant calculator from the Sosnick group (http://sosnick.uchicago.edu/gdmcl.html).

5.3.2   Isothermal chemical denaturation

The experiment was performed as described in our earlier work[55]. Briefly, the protein stock solution in the formulation buffer was combined with various amounts of formulation buffer and denaturant stock solution in formulation buffer. The samples were prepared in 384-nonbinding well plates (Corning, Corning, NY) with a Viaflo Assist pipetting platform (Integra

Biosciences, Konstanz, Germany) equipped with suitable multichannel pipettes. After mixing, the well plate was sealed and incubated at room temperature for the desired time. The degree of protein unfolding was assessed by measuring the intrinsic protein fluorescence intensity at 330 nm and 350 nm after excitation at 280 nm with a FLUOstar Omega microplate reader (BMG Labtech, Ortenberg, Germany). The intrinsic fluorescence intensity ratio FI350/FI330 (fluorescence intensity at 350 nm)/(fluorescence intensity at 330 nm) was plotted against the denaturant concentration to obtain protein isothermal unfolding curves. The denaturant concentration needed to unfold 50% of the protein was calculated for the first (C_{m1}) and second (C_{m2}) transition from the best fit to a 3-state unfolding model in the CDpal software[50,55].

5.3.3 Dynamic light scattering

The samples are centrifuged for 10 minutes at 8200g. Next, ten microliters of each solution were pipetted in triplicates into a clear bottom 1534-well plate (Aurora). The plate was centrifuged for 2 minutes using a Heraeus Megafuge 40 centrifuge equipped with an M-20 well plate rotor (Thermo Fisher Scientific). The plate was then sealed with a transparent foil and centrifuged again for 2 minutes. Subsequently, the samples were measured with a DynaPro III DLS plate reader (Wyatt Technology Europe, Dernbach, Germany) using 5 acquisitions of 5 seconds at 25 ºC. The collected data was evaluated with the Dynamics V7.8 software. The fluctuations of the scattered light were used to obtain autocorrelation functions. Cumulant analysis was used to derive mutual diffusion coefficient (D) and the polydispersity index (PDI). The Stokes-Einstein equation was used to calculate the apparent hydrodynamic radius (R_h) at 25°C from the D and the sample viscosity.

5.3.4 Size exclusion chromatography with multi-angle light scattering

The system used includes an Agilent 1100 Series HPLC (Santa Clara, CA, USA), an Agilent 1100 multiple wavelength detector (Santa Clara, CA, USA), Agilent 1100 refractive index detector and a DAWN HELEOS multi-angle light scattering (MALS) detector (Wyatt Technology, Santa Barbara, USA). The samples were injected on a TSKgel G3000SWxl, 7.8x300 mm, 5 μm column (Tosoh Bioscience, Tokyo, Japan) and protein elution was detected with the absorption at 280 nm. The running buffer for samples without denaturant consisted of 100 mM potassium phosphate, 200 mM sodium chloride and 0,05 % w/v sodium azide. The

buffer pH was adjusted to 7.0 with 2 M sodium hydroxide. The running buffer for samples with denaturant consisted of 50 mM histidine/histidine hydrochloride with pH 5 or pH 6.5 and the respective concentration of guanidine hydrochloride. Data collection and processing were performed using the ASTRA software v7.1 (Wyatt Technology, Santa Barbara, USA).

5.3.5 Microdialysis-based unfolding/refolding experiments

100 µL of LMU-1 solution with a concentration of 1, 5, 10, 25 or 50 g/L in 50 mM histidine buffer with pH 5 or 6.5 was filled in Pierce™ microdialysis devices (3.5 kDa MWCO). The samples were dialysed in a deep well-plate against 1.5 mL of 8 M guanidine hydrochloride or 10 M urea solution in the respective formulation buffer. The denaturant solutions were changed after 4 and 8 hours to ensure a constant concentration gradient across the membrane. After the last change, the dialysis was continued in total for 24 hours. Subsequently, the mAb samples dialysed against denaturant were dialysed against 1.5 mL of the respective denaturant-free formulation buffer. The buffer was changed after 4 and 8 hours; the dialysis continued in total for 24 hours. During the entire dialysis procedure, the deep well plate was agitated at 700 rpm with a Thermomixer Comfort (Eppendorf AG, Hamburg, Germany). Subsequently, the samples were collected from the dialysis devices, and the weight of each sample was added to 1.0 g using the respective denaturant-free buffer. Finally, the samples were centrifuged at 10 000 x g for 10 minutes to remove insoluble protein aggregates. Further measurements were performed on the supernatant.

5.4   Results and discussion

5.4.1   Effect of denaturant type on the isothermal antibody unfolding

I investigated if different denaturants can be used to obtain isothermal unfolding curves of a model antibody in different formulations. A comparison between isothermal unfolding curves of LMU-1 with different denaturants is presented in Fig. 27. GuSCN causes protein unfolding at lowest denaturant concentrations but also causes protein precipitation which results in a loop in the pre-unfolding baseline. This precipitation was more pronounced in formulations with lower pH and at GuSCN concentrations that cause partial protein unfolding (Master thesis, Uroš Markoja). This phenomenon could arise from the binding of the weakly hydrated guanidine and thiocyanate ions to the protein[183]. However, the exact mechanism by which

GuSCN reduces the solubility of the partially unfolded antibody will be topic of separate research. GuHCl unfolds the protein at higher concentrations than GuSCN, and good pre- and post-transition baselines are obtained. Dimethylurea causes only partial protein unfolding. Urea causes full protein unfolding, but denaturant concentrations up to 9 M are required to obtain a good post-transition baseline. I also tested several urea derivatives, i.e. methylurea, ethylurea, dimethylurea, that do not cause full unfolding of the protein in the concentration range where the denaturant was soluble. Other groups also observed uncomplete protein unfolding of a model protein like ribonuclease A in alkylureas[184]. Another urea derivative, i.e. tetramethylurea, precipitated the model antibody. Based on this data, guanidine hydrochloride and urea seem to be the most suitable denaturants for ICD experiments with LMU-1.
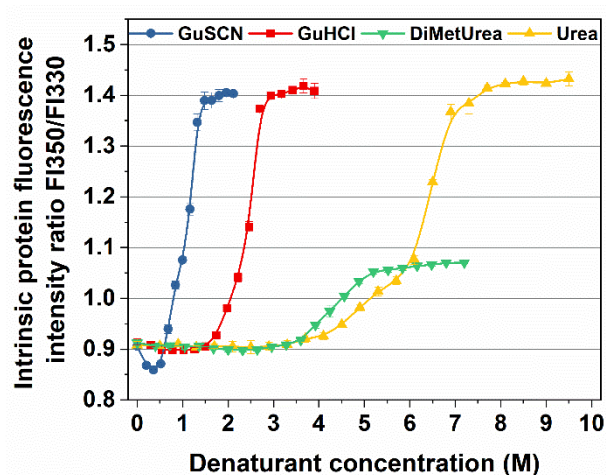
Figure 27. Effect of denaturant type on the isothermal unfolding of LMU-1. 50 mM histidine with pH 5 is used as a sample buffer. The protein concentration is 1 g/L. The samples were incubated for 24 hours at room temperature before measurement. The symbols are mean of triplicates; the error bar is the standard deviation.

5.4.2 Effect of incubation time on the denaturant-induced antibody unfolding

After identifying guanidine hydrochloride and urea as suitable for further experiments, I studied the effect of incubation time with these two denaturants on the isothermal unfolding of the antibody in two formulations with different pH - pH 5 and pH 6.5. The isothermal chemical denaturation curves in all tested conditions shift quickly in the first hours of incubation (Fig 28). I also used circular dichroism on selected samples to confirm that the observations from fluorescence measurements arise from structural changes (see

supplementary data to this chapter). After 24 hours of incubation, the curve shift is very slow but continues for weeks and depends on the formulation buffer and pH (data not shown). This shift was already observed for antibodies[153] and indicates that the unfolding does not reach equilibrium. The shifts mentioned above are a complication in cases when an isothermal chemical denaturation experiment aims to accurately determine correct thermodynamic parameters like the true Gibbs free energy of unfolding. In the best case, the effect of incubation time on the unfolding of the protein should be assessed on a case-by-case basis.
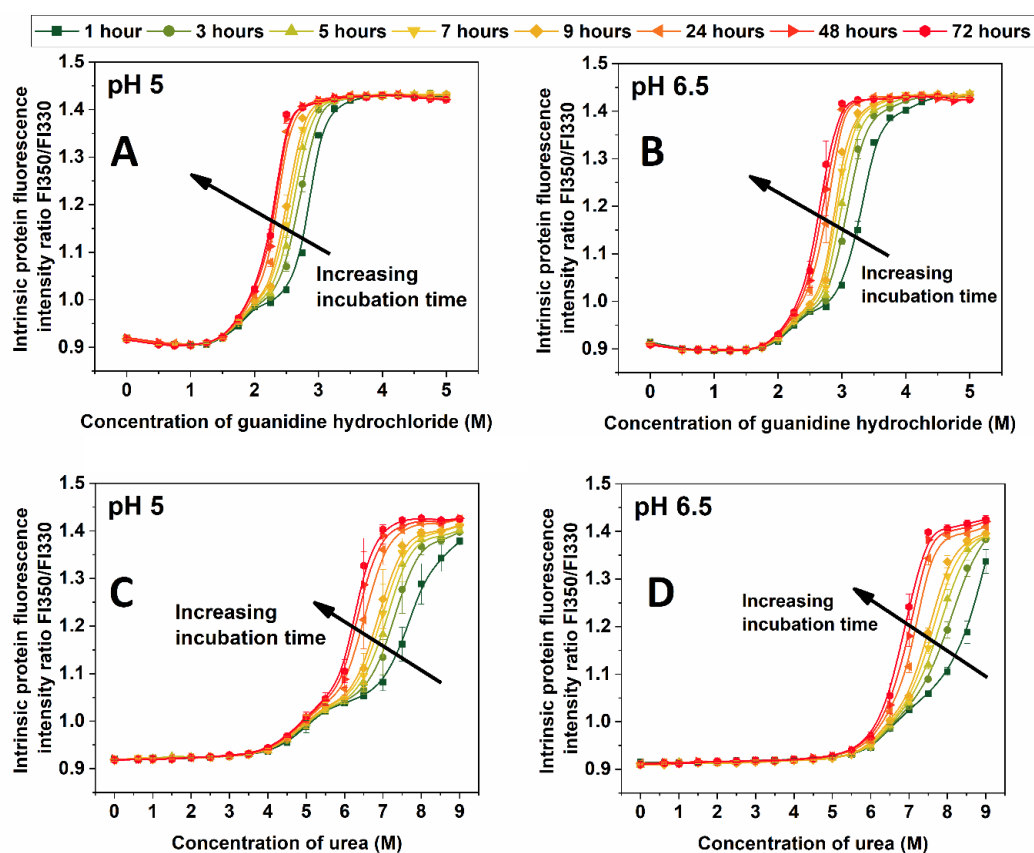
Figure 28. Effect of time and denaturant on the isothermal unfolding of LMU-1 in formulations with different pH. Unfolding in (**A**) pH 5 with guanidine hydrochloride, (**B**) pH 6.5 with guanidine hydrochloride, (**C**) pH 5 with urea, and (**D**) pH 6.5 with urea.

5.4.3 Effect of guanidine hydrochloride and urea on the isothermal antibody unfolding in formulations with different pH

I was interested to compare more in detail how guanidine hydrochloride and urea unfold the model antibody in formulations with different pH because these two denaturants have very different properties. Guanidine hydrochloride is a salt and masks the electrostatic interactions in solution, while urea does not change the ionic strength and respectively does not largely affect the electrostatics. Earlier work employed these differences in the denaturant properties to demonstrate that comparing isothermal chemical denaturation data obtained with guanidine hydrochloride and urea can be used to provide information about the contribution of electrostatic interactions to the conformational protein stability[185]. From the perspective of formulation development, a big change in the ionic strength can affect the protein in different ways. To study if using different denaturants affects the results obtained for different protein formulations, I tested the effect of urea and guanidine hydrochloride on the unfolding of the model mAb in the pH range 5 to 7 (Fig 29). With an increase in pH, higher denaturant concentration is needed to unfold the protein with a maximum reached around pH 7. At lower pH the protein was unfolded by lower denaturant concentrations. This observation is the same when using either guanidine hydrochloride or urea.
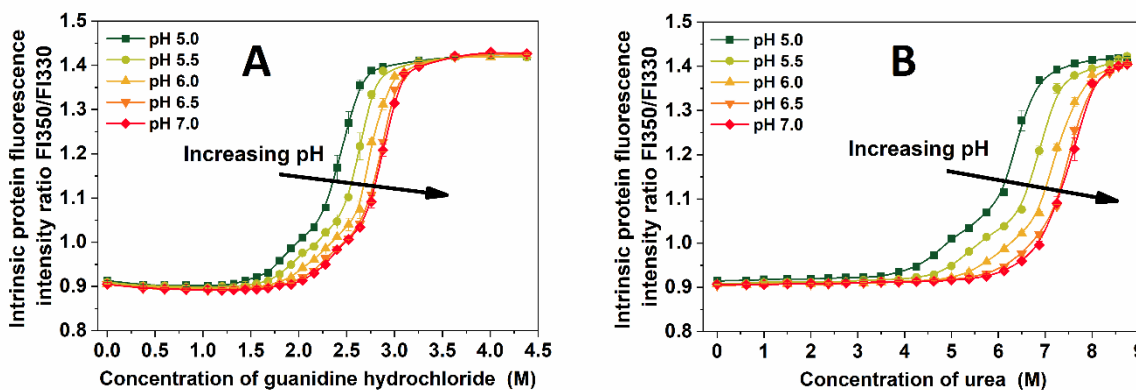
Figure 29. Effect of denaturant on the isothermal unfolding of LMU-1 in formulations with different pH. Isothermal chemical denaturation curves obtained with (**A**) guanidine hydrochloride and (**B**) urea. The samples are incubated for 24 hours at 25 °C. The protein concentration is 1 g/L.

I used the obtained curves in Fig 29 to derive the apparent melting denaturant concentrations for the first (C_{m1}) and the second transition (C_{m2}) (Table 4). The melting denaturant concentration shows what denaturant concentration is needed to unfold 50 % of the protein. Next, I calculated the ratios between the C_m values for the two unfolding transitions obtained in urea and guanidine hydrochloride to assess whether the relationship between the "strength" of the two denaturants is the same in all formulations (Fig 30). What is evident from Fig 30 is that the ratios of the C_m values obtained with urea or guanidine hydrochloride change with the formulation pH. Moreover, the change is different for the two unfolding transitions. The shift around pH 6 in Fig 30 could be a result of the change in the protonation state of histidine residues in the protein structure, which could change the electrostatics contributing to the conformational protein stability. However, the exact reason for these results must be studied in detail on smaller model proteins like single antibody domains.

Table 4. Apparent parameters extracted from the isothermal chemical denaturation graphs of LMU-1. The ± is the error from the Jackknife error from the fit to a three-state model in CDpal.

Denaturant	Parameter	pH 5.0	pH 5.5	pH 6.0	pH 6.5	pH 7.0
GuHCl	C_{m1} (M)	1.79 ±0.15	2.08 ±0.12	2.11 ±0.2	2.29 ±0.07	2.50 ±0.07
	C_{m2} (M)	2.46 ±0.03	2.64 ±0.01	2.76 ±0.04	2.86 ±0.02	2.86 ±0.02
Urea	C_{m1} (M)	4.58 ±0.33	5.26 ±0.21	5.74 ±0.32	6.68 ±0.32	7.24 ±0.07
	C_{m2} (M)	6.42 ±0.1	6.89 ±0.04	7.2 ±0.21	7.54 ±0.04	7.77 ±0.25
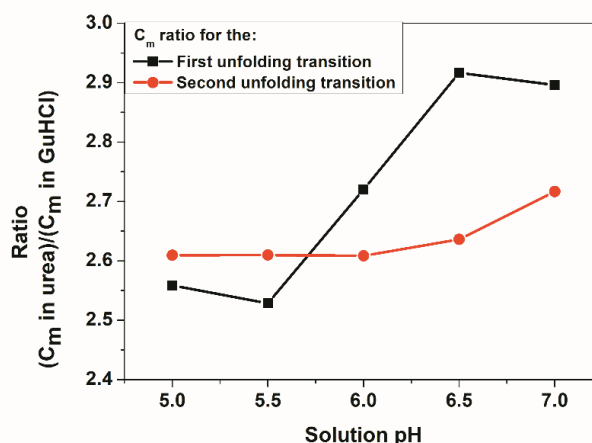
Figure 30. The ration between the melting denaturant concentrations obtained with urea and guanidine hydrochloride for the first (**squares**) and the second (**circles**) unfolding transition of LMU-1 in formulations with different pH

5.4.4 The impact of the denaturant and formulation pH on the aggregation of a partially unfolded antibody

Earlier, I observed that the isothermal chemical denaturation curves of the model antibody continuously shift during incubation. I assumed that the reason for these shifts could be aggregation or precipitation that can occur in the samples[89,181,186]. Such aggregation was observed for other monoclonal antibodies, although the effect of denaturant type and pH on that phenomenon was not studied in detail[53,187].
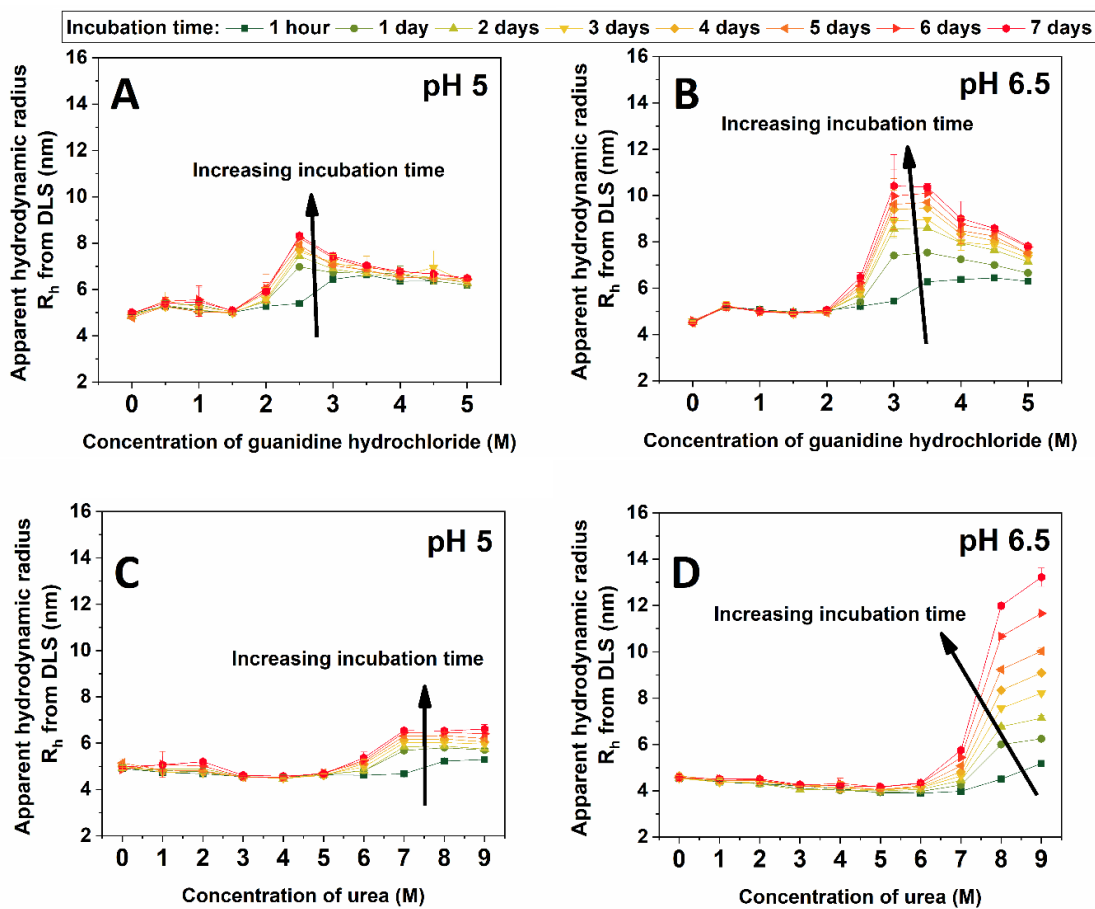
Figure 31. Effect of pH, denaturant type and denaturant concentration on the aggregation of LMU-1 assessed by the change in the apparent hydrodynamic radius R_h from dynamic light scattering. Aggregation in (**A**) GuHCl at pH 5; (**B**) GuHCl at pH 6.5; (**C**) urea at pH 5; and (**D**) urea at pH 6.5; The protein concentration is 10 g/L.

I wanted to study if the partially unfolded antibody in a denaturant solution aggregates and, if so, whether this aggregation is different in formulations with different pH. To investigate

that, I used dynamic light scattering to assess the aggregation of the partially unfolded protein in two formulations with pH 6.5 and pH 5 over the time course of seven days (Fig 31). A slow aggregation was observed at denaturant concentrations that cause partial protein unfolding (see Fig 29). This aggregation occurred in both guanidine hydrochloride and urea and was significantly more pronounced at pH 6.5 compared to pH 5 (Fig 31).

To confirm the results from the fluorescence and DLS analysis that the protein unfolds slowly (Fig 28) and simultaneously forms aggregates (Fig 31), I used size exclusion chromatography coupled to multi-angle light scattering to determine the molecular weight of the eluting species. The LMU-1 samples were incubated in the respective denaturant concentration and injected in the SEC-MALS system running with the same buffer and denaturant concentration like the incubated sample.
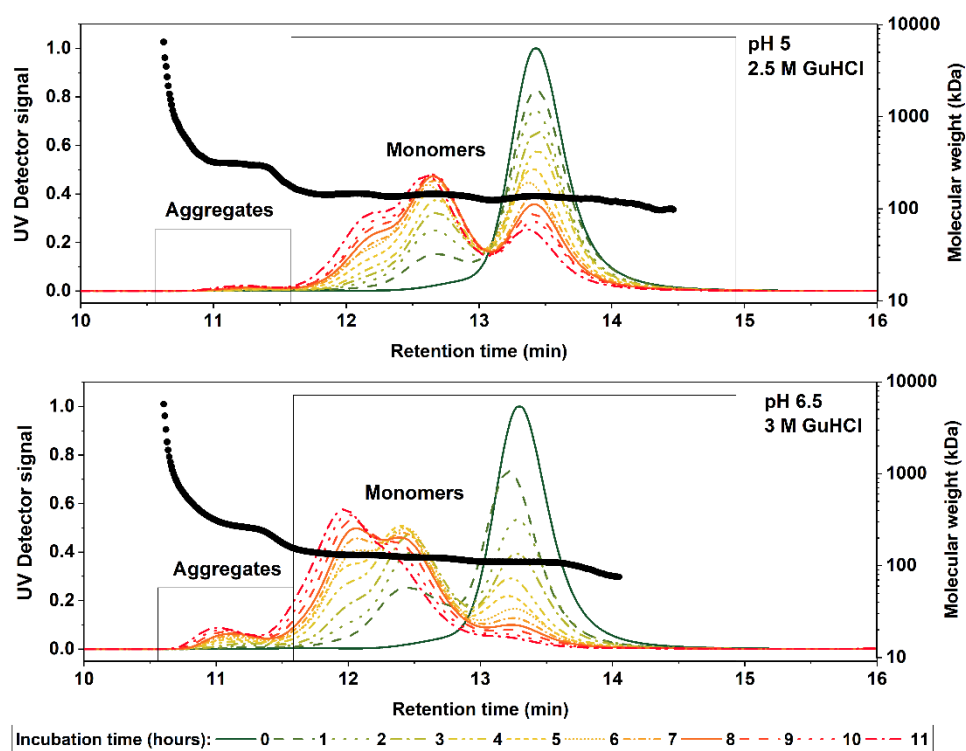
Figure 32. Formation of multiple unfolded species with simultaneous formation of aggregates when 10 g/L LMU-1 are incubated at 25 °C in (**A**) 2.5 M guanidine hydrochloride in 50 mM histidine pH 5; and (**B**) 3 M guanidine hydrochloride in 50 mM histidine pH 6,5;

The incubation in the denaturant that induces partial unfolding in Fig 28 causes the formation of multiple monomeric species that elute earlier than the native protein (Fig 32). Such species have a different degree of unfolding which results in different hydrodynamic radius and respectively different elution times. I also observed that aggregates form simultaneously with the unfolding of the protein. The DLS and SEC-MALS results both show that the isothermal chemical denaturation curves shift during longer incubation due to protein aggregation. Important to note, the aggregation of the partially unfolded antibody is more pronounced in a formulation with pH 6.5 compared to the counterpart with pH 5 (Fig 33).
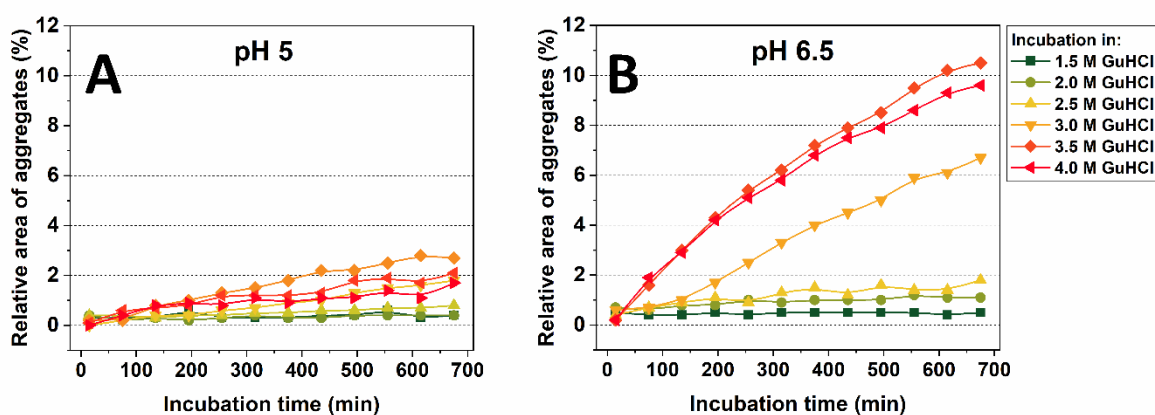
Figure 33. Effect of guanidine hydrochloride concentration on aggregation of LMU-1 at (**A**) pH 5 and (**B**) pH 6.5 measured with SEC-MALS. The protein concertation in the experiment is 10 g/L. The samples are incubated at 25 ºC.

5.4.5 The aggregation during refolding of an antibody depends on the formulation

I assumed that the formulation conditions (e.g. pH) would affect in the same way the aggregation of a partially unfolded antibody in the presence of a denaturant and the aggregation of a fully unfolded antibody during refolding from a denaturant. To test this, I performed microdialysis unfolding/refolding experiments on the antibody in formulations with pH 5 and pH 6.5. Further, I was interested in how the protein concentration (from 1 to 50 g/L) affects the antibody aggregation during refolding in the formulations with different pH. Before and after refolding, I used size exclusion chromatography to measure the area of the monomer peak in each sample. I divided the monomer area after unfolding/refolding by the monomer area before unfolding/refolding to obtain a parameter called relative monomer yield (RMY). A RMY of 0

shows that no monomer is recovered after refolding, while an RMY of 1 shows that all the monomer is recovered after refolding.

The RMY of the antibody is higher, i.e. less protein is aggregated, when the refolding is performed in urea compared to guanidine hydrochloride (Fig 34). This effect is more pronounced at protein concentrations less than 25 g/L. The difference between urea and guanidine hydrochloride can be explained by the fact that in urea solutions the electrostatic interactions between the monomers are not screened and contribute to significant repulsion between the molecules, especially in dilute solutions. The addition of guanidine hydrochloride screens these electrostatic repulsions and the antibody aggregates more after refolding. I also observed that more monomer was recovered when the refolding was performed in formulations with pH 5 compared to counterparts with pH 6.5. These differences were more pronounced when urea was used and at lower protein concentration.
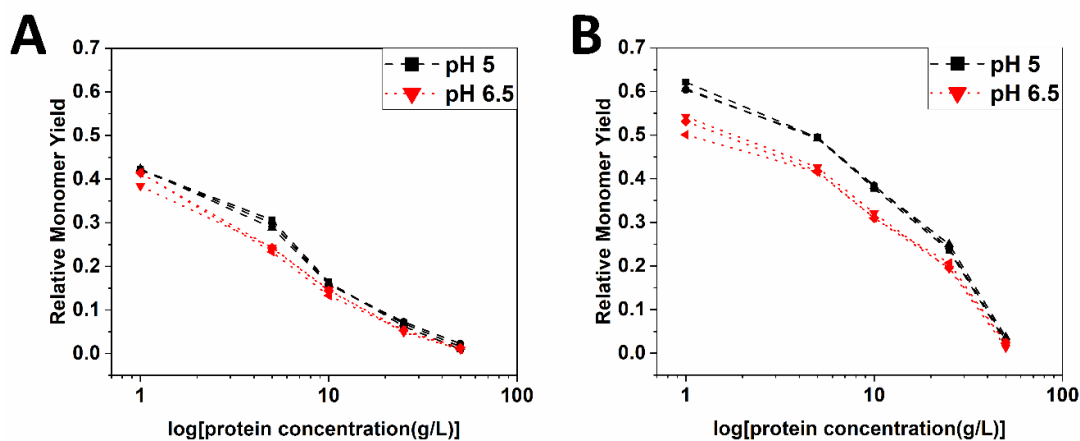
Figure 34. Effect of pH and protein concentration on the relative monomer yield of LMU-1 after refolding from (**A**) guanidine hydrochloride, and (**B**) urea.

Earlier, I showed that the partially unfolded antibody in urea and guanidine hydrochloride aggregates more in a formulation with pH 6.5 compared to a formulation with pH 5. These observations agree with the results that the protein aggregates more during refolding from a denaturant in formulations with pH 6.5 compared to pH 5. This reveals an interesting opportunity that the effect of the formulation on the aggregation of partially unfolded protein species can be assessed by microdialysis unfolding/refolding experiments like the one used here.

5.5 Conclusions

In this chapter, I explored several variables that affect the unfolding and aggregation of an antibody in different formulations. At the beginning, I tested if different denaturants can be used for isothermal chemical denaturation studies to find that only guanidine hydrochloride and urea were suitable in this work. Other denaturants like alkylureas or guanidine thiocyanate had poor solubility in the formulation buffers, induced only partial protein unfolding or caused protein precipitation. Next, I studied how the incubation time affects the denaturant-induced unfolding of the antibody in two formulations with pH 5 and pH 6.5. The isothermal chemical denaturation curves of the antibody shift quickly in the first hours of incubation. After 24 hours, the curves continue to shift very slowly, the shift continues for weeks. Further, I used dynamic light scattering and size exclusion chromatography coupled to multi-angle light scattering to show that the partially unfolded antibody aggregates in the presence of denaturants. The aggregation is faster in a formulation with pH 6.5 compared to a formulation with pH 5. Then, I hypothesised that the formulation conditions (i.e. pH) would have the same effect on the aggregation of the partially unfolded protein in the presence of a denaturant and on the aggregation during refolding of the fully unfolded protein from a denaturant. I performed microdialysis unfolding/refolding experiments to find that the antibody aggregates more during refolding in formulations with pH 6.5 compared to formulations with pH 5, confirming the hypothesis mentioned above.

The findings in this chapter indicate that a microdialysis-based unfolding/refolding assay with urea could be employed to assess how the formulation affects the aggregation of the partially unfolded antibody. In the next two chapters, I explore if such an assay can predict formulations that impede protein aggregation during long-term storage.

5.6 Supplementary data
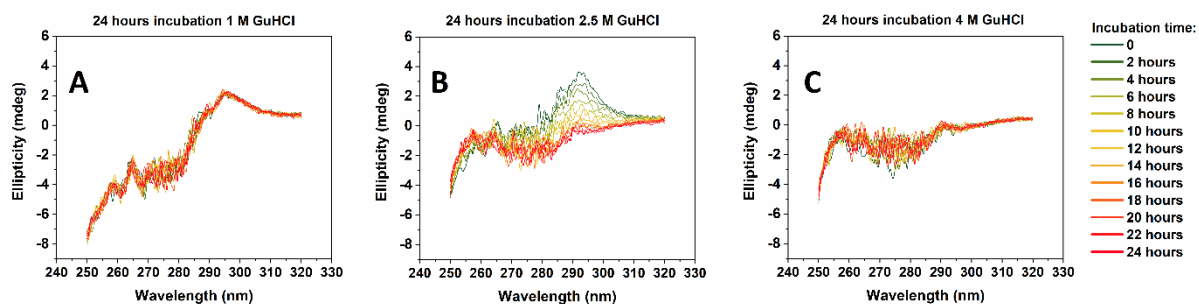
Figure S16. Near-UV CD spectra of 10 g/L LMU-1 in 50 mM histidine pH 5 during 24 hours of incubation in (**A**) 1 M guanidine hydrochloride; (**B**) 2.5 M guanidine hydrochloride; and (**C**) 4 M guanidine hydrochloride; The incubation time step between the different spectra is 2 hours. The measurements are made with a Jasco J-810 spectrometer (JASCO Deutschland GmbH, Pfungstadt, Germany) using 1 mm quartz cuvettes (Hellma GmbH, Muellheim, Germany). Each spectrum is an average of 3 scans measured with 20 min/min scan speed.

Chapter 6 The ReFOLD assay for therapeutic antibody formulation studies and selection of formulation conditions for long-term storage

This chapter is published as:

Svilenov, H.[*] and Winter, G. [*], **2019**. The ReFOLD assay for protein formulation studies and prediction of protein aggregation during long-term storage. European Journal of Pharmaceutics and Biopharmaceutics, 137, pp. 131-139

[*]Department of Pharmacy, Pharmaceutical Technology and Biopharmaceutics, Ludwig-Maximilians-University, Butenandtstrasse 5-13, Munich D-81377, Germany

Author contributions:

H.S. performed the experiments, evaluated the data and wrote the paper. H.S. and G.W. conceived the presented idea and planned the experiments. G.W. supervised the work, provided conceptual guidance and corrected the manuscript.

Note from the authors:

The version included in this thesis is identical with the published article apart from minor changes. The reference, figure and table numbers were changed to fit into the coherent numbering of this document. The text was edited to meet the norms for British English.

The published article can be accessed online via:

https://doi.org/10.1016/j.ejpb.2019.02.018

6.1 Abstract

The formulation of novel therapeutic proteins is a challenging task which aims at finding formulation conditions that will minimise protein degradation during long-term storage. In this chapter, we suggest a novel approach for the selection of formulations that will suppress the formation of protein aggregates during long-term storage. We postulate that conditions (i.e. pH, buffer type, ionic strength) that reduce the isothermal aggregation of various denaturant-induced partially folded protein species will be conditions that impede protein aggregation during long-term storage. To test our hypothesis, we developed an isothermal microdialysis-based unfolding/refolding assay, named ReFOLD, which we use to induce moderate aggregation of partially folded proteins. Next, we assessed the relative monomer yield after isothermal unfolding/refolding of two monoclonal antibodies, each formulated in 12 different conditions. Using the proposed approach, we were able to accurately rank the formulations in order of their effect on the amount of protein aggregates detected after storage for 12 months at 4 °C and 25 °C, while widely-used stability-indicating parameters like protein melting and aggregation onset temperatures failed to provide accurate predictive formulation rankings.

Keywords - Proteins; Protein formulation; Protein folding; Protein unfolding; Protein Aggregation; Monoclonal antibody; Storage Stability; Stability prediction;

Abbreviations - CD – Circular dichroism; dG – the Gibbs free energy of protein unfolding; DLS – Dynamic Light Scattering; DSF - Differential Scanning Fluorimetry; ICD – Isothermal Chemical Denaturation; mAb – monoclonal antibody; nanoDSF™ – Microscale Differential Scanning Fluorimetry; RMY – Relative Monomer Yield after refolding; SEC-MALS – size exclusion chromatography coupled to a multi-angle light scattering detector; T_{agg} – Protein aggregation onset temperature; T_m – Protein melting temperature;
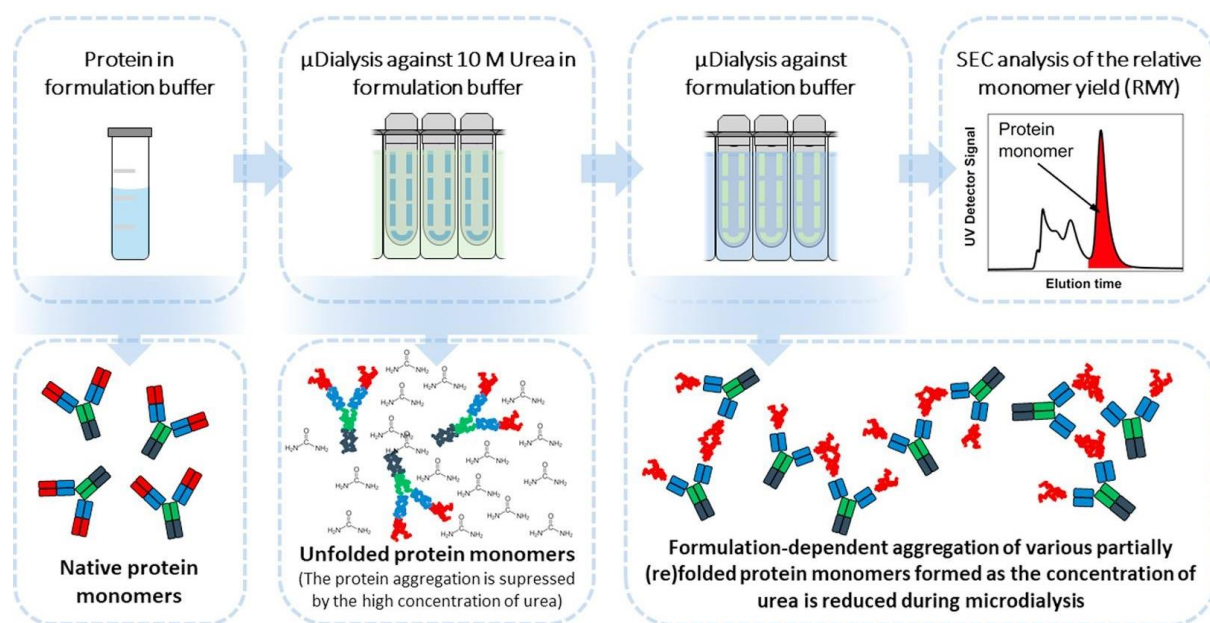
Figure 35. Graphical abstract of Chapter 6 - Schematic diagram of the ReFOLD assay

6.2 Introduction

Non-native protein aggregation (referred to as just "protein aggregation" in this paper) is a major concern during the long-term storage of liquid protein formulations[18,47,85,93]. This pathway of protein aggregation typically occurs through partially unfolded intermediates (often termed as reactive species[188]), which can form irreversible aggregate nuclei that can further grow by various mechanisms. The latter are extensively discussed in the literature and are outside the scope of this article[85,87,90,189,190]. Regardless of the exact mechanism of aggregate nucleation and growth, the formation and presence of protein aggregates in parenteral products should be controlled and minimised for various reasons, e.g. immunogenicity concerns[101,102,191,192], reduced biological activity[135,136] or non-compliance with regulatory frameworks[103,138,193]. The formation of protein aggregates during long-term storage can be suppressed by choosing suitable formulation conditions, e.g. pH, buffer type, ionic strength, etc.[1,104]. The process of selecting the optimal formulation for a new therapeutic protein candidate usually includes the testing of dozens of different conditions[62,194]. Screening all these formulation conditions with long-term or accelerated stability studies is impractical as this would require a lot of resources. Therefore, many researchers turn to short-term biophysical

techniques that could provide predictions for the protein aggregation during storage, thereby reducing the number of formulations for long-term stability studies.

Such biophysical techniques usually require small amounts of sample, can be performed in short timeframes and are suitable for automatization and high-throughput formats[116,139,155,195]. Two of these techniques that are frequently used in the industry are differential scanning fluorimetry (DSF) and dynamic light scattering (DLS)[46,47,146,165,196–198]. The latter can provide the (apparent) protein melting temperature (T_m) and the aggregation onset temperature (T_{agg}) respectively. Earlier publications show that in some cases, and on a limited set of formulation conditions, a high T_m or a high T_{agg} can be an indicator for formulation conditions where protein aggregation is suppressed during accelerated stability studies (e.g. 40 ºC and 50 ºC)[47,105,199]. However, recent work on larger sets of proteins indicates that these parameters show a very weak or no correlation with the aggregation behaviour of many therapeutic proteins, especially mAbs, during storage at 4 ºC and 25 ºC[62,63,105,200].

Probably due to the reason mentioned above, researchers have started to explore orthogonal techniques that could provide better stability predictions for the aggregation behaviour of novel therapeutic proteins during long-term storage. One such technique is isothermal chemical denaturation (ICD)[4,54,165]. Although ICD is the gold standard to obtain the Gibbs free energy of protein unfolding (and thereby assess the conformational stability of a protein)[162], the data evaluation from this method is valid only in cases where the protein of interest undergoes reversible unfolding in the denaturant solution[52,55,173]. Most of the published work including ICD experiments is on small globular single-domain proteins[174,201,202]. However, the vast majority of therapeutic proteins under development in the moments have large, multi-domain structures (e.g. mAbs, bispecifics, fusion proteins, antibody-drug conjugates) that can undergo complex, multi-step unfolding during an ICD experiment which could require sophisticated fitting to a model[50,165]. Furthermore, the reversibility of unfolding of these proteins in different formulation conditions might vary[52,54,55]. Recently, it was suggested that one could use ICD experiments to investigate non-reversibility effects during protein unfolding in a denaturant[6,154]. Such experiments study how the apparent Gibbs free energy of protein unfolding changes when different protein concentrations are used to obtain the ICD curves. It was already demonstrated that the latter approach can provide complementary stability-

indicating information to DSF and DLS[54,203]. Still, ICD experiments that study the concentration dependence of dG are tedious, require dedicated laboratory equipment and rely on the quality of the fitting to a certain unfolding model.

Rather than using ICD as an "indirect" way to look into the effect of the formulation conditions on the reversibility of isothermal protein unfolding, we recently suggested that one could directly study the aggregation after dilution from a denaturant[55]. Shortly after that and independently of us, Rowe et al. proposed a similar approach[53]. In our previous work, we showed that when the dilution refolding experiments are performed with certain denaturant concentrations, the protein aggregation during refolding can be linked to other stability-indicating parameters, e.g. the melting denaturant concentration C_m and the interaction parameter k_D[55]. The dilution approach we proposed is valuable to probe which denaturant concentrations will cause extensive protein aggregation after dilution refolding and also to study if there is a difference in the physical stability of a protein in conditions with overlapping ICD curves[55].

However, different concentrations of a denaturant cause different degrees of protein unfolding and different aggregation-prone intermediates. Each of the latter could be important for the non-native protein aggregation during long-term storage. Rather than diluting the protein from dozens of different denaturant concentrations, we decided to perform microdialysis on the protein against a denaturant and subsequently against a denaturant-free formulation buffer. This procedure will cause various unfolding (refolding) protein intermediates. We hypothesised that these intermediates will aggregate depending on the formulation conditions, e.g. pH, buffer type, ionic strength, protein concentration. The rationale behind using this phenomenon as a protein formulation tool is that formulation conditions which suppress the aggregation of various partially folded states would be formulation conditions that would suppress protein aggregation during long-term storage. Since the isolation of the individual aggregation-prone intermediates or aggregates formed could be a challenging task, we adopted an approach where we assess the relative monomer yield (RMY) after the isothermal unfolding and refolding is completed. Important to note, determining the RMY after isothermal unfolding/refolding of the protein for the purpose of formulation development would be quite different compared to unfolding/refolding experiments to increase the monomer yield after

protein expression as inclusion bodies. The latter experiments usually include a reduction and new formation of disulphide bonds, as well as extremities in the pH, excipient concentration and the type of excipients used[166,168,169,204,205]. Assessing the aggregation during isothermal unfolding/refolding of the protein as a formulation tool is focused on a pH range which is realistic for long-term storage and administration in patients due to chemical stability and tolerability considerations respectively. Furthermore, the excipients used, as well as their concentrations, would be approved for parenteral application[206].

To study our hypothesis, we developed a microdialysis unfolding/refolding assay which we called ReFOLD. Next, we investigated the effect of realistic for long-term storage formulation conditions on the relative monomer yield after isothermal unfolding/refolding of two monoclonal antibodies. We validated the predictions from the ReFOLD assay by performing a 12-month stability study at 4 ⁰C and 25 ⁰C. Additionally, we characterised the antibodies in the presence of urea to show that this denaturant causes partially unfolded states and suppresses the protein aggregation in all conditions tested. The latter phenomena allow us to see formulation-dependent differences in the monomer loss caused by aggregation of partially folded protein species during unfolding/refolding.

6.3 Materials and Methods

6.3.1 Monoclonal antibodies and chemicals

Two IgG1 monoclonal antibodies were used in this work - LMU-1 and PPI03. The monomeric state and the purity of the proteins in the bulk solution were confirmed as described earlier[55]. The buffer of the mAbs was exchanged by extensive dialysis overnight as previously described[55]. Unless otherwise stated, the final mAb solutions after dialysis contained 10 mM histidine/histidine hydrochloride buffer, 10 mM sodium citrate/citric acid buffer with a pH 5, 5.75 or 6.5. The PPI03 samples containing 70 mM sodium chloride were prepared by spiking in the salt from a 10X stock solution. All LMU-1 samples contained 0,05 % w/v polysorbate 20 which was spiked in the protein solution after dialysis. All PPI03 solutions were free of surfactants. For an overview of the formulations see Tables 5 and S4. The protein concentration was measured by UV spectrometry at 280 nm with a Nanodrop 2000 (Thermo Fisher Scientific, Wilmington, DE) using the respective protein extinction coefficient. Reagent chemicals from

the highest grade available were purchased from Sigma Aldrich (Steinheim, Germany), VWR International (Darmstadt, Germany) or Fisher Scientific (Schwerte, Germany). Highly purified water was used for the preparation of all buffers.

6.3.2 Isothermal protein unfolding and refolding with microdialysis

100 µL of formulated mAb solution was filled in Pierce™ microdialysis devices with a membrane having 3.5 kDa MWCO. The samples were dialysed in a deep well-plate against 1.5 mL of 10 M urea solution in the respective formulation buffer. The urea solution was changed 4 and 8 hours after the beginning. After the last change, the dialysis was continued for another 16 hours. Next, the mAb samples dialysed against 10 M urea were dialyzed against 1.5 mL of the respective urea-free formulation buffer. The buffer was changed 4 and 8 hours after the beginning, and the dialysis continued in total for 24 hours. During the entire dialysis procedure, the deep well plate was attached to a Thermomixer Comfort (Eppendorf AG, Hamburg, Germany) which was adjusted to agitate the plate at 700 rpm. Finally, the samples were collected from the dialysis devices and the weight of each sample was added to 1.0 g with the respective urea-free buffer to avoid variations in the sample volume that might arise during dialysis. Finally, the samples were centrifuged at 10 000 x g for 10 minutes to remove any insoluble matter. The supernatant was used for further measurements.

6.3.3 Size Exclusion Chromatography

A Dionex Summit 2 system (Thermo Fisher, Dreieich, Germany) and a TSKgel G3000SWxl, 7,8x300 mm, 5 µm column (Tosoh Bioscience, Tokyo, Japan) were used for the size exclusion chromatography. Protein elution was detected at 280 nm unless otherwise stated. The running buffer consisted of 100 mM potassium phosphate, 200 mM sodium chloride and 0,05 % w/v sodium azide. The buffer pH was adjusted to 7.0 with 2 M sodium hydroxide. The chromatograms were integrated with Chromeleon V6.8 (Thermo Fisher, Dreieich, Germany). The relative content of the high molecular weight (HMW) species formed after long-term storage was calculated by dividing the peak area of the high molecular weight species by the total area of all protein peaks in the chromatogram which provides a number representing the relative content of high molecular weight species in percentage. Representative chromatograms with integration times and more explanations are presented in the supplementary data to this

chapter. The relative monomer yield (RMY) of the proteins after isothermal unfolding/refolding, i.e. the ReFOLD assay, was calculated by dividing the area of the monomer peak of the refolded sample by the area of the monomer peak of the sample before unfolding/refolding which gives a value between 0 and 1, where 0 means that no protein monomer is recovered in the sample after refolding and 1 means the same amount of monomer is recovered after refolding.

6.3.4 Size Exclusion Chromatography with Multi-angle Light Scattering

An Agilent 1100 Series HPLC system (Santa Clara, CA, USA) with an Agilent 1100 multiple wavelength detector (Santa Clara, CA, USA), Agilent 1100 refractive index detector and a DAWN HELEOS multi-angle light scattering (MALS) detector (Wyatt Technology, Santa Barbara, USA) were used for the SEC-MALS measurements. Sample elution was monitored at 280 nm and with the change in the refractive index. The same column and running buffer like for the SEC method above were used. Data collection and processing were performed using the ASTRA software, Version 7.1 (Wyatt Technology, Santa Barbara, USA).

6.3.5 Isothermal Chemical Denaturation (ICD)

Samples for isothermal chemical denaturation experiments were prepared by combining protein stock solution in formulation buffer with different amounts of formulation buffer and 10 M urea stock solution in formulation buffer in a non-binding 384-well plate as described earlier[54,55]. The samples were incubated for 24 hours at room temperature and the protein intrinsic fluorescence intensity at 330 and 350 nm was measured after excitation at 280 nm with a FLUOstar Omega microplate reader (BMG Labtech, Ortenberg, Germany). The intrinsic protein fluorescence intensity ratio (FI350/FI330) was plotted against the urea concentration to obtain isothermal chemical unfolding curves of the mAbs in different buffers[54,55,116].

6.3.6 Microscale Differential Scanning Fluorimetry

The protein samples were filled in standard nanoDSF™ grade capillaries, the capillaries were sealed and the thermal unfolding of the proteins was studied by applying a temperature ramp of 1 ºC/min from 20 to 100 ºC with the Prometheus NT.48 (NanoTemper Technologies, Munich, Germany) system that measures the intrinsic protein fluorescence intensity at 330 and 350 nm after excitation at 280 nm. At the same time, the device detects precipitation of the

samples by measuring the back-reflection intensity of a light beam that passes twice through the capillary, this signal can be normalised to a value called "Excess Scattering". The apparent protein melting temperatures (T_m) were determined with the PR.ThermControl software V2.1 (NanoTemper Technologies, Munich, Germany) from the maximum of the first derivatives of the thermal unfolding curves[148,207].

6.3.7 Circula Dicroism (CD) Spectroscopy

Near-UV circular dichroic spectra of the mAb samples were measured at 25 ⁰C with a Jasco J-810 spectrometer (JASCO Deutschland GmbH, Pfungstadt, Germany). Quartz cuvettes (Hellma GmbH, Muellheim, Germany) with 10 mm wavelength path were used for the measurements. All measurements were performed with 3 accumulations and a speed of 20 nm/min. The spectrum of the respective buffer was subtracted for each sample, Savitzky-Golay algorithm with 9 smoothing points was applied and the mean residue ellipticity (MRE) of the protein at each wavelength was calculated as described elsewhere[120].

6.3.8 Fourier-transform Infrared Spectroscopy

FT-IR spectra of the mAb samples were collected at 25 °C using a Tensor 27 (Bruker Optik GmbH, Ettlingen, Germany) with a BioATR (Attenuated Total Reflectance) cell™ II (Harrick) connected to a thermostat (DC30-K20, Thermo Haake). 120 scans with a resolution of 4 cm^{-1} were taken to measure each spectrum. The raw data of each sample was analysed with the Opus 7.5 (Bruker Optik GmbH) software and shown as a vector-normalised second-derivative spectrum. The data were smoothed using a Savitzky-Golay algorithm with 17 smoothing points[119].

6.3.9 Long-term stability studies

The mAb solutions with different formulation conditions were sterile filtered with a 0.22 μm cellulose acetate filter and aseptically filled into pre-sterilized DIN2R glass type I vials (MGlass AG, Germany). Next, the vials were crimped with rubber chlorobutyl stoppers with FluroTec® coating (West Pharmaceutical Services, USA) and stored at 4 ⁰C and 25 ⁰C for the desired time. Three different vials were used for the SEC analysis of each condition.

6.4 Results and Discussion

6.4.1 The isothermal protein unfolding/refolding leads to a formulation-dependent protein aggregation and monomer loss

Both antibodies used in this work show substantial aggregation after microdialysis against 10 M urea (unfolding) and subsequently against urea-free formulation buffer (refolding). The visual appearance of the samples after refolding is dependent on the formulation conditions in which the refolding is performed. For example, after the ReFOLD assay, LMU-1 formulations with a concentration 10 g/L in 10 mM histidine buffer with pH 6.5 remain transparent, while counterparts with 10 mM citrate buffer show increased turbidity and form a pellet after centrifugation. These observations confirm earlier reports that the aggregate formation of antibodies after dilution/dialysis from a denaturant is formulation-dependent[53,55]. SEC-MALS analysis of the supernatant of the refolded samples shows that the samples contain a considerable amount of high molecular weight species ranging from dimers to oligomers larger than 1000 kDa. (Fig 36). The aggregates are not reversible, and their relative area is the same even several days after the dialysis (data not shown). A monomer peak having the same retention time as the native protein is detected in the refolded samples. The area of the monomer peak is largely dependent on the formulation buffer in which the ReFOLD assay is performed. Since the evaluation of the exact size, concentration and type of aggregates formed is challenging in such a complex mixture, we decided to focus on the fraction of the protein that remains monomeric after isothermal unfolding/refolding (i.e. the relative monomer yield - RMY) as a parameter providing a comparison between the formulations.
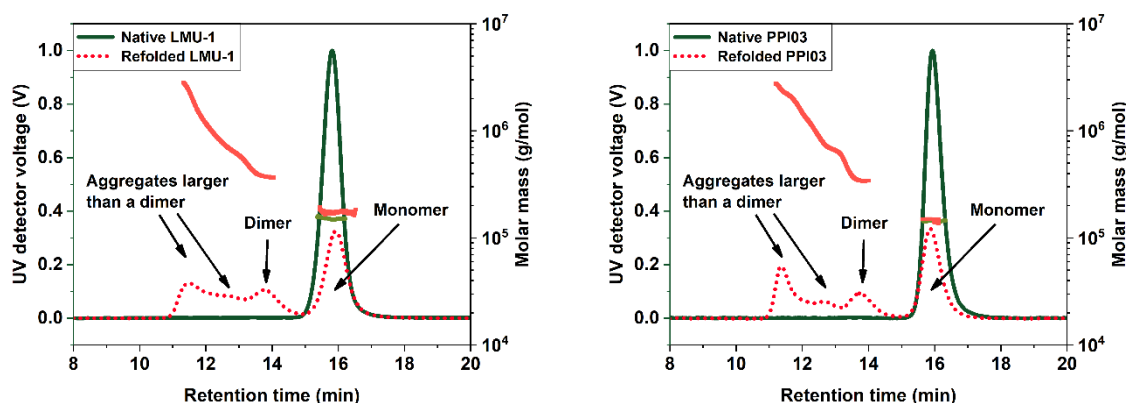
Figure 36. SEC-MALS of native and refolded samples of LMU-1 and PPI03

6.4.2 The relative monomer yield after isothermal protein unfolding/refolding correlates with the relative amount of protein aggregates detected after long-term storage

The relative monomer yield after the ReFOLD assay is highly dependent on the formulation conditions of both LMU-1 (Tables 5 and S3) and PPI03 (Table S4). The formulation conditions also have an influence on the relative area of high molecular weight (HMW) species, i.e. protein aggregates, detected by SEC after storing the respective denaturant-free protein samples for 12 months at 4 °C and 25 °C (Table 5 and S3). LMU-1 samples contain more HMW species after long-term storage compared to PPI03. Both proteins form fewer HMW species when stored at 4 °C compared to storage at 25 °C. We also used flow microscopy to study the presence of subvisible particles in the samples after 12 months of storage at 4 °C and 25 °C (Fig S18). Calculations on the monomer recovery from the size-exclusion chromatography method used for the stability study are also included in the supplementary data. A very strong correlation between the relative monomer yield from the ReFOLD assay and the relative area of high molecular weight species detected after 12 months of storage is observed in the case of LMU-1 (Fig 37). Interestingly, the first and second apparent melting temperatures of LMU-1 measured nanoDSF™ show reversed correlations with the relative area of HMW species detected after storage, therefore providing misleading predictions for the long-term physical stability of these samples (Figs S19 and S20). The aggregation onset temperatures of LMU-1 show only a moderate to weak correlation with the amount of aggregates formed after storage for 12 months (Fig S21). In the case of PPI03 the Spearman's R between the RMY from the

ReFOLD assay and the aggregates formed after storage at 4 ⁰C and 25 ⁰C is -0.762 and -0.686 respectively, showing a strong correlation between these parameters (Fig S22). Like the case of LMU-1, the melting temperatures of the PPI03 samples show an inverse correlation with the aggregates formed after storage, therefore providing wrong predictions for these formulations (Figs S23 and S24). The aggregation onset temperatures of the PPI03 samples show a very weak correlation with the amount of high molecular species formed after long-term storage at 4 ⁰C and 25 ⁰C (Fig S25). In general, PPI03 exhibits a very low aggregation propensity and small differences between the formulations during long-term storage. The latter observations can contribute to the lower correlation between the RMY and the aggregates formed after 12 months of storage in comparison to LMU-1. Almost all LMU-1 and PPI03 formulations contain less than 10 000 particles $\geq$ 2 μm per mL after 12 months of storage at 25 ⁰C and 4 ⁰C (Fig S18). One exception is the LMU-1 formulation with protein concentration 50 g/L formulated in 10 mM histidine pH 6.5 which contains around 150 000 particles $\geq$ 2 μm per mL. Interestingly, this is also the formulation with the lowest relative monomer yield after the ReFOLD assay (Table 5). There, are small differences, i.e. $\pm$ 5 %, in the monomer recovery of the antibodies at the end of the stability study. The samples with high RMY from the ReFOLD assay show 100 % ($\pm$ 1 %) monomer recovery after 12-month storage at 4 ⁰C and 25 ⁰C (Tables S5 and S6).

It is important to underline that the RMY-based predictions from the ReFOLD assay provide reliable ranking of the formulations in order of their effect on the relative area of protein HMWs formed after 12 months of storage at 4 ⁰C and 25 ⁰C, while often-used stability-indicating parameters (i.e. apparent protein melting temperatures from nanoDSF™ and the aggregation onset temperatures from dynamic light scattering) provided misleading or weak predictions.

Table 5. Relative Monomer Yield (RMY) of LMU-1 formulations after the ReFOLD assay and the relative content of high molecular weight species after long term storage of the respective LMU-1 formulations. The values are mean of triplicates and the error represents the standard deviation. The value from each replicate is provided in the supplementary data to this chapter.

Formulation number	Protein conc. [g/L]	Buffer	pH	RMY after refolding from 10 M urea		% HMW after 12 months at 25 °C		% HMW after 12 months at 4 °C	
				Mean	StDev	Mean	StDev	Mean	StDev
1	10	histidine	5	0.387	0.0145	0.207	0.0252	0.153	0.0513
2	10	histidine	5.75	0.378	0.0125	0.167	0.0153	0.197	0.0462
3	10	histidine	6.5	0.269	0.0035	0.447	0.0907	0.283	0.0808
4	10	citrate	5	0.241	0.0021	0.51	0.0346	0.313	0.0231
5	10	citrate	5.75	0.168	0.0032	0.723	0.0651	0.363	0.0586
6	10	citrate	6.5	0.159	0.0067	0.94	0.1082	0.607	0.0404
7	50	histidine	5	0.096	0.0032	0.703	0.0289	0.47	0.04
8	50	histidine	5.75	0.083	0.0046	0.863	0.0306	0.587	0.0723
9	50	histidine	6.5	0.005	0.0038	1.607	0.0551	0.923	0.0208
10	50	citrate	5	0.071	0.0052	0.977	0.0808	0.437	0.0643
11	50	citrate	5.75	0.035	0.0046	1.15	0.0819	0.593	0.0208
12	50	citrate	6.5	0.021	0.0032	1.757	0.0929	1.01	0.0755
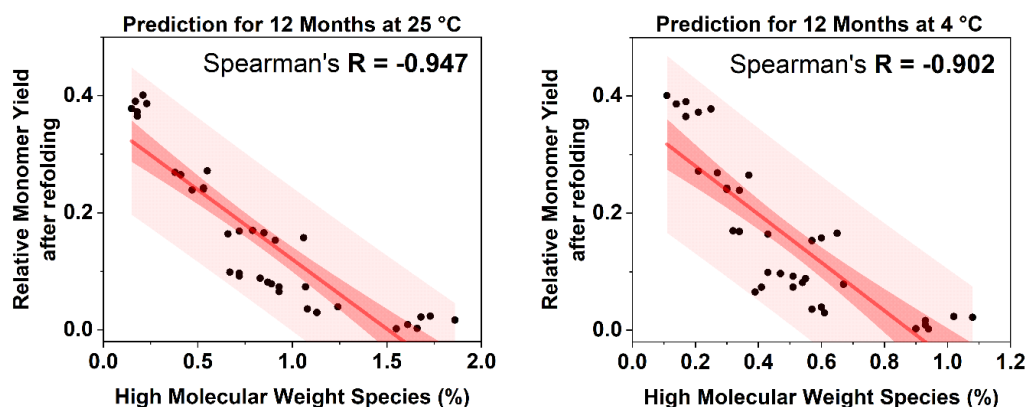
Figure 37. Correlation between the relative monomer yield of LMU-1 from the ReFOLD assay and the relative content of high molecular weight species, i.e. protein aggregates, detected by size exclusion chromatography after 12 months of storage at 25 °C (**left**) and at 4 °C (**right**). The value of each replicate is shown on the graph. The solid red line is linear fit of the data, the dark red zone represents the 95 % confidence interval of the fit and the light red zone the 95 % prediction interval.

6.4.3 Urea causes partially unfolded species, reduces the melting temperatures and suppresses the aggregation of LMU-1 and PPI03

To study whether the proteins in this work form partially folded states in urea, we performed isothermal chemical denaturation experiments on all 24 LMU-1 and PPI03 formulations. The isothermal unfolding curves of LMU-1 (Fig 38) and PPI03 (Fig S26) are dependent on the formulation conditions (i.e. pH, buffer type, sodium chloride concentration). However, in all conditions tested the intrinsic protein fluorescence ratio reached the same value at urea concentration of 9.5 M (around 1.3 in the case of LMU-1 and around 1.2 in the case of PPI03). This indicates that the unfolding was complete at this concentration of urea. The latter was also later confirmed by the loss of the typical peaks in the near-UV CD spectra related to the protein tertiary structure (see below). Our aim by performing the isothermal chemical denaturation experiments was not to fit the data and extract thermodynamic parameters from it. Our purpose was to show that different concentrations of urea cause different states of the unfolding of the protein in the formulations tested.
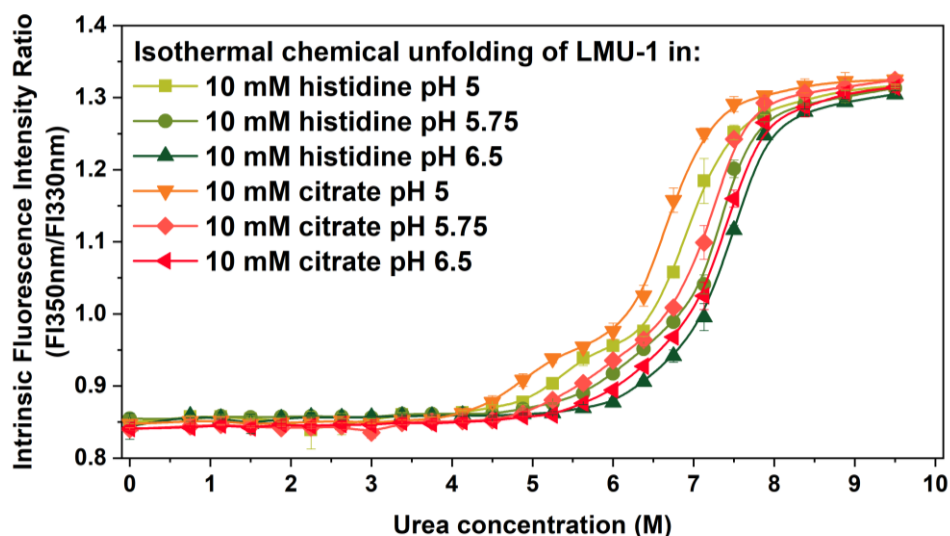
Figure 38. Isothermal unfolding curves of LMU-1 in different formulation buffers. The symbols are means of triplicates and the bars represent the standard deviation. The lines are a guide to the eye. The concentration of LMU-1 in all samples is 1 g/L.

Further, we studied how urea affects the melting temperatures and the aggregation behaviour of the protein with nanoDSF™. Moderate urea concentrations (up to 4.5 M) shift the apparent

112

melting temperatures of both proteins to a lower temperature, while higher urea concentrations (6-7.5 M) cause partial protein unfolding at room temperature (Figs 39 and S27). A similar effect of urea on the melting temperatures of a mAb was reported from differential scanning calorimetry experiments[208]. No unfolding upon heating is detected in 9.5 M urea, indicating that the proteins are already unfolded at 20 ºC in this urea concentration (Figs 39 and S27). This is in good agreement with the ICD (Figs 38 and S26) and the Far-UV circular dichroism data (see below). The latter observations are consistent among all 24 formulations in this work (data not shown). These results confirm our hypothesis that different urea concentrations (which the protein will inevitably experience during the ReFOLD assay) cause various partially folded protein species in all formulations tested here.

Additionally, we observed that an increasing concentration of urea suppresses the aggregation of the mAbs even at high temperatures (Figs 39 and S27). Similar observations were reported earlier for another antibody[208]. No protein aggregation was detected with the Prometheus NT.48 during the temperature ramp when the protein was in solutions with 5 to 9.5 M urea (Figs 39 and S27), while rapid aggregation was observed around 70-80 ºC in the urea-free LMU-1 and PPI03 formulations. We should note that the nature of the aggregate detection with the Prometheus NT.48 allows us to see only aggregates with a size starting from about 40-50 nm. Therefore, we cannot conclude that the aggregate formation is completely absent in the presence of urea. However, the aggregation growth is greatly inhibited. Furthermore, the isothermal aggregation of the unfolded protein in presence of 9 M urea was very slow at 25 ºC measured by the change in the apparent hydrodynamic radius of the samples with dynamic light scattering (Figure S28).

Moderate isothermal aggregation of partially unfolded mAbs was already reported in the presence of another denaturant - guanidine hydrochloride[53,187]. This confirms that the aggregation of the proteins unfolded in presence of urea is suppressed in comparison to aggregation induced by high temperatures. Noteworthy, the moderate aggregation in urea allows a large fraction of the (partially) unfolded protein to remain monomeric and allows the observation of formulation-dependent differences based on the relative monomer yield after refolding.
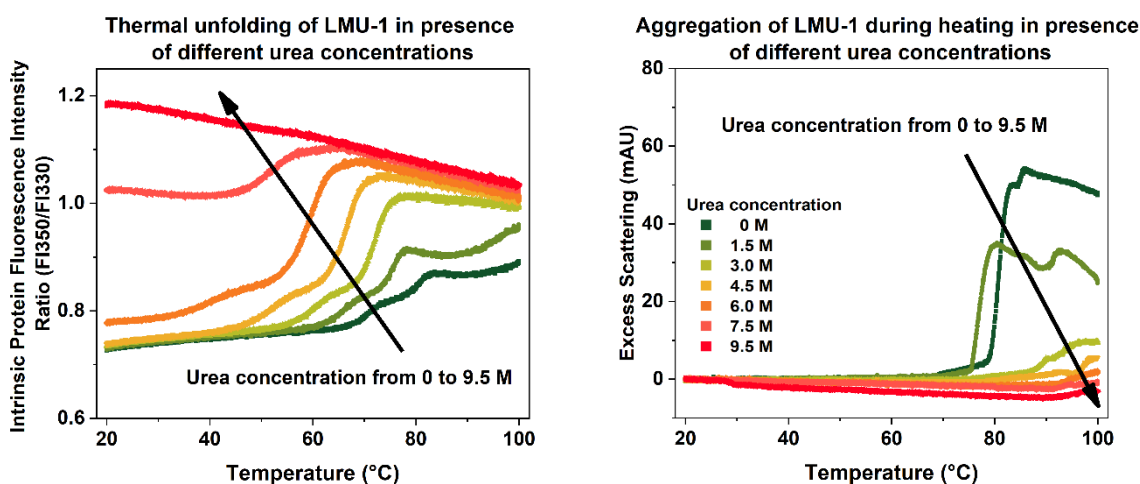
Figure 39. Thermal unfolding traces (**left**) and aggregation during unfolding (**right**) of LMU-1 in presence of different concentrations of urea. The buffer is 10 mM citrate pH 6.5. The samples were incubated for 24 hours in the urea before the measurements. The concentration of LMU-1 in all samples is 1 g/L.

6.4.4 The samples after isothermal unfolding/refolding have native-like far-UV circular dichroic spectra and increased intermolecular beta sheet content

The near-UV CD spectra of both proteins show typical spectra arising from the signals of the tryptophan, tyrosine, phenylalanine and disulphide bonds having a certain environment in the tertiary protein structure (Figs 40 and S29)[209–211]. The formulation conditions (i.e. pH, buffer type and sodium chloride concentration) of the native samples do not affect the characteristics of the spectra – positive peak around 295 nm and several negative peaks between 280 and 250 nm. The near-UV CD spectra of LMU-1 and PPI03 samples incubated in 9.5 M urea do not contain most of the features of the native samples (Figs 40 and S29). Interestingly, the proteins in the supernatant of the refolded samples from the ReFOLD assay have the typical components of the near-UV CD spectra of the native monomers (Figs 40 and S29). Hawe et al. reported that the near-UV CD spectra of a heat or freeze-stressed mAbs resemble the native protein[212]. Another group showed that the near-UV spectra of thermally-induced mAb oligomers resemble the spectra of the native protein[213]. Additionally, the near-UV spectra of a mAb exhibited the same changes during thermal unfolding like the changes we observed during urea-induced isothermal unfolding[41].

114
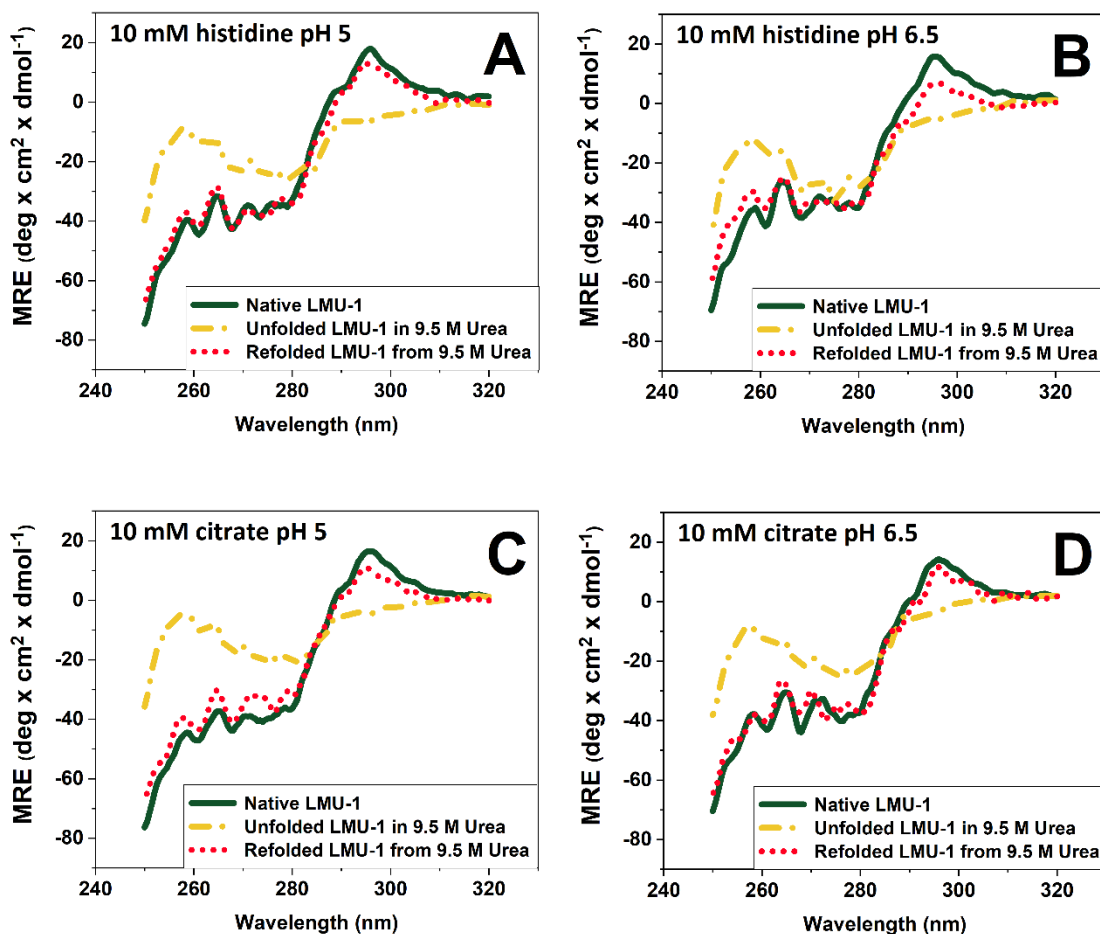
Figure 40. Near-UV CD spectra of LMU-1 - native (green solid line), unfolded with 10 M urea (yellow dot and dash) and refolded protein (red dot) after the ReFOLD assay was performed with (**A**) 10 mM histidine pH 5, (**B**) 10 mM histidine pH 6.5, (**C**) 10 mM citrate pH 5 and (**D**) 10 mM citrate pH 6.5. The CD spectra of the refolded samples represent the mixture of protein aggregates and monomer after refolding without any prior fractionation.

Further, we used FTIR to investigate the secondary protein structure of the native and refolded protein. A minimum around 1638 cm^{-1} is observed in the Amide I region of the second-derivative FTIR spectra of native LMU-1 samples (Fig 41). This is typical for a native beta-sheet secondary structure and is already reported for monoclonal antibodies[80,214,215]. The refolded LMU-1 samples show a minimum in the Amide I band which is shifted to 1630 cm^{-1}. The latter is typical when intermolecular beta-sheets are formed[80,214,215]. The above-mentioned observations were consistent among various formulation conditions we tested in this work. The

intermolecular beta-sheets are an often-reported secondary structure of non-native protein aggregates[216–218].
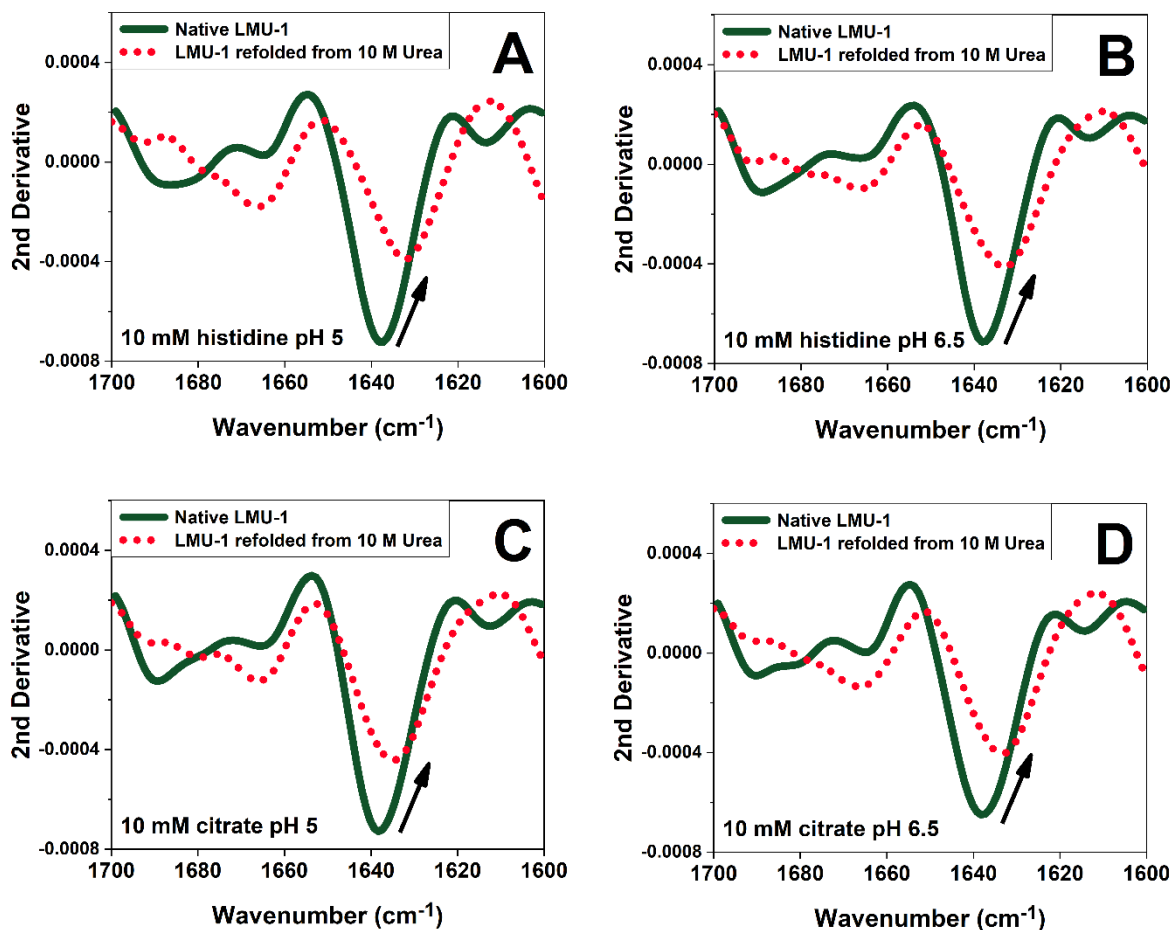
Figure 41. FT-IR second derivative spectra of native and refolded LMU-1 after the ReFOLD assay was performed with (**A**) 10 mM histidine pH 5, (**B**) 10 mM histidine pH 6.5, (**C**) 10 mM citrate pH 5 and (**D**) 10 mM citrate pH 6.5. The CD spectra of the refolded samples represent the mixture of protein aggregates and monomer after refolding without any prior fractionation.

6.5   Conclusions

This work presents a novel perspective on how to quickly select formulation conditions that will suppress the formation of protein aggregates during long-term storage at 4 ⁰C and 25 ⁰C. The proposed approach is based on the hypothesis that formulation conditions which suppress the isothermal aggregation of various partially folded species would be formulation conditions that suppress protein aggregation during long-term storage. An isothermal microdialysis-based

unfolding/refolding assay, named ReFOLD, is presented and used to assess the relative monomer yield after isothermal unfolding/refolding with 10 M urea of two mAbs, each in 12 different formulation conditions. The relative monomer yield of the proteins in different formulation conditions from the ReFOLD assay shows a very strong to strong correlation with the amount of aggregates formed by the proteins after storage for 12 months at 4 ⁰C and 25 ⁰C. Other stability-indicating parameters like the apparent protein melting temperatures and aggregation onset temperatures show inverse or weak correlations with the amount of aggregates formed after storage. The refolded protein samples have a native-like near-UV circular dichroic spectra and a peak position in the Amide I band which is typical for aggregated beta-sheets.

The concept of the ReFOLD assay presented here opens several directions for future work. First, the ReFOLD assay must be tested with more proteins and on a larger set of formulation conditions to study whether the technique can be used as a universal tool for formulation development. Second, it will be interesting to study in detail the effect of various excipients, i.e. sugars, polyols, amino acids, surfactants, on the relative monomer yield of different proteins and investigate whether excipients that inhibit the aggregation of partially folded species are the excipients that stabilize the proteins during long-term storage. Third, the aggregates and monomers formed after unfolding and refolding in urea can be fractionated and their morphology and structure can be studied more in detail. It would be interesting to see whether the aggregates formed during long-term storage exhibit the same characteristics with the aggregates formed after refolding. Finally, development of dedicated devices for fully automated and controlled microdialysis with online detection of aggregation and protein unfolding will pave the way for a more comprehensive understanding of the concept behind the ReFOLD assay.

6.6   Supplementary data

Determination of aggregation onset temperature with dynamic light scattering

25 µL of protein solution was filled in a 384 well plate (Corning) and the plate was centrifuged at 2200 rpm for 2 minutes using a Heraeus Megafuge 40 centrifuge equipped with an M-20 well plate rotor (Thermo Fisher Scientific, Wilmington, USA). Next, a drop of silicone oil was used to seal each well and the samples were centrifuged again at 2200 rpm for 2 minutes. Unless otherwise stated, the well plate was placed in a Dyna Pro DLS plate reader (Wyatt Technology, Santa Barbara, USA) and a temperature ramp of 0.25 °C/min was applied from 25 to 80 °C. During the temperature ramp, the samples were measured with 3 acquisitions of 3 seconds. The autocorrelation function (ACF) of each sample was calculated from the fluctuation of the light scattering intensity using the Dynamics V7.8 software. Cumulant analysis was performed with the same software to derive the apparent coefficient of self-diffusion (D) and the polydispersity index (PDI). Next, the apparent protein hydrodynamic radius from DLS (R_h) was calculated using the Stokes-Einstein equation. The aggregation onset temperature (Ton) from the increase in the R_h from DLS was determined using the Dynamics V7.8 software. All measurements were performed in triplicates.

Table S3. Relative Monomer Yield (RMY) of LMU-1 formulations after the ReFOLD assay and the relative content of high molecular weight species after long term storage of the respective LMU-1 formulations

Formulation number	Protein conc. [g/L]	Buffer	pH	RMY after refolding from 10 M urea			% HMW after 12 months at 25 °C			% HMW after 12 months at 4 °C		
1	10	histidine	5	0.401	0.387	0.372	0.21	0.23	0.18	0.11	0.14	0.21
2	10	histidine	5.75	0.378	0.365	0.390	0.15	0.18	0.17	0.25	0.17	0.17
3	10	histidine	6.5	0.269	0.272	0.265	0.38	0.55	0.41	0.27	0.21	0.37
4	10	citrate	5	0.239	0.243	0.240	0.47	0.53	0.53	0.34	0.30	0.30
5	10	citrate	5.75	0.17	0.164	0.169	0.79	0.66	0.72	0.32	0.43	0.34
6	10	citrate	6.5	0.153	0.166	0.157	0.91	0.85	1.06	0.57	0.65	0.60
7	50	histidine	5	0.098	0.097	0.092	0.67	0.72	0.72	0.43	0.47	0.51
8	50	histidine	5.75	0.082	0.079	0.088	0.87	0.89	0.83	0.54	0.67	0.55
9	50	histidine	6.5	0.003	0.009	0.002	1.66	1.61	1.55	0.90	0.93	0.94
10	50	citrate	5	0.065	0.074	0.074	0.93	0.93	1.07	0.39	0.51	0.41
11	50	citrate	5.75	0.036	0.030	0.039	1.08	1.13	1.24	0.57	0.61	0.60
12	50	citrate	6.5	0.022	0.023	0.017	1.68	1.73	1.86	1.08	1.02	0.93

Table S4. Relative Monomer Yield (RMY) of PPI03 formulations after the ReFOLD assay and the relative content of high molecular weight species, i.e. protein aggregates, after long term storage* of the respective PPI03 formulations. The concentration of PPI03 is 5 g/L in all 12 formulations.

Form. number	Buffer	pH	NaCl	RMY after refolding from 10 M urea			% HMW after 12 months at 25 °C			% HMW after 12 months at 4 °C		
1	histidine	5	No	0.519	0.535	0.553	0.11	0.11	0.14	0.16	0.16	0.14
2	histidine	5.75	No	0.47	0.47	0.495	0.15	0.13	0.13	0.15	0.13	0.14
3	histidine	6.5	No	0.514	0.474	0.461	0.18	0.18	0.18	0.14	0.16	0.16
4	histidine	5	70 mM	0.352	0.359	0.355	0.22	0.24	0.26	0.17	0.16	0.17
5	histidine	5.75	70 mM	0.334	0.338	0.335	0.23	0.24	0.24	0.17	0.17	0.17
6	histidine	6.5	70 mM	0.336	0.305	0.317	0.41	0.46	0.43	0.24	0.26	0.24
7	citrate	5	No	0.418	0.417	0.397	0.5	0.44	0.43	0.24	0.23	0.22
8	citrate	5.75	No	0.303	0.294	0.296	0.55	0.48	0.46	0.31	0.33	0.32
9	citrate	6.5	No	0.255	0.284	0.285	0.65	0.67	0.64	0.56	0.54	0.54
10	citrate	5	70 mM	0.431	0.399	0.421	0.5	0.45	0.48	0.24	0.23	0.22
11	citrate	5.75	70 mM	0.364	0.339	0.323	0.41	0.44	0.44	0.29	0.3	0.29
12	citrate	6.5	70 mM	0.337	0.346	0.353	0.63	0.63	0.6	0.55	0.55	0.56

*The relative content of high molecular weight species of PPI03 after storage was measured with the same SEC method described in materials and methods. However, the elution of the protein was detected with a Dionex RF2000 fluorescence detector (Thermo Fisher, Dreieich, Germany) using the following parameters - excitation at 280 nm, emission at 343 nm, gain 4.0 and medium sensitivity. There is a linear correlation ($R^2 > 0.98$) between the relative area of high molecular weight species of PPI03 detected by UV absorption at 280 nm and by intrinsic fluorescence (data not shown). However, in the case of PPI03 many of the samples contained less than 0.2 % aggregates and the use of the fluorescence detector provided a better signal-to-noise ratio compared to the UV detector.

Table S5. Monomer recovery of LMU-1 after 12 months of storage at 25 ⁰C and 4 ⁰C. The monomer recovery was calculated by dividing the area of the monomer peak in the SEC chromatograms after 12 months of storage by the area of the monomer peak at the beginning of the stability study, and finally multiplying this value by 100. A value of 100 % therefore indicates that the same monomer area was fond after storage, while a value lower than 100 % indicates that the area of the monomer was smaller.

Formulation number	Protein conc. [g/L]	Buffer	pH	SEC monomer recovery (%) after 12 months at 25 ⁰C		SEC monomer recovery (%) after 12 months at 4 ⁰C	
				Mean	StDev	Mean	StDev
1	10	histidine	5	99.96	0.05	100.54	0.22
2	10	histidine	5.75	100.91	1.46	100.24	0.08
3	10	histidine	6.5	100.43	1.14	99.99	0.14
4	10	citrate	5	101.23	0.65	101.18	0.20
5	10	citrate	5.75	100.15	0.66	100.13	0.38
6	10	citrate	6.5	99.94	0.17	100.02	0.18
7	50	histidine	5	96.15	1.17	99.50	0.54
8	50	histidine	5.75	96.34	0.41	99.56	0.25
9	50	histidine	6.5	95.48	1.20	99.06	0.26
10	50	citrate	5	95.29	1.05	97.94	0.24
11	50	citrate	5.75	95.38	0.51	98.36	0.41
12	50	citrate	6.5	95.36	0.22	97.68	0.77

Table S6. Monomer recovery of PPI03 after 12 months of storage at 25 ⁰C and 4 ⁰C. The monomer recovery was calculated by dividing the area of the monomer peak in the SEC chromatograms after 12 months of storage by the area of the monomer peak at the beginning of the stability study, and finally multiplying this value by 100. A value of 100 % therefore indicates that the same monomer area was fond after storage, while a value lower than 100 % indicates that the area of the monomer was smaller.

Formulation number	Buffer	pH	NaCl	SEC monomer recovery (%) after 12 months at 25 ⁰C		SEC monomer recovery (%) after 12 months at 4 ⁰C	
				Mean	StDev	Mean	StDev
1	histidine	5	No	99.57	0.57	100.15	0.36
2	histidine	5.75	No	98.87	0.37	99.48	0.20
3	histidine	6.5	No	99.14	0.10	98.97	0.40
4	citrate	5	70 mM	98.39	0.08	98.88	0.24
5	citrate	5.75	70 mM	99.21	1.50	98.77	0.45
6	citrate	6.5	70 mM	98.80	0.34	98.99	0.18
7	histidine	5	No	96.91	0.34	98.67	0.36
8	histidine	5.75	No	96.86	0.35	97.82	0.37
9	histidine	6.5	No	98.11	0.60	98.47	0.35
10	citrate	5	70 mM	96.78	0.45	98.19	0.62
11	citrate	5.75	70 mM	96.76	0.92	96.86	0.55
12	citrate	6.5	70 mM	98.32	0.53	98.67	0.79
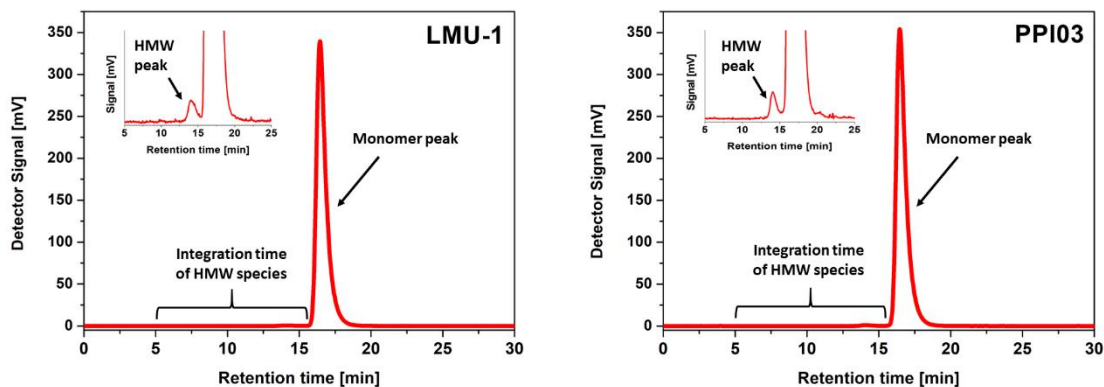
The % of high molecular weight (HMW) species after long-term storage is calculated using the following equation: HMW Species (%) = ((Area of HMW)/(Area of all peaks))*100

Figure S17. Representative chromatograms of LMU-1 and PPI03 obtained with the size-exclusion chromatography method used during the long-term stability studies. The area of high molecular weight (HMW) species is integrated between 5 and 15.1 minutes retention time. The protein monomer is integrated between 15.1 and 22 minutes.
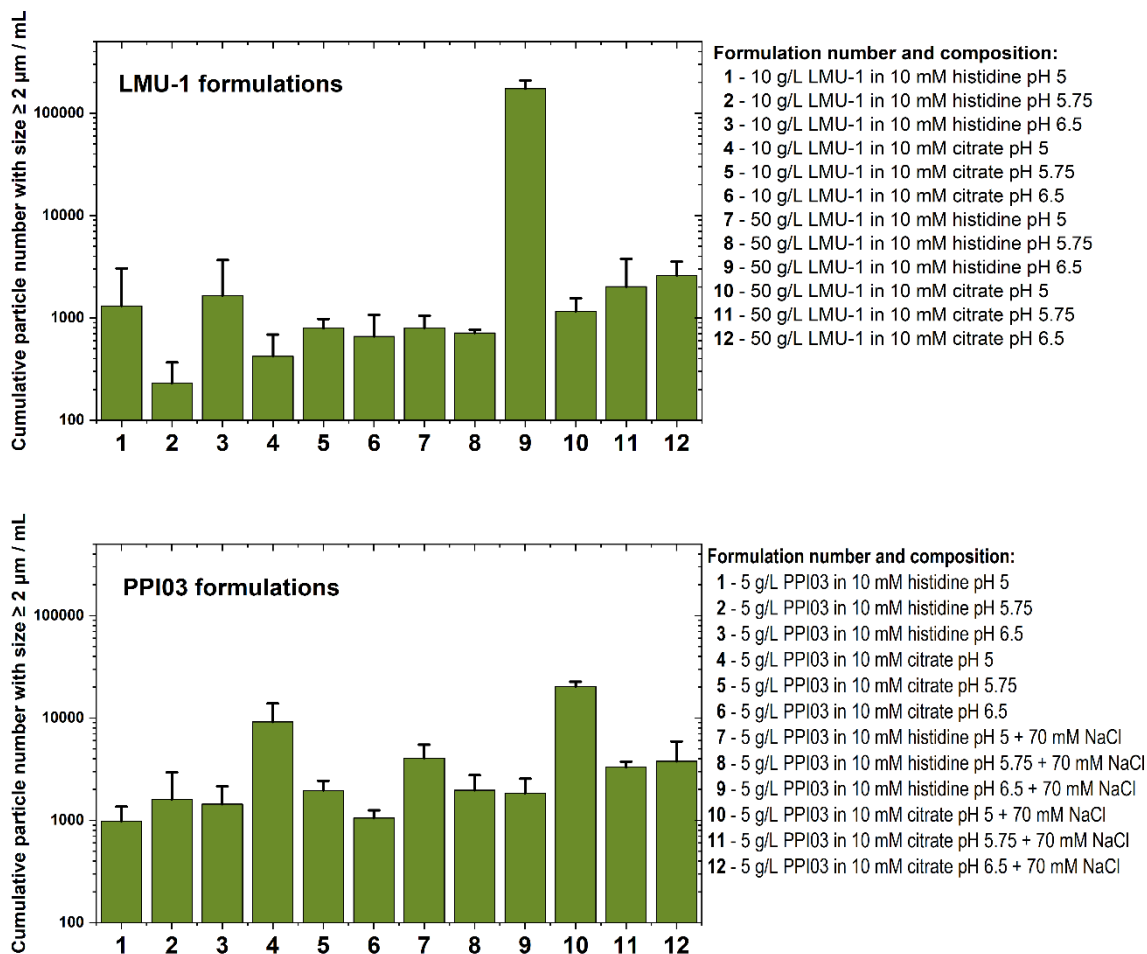
Figure S18. Subvisible particles in the LMU-1 and PPI03 formulations after 12 months of storage at 25 °C. The numbers represent cumulative particles larger than 2 μm in 1 mL. After 12 months of storage at 4 °C, all formulations contained less than 5000 particles ≥ 2 μm per mL (data not shown). The measurements were performed with a FlowCAM® 8100 (Fluid Imaging Technologies, Inc., Scarborough, ME, USA). The system was equipped with a 10x magnification cell (81 μm x 700 μm). Before each measurement, the cleanliness of the cell was checked visually. 200 μL of sample were used for the analysis and the images are collected with a flow rate of 0.15 mL/min, auto image frame rate of 29 frames/second and a sampling time of 74 seconds. The following settings were used for particle identification - 3 μm distance to the nearest neighbour, particle segmentation thresholds of 13 and 10 for the dark and light pixels respectively. The particle size was reported as the equivalent spherical diameter (ESD). The VisualSpreadsheet® 4.7.6 software was used for data collection and evaluation.
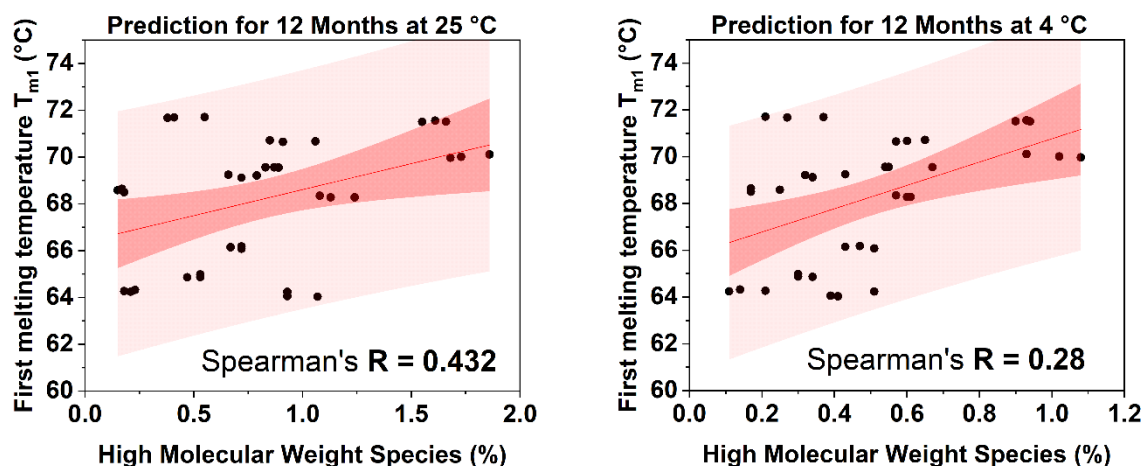
Figure S19. Correlation between the first melting temperature T_{m1} of LMU-1 and the relative content of high molecular weight species detected by size exclusion chromatography after 12 months of storage at 25 ⁰C (left) and at 4 ⁰C (right). The value of each replicate is shown on the graph. The solid red line is linear fit of the data, the dark red zone represents the 95 % confidence interval of the fit and the light red zone the 95 % prediction interval.
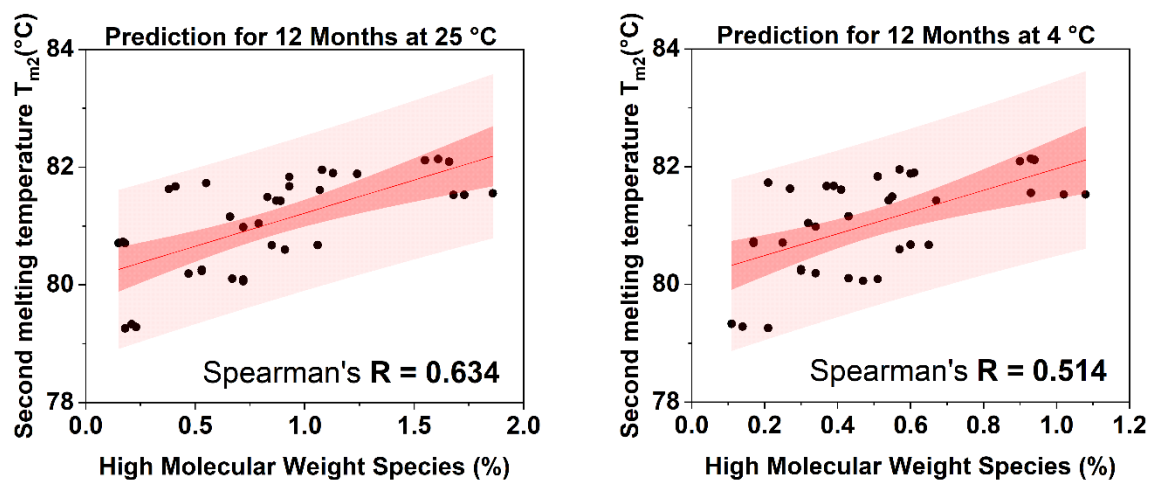
Figure S20. Correlation between the second melting temperature T_{m2} of LMU-1 and the relative content of high molecular weight species detected by size exclusion chromatography after 12 months of storage at 25 ⁰C (left) and at 4 ⁰C (right). The value of each replicate is shown on the graph. The solid red line is linear fit of the data, the dark red zone represents the 95 % confidence interval of the fit and the light red zone the 95 % prediction interval.
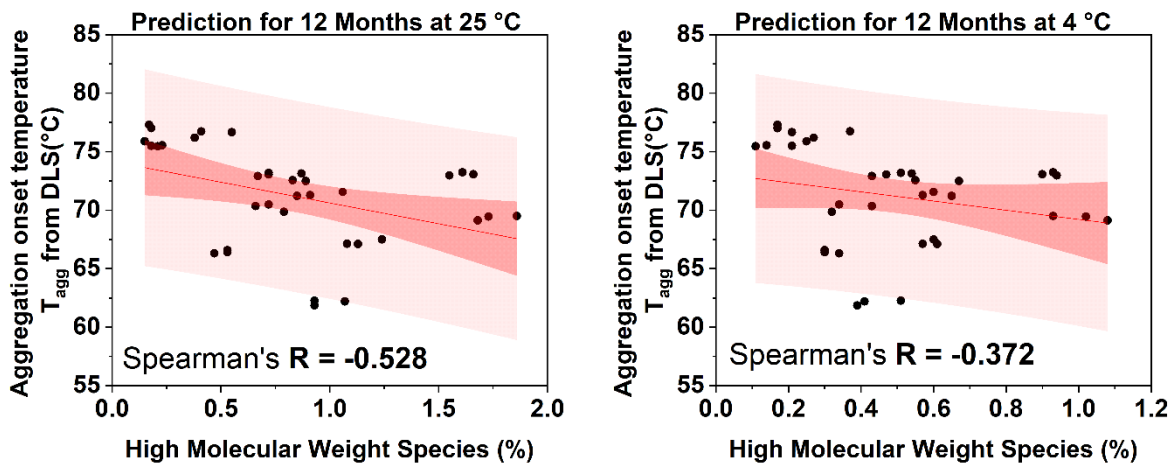
Figure S21. Correlation between the aggregation onset temperature from DLS of LMU-1 and the relative content of high molecular weight species detected by size exclusion chromatography after 12 months of storage at 25 °C (left) and at 4 °C (right). The value of each replicate is shown on the graph. The solid red line is linear fit of the data, the dark red zone represents the 95 % confidence interval of the fit and the light red zone the 95 % prediction interval.
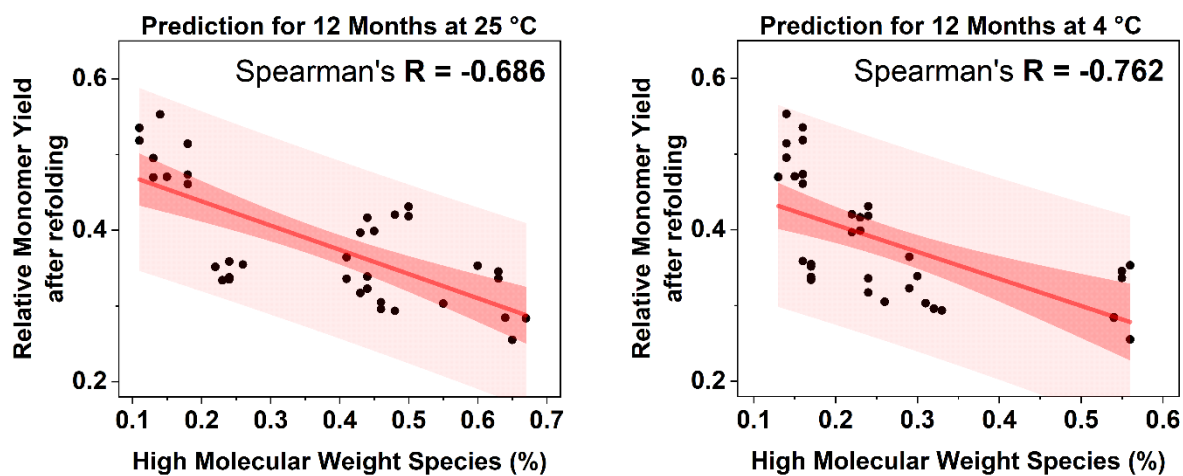
Figure S22. Correlation between the relative monomer yield of PPI03 from the ReFOLD assay and the relative content of high molecular weight species detected by size exclusion chromatography after 12 months storage at 25 °C (left) and at 4 °C (right). The value of each replicate is shown on the graph. The solid red line is linear fit of the data, the dark red zone represents the 95 % confidence interval of the fit and the light red zone the 95 % prediction interval.
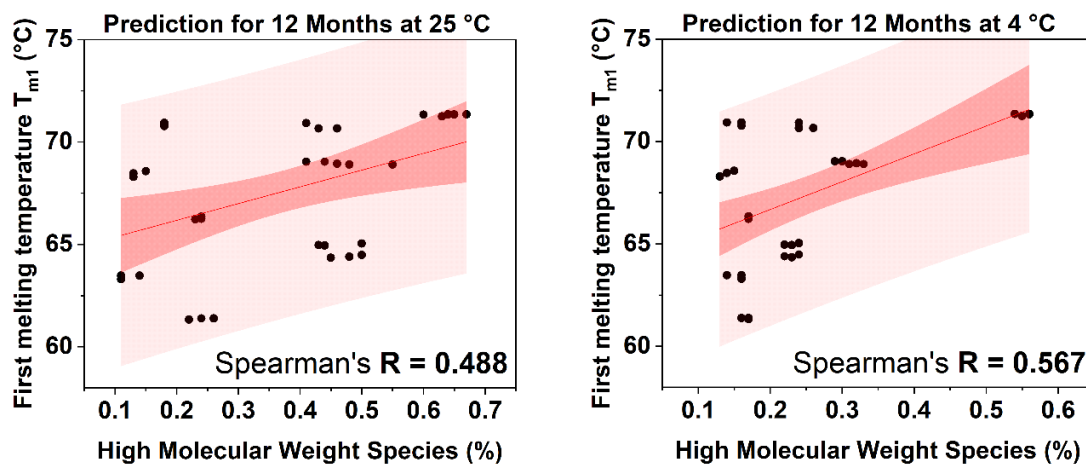
Figure S23. Correlation between the first melting temperature T_{m1} of PPI03 and the relative content of high molecular weight species detected by size exclusion chromatography after 12 months of storage at 25 °C (left) and at 4 °C (right). The value of each replicate is shown on the graph. The solid red line is linear fit of the data, the dark red zone represents the 95 % confidence interval of the fit and the light red zone the 95 % prediction interval.
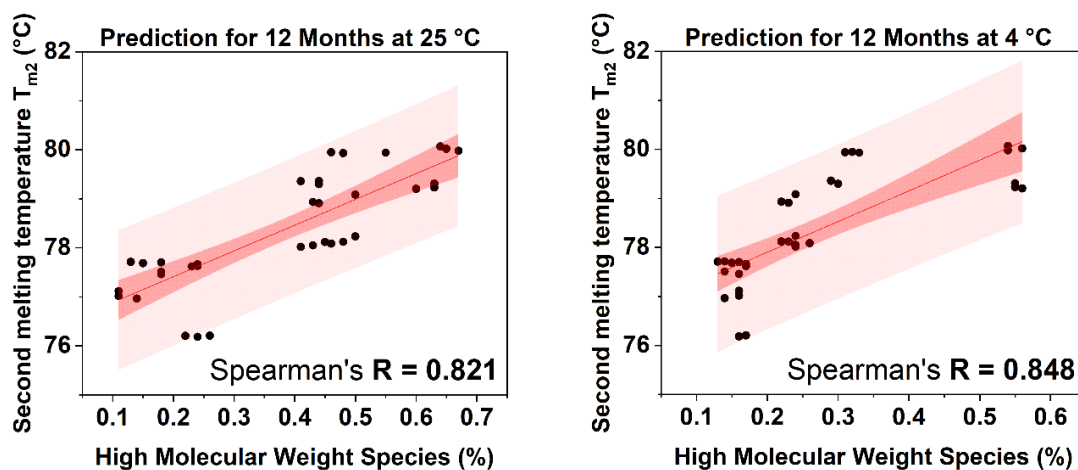
Figure S24. Correlation between the second melting temperature T_{m2} of PPI03 and the relative content of high molecular weight species detected by size exclusion chromatography after 12 months of storage at 25 °C (left) and at 4 °C (right). The value of each replicate is shown on the graph. The solid red line is linear fit of the data, the dark red zone represents the 95 % confidence interval of the fit and the light red zone the 95 % prediction interval.
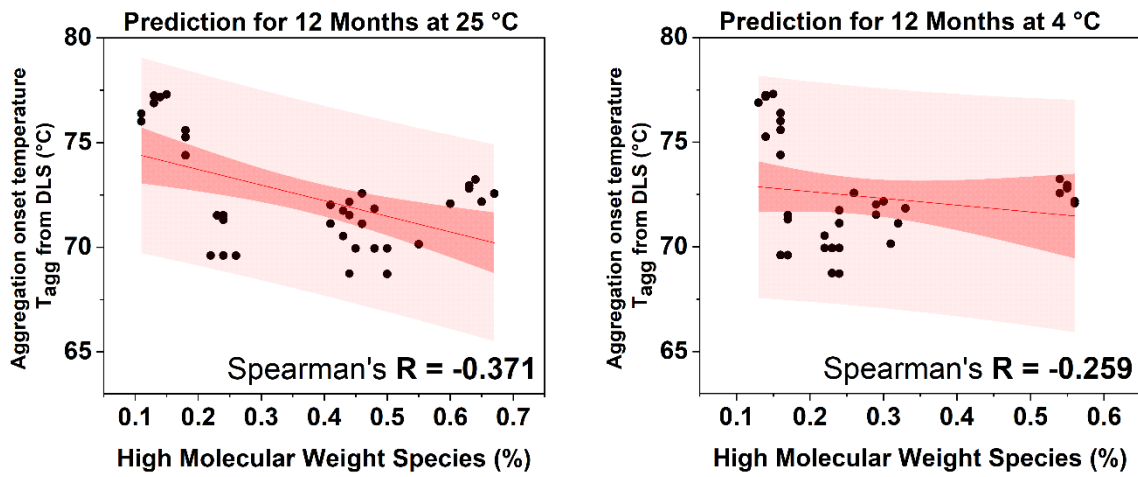
Figure S25. Correlation between the aggregation onset temperature from DLS of PPI03 and the relative content of high molecular weight species detected by size exclusion chromatography after 12 months of storage at 25 ºC (left) and at 4 ºC (right). The value of each replicate is shown on the graph. The solid red line is linear fit of the data, the dark red zone represents the 95 % confidence interval of the fit and the light red zone the 95 % prediction interval.
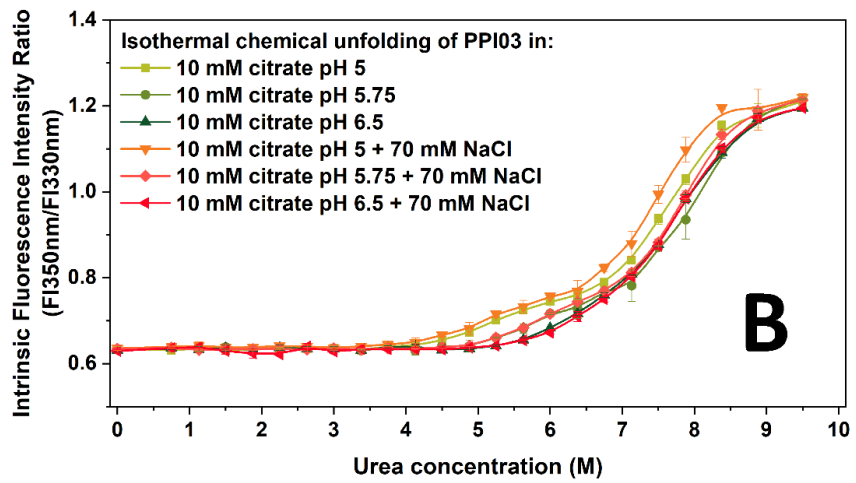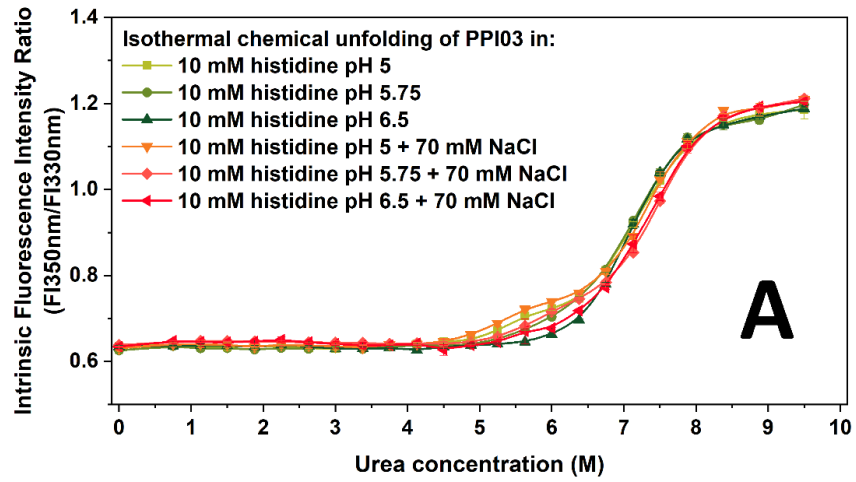
Figure S26. Isothermal unfolding curves of PPI03 in histidine (**A**) and citrate (**B**) buffer with different pH and different ionic strength. The symbols are means of triplicates and the bars represent the standard deviation. The lines are a guide to the eye. The protein concentration in all samples is 0.5 g/L.
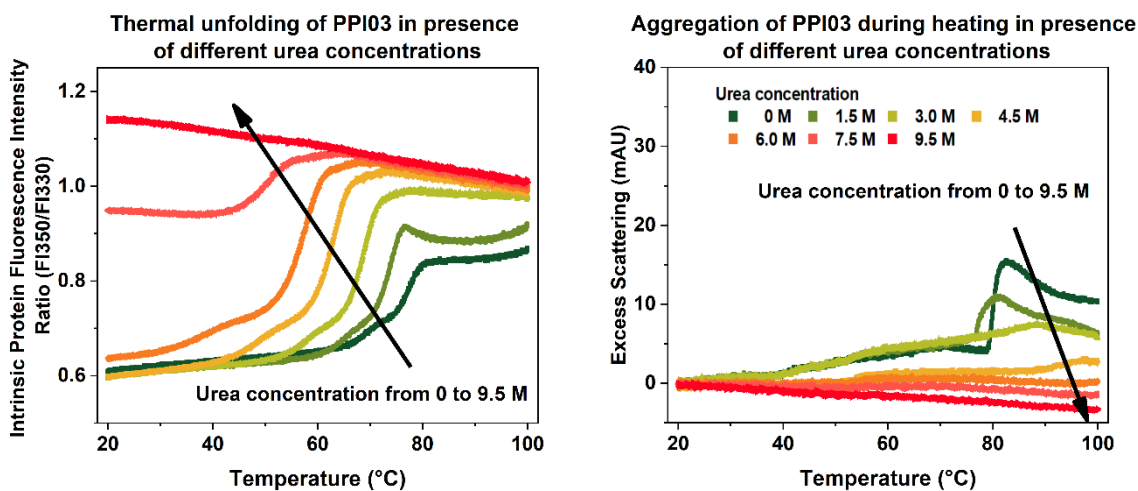
Figure S27. Thermal unfolding traces (left) and aggregation during unfolding (right) of PPI03 in presence of different concentrations of urea. The buffer is 10 mM histidine pH 6.5 with 70 mM sodium chloride. The protein concentration in all samples is 0.5 g/L.
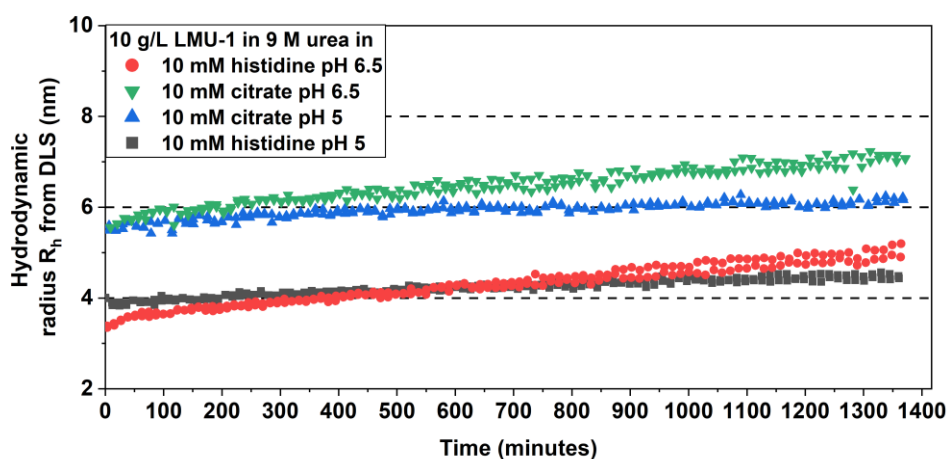
Figure S28. Isothermal aggregation of LMU-1 in presence of 9 M urea in different formulation conditions measured by the change in the apparent protein hydrodynamic radius from DLS. The samples are prepared, measured and evaluated as described in the Supplementary data. The measurements are performed at 25 °C with 5 acquisitions of 5 seconds. The samples are corrected for viscosity using a value of 1.93 cP for the 9 M urea solutions.
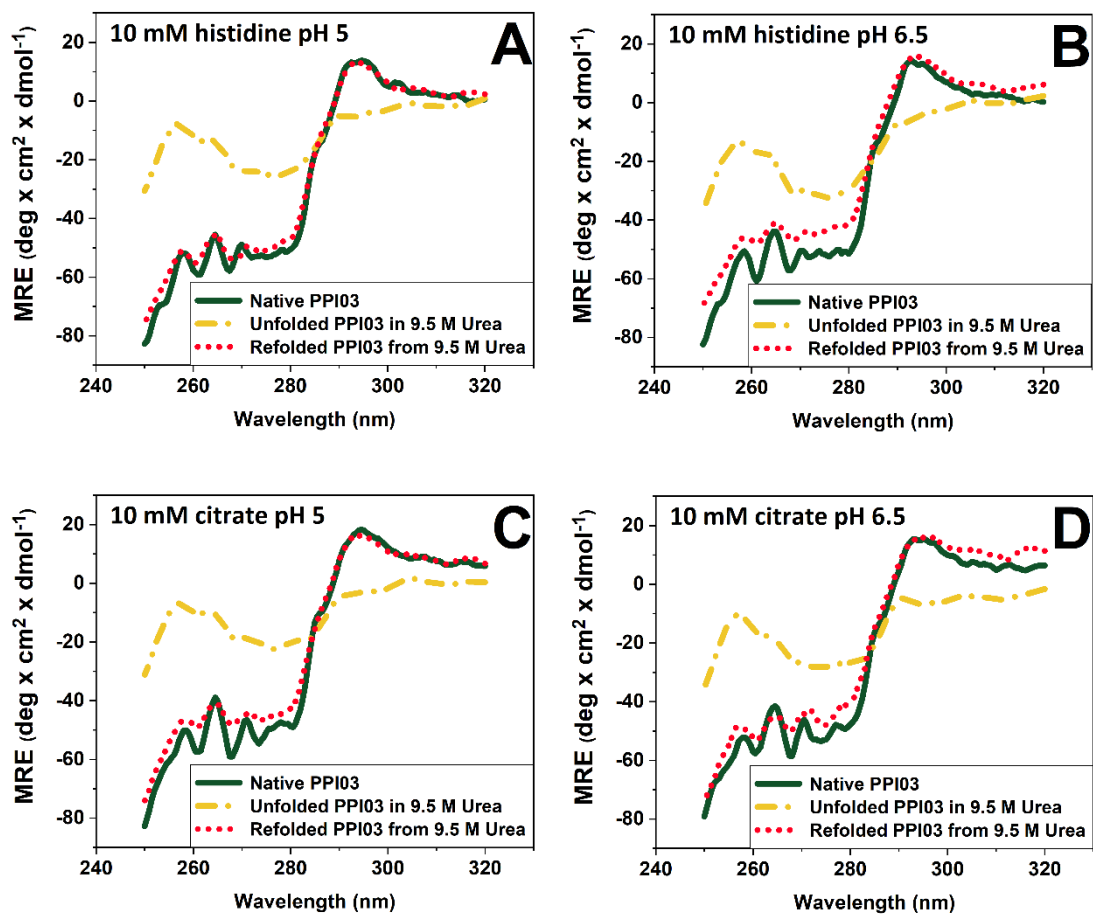
Figure S29. Near-UV CD spectra of PPI03 native (green solid line), unfolded with 10 M urea (yellow dot and dash) and refolded protein (red dot) after the ReFOLD assay was performed with 10 mM histidine pH 5 (**A**), 10 mM histidine pH 6.5 (**B**), 10 mM citrate pH 5 (**C**) and (**D**) 10 mM citrate pH 6.5.

Chapter 7 Orthogonal techniques to study the effect of pH, sucrose and arginine salts on monoclonal antibody thermal unfolding, aggregation and long-term storage stability

This chapter is prepared for submission and peer review as:

Svilenov, H.[*] and Winter, G.[*], Orthogonal techniques to study the effect of pH, sucrose and arginine salts on monoclonal antibody thermal unfolding, aggregation and long-term storage stability

[*]Department of Pharmacy, Pharmaceutical Technology and Biopharmaceutics, Ludwig-Maximilians-University, Butenandtstrasse 5-13, Munich D-81377, Germany

Author contributions:

H.S. performed the experiments, evaluated the data and wrote the manuscript. H.S. and G.W. conceived the presented idea and planned the experiments. G.W. provided conceptual guidance and corrected the manuscript.

7.1 Abstract

Additives like sucrose and arginine salts can have effects on protein long-term storage stability. Predicting these effects with prompt biophysical characterisation could accelerate the therapeutic protein development process. In this work, we apply several high-throughput methods to study the thermal unfolding and aggregation of a model antibody at pH 5 and pH 6.5 in the presence of 280 mM sucrose, 140 mM arginine hydrochloride, and 70 mM arginine glutamate. The colloidal protein stability is reduced upon addition of the arginine salts which results in reduced protein aggregation onset temperature, reduction in the interaction parameter k_D and lower relative monomer yield after refolding from urea. The low colloidal stability in the presence of arginine salts together with the thermal unfolding at a lower temperature at pH 5 concurs with the formation of subvisible particles during storage for 12 months at 25 ºC. 280 mM sucrose does not affect the colloidal protein stability, shifts the thermal protein unfolding to a higher temperature and increases the relative monomer yield after refolding from urea which agrees with a stabilising effect during long-term storage. This study shows how contemporary techniques for protein characterisation can be applied to select additives for stable therapeutic protein formulations.

Keywords - Proteins; Protein formulation; Protein folding; Protein unfolding; Protein Aggregation; Monoclonal antibody; Storage Stability; Stability prediction; Excipients;

Abbreviations - DLS - Dynamic Light Scattering; mAb - monoclonal antibody; nanoDSF™ - Microscale Differential Scanning Fluorimetry; RMY - Relative Monomer Yield after refolding; SEC - size exclusion chromatography; T_{agg} - Protein aggregation onset temperature from DLS; IP1 - Inflection point of the thermal unfolding transition at a lower temperature; IP2 - Inflection point of the thermal unfolding transition at a higher temperature; k_D - interaction parameter; A_2 - second osmotic virial coefficient; SLS – static light scattering;

7.2   Introduction

One fundamental aim during the development of therapeutic proteins is finding formulations that increase protein stability during long-term storage. Some of the critical variables in these formulations are solution pH, ionic strength, and the presence of additives. The additives usually belong to the group of sugars, polyols, amino acids or polymers[219,220]. Among these, sucrose is the most frequently used in marketed therapeutic protein formulations[219]. From the amino acids, arginine is of considerable interest as in some cases it can suppress protein aggregation or reduce the viscosity of highly concentrated protein solutions[221,222]. Also, the use of different arginine salts is a topic of intense research since the arginine counterion can determine the effect on protein stability[199,222–224].

Sucrose and arginine salts can affect the thermal protein unfolding and aggregation in different directions depending on the protein molecule[199,225–228]. Especially arginine can have complex effects on the protein unfolding, aggregate formation and aggregate growth[229]. The concentration of the additive is also essential but limited by the osmotic pressure of the formulation that typically should be close to physiological[230]. Many of the studies with sucrose and arginine salts observe effects on protein stability that depend on the additive concentration[199,225,226,228]. Often, 0.5-1 M of sucrose or arginine have beneficial effects on protein stability[8,169,225,231,232]. However, such solutions are hypertonic and thus unsuitable for the development of therapeutic protein formulations that will be injected undiluted in patients. Further, published work about the effect of additives on protein stability is typically not supported by long-term stability data to confirm that an additive will have a stabilising or destabilising effect during storage at temperatures relevant for therapeutic proteins.

Here, we apply high-throughput methods to study the effect of three additives, 280 mM sucrose, 140 mM arginine hydrochloride, and 70 mM arginine glutamate, on the thermal unfolding and aggregation of a model monoclonal antibody at pH 5 and pH 6.5. In addition, we assess the impact of the additives on the colloidal protein stability, and on the protein aggregation during refolding from urea using a new assay, named ReFOLD. Finally, we perform long-term stability for 12 months at 4 ºC and 25 ºC to see if the prompt biophysical characterisation can predict the effects of the additives on the protein storage stability.

7.3 Materials and methods

7.3.1 Monoclonal antibodies and chemicals

The monoclonal antibody PPI13 used in this work is a human IgG1κ with a molecular mass of 148.9 kDa and an isoelectric point around 9. The protein bulk solution is surfactant-free and contains 98 % monomer and 2 % dimer, assessed with size exclusion chromatography. The bulk buffer was exchanged to 10 mM histidine/histidine hydrochloride with pH 5, pH 5.75 and pH 6.5 using extensive dialysis as described earlier[182]. The absorption of PPI13 at 280 nm was measured with a Nanodrop 2000 UV spectrophotometer (Thermo Fisher Scientific, Wilmington, DE) and the protein concentration was calculated using the protein extinction coefficient. Stock solutions of the additives (sucrose, arginine hydrochloride, arginine glutamate, guanidine hydrochloride and sodium chloride) were prepared in the respective histidine buffer and spiked to the dialysed protein solution. All chemicals were high purity grade and were purchased from Sigma Aldrich (Steinheim, Germany), VWR International (Darmstadt, Germany) or Fisher Scientific (Schwerte, Germany). Highly purified water was used to prepare all solutions.

7.3.2 Long-term stability study

PPI13 samples with protein concentration 5 g/L in the respective buffer (or buffer plus additive) were sterile filtered with a 0.22 μm cellulose acetate filter, aseptically filled into sterilised DIN2R glass type I vials (MGlass AG, Germany), crimped with FluroTec® coated rubber chlorobutyl stoppers (West Pharmaceutical Services, USA), and stored at 4 ⁰C and 25 ⁰C for the desired time. Three different vials were used for the analysis of each condition and time.

7.3.3 Dynamic light scattering

Before DLS measurements, all samples were centrifuged at 10 000g for 10 minutes. Next, 10 μL of PPI13 solution with 5 g/L protein concentration unless otherwise stated were filled in a 1534 microwell plate (Aurora, Whitefish, USA). The plate was centrifuged at 2200 rpm for 2 minutes using a Heraeus Megafuge 40 centrifuge equipped with an M-20 well plate rotor (Thermo Fisher Scientific, Wilmington, USA). Each well was subsequently sealed with 5 μL silicon oil and the plate was centrifuged again. The samples were then measured on a DynaPro plate reader III (Wyatt Technology, Santa Barbara, USA) using 3 acquisitions of 3 seconds

during a linear temperature ramp of 0.1 °C/min from 25 to 85 ºC. The Dynamics V7.8 software was used to create autocorrelation functions (ACF) and to apply cumulant analysis giving the mutual self-diffusion coefficient (D) and the polydispersity index (PDI). The apparent protein hydrodynamic radius (R_h) was calculated with the Stokes-Einstein equation from the D and the sample viscosity. The sample viscosity was measured with a falling ball viscometer. The aggregation onset temperature (T_{agg}) was determined using the Dynamics V7.8 software from the R_h increase during heating.

To derive the interaction parameter k_D, PPI13 samples with different protein concentration (see the results section) were filled in 1534 microwell plates as described above. The samples were then measured at 25 ºC with 10 acquisitions of 5 seconds. The mutual self-diffusion coefficient D was calculated as described above and the following equation was used to extract k_D:

$$D=D_0(1+k_Dc)$$

where D_0 is the diffusion coefficient at infinite dilution and c is the protein concentration. All DLS measurements were performed in triplicates.

7.3.4   High-throughput Fluorimetric Analysis of Thermal Protein Unfolding

The thermal unfolding of 5 g/L PPI13 in different formulations was studied with nanoDSF®[116,117]. The samples were filled in standard glass capillaries, the capillaries were sealed and placed in a Prometheus® NT.48 (NanoTemper Technologies, Munich, Germany). The device was used to linearly change the sample temperature from 25 to 100 °C with a ramp of 0.1 °C/min. During the temperature increase, the intrinsic protein fluorescence intensity at 330 nm and 350 nm was measured after excitation at 280 nm. Simultaneously, the back-reflection intensity of a light beam that passes through the capillary was measured to detect protein aggregation/precipitation. The scattering signal was normalised to a value called "Excess Scattering". The fluorescence intensity ratio (F350/F330) was plotted versus temperature, and the first (IP1) and second (IP2) inflection points of the protein thermal unfolding curve were determined from the maxima of the first derivative using the PR.ThermControl V2.1 software (NanoTemper Technologies, Munich, Germany).

7.3.5 Isothermal unfolding and refolding with urea (ReFOLD assay)

The assay was performed as described earlier[182]. Briefly, 50 µL of 5 g/L PPI13 solution in the respective buffer (or buffer plus additive) were filled in Pierce™ microdialysis devices (3.5 kDa MWCO). The samples were dialysed in a deep well-plate against 1.5 mL of 9 M urea dissolved in the respective formulation buffer (or buffer plus additive). The urea solution was changed after 4 and 8 hours and the dialysis continued for 24 hours in total. Next, the PPI13 samples in 9 M urea were dialysed using the same procedure against 1.5 mL of the respective urea-free formulation buffer (or buffer plus additive). During dialysis, the deep well plate was agitated at 700 rpm with a Thermomixer Comfort (Eppendorf AG, Hamburg, Germany). Subsequently, the samples were collected from the dialysis devices, and the weight of each sample was added to 250 mg on a microbalance. Finally, the samples were centrifuged at 10 000g for 10 minutes, and the supernatant was used for further measurements.

7.3.6 Size exclusion chromatography

A Dionex Summit 2 system equipped with a UVD170U UV/Vis detector (Thermo Fisher, Dreieich, Germany) was used to inject PPI13 samples on a TSKgel G3000SWxl, 7,8x300 mm, 5 µm column (Tosoh Bioscience, Tokyo, Japan). The mobile phase with pH 7.0 consisted of 100 mM potassium phosphate, 200 mM sodium chloride and 0,05 % w/v sodium azide. The elution of the samples was detected at 280 nm. The chromatograms were collected and integrated with Chromeleon V6.8 (Thermo Fisher, Dreieich, Germany). The relative monomer yield (RMY) of the protein after isothermal unfolding/refolding in urea was calculated after dividing the area of the monomer peak of the refolded sample by the area of the monomer peak of the sample before unfolding/refolding[182]. The relative area of aggregates and the monomer recovery of PPI13 during long-term storage were calculated as earlier described[182].

7.3.7 Flow imaging microscopy

The subvisible particles formed during long-term storage of PPI13 were measured with a FlowCAM® 8100 (Fluid Imaging Technologies, Inc., Scarborough, ME, USA) equipped with a 10x magnification cell (81 µm x 700 µm). Particle images were obtained using 150 µL sample volume, a flow rate of 0.15 mL/min, an auto image frame rate of 29 frames/second and a sampling time of 74 seconds. The particle identification settings were 3 µm distance to the

nearest neighbour, particle segmentation thresholds of 13 and 10 for the dark and light pixels respectively. The particle size reported represents the equivalent spherical diameter (ESD). The data was collected and processed with the VisualSpreadsheet® 4.7.6 software.

7.4 Results and discussion

7.4.1 Effect of pH and additives on the thermal unfolding and aggregation of PPI13

PPI13 shows two unfolding transitions detected by the change in the intrinsic protein fluorescence ratio (Fig 42A). These transitions correspond well to the temperatures of circular dichroism changes in the near-UV protein spectra (Fig S30).
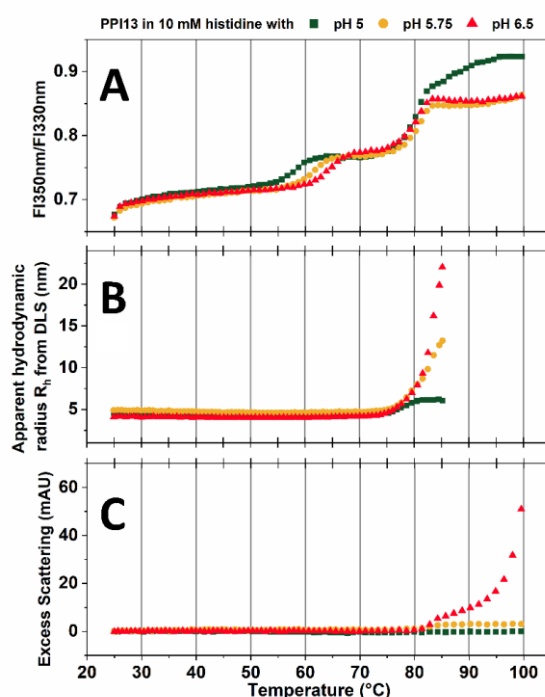
Figure 42. Simultaneous thermal unfolding and aggregation of 5 g/L PPI13 in 10 mM histidine with pH 5 (**squares**), 5.75 (**circles**) and 6.5 (**triangles**) assessed by the change in the (**A**) intrinsic protein fluorescence intensity ratio from nanoDSF®, (**B**) apparent hydrodynamic radius R_h from DLS, and (**C**) the excess scattering from nanoDSF®; In A and C the datapoint density is reduced to improve clarity.

Increasing pH from 5 to 6.5 shifts the inflection point of the first unfolding transition to a higher temperature, while the effect on the second inflection point is minimal. At pH 5, the protein aggregation onset temperature measured with dynamic light scattering is around 78 ºC and the R_h does not become larger than 7-8 nm up to 85 ºC (Fig 42B). Correspondingly, no precipitation

137

or formation or large aggregates is detected with the Prometheus NT.48® up to 100 ºC (Fig 42C). At pH 6.5, the T_{agg} from DLS is slightly lower (76.7 ºC), and the sample R_h and excess scattering rapidly increase which indicates the formation of large aggregates and precipitation (Figs 42B and 42C). Such pH dependence of thermal unfolding and aggregation is already reported for several monoclonal antibodies[54,116,140,233]. We then focused on the effect of several additives on the stability of PPI13 at pH 5 and pH 6.5 since the protein behaves differently in these conditions concerning its thermal unfolding and aggregation. The addition of 280 mM sucrose shifts the inflection points of the unfolding transitions and the aggregation onset to a slightly higher temperature independent of pH and without affecting the aggregate growth (Figs 43 and 44) (for values see Table 6). The stabilisation effect of sucrose is known and can be explained by preferential exclusion[140,233–236].
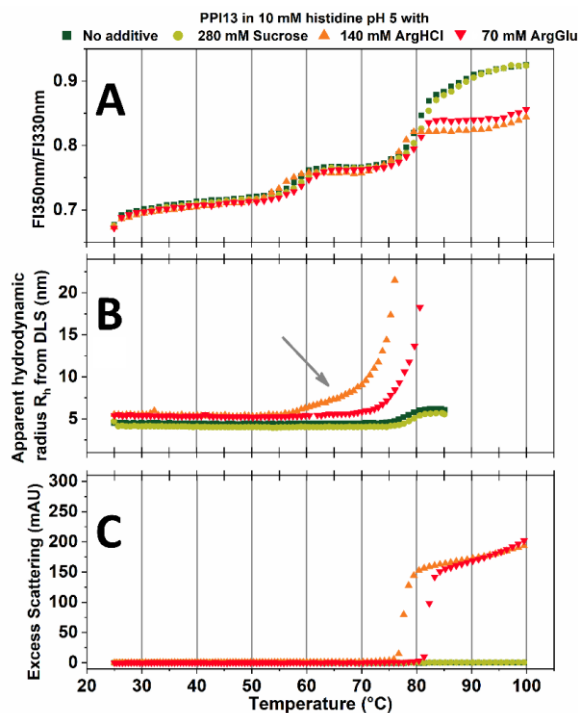
Figure 43. Simultaneous thermal unfolding and aggregation of 5 g/L PPI13 in 10 mM histidine pH 5 with no additive (**squares**), 280 mM sucrose (**circles**), 140 mM arginine hydrochloride (**triangles up**), 70 mM arginine glutamate (**triangles down**) assessed by the change in the (**A**) intrinsic protein fluorescence intensity ratio from nanoDSF®, (**B**) apparent hydrodynamic radius R_h from DLS, and (**C**) the excess scattering from nanoDSF®; In A and C the datapoint density is reduced to improve clarity.

Contrary to sucrose, the addition of 140 mM arginine hydrochloride at pH 5 shifts the protein aggregation onset and the inflection points of both unfolding transitions to lower temperatures (Figs 43 and 44) (Table 6). 70 mM arginine glutamate has a more complex effect on the stability of PPI13 at pH 5, reducing the aggregation onset temperature, but in most cases slightly increasing the temperature of both thermal unfolding inflection points (Table 6). The addition of arginine salts causes the formation of larger protein aggregates at pH 5 (Figs 43B and 43C). At pH 6.5, 140 mM arginine hydrochloride and 70 mM arginine glutamate affect the T_{agg}, IP1 and IP2 of PPI13 in a similar direction but with a smaller magnitude compared to pH 5 (Table 6). The early onset of protein aggregation induced by ArgHCl at pH 5 (indicated by an arrow in Fig 43B) is not observed at pH 6.5. Our findings agree well with published data about the effect of arginine hydrochloride on the thermal unfolding of other proteins[47,226,237].
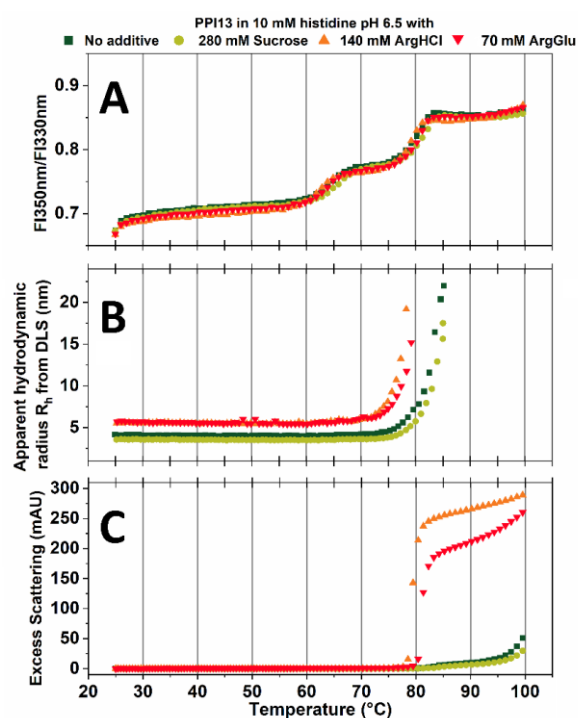
Figure 44. Simultaneous thermal unfolding and aggregation of 5 g/L PPI13 in 10 mM histidine pH 6.5 with no additive (**squares**), 280 mM sucrose (**circles**), 140 mM arginine hydrochloride (**triangles up**), 70 mM arginine glutamate (**triangles down**) assessed by the change in the (**A**) intrinsic protein fluorescence intensity ratio from nanoDSF®, (**B**) apparent hydrodynamic radius R_h from DLS, and (**C**) the excess scattering from nanoDSF®; In A and C the datapoint density is reduced to improve clarity.

The unfavourable effect of arginine salts on the aggregation onset temperature of PPI13 encouraged us to further investigate how the additives affect the colloidal protein stability.

Table 6. Stability-indicating parameters of PPI13 in 10 mM histidine buffer with pH 5 and pH 6.5 in presence of different additives.

	Additive	From nanoDSF®		From DLS		
		IP1, °C	IP2, °C	T_{agg}, °C	k_D (mL/g)	D_0 (cm^2/s)
pH 5	No	**58.2** ±0.05	**80.17** ±0.07	**78.11** ±0.29	**34.20**	4.70E-07
	280 mM Sucrose	**59.32** ±0.06	**81.04** ±0.05	**78.86** ±0.14	**16.70**	4.16E-07
	140 mM ArgHCl	**55.43** ±0.06	**76.99** ±0.03	**60.76** ±0.86	**-13.90**	4.48E-07
	70 mM ArgGlu	**59.7** ±0.09	**80.37** ±0.01	**73.32** ±0.24	**-11.10**	4.48E-07
pH 6.5	No	**64.33** ±0.1	**80.11** ±0.04	**76.68** ±0.38	**27.30**	5.01E-07
	280 mM Sucrose	**65.86** ±0.11	**81.24** ±0.03	**77.38** ±0.42	**10.40**	4.62E-07
	140 mM ArgHCl	**62.25** ±0.06	**78.97** ±0.04	**73.26** ±0.50	**-15.80**	4.55E-07
	70 mM ArgGlu	**63.84** ±0.02	**80.36** ±0.01	**74.11** ±0.45	**-16.80**	4.47E-07

7.4.2 Effect of additives on the colloidal stability of PPI13

Dynamic light scattering was used to study the effect of the additives on the colloidal stability of PPI13. In 10 mM histidine buffer with pH 5 and pH 6.5, the mutual diffusion coefficient of the protein increases with an increase in protein concentration (Fig 45). The addition of 280 mM sucrose does not change the sign of this concentration dependence. However, when 140 mM arginine hydrochloride or 70 mM arginine glutamate is added, the mutual diffusion coefficient of the protein decreases with protein concentration (Fig 45). This effect can be explained with the increase in ionic strength upon addition of the arginine salts which leads to screening of the electrostatic repulsion between the protein molecules[57]. We also used the data in Fig 45 to derive the interaction parameter k_D of PPI13 in these formulations (Table 6). Here, we would like to make a note that the k_D values obtained at pH 6.5 without arginine salts could be overestimated due to the low ionic strength of the solution[59], but their sign should not be affected. To confirm the observations in Fig. 45, we used microwell plate-based static light scattering method to measure second virial coefficients A_2 of PPI13 in presence of the additives and found good agreement between k_D and A_2 (Figure S31) that is already reported earlier[56].
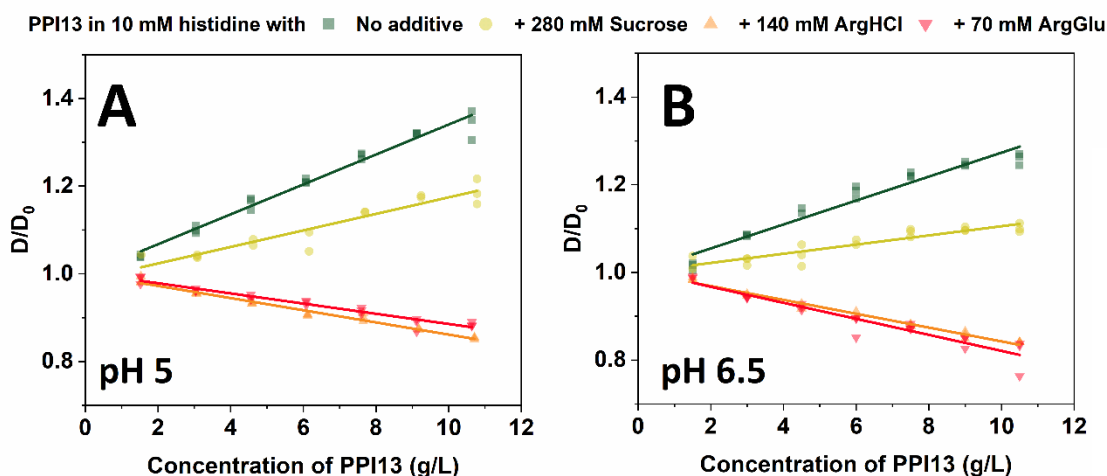
Figure 45. Concentration dependence of the mutual diffusion coefficient of PPI13 at pH 5 (**A**) and pH 6.5 (**B**) in presence of no additive (**squares**), 280 mM sucrose (**circles**), 140 mM arginine hydrochloride (**triangles up**) and 70 mM arginine glutamate (**squares down**). The data is overlay of triplicates. The lines present a linear fit to the points.

Based on the k_D and A_2 data we could confirm that the addition of both arginine salts reduces the repulsive protein interactions, thus reducing the colloidal stability of PPI13 which corresponds well with the lower aggregation onset temperatures (Table 6) and the larger aggregate growth at pH 5 (Figs 43B and 43C). 280 mM Sucrose has a much smaller effect on the k_D and A_2 of PPI13 compared to the arginine salts (Tables 6 and S7).

7.4.3 Do arginine salts reduce the colloidal and thermal stability of PPI13 only due to an increase in ionic strength?

Looking for a better understanding how the additives affect the stability of PPI13, we assessed the IP1, IP2, T_{agg}, k_D and A_2 of PPI13 in guanidine hydrochloride and sodium chloride solutions having the same molar concentration as the arginine salts used above (Table S7). Both 140 mM guanidine hydrochloride and 140 mM sodium chloride cause PPI13 unfolding and aggregation at a lower temperature in a similar way to arginine hydrochloride (Table S7). Although there are some differences between the effects of ArgHCl, GuHCl and NaCl, these results indicate that the negative impact on PPI13 is not exclusively due to the arginine cation but also due to an increase in ionic strength and subsequent reduction in the colloidal protein stability. Interestingly, 70 mM arginine glutamate has a less negative impact on the thermal protein

unfolding and aggregation compared to 70 mM guanidine hydrochloride or 70 mM sodium chloride. This indicates once again the advantage of ArgGlu over ArgHCl but also raises the question of whether ArgGlu is superior to ArgHCl due to the glutamate counterion or ArgHCl is inferior to ArgGlu due to the chloride ion. A hint about the answer to this question can be found in a recent study showing that arginine acetate stabilises proteins as good as arginine glutamate and that both are better than arginine hydrochloride[224]. In addition, we measured the osmotic pressure of the solutions. The osmolarity of the formulations with all salts tested corresponds to the expected osmolarity of strong binary electrolytes (Table S8), indicating that the ionic strength of formulations including salts with the same molar concentration will be similar. Small differences from the expected osmolarity were observed in some cases, e.g. for arginine hydrochloride and guanidine hydrochloride. These differences could be due to the way of interaction of the excipients with the protein[238]. In future, we will explore if we can use vapour pressure osmometry to assess quantitatively the interaction of the additives with PPI13.

7.4.4 Effect of additives on the aggregation during refolding of PPI13

We recently developed an unfolding/refolding assay, named ReFOLD, that can be used to assess the aggregation of urea-induced partially unfolded protein species[182]. We applied this assay to see whether the additives tested here suppress the aggregation of the partially unfolded protein at pH 5 and pH 6.5. The 9 M concentration of urea was selected since it causes significant perturbations in the protein structure as shown by the change in the circular dichroism protein spectra (Fig S32). Also, 280 mM sucrose, 140 mM ArgHCl and 70 mM ArgGlu can be dissolved in this urea concentration.

After isothermal unfolding and refolding of PPI13, there is a significant reduction in the monomer peak detected by size exclusion chromatography (Fig 46A). This decrease is due to protein aggregation during refolding from urea as we reported earlier for two other monoclonal antibodies[182]. We then calculated the relative monomer yield (RMY) after refolding and observed that the RMY was lowest when the refolding was performed at pH 5 in the presence of 140 mM ArgHCl or 70 mM ArgGlu (Fig 46B). This corresponds well with the detrimental effect of these salts on the colloidal stability of PPI13. The addition of 280 mM sucrose results in higher RMY at both pH 5 and pH 6.5 which agrees with the stabilising effect of this sugar during thermal denaturation of PPI13 (Figs 46B and 46C). In addition, the mean values of

RMY are slightly higher at pH 6.5 compared to their counterparts at pH 5. That concurs with the other stability-indicating parameters measured earlier at these pH values (Table 6). The near-UV CD spectra of the refolded PPI13 resembled the spectra of the native PPI13 in all formulation that we tested (Fig S32).
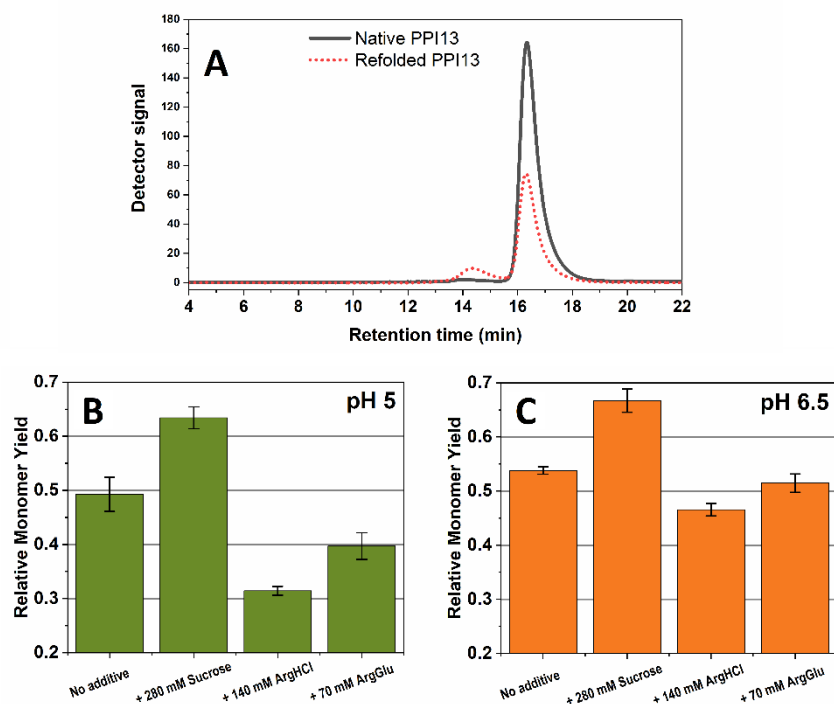
Figure 46. (**A**) SEC chromatogram of native and refolded PPI13 in 10 mM histidine pH 5. In a separate experiment, the peak at 14.2 minutes was identified as a dimer using SEC coupled to multi-angle light scattering. Relative monomer yield of PPI13 when the protein is refolded from 9 M urea at pH 5 (**B**) and pH 6.5 (**C**) with no additive, 280 mM sucrose, 140 mM arginine hydrochloride or 70 mM arginine glutamate. The values in B and C are mean of triplicates, the error bar is the standard deviation.

The results that arginine salts reduce the relative monomer yield after refolding from urea might appear surprising at first since arginine is often used at high concentrations (i.e. 0.5-1.0 M) to suppress aggregation during refolding[239]. However, the formulations of PPI13 present an interesting case. As we showed earlier, PPI13 has high colloidal stability at low ionic strength in 10 mM histidine with pH 5 or pH 6.5. The addition of salts in concentration 70-140 mM negatively affects the colloidal protein stability and reduces the repulsive protein-protein interactions as shown by the reduction in the interaction parameter k_D and the aggregation onset

temperature (Tables 6 and S7). Published work shows that the protein-protein interactions are directly linked to the aggregation during refolding of some proteins[169,240]. This reveals that the effects of additives on the protein colloidal stability should be carefully considered from case to case to have a better understanding why specific concentrations of some additives have a negative impact on protein aggregation during heating and refolding.

7.4.5 Effect of additives on the aggregation during long-term stability of PPI13

The stability of PPI13 during long-term storage at 4 ºC and 25 ºC was assessed with size exclusion chromatography and flow imaging microscopy. PPI13 presents a peculiar case in which the amount of soluble aggregates detected by SEC remained constant or decreased a little bit during storage (Fig S33). These aggregates were present in the bulk solution which has about ten-fold higher protein concentration than the 5 g/L we used in our stability studies. The observation with SEC that the amount of soluble aggregates in the samples does not increase after storage were confirmed with dynamic light scattering (data not shown). Future work can focus on the aggregation mechanism and type of aggregates formed by PPI13, and how the aggregation depends on protein concentration.

A decrease in the monomer recovery of PPI13 was observed after storage which indicated a loss of soluble protein probably due to the formation of larger aggregates that are filtered out by the SEC column (Fig 47). The decrease in monomer recovery was more pronounced at pH 5 compared to pH 6.5, and during storage at 25 ºC compared to 4 Cº. The formulations including 280 mM sucrose showed the highest recovery at both storage temperatures and both at pH 5 and pH 6.5. Interestingly, the formulations with 70 mM arginine glutamate had monomer recoveries close to 100 % at pH 6.5 but not at pH 5.

We confirmed our hypothesis for the monomer loss due to the formation of larger aggregates by observing the formation of subvisible particles in PPI13 formulations (Fig 48). At pH 5, the two arginine salts induced the formation of the largest number of particles in all three size ranges. 280 mM sucrose reduced the number of particles formed at pH 5 compared to no additive. These results concur well with the monomer recovery in Fig 47A. At pH 6.5 the particle counts were very low independent of the presence of additives. The samples stored at 4 ºC showed very low particle numbers at both pH 5 and pH 6.5, and no clear difference between effect of different additives could be observed (Fig S34).

144
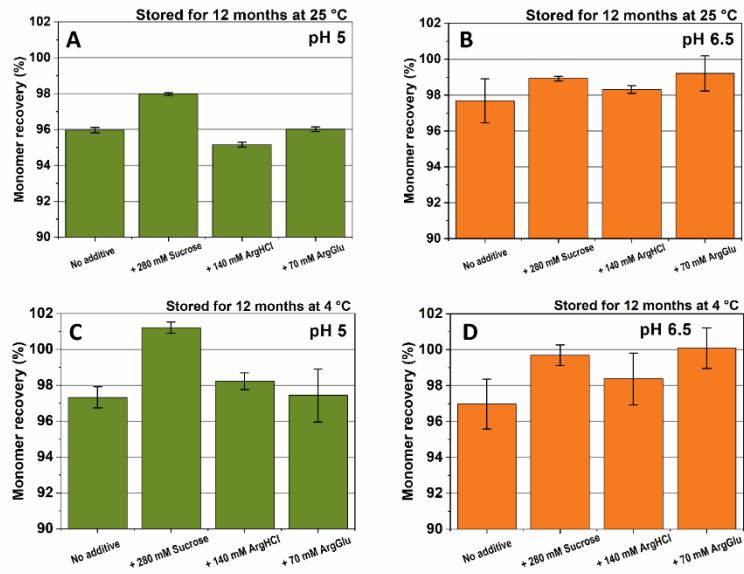
Figure 47. Effect of additives on the monomer recovery of PPI13 from size exclusion chromatography after 12 months of storage. (**A**) storage at 25 ºC at pH 5, (**B**) storage at 25 ºC at pH 6.5, (**C**) storage at 4 ºC at pH 5, (**D**) storage at 4 ºC at pH 6.5;
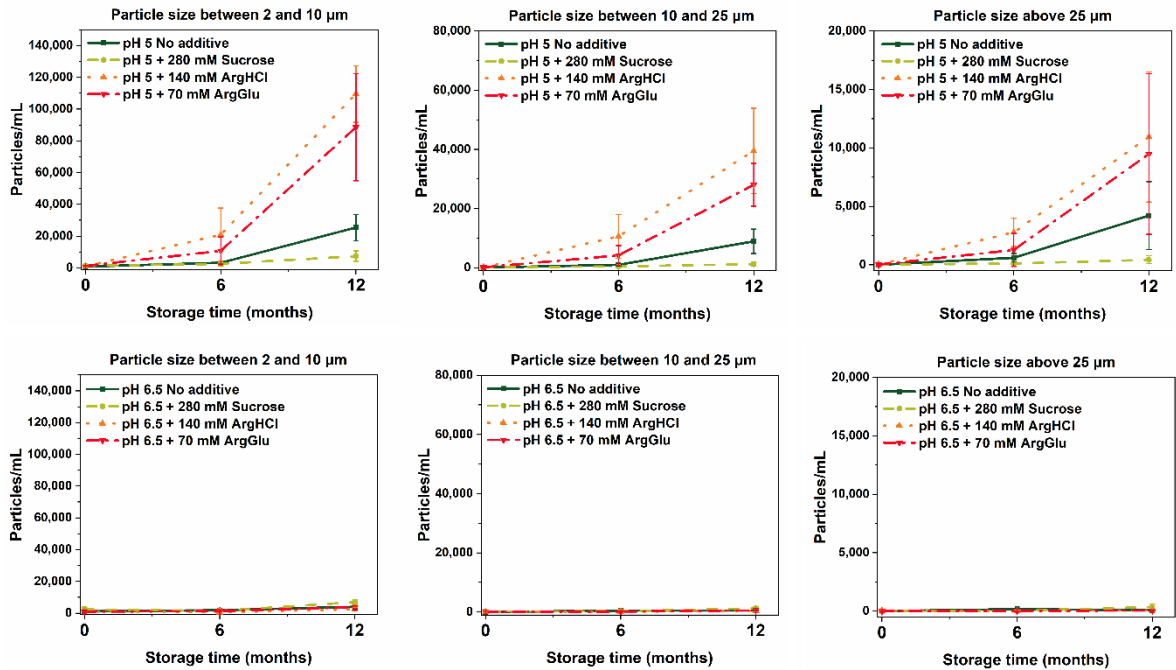
Figure 48. Subvisible particles of PPI13 measured during storage for 12 months at 25 ºC

7.4.6 Correlation between stability-indicating parameters and long-term stability

To conclude the study, we looked for correlations between the different biophysical parameters and the monomer recovery and particle numbers after long-term storage at 25 °C. Almost all parameters indicated that the formulations comprising arginine salts at pH 5 will have inferior stability compared to others. The rankings from the first thermal unfolding inflection point and the relative monomer yield after refolding from urea showed the strongest correlation with long-term stability data (Fig S35). In general, some of the correlations (Fig S35 – A, B, C, D, E) are weak due to the low particle numbers and small differences between most of the formulations that causes the points to cluster in a narrow range. The least stable formulations during long-term storage were the two formulations where the protein unfolds at lower temperature and has the lowest aggregation onset temperature, the lowest relative monomer yield after refolding from urea, and a negative interaction parameter k_D. 280 mM sucrose increase the temperature of thermal unfolding and the relative monomer yield after refolding from urea at pH 5. This corresponds well to the stabilising effect of sucrose observed during storage compared to no additive. Many of the formulations, e.g. at pH 6.5, exhibit high monomer recovery and low particle numbers independent of the presence of an additive. It remains an open question, whether a difference between these formulations would be seen after longer storage time. Here, we should note that the although the strength of the correlations in Fig S35 differ, there was good agreement between the stability-indicating techniques, and they were all useful for identifying the two PPI13 formulations that were least stable during long-term storage. Taking a decision which protein formulations should (or should not) be developed is easier in cases like this due to the consensus between the stability-indicating techniques.

An interesting observation is that during long-term stability studies with PPI13 we did not detect an increase in the amount of soluble aggregates but found that the protein aggregates by forming large particles which contributes to monomer loss. When the protein is refolded from 9 M urea using the ReFOLD assay, we observe substantial monomer loss but only a small increase in the soluble aggregates, identified as dimers (Fig 46). For a comparison, two other antibodies form much more soluble aggregates with various sizes after refolding from urea[182]. These results indicate that the aggregation mechanisms of PPI13 during long-term storage and during refolding from urea in different formulations are probably similar.

146

7.5 Conclusion

In this work, we applied orthogonal high-throughput techniques to probe the effect of 280 mM sucrose, 140 mM arginine hydrochloride and 70 mM arginine glutamate on the stability of a monoclonal antibody named PPI13. We found good agreement between various parameters showing that sucrose stabilises the protein, while arginine salts in this concentration reduce the colloidal protein stability at both pH 5 and pH 6.5. This reduction can be explained with the increase in ionic strength and the screening of electrostatic repulsion between the protein monomers. We also performed long-term stability studies to validate the observations from the prompt biophysical characterisation. The two parameters that show the strongest correlation with the long-term stability data are the temperature of the first thermal unfolding inflection point and the relative monomer yield after isothermal refolding from urea. Formulations in which PPI13 unfolds at lower temperature and has low colloidal stability are the formulations in which a considerable amount of subvisible particles were formed after 12-month storage at 25 ºC. Our work is important in two directions. First, it shows that the effect of additives on the long-term stability of PPI13 can be predicted with the biophysical techniques used here. And second, we show that a more comprehensive approach is needed to predict whether arginine salts will inhibit or promote aggregation. Although arginine can undoubtedly bring benefits in formulations where the short-ranged hydrophobic interactions are important (e.g. at high protein concentration), arginine salts can have a detrimental effect on the protein colloidal stability in protein formulations where electrostatic repulsion is important to suppress protein aggregation (e.g. dilute protein solutions with low ionic strength).

7.6   Supplementary data

	Additive	From nanoDSF®		From DLS			From SLS
		IP1, °C	IP2, °C	T_{agg}, °C	k_D (mL/g)	D_0 (cm^2/s)	A_2 (mol.mL/g^2)
pH 5	No	**58.2** ±0.05	**80.17** ±0.07	**78.11** ±0.29	34.20	4.70E-07	3.6296E-4
	280 mM Sucrose	**59.32** ±0.06	**81.04** ±0.05	**78.86** ±0.14	16.70	4.16E-07	3.9649E-4
	140 mM ArgHCl	**55.43** ±0.06	**76.99** ±0.03	**60.76** ±0.86	-13.90	4.48E-07	2.5636E-5
	140 mM GuHCl	**54.41** ±0.05	**76.21** ±0.01	**60.35** ±0.93	-15.40	4.66E-07	2.1202E-5
	140 mM NaCl	**55.25** ±0.02	**76.78** ±0.04	**57.37** ±0.08	-33.40	4.56E-07	-7.8494E-5
	70 mM ArgGlu	**59.7** ±0.09	**80.37** ±0.01	**73.32** ±0.24	-11.10	4.48E-07	1.0445E-4
	70 mM GuHCl	**55.55** ±0.03	**77.5** ±0.05	**65.76** ±0.89	-16.50	4.67E-07	1.7217E-5
	70 mM NaCl	**55.95** ±0.04	**77.81** ±0.04	**61.13** ±0.18	-28.70	4.55E-07	-1.7224E-5
pH 6.5	No	**64.33** ±0.1	**80.11** ±0.04	**76.68** ±0.38	27.30	5.01E-07	2.8685E-4
	280 mM Sucrose	**65.86** ±0.11	**81.24** ±0.03	**77.38** ±0.42	10.40	4.62E-07	4.4982E-4
	140 mM ArgHCl	**62.25** ±0.06	**78.97** ±0.04	**73.26** ±0.50	-15.80	4.55E-07	2.3052E-5
	140 mM GuHCl	**61.93** ±0.07	**78.1** ±0.08	**71.76** ±0.29	-18.70	4.72E-07	1.4398E-5
	140 mM NaCl	**63.33** ±0.06	**79.3** ±0.03	**71.46** ±0.62	-35.70	4.63E-07	-1.9252E-4
	70 mM ArgGlu	**63.84** ±0.02	**80.36** ±0.01	**74.11** ±0.45	-16.80	4.47E-07	2.6366E-5
	70 mM GuHCl	**62.95** ±0.02	**79.13** ±0.11	**72.08** ±0.53	-24.70	4.73E-07	-1.1819E-5
	70 mM NaCl	**64.08** ±0.14	**79.2** ±0.05	**69.75** ±0.72	-40.80	4.61E-07	-9.2413E-5

Table S7. Stability indicating parameters of PPI13 at pH 5 and pH 6.5 in the presence of different additives

Additive	No	280 mM sucrose	140 mM ArgHCl	140 mM GuHCl	140 mM NaCl	70 mM ArgGlu	70 mM GuHCl	70 mM NaCl
pH 5	13 (±5.5)	287 (±2.3)	244 (±3.5)	261 (±5.6)	274 (±1.5)	138 (±6.7)	138 (±2.9)	143 (4.6)
pH 6.5	2 (±1)	294 (±7.8)	235 (±5.7)	259 (±3.8)	254 (±2.5)	123 (±3.8)	134 (±4.5)	134 (±5.5)

Table S8. Osmolarity of 5 g/L PPI13 solutions in 10 mM histidine buffer with pH 5 and pH 6.5 including different additives. The values are mean of triplicates, the error is the standard deviation. The osmolarity was measured with a VAPRO® Vapor Pressure Osmometer using 10 µL sample volume. The device was calibrated before use according to the manual from the manufacturer.

Circular dichroism (CD) spectroscopy method used in this work:

The 5 g/L PPI13 solution was filled in a quartz cuvette with 1 mm wavelength path and placed in a Jasco J-810 spectrometer (JASCO Deutschland GmbH, Pfungstadt, Germany). The sample temperature was increased with a gradient of 0.1 ºC/min. In 10 ºC interval, the near-UV spectra were collected with 3 accumulations and a speed of 20 nm/min. The spectra we smoothed using Savitzky-Golay algorithm with 9 smoothing points and plotted against temperature.
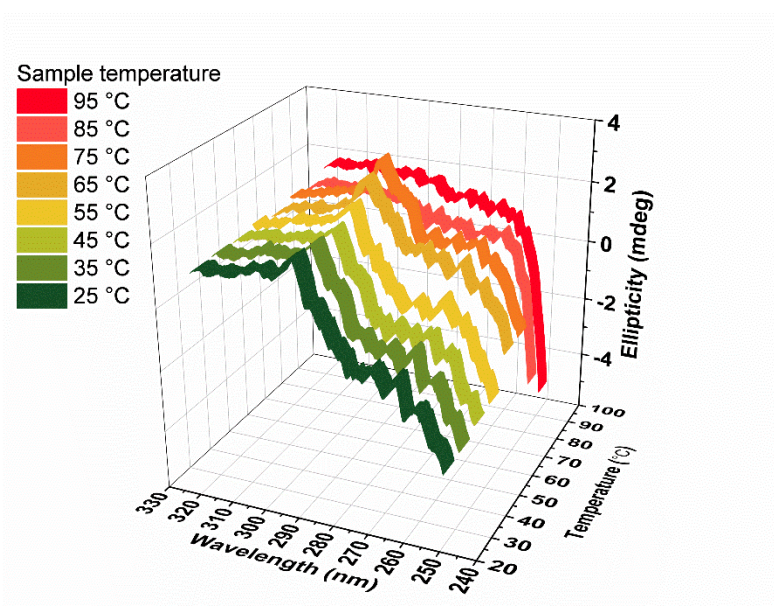
Figure S30. Near-UV CD spectra of 5 g/L PPI13 in 10 mM histidine pH 5 at different temperatures.

Static light scattering method used in this work:

Different concentrations of PPI13 in the respective buffer and additive were filled in 1532 microwell plates as described for the dynamic light scattering measurements. The static light scattering measurements were performed with the DynaPro plate reader III using 2 % laser power, 0 % attenuation level and 30 acquisitions of 3 seconds. The light scattering of the pure buffers without protein was measured to determine the solvent offsets. The microwell plate was calibrated using concentration series of dextran solutions with known molecular weight and second virial coefficient.
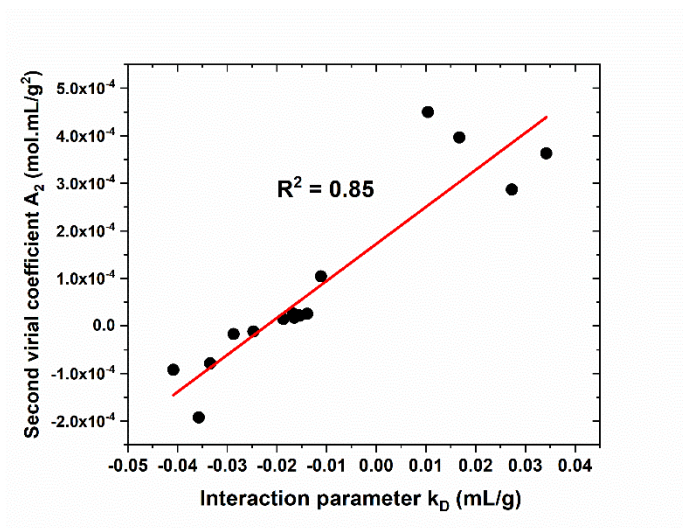
Figure S31. Correlation between the interaction parameter k_D from dynamic light scattering and the second virial coefficient A_2 from static light scattering.
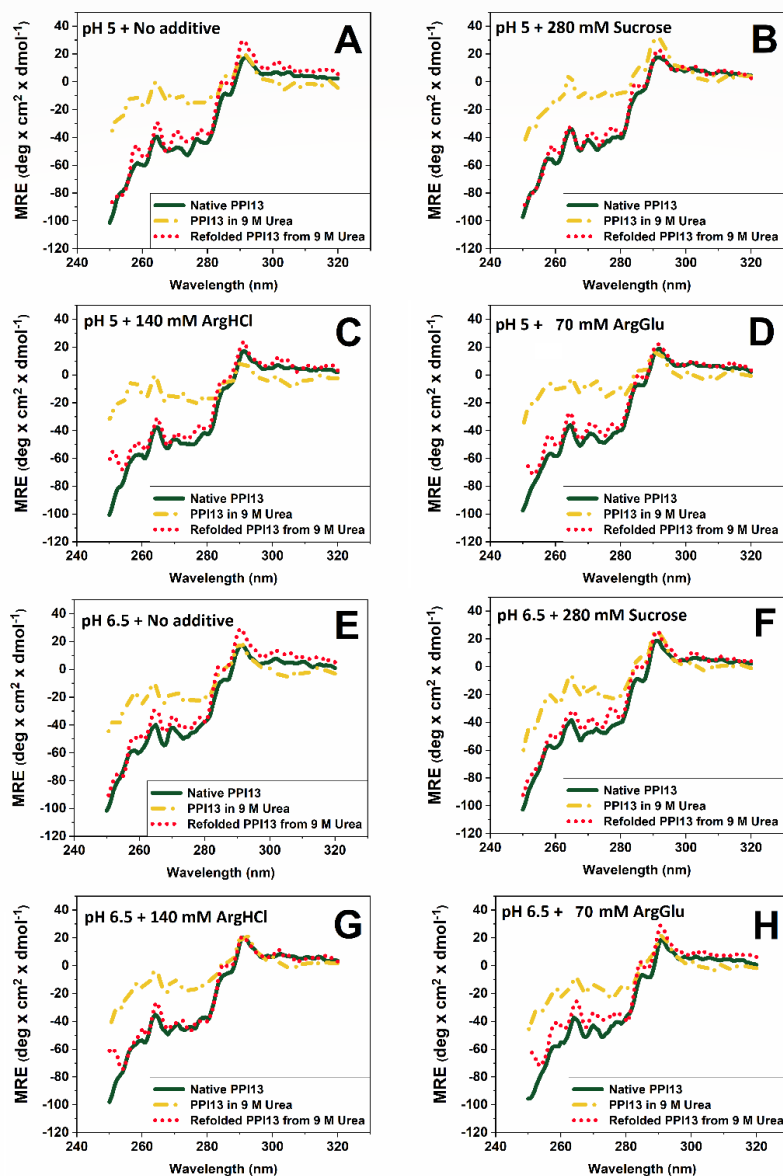
Figure S32. Effect of pH and additives on the near-UV CD spectra of native PPI13 (green line), PPI13 incubated for 24 hours in 9 M urea (yellow dash and dot), and PPI13 refolded from 9 M urea (red dots). (**A**) pH 5 with no additive; (**B**) pH 5 with 280 mM sucrose; (**C**) pH 5 with 140 mM arginine hydrochloride; (**D**) pH 5 with 70 mM arginine glutamate; (**E**) pH 6.5 with no additive; (**F**) pH 6.5 with 280 mM sucrose; (**G**) pH 6.5 with 140 mM arginine hydrochloride; (**H**) pH 6.5 with 70 mM arginine glutamate; *The addition of 9 M urea perturbs the structure of PPI13 as seen by the change in the near-UV CD spectra (yellow dash and dot). The refolded PPI13 (red dots) has the typical near-UV CD spectrum of the native protein (green line) in all tested formulations.*
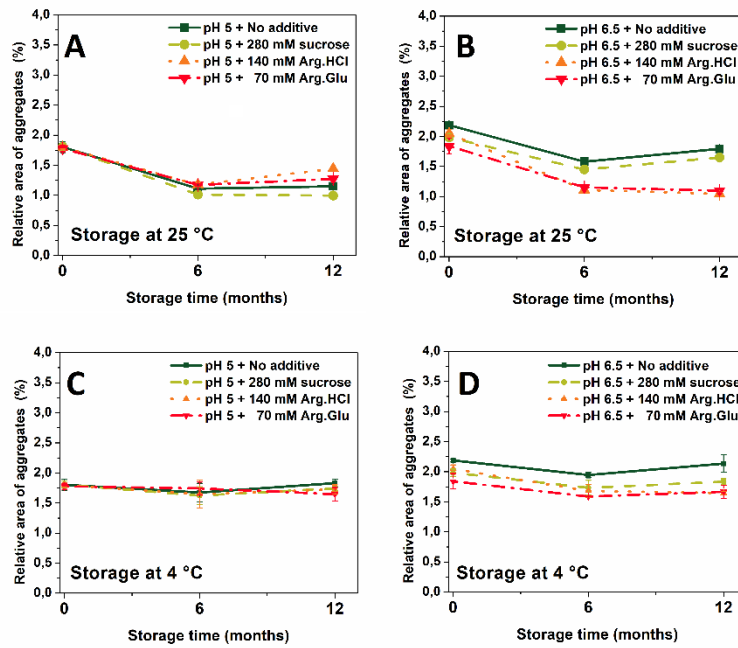
Figure S33. Relative area of aggregates detected by size exclusion chromatography during storage of PPI13 with different additives at (**A**) 25 ºC and pH 5, (**B**) 25 ºC and pH 6.5, (**C**) 4 ºC and pH 5, (**D**) 4 ºC and pH 6.5.
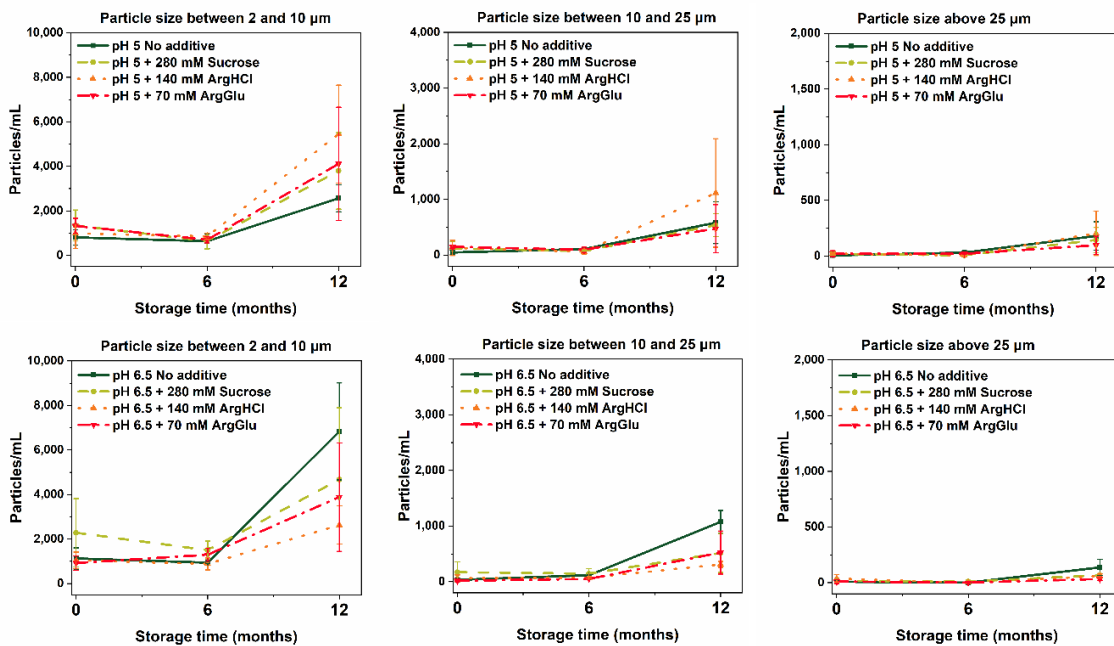
Figure S34. Subvisible particles of PPI13 measured during storage for 12 months at 4 ºC
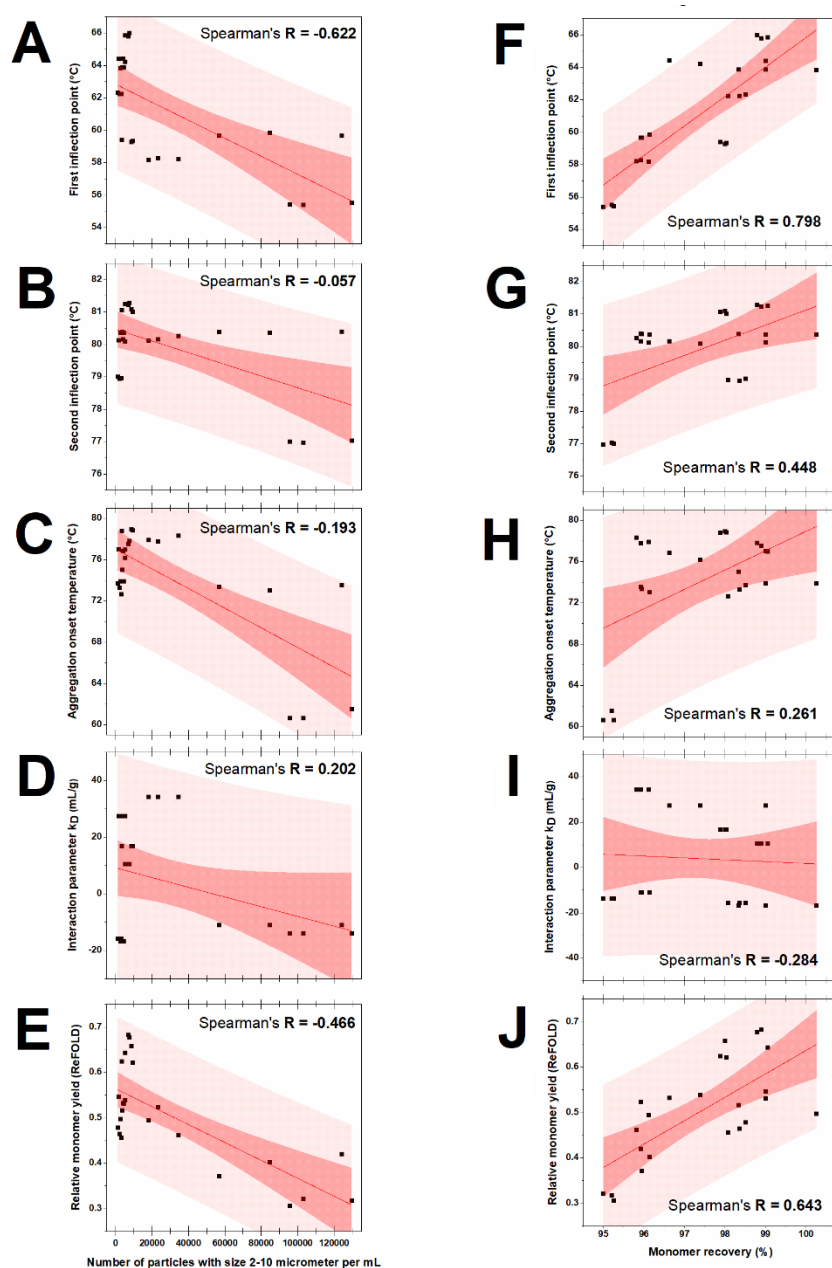
Figure S35. Correlations between long-term stability data and stability indicating parameters and long-term stability data obtained after storage for 12 months at 25 C. Correlation between the number of subvisible particles after storage and (**A**) the first thermal unfolding inflection point, (**B**) the second thermal unfolding inflection point (**C**) the aggregation onset temperature, (**D**) the interaction parameter k_D, (**E**) the relative monomer yield after refolding from 9M urea; Correlation between the monomer recovery after storage and (**F**) the first thermal unfolding inflection point, (**G**) the second thermal unfolding inflection point (**H**) the aggregation onset temperature, (**I**) the interaction parameter k_D, (**J**) the relative monomer yield after refolding from 9M urea;

Chapter 8 **Summary of the thesis**

The primary aim of this thesis was to investigate whether techniques used for prompt biophysical characterisation can be used to accurately rank and select therapeutic protein formulations stable during long-term storage.

In *Chapter 1*, I started the thesis with a brief overview of protein stability from the perspective of a protein formulation scientist. This chapter can serve as an introduction to people that are new to the topic and that want to learn about the various aspects that must be considered to obtain a stable protein formulation. In *Chapter 2*, I applied some of the state-of-the-art protein characterisation techniques on interferon alpha2a. Using these techniques and a systematic approach I selected four leading formulations and performed long-term stability studies on them. The formulation indicated as most stable by the largest number of stability-indicating parameters was also the most stable during long-term storage. I then moved to *Chapter 3*, where I discussed some disadvantages of the thermal denaturation techniques. I demonstrated that using these methods on formulations that exhibit a change in their properties (i.e. pH) during heating can lead to misleading stability rankings. These findings also explained some observations in the literature that proteins have lower melting temperatures in histidine buffer compared to acetate and citrate buffer, for example. To tackle the problems arising from sample heating, I developed a microwell plate-based method for isothermal chemical denaturation in our laboratory and applied it to investigate non-reversibility unfolding effects (i.e. the concentration dependence of the Gibbs free energy of unfolding) and by this to find antibody formulations stable during storage. Encouraged by the agreement between storage stability data and the non-reversibility effects measured with isothermal chemical denaturation, I started *Chapter 4* in which I studied the aggregation of two antibodies after dilution from different concentrations of a denaturant. I showed that there is a connection between several stability-indicating parameters and the level of aggregation after refolding by dilution in different formulations. Based on the results in Chapter 4, I developed a hypothesis that the aggregation of the partially folded proteins will depend on the formulation conditions. *In Chapter 5*, I prove this hypothesis by systematically studying the effect of denaturants on the unfolding and aggregation of an antibody. I demonstrate with orthogonal techniques that a

partially unfolded antibody exhibits more aggregation at pH 6.5 compared to pH 5. I then show that the aggregation of the partially unfolded protein in the presence of denaturants agrees well with the aggregation of the protein during isothermal refolding from denaturants. From these observations, I assumed that the aggregation during refolding from urea in different formulations could be used to rank formulations in order of their effect on the aggregation of the protein during long-term storage. To study this, in *Chapter 6*, I develop a microdialysis-based unfolding/refolding assay, named ReFOLD. I show that the parameters obtained from the ReFOLD assay correlate very well with the aggregation of two antibodies, each in 12 different formulations, during storage at 4 ºC and 25 ºC. Until that point, most of the work in this thesis was focused on the effect of pH, buffer type, ionic strength and protein concentration. Besides these variables, another essential part of formulation development is the inclusion of additives. Such additives are typically sugars or amino acids, and their effect on protein stability can be either positive or negative. To cover this aspect, I included Chapter 7 in which I investigate the effect of sucrose and arginine salts on the stability of a model antibody. A combination of complementary techniques, including the newly developed ReFOLD assay, was able to determine and explain the effect of these additives on the different aspects of protein stability and the predictions were confirmed by long-term stability data. The thesis is concluded with this summary and general suggestions for rational therapeutic protein formulation approach.

This thesis is relevant to both basic and applied research as it shows several protein formulation case studies. Most of the techniques I used require small sample amounts which makes the approaches presented here especially interesting for people involved in the early-stage development of therapeutic protein candidates. Also, the presented ReFOLD assay is a new stability-predicting tool that can become an integral part of protein formulation design and the concept behind it carries the potential of many creative follow-up studies. The part of the thesis which is rarely seen in published work and therefore carries particularly high value are the comparisons between stability-indicating parameters and long-term stability data after storage at 4 ºC and 25 ºC of the proteins in different formulations.

A rational approach to develop protein formulations stable during long-term storage

Stepping into formulation studies of a new therapeutic protein raises two questions:

1. What techniques should be used? and 2. What formulation variables should be studied?

Regarding the first question, the main message from this thesis is that no single technique can provide a reliable prediction for protein aggregation in all cases. Attempts to correlate a single parameter to long-term stability data will sometimes succeed and sometimes fail depending on the protein. The best formulation approach is to apply a combination of several orthogonal methods to study the protein thermal unfolding, aggregation, colloidal stability, monomer recovery after refolding, and, if necessary, other relevant parameters like viscosity. An approach that employs a combination of many techniques in the very early-stage development of proteins was unthinkable several years ago since many of the methods like differential scanning microcalorimetry required large sample amounts and suffered from low throughput. Fortunately, the technological progress has greatly decreased the sample volume and increased the throughput of most machinery enabling us to make the formulation development of therapeutic proteins more efficient.

Regarding the second question, as discussed in Chapter 1, protein formulation is a compromise. Much like in diplomacy, the formulation scientists are looking for conditions where all aspects of protein stability are satisfied. This compromise can be achieved by optimising several formulation variables. These variables are typically solution pH and ionic strength; the type and concentration of buffer, osmolytes, surfactants, antioxidants; protein concentration; and the primary package. Some directions how to investigate these variables are listed below:

Study the effect of pH - A successful and effective pH screen starts with a sound theoretical preparation before the experiments. Most of the chemical changes that I briefly discussed in Chapter 1 are greatly accelerated at very acidic or basic pH. This means that typically only the pH range of 3.5 to 8.0 is feasible for long-term protein storage at 4 ºC and 25 ºC. Good knowledge of the molecule can narrow this pH range even more. For example, if the protein under development is an IgG1 antibody, it is known that the optimal pH range for storage of these proteins is between 5 and 7. Next, several complementary techniques can be applied to

study the unfolding and aggregation of the protein in the selected pH range. If the sample amount is limited, a combination of sample-saving high-throughput techniques like the ones used in Chapter 2 can be applied. In case more sample is available, isothermal methods like isothermal chemical denaturation (Chapter 3) and isothermal refolding from denaturant (Chapter 6) can be used. The aim during the pH screen is to discard formulations that have very low melting and aggregation onset temperatures, as well as formulations that have low Gibbs free energy of unfolding or low monomer yield after refolding from urea. Although it is difficult to define a threshold for these values that will be valid for all proteins, one could, for example, adopt an approach where the worst 25-50 % of all formulations are discarded.

Study the effect of different buffers – After the pH range (±1 pH unit) of optimal stability is defined, different buffer systems must be tested. The main requirement is to select buffers that have a high buffer capacity in the desired pH range. To keep the ionic strength of the buffer low, the buffer concentration typically should be low (e.g. $\leq$ 50 mM) and the final pH should be achieved by combining the appropriate amounts of the two buffer components. Further, the buffer molecules are not inert towards the protein and as I show in Chapter 6 a change from citrate to histidine can have a positive effect on the protein stability during storage. It is important that buffers having different pH shift with temperature are not compared with each other using non-isothermal techniques as we show in Chapter 3. The effect of the buffers on the protein stability can be studied by assessing parameters like the interaction parameter k_D, the second osmotic virial coefficient A_2, the Gibbs free energy of protein unfolding, or the relative monomer yield after refolding from urea.

Study the effect of ionic strength – the ionic strength of the solution can have a significant influence on the protein aggregation during storage when electrostatic interactions between the monomers are contributing to high colloidal protein stability. The effect of an increase in ionic strength on the protein unfolding and aggregation can be studied with thermal denaturation techniques as I demonstrate in Chapter 2 or with isothermal methods like the ReFOLD assay in Chapter 6 and dynamic light scattering in Chapter 7. These studies will aim to define if low (e.g. $\leq$20 mM), moderate (e.g. 20 – 140 mM) or high (e.g. $\geq$ 140 mM) ionic strength will have favourable effects on the protein stability-indicating parameters.

Study the effect of additives – After the optimal pH, buffer and ionic strength are defined, the formulation scientist can include various additives, e.g. osmolytes, in the formulation. Such additives might not always be needed to stabilise the protein but, for example, could be used to adjust the tonicity of the solution. Additives can positively or negatively affect protein stability as we also show in this thesis. A systematic approach with stability-indicating techniques like the one in Chapter 7 is needed to assess the effects of additives on protein stability and to predict their impact on protein aggregation during long-term storage.

Effect of protein concentration – Increasing protein concentration typically results in more aggregation during storage as also we show with the antibody LMU-1 in Chapter 6. These effects were predictable by assessing the aggregation onset temperature of the protein and the relative monomer yield after refolding from urea. A critical point here is that there is an increased demand for highly concentrated protein formulations, e.g. 150-200 g/L for antibodies. The development of such formulations brings additional challenges that were unfortunately outside the scope of this thesis. Such complications are, for example, related to high viscosity, phase separation and aggregation driven by short-ranged hydrophobic interactions. Studying and tackling these phenomena requires the adoption of more methods and the use of viscosity-lowering agents. Future work will have to address these challenges.

Study the effect of surfactants – Although outside the scope of this thesis, the interfacial protein stability is another important aspect of protein formulation. The impact of several surfactants, e.g. polysorbates and poloxamers, on the protein stability should be studied by a combination of appropriate analytical techniques mentioned in Chapter 1 and suitable mechanical stress like agitation, shaking, freeze/thaw and after repetitive drops.

Study the effect of antioxidants – after several leading formulations with optimised pH, ionic strength, osmolyte and surfactant are selected, the sensitivity to oxidation of the protein should be tested. This can be done by stress like light exposure, the addition of oxidants, purging with oxygen or exposure to high temperature coupled to a suitable analytical technique (see Chapter 1). It is essential that these studies are also done after the surfactants and all other excipients are added since they can impact the oxidation rates. If needed, an antioxidant like

methionine can be included in the formulation or the solution can be filled and closed under oxygen-poor atmosphere.

Study the effect of the primary package – Finally, the effect of the primary package on the protein stability should be extensively studied. The package material, transparency, fill volume, type of overhead gas, presence of tungsten or silicon oil can all affect the stability of the protein in the lead formulations. In the best case, several primary packages should be tested with stress and accelerated stability studies to access their impact on the product.

The suggestions above can serve as some starting points for protein formulation studies. One should not look at all these steps of protein formulation development separately but always think about the connection between them and how changing one variable positively or negatively affects different aspects of protein stability. Complex and non-evident relationships between variables can be better studied by applying design of experiments (DoE). Although the application of DoE was not part of this thesis, this concept can also be applied to simultaneously and quickly study the effect of various formulation variables (e.g. pH, ionic strength, buffer system) on several stability-indicating parameters. For example, a screen for optimal pH and ionic strength like the one in Chapter 2 can also be integrated into DoE and can be completed in a couple of days by consuming only several micrograms of protein. The presented ReFOLD assay can also be used in the design of protein formulation studies as an orthogonal stability-indicating technique that provides good predictions which formulations will impede protein aggregation during storage.

Finally, the selection of the leading formulations should be performed also considering the entire life cycle of a potential therapeutic protein drug starting from protein expression and finishing with the administration in patients.

References

1. Manning, M. C., Liu, J., Li, T. & Holcomb, R. E. *Rational Design of Liquid Formulations of Proteins*. *Advances in Protein Chemistry and Structural Biology* **112,** 1–59 (Academic Press, 2018).

2. Dobson, C. M. Protein folding and misfolding. *Nature* **426,** 884–890 (2003).

3. Pace, C. N., Shirley, B. & Thomson, J. Measuring the conformational stability of a protein. in *Protein Structure: A Practical Approach* 311–330 (Oxford University Press, 1997).

4. Freire, E., Schön, A., Hutchins, B. M. & Brown, R. K. Chemical denaturation as a tool in the formulation optimization of biologics. *Drug Discov. Today* **18,** 1007–1013 (2013).

5. Chi, E. Y., Krishnan, S., Randolph, T. W. & Carpenter, J. F. Physical stability of proteins in aqueous solution: Mechanism and driving forces in nonnative protein aggregation. *Pharm. Res.* **20,** 1325–1336 (2003).

6. Clarkson, B. R., Schön, A. & Freire, E. Conformational stability and self-association equilibrium in biologics. *Drug Discov. Today* **21,** 342–347 (2016).

7. De Young, L. R., Fink, A. L. & Dills, K. A. *Aggregation of Globular Proteins*. *Acc. Chem. Res* **26,** (1993).

8. Chi, E. Y. E. *et al.* Roles of conformational stability and colloidal stability in the aggregation of recombinant human granulocyte colony-stimulating factor. *Protein Sci.* **12,** 903–913 (2003).

9. Blaffert, J., Haeri, H. H., Blech, M., Hinderberger, D. & Garidel, P. Spectroscopic methods for assessing the molecular origins of macroscopic solution properties of highly concentrated liquid protein solutions. *Anal. Biochem.* **561–562,** 70–88 (2018).

10. Connolly, B. D. *et al.* Weak interactions govern the viscosity of concentrated antibody solutions: High-throughput analysis using the diffusion interaction parameter. *Biophys. J.* **103,** 69–78 (2012).

11. Calero-Rubio, C., Saluja, A. & Roberts, C. J. Coarse-Grained Antibody Models for "Weak" Protein–Protein Interactions from Low to High Concentrations. *J. Phys. Chem. B* **120,** 6592–6605 (2016).

12. Gangele, K. & Poluri, K. M. Imidazole derivatives differentially destabilize the low pH conformation of lysozyme through weak electrostatic interactions. *RSC Adv.* **6,** 101395–101403 (2016).

13. Raut, A. S. & Kalonia, D. S. Pharmaceutical Perspective on Opalescence and Liquid-Liquid Phase Separation in Protein Solutions. *Mol. Pharm.* **13,** 1431–1444 (2016).

14. Ben-Naim, A. *Statistical Thermodynamics for Chemists and Biochemists*. (Springer US, 1992). doi:10.1007/978-1-4757-1598-9

15. Hedberg, S. H. M., Lee, D., Mishra, Y., Haigh, J. M. & Williams, D. R. Mapping the mAb Aggregation Propensity Using Self-Interaction Chromatography as a Screening Tool. *Anal. Chem.* **90,** 3878–3885 (2018).

16. Quigley, A. & Williams, D. R. The second virial coefficient as a predictor of protein aggregation propensity: A self-interaction chromatography study. *Eur. J. Pharm. Biopharm.* **96,** 282–90 (2015).

17. Saito, S. *et al.* Effects of ionic strength and sugars on the aggregation propensity of monoclonal antibodies: Influence of colloidal and conformational stabilities. *Pharm. Res.* **30,** 1263–1280 (2013).

18. Manning, M. C., Chou, D. K., Murphy, B. M., Payne, R. W. & Katayama, D. S. Stability of protein pharmaceuticals: An update. *Pharm. Res.* **27,** 544–575 (2010).

19. Zhang, W., Xiao, S. & Ahn, D. U. Protein Oxidation: Basic Principles and Implications for Meat Quality. *Crit. Rev. Food Sci. Nutr.* **53,** 1191–1201 (2013).

20. Li, S., Schöneich, C. & Borchardt, R. T. Chemical instability of protein pharmaceuticals: Mechanisms of oxidation

and strategies for stabilization. *Biotechnol. Bioeng.* **48,** 490–500 (1995).

21. Torosantucci, R., Schöneich, C. & Jiskoot, W. Oxidation of Therapeutic Proteins and Peptides: Structural and Biological Consequences. *Pharm. Res.* **31,** 541–553 (2014).

22. Wakankar, A. A. & Borchardt, R. T. Formulation considerations for proteins susceptible to asparagine deamidation and aspartate isomerization. *J. Pharm. Sci.* **95,** 2321–2336 (2006).

23. Robinson, A. B. & Rudd, C. J. Deamidation of Glutaminyl and Asparaginyl Residues in Peptides and Proteins. *Curr. Top. Cell. Regul.* **8,** 247–295 (1974).

24. Pan, B., Ricci, M. S. & Trout, B. L. A Molecular Mechanism of Hydrolysis of Peptide Bonds at Neutral pH Using a Model Compound. *J. Phys. Chem. B* **115,** 5958–5970 (2011).

25. Gaza-Bulseco, G. & Liu, H. Fragmentation of a Recombinant Monoclonal Antibody at Various pH. *Pharm. Res.* **25,** 1881–1890 (2008).

26. Oliyai, C. & Borchardt, R. T. Chemical Pathways of Peptide Degradation. IV. Pathways, Kinetics, and Mechanism of Degradation of an Aspartyl Residue in a Model Hexapeptide. *Pharm. Res.* **10,** 95–102 (1993).

27. Schultz, J. [28] Cleavage at aspartic acid. *Methods Enzymol.* **11,** 255–263 (1967).

28. Ledvina, M. & Labella, F. S. Fluorescent substances in protein hydrolyzates I. Acid "Hydrolyzates" of individual amino acids. *Anal. Biochem.* **36,** 174–181 (1970).

29. Sepetov, N. F. *et al.* Rearrangement, racemization and decomposition of peptides in aqueous solution. *Pept. Res.* **4,** 308–13

30. Quan, C. *et al.* A study in glycation of a therapeutic recombinant humanized monoclonal antibody: Where it is, how it got there, and how it affects charge-based behavior. *Anal. Biochem.* **373,** 179–191 (2008).

31. Wypych, J. *et al.* Human IgG2 antibodies display disulfide-mediated structural isoforms. *J. Biol. Chem.* **283,** 16194–205 (2008).

32. Lee, H. J., McAuley, A., Schilke, K. F. & McGuire, J. Molecular origins of surfactant-mediated stabilization of protein drugs. *Adv. Drug Deliv. Rev.* **63,** 1160–1171 (2011).

33. Randolph, T. W. *et al.* Do Not Drop: Mechanical Shock in Vials Causes Cavitation, Protein Aggregation, and Particle Formation. *J. Pharm. Sci.* **104,** 602–611 (2015).

34. Kiese, S., Papppenberger, A., Friess, W. & Mahler, H.-C. Shaken, Not Stirred: Mechanical Stress Testing of an IgG1 Antibody. *J. Pharm. Sci.* **97,** 4347–4366 (2008).

35. Koepf, E., Eisele, S., Schroeder, R., Brezesinski, G. & Friess, W. Notorious but not understood: How liquid-air interfacial stress triggers protein aggregation. *Int. J. Pharm.* **537,** 202–212 (2018).

36. Koepf, E., Schroeder, R., Brezesinski, G. & Friess, W. The film tells the story: Physical-chemical characteristics of IgG at the liquid-air interface. *Eur. J. Pharm. Biopharm.* **119,** 396–407 (2017).

37. Norde, W. Adsorption of proteins from solution at the solid-liquid interface. *Adv. Colloid Interface Sci.* **25,** 267–340 (1986).

38. Wang, W., Nema, S. & Teagarden, D. Protein aggregation-Pathways and influencing factors. *Int. J. Pharm.* **390,** 89–99 (2010).

39. Martos, A. *et al.* Trends on Analytical Characterization of Polysorbates and Their Degradation Products in Biopharmaceutical Formulations. *J. Pharm. Sci.* **106,** 1722–1735 (2017).

40. Johnson, C. M. Differential scanning calorimetry as a tool for protein folding and stability. *Arch. Biochem. Biophys.* **531,** 100–109 (2013).

41. Vermeer, A. W. P. & Norde, W. The thermal stability of immunoglobulin: unfolding and aggregation of a multi-domain protein. *Biophys. J.* **78,** 394–404 (2000).

42. Nataˇ Sa Poklar, S. & Vesnaver, G. *Thermal Denaturation of Proteins Studied by UV*. *J. Chem. Educ* **77,** (2000).

43. Hawe, A. & Friess, W. Development of HSA-free formulations for a hydrophobic cytokine with improved stability. *Eur. J. Pharm. Biopharm.* **68,** 169–182 (2008).

44. Menzen, T. & Friess, W. High-throughput melting-temperature analysis of a monoclonal antibody by differential scanning fluorimetry in the presence of surfactants. *J. Pharm. Sci.* **102,** 415–428 (2013).

45. Garidel, P., Hegyi, M., Bassarab, S. & Weichel, M. A rapid, sensitive and economical assessment of monoclonal antibody conformational stability by intrinsic tryptophan fluorescence spectroscopy. *Biotechnol. J.* **3,** 1201–1211 (2008).

46. Malik, K., Matejtschuk, P., Thelwell, C. & Burns, C. J. Differential scanning fluorimetry: Rapid screening of formulations that promote the stability of reference preparations. *J. Pharm. Biomed. Anal.* **77,** 163–166 (2013).

47. Goldberg, D. S., Bishop, S. M., Shah, A. U. & Sathish, H. A. Formulation Development of Therapeutic Monoclonal Antibodies Using High-Throughput Fluorescence and Static Light Scattering Techniques: Role of Conformational and Colloidal Stability. *J. Pharm. Sci.* **100,** 1306–1315 (2011).

48. Youssef, A. M. K. & Winter, G. A critical evaluation of microcalorimetry as a predictive tool for long term stability of liquid protein formulations: Granulocyte Colony Stimulating Factor (GCSF). *Eur. J. Pharm. Biopharm.* **84,** 145–155 (2013).

49. Maddux, N. R. *et al.* High throughput prediction of the long-term stability of pharmaceutical macromolecules from short-term multi-instrument spectroscopic data. *J. Pharm. Sci.* **103,** 828–839 (2014).

50. Niklasson, M. *et al.* Robust and convenient analysis of protein thermal and chemical stability. *Protein Sci.* **24,** 2055–2062 (2015).

51. Pace, C. N. & Shaw, K. L. Linear extrapolation method of analyzing solvent denaturation curves. *Proteins* **Suppl 4,** 1–7 (2000).

52. Wafer, L., Kloczewiak, M., Polleck, S. M. & Luo, Y. Isothermal chemical denaturation of large proteins: Path-dependence and irreversibility. *Anal. Biochem.* **539,** 60–69 (2017).

53. Rowe, J. B. *et al.* Submicron Aggregation of Chemically Denatured Monoclonal Antibody. *Mol. Pharm.* **15,** 4710–4721 (2018).

54. Svilenov, H., Markoja, U. & Winter, G. Isothermal chemical denaturation as a complementary tool to overcome limitations of thermal differential scanning fluorimetry in predicting physical stability of protein formulations. *Eur. J. Pharm. Biopharm.* **125,** 106–113 (2018).

55. Svilenov, H., Gentiluomo, L., Friess, W., Roessner, D. & Winter, G. A New Approach to Study the Physical Stability of Monoclonal Antibody Formulations—Dilution From a Denaturant. *J. Pharm. Sci.* **107,** 3007–3013 (2018).

56. Menzen, T. & Friess, W. Temperature-Ramped Studies on the Aggregation, Unfolding, and Interaction of a Therapeutic Monoclonal Antibody. *J. Pharm. Sci.* **103,** 445–455 (2014).

57. Roberts, D. *et al.* The Role of Electrostatics in Protein–Protein Interactions of a Monoclonal Antibody. *Mol. Pharm.* **11,** 2475–2489 (2014).

58. Woldeyes, M. A. *et al.* How Well Do Low- and High-Concentration Protein Interactions Predict Solution Viscosities of Monoclonal Antibodies? *J. Pharm. Sci.* **108,** 142–154 (2018).

59. Sorret, L. L., DeWinter, M. A., Schwartz, D. K. & Randolph, T. W. Challenges in Predicting Protein-Protein

Interactions from Measurements of Molecular Diffusivity. *Biophys. J.* **111,** 1831–1842 (2016).

60. Calero-Rubio, C., Ghosh, R., Saluja, A. & Roberts, C. J. Predicting protein-protein interactions of concentrated antibody solutions using dilute solution data and coarse-grained molecular models. *J. Pharm. Sci.* **107,** 1269–1281 (2017).

61. Woldeyes, M. A., Calero-Rubio, C., Furst, E. M. & Roberts, C. J. Predicting Protein Interactions of Concentrated Globular Protein Solutions Using Colloidal Models. *J. Phys. Chem. B* **121,** 4756–4767 (2017).

62. Goldberg, D. S. *et al.* Utility of High Throughput Screening Techniques to Predict Stability of Monoclonal Antibody Formulations During Early Stage Development. *J. Pharm. Sci.* **106,** 1971–1977 (2017).

63. Thiagarajan, G., Semple, A., James, J. K., Cheung, J. K. & Shameem, M. A comparison of biophysical characterization techniques in predicting monoclonal antibody stability. *MAbs* **8,** 1088–1097 (2016).

64. Deszczynski, M., Harding, S. E. & Winzor, D. J. Negative second virial coefficients as predictors of protein crystal growth: Evidence from sedimentation equilibrium studies that refutes the designation of those light scattering parameters as osmotic virial coefficients. **120,** 106–113 (2005).

65. Mosbæk, C. R., Konarev, P. V., Svergun, D. I., Rischel, C. & Vestergaard, B. High Concentration Formulation Studies of an IgG2 Antibody Using Small Angle X-ray Scattering. *Pharm. Res.* **29,** 2225–2235 (2012).

66. Liu, Z., Gong, Z., Dong, X. & Tang, C. Transient protein–protein interactions visualized by solution NMR. *Biochim. Biophys. Acta - Proteins Proteomics* **1864,** 115–122 (2016).

67. Tessier, P. M., Jinkoji, J., Cheng, Y.-C., Prentice, J. L. & Lenhoff, A. M. Self-Interaction Nanoparticle Spectroscopy: A Nanoparticle-Based Protein Interaction Assay. **130,** 3106–3112 (2008).

68. Toprani, V. M. *et al.* A Micro Polyethylene Glycol Precipitation Assay as a Relative Solubility Screening Tool for Monoclonal Antibody Design and Formulation Development. *J. Pharm. Sci.* **105,** 2319–2327 (2016).

69. Sun, T. *et al.* High throughput detection of antibody self-interaction by bio-layer interferometry. **5,** 838–841 (2013).

70. Hawe, A. *et al.* Forced degradation of therapeutic proteins. *J. Pharm. Sci.* **101,** 895–913 (2012).

71. Nowak, C. *et al.* Forced degradation of recombinant monoclonal antibodies: A practical guide. *MAbs* **9,** 1217–1230 (2017).

72. Tamizi, E. & Jouyban, A. Forced degradation studies of biopharmaceuticals: Selection of stress conditions. *Eur. J. Pharm. Biopharm.* **98,** 26–46 (2016).

73. Kroon, D. J., Baldwin-Ferro, A. & Lalan, P. Identification of Sites of Degradation in a Therapeutic Monoclonal Antibody by Peptide Mapping. *Pharm. Res.* **09,** 1386–1393 (1992).

74. Loew, C. *et al.* Analytical Protein A Chromatography as a Quantitative Tool for the Screening of Methionine Oxidation in Monoclonal Antibodies. *J. Pharm. Sci.* **101,** 4248–4257 (2012).

75. Fekete, S., Dong, M. W., Zhang, T. & Guillarme, D. High resolution reversed phase analysis of recombinant monoclonal antibodies by ultra-high pressure liquid chromatography column coupling. *J. Pharm. Biomed. Anal.* **83,** 273–278 (2013).

76. Kunitani, M. *et al.* Reversed-phase chromatography of interleukin-2 muteins. *J. Chromatogr. A* **359,** 391–402 (1986).

77. Farnan, D. & Moreno, G. T. Multiproduct High-Resolution Monoclonal Antibody Charge Variant Separations by pH Gradient Ion-Exchange Chromatography. *Anal. Chem.* **81,** 8846–8857 (2009).

78. Haverick, M., Mengisen, S., Shameem, M. & Ambrogelly, A. Separation of mAbs molecular variants by analytical hydrophobic interaction chromatography HPLC: overview and applications. *MAbs* **6,** 852–858 (2014).

79. Torisu, T. *et al.* Friability Testing as a New Stress-Stability Assay for Biopharmaceuticals. *J. Pharm. Sci.* **106,** 2966–

164

2978 (2017).

80. Mahler, H.-C. & Jiskoot, W. *Analysis of aggregates and particles in protein pharmaceuticals*. (John Wiley & Sons, 2012).

81. Zölls, S. *et al.* Particles in Therapeutic Protein Formulations, Part 1: Overview of Analytical Methods. *J. Pharm. Sci.* **101,** 914–935 (2012).

82. Koepf, E., Schroeder, R., Brezesinski, G. & Friess, W. The missing piece in the puzzle: Prediction of aggregation via the protein-protein interaction parameter A∗2. *Eur. J. Pharm. Biopharm.* **128,** 200–209 (2018).

83. Laidler, K. J. The Development of the Arrhenius Equation. *J. Chem. Educ.* **61,** 494 (1984).

84. Ershadi, S., Rashedi, H. & Fazeli, A. A Study on the Mechanism of Aggregation of Therapeutic Reteplase Protein by Using the Monomer-Loss Model. **2,** 191–197 (2015).

85. Roberts, C. J. Non-Native Protein Aggregation Kinetics. *Biotechnol. Bioeng.* **98,** 927–938 (2007).

86. Barnett, G. V., Drenski, M., Razinkov, V., Reed, W. F. & Roberts, C. J. Identifying protein aggregation mechanisms and quantifying aggregation rates from combined monomer depletion and continuous scattering. *Anal. Biochem.* **511,** 80–91 (2016).

87. Li, Y. & Roberts, C. J. Protein Aggregation Pathways, Kinetics, and Thermodynamics. in *Aggregation of Therapeutic Proteins* 63–102 (John Wiley & Sons, Inc., 2010). doi:10.1002/9780470769829.ch2

88. Smith, N., Mori, S. a & Henderson, A. *Aggregation of Therapeutic Proteins*. (John Wiley & Sons, Inc., 2010).

89. Bam, N. B., Cleland, J. L. & Randolph, T. W. Molten globule intermediate of recombinant human growth hormone: Stabilization with surfactants. *Biotechnol. Prog.* **12,** 801–809 (1996).

90. Andrews, J. M. & Roberts, C. J. Non-Native Aggregation of α-Chymotrypsinogen Occurs through Nucleation and Growth with Competing Nucleus Sizes and Negative Activation Energies. (2007). doi:10.1021/BI700296F

91. Bam, N. B. *et al.* Tween protects recombinant human growth hormone against agitation- induced damage via hydrophobic interactions. *J. Pharm. Sci.* **87,** 1554–1559 (1998).

92. Wang, W. & Roberts, C. J. Non-Arrhenius Protein Aggregation. *AAPS J.* **15,** 840–851 (2013).

93. Roberts, C. J., Das, T. K. & Sahin, E. Predicting solution aggregation rates for therapeutic proteins: Approaches and challenges. *Int. J. Pharm.* **418,** 318–333 (2011).

94. Ce Nicoud, L. *et al.* Kinetic Analysis of the Multistep Aggregation Mechanism of Monoclonal Antibodies. *J. Phys. Chem. B* **118,** 10595–10606 (2014).

95. Kalonia, C. *et al.* Effects of Protein Conformation, Apparent Solubility, and Protein-Protein Interactions on the Rates and Mechanisms of Aggregation for an IgG1Monoclonal Antibody. *J. Phys. Chem. B* **120,** 7062–7075 (2016).

96. Kim, N. *et al.* Aggregation of anti-streptavidin immunoglobulin gamma-1 involves Fab unfolding and competing growth pathways mediated by pH and salt concentration. *Biophys. Chem.* **172,** 26–36 (2013).

97. Meric, G., Robinson, A. S. & Roberts, C. J. Driving Forces for Nonnative Protein Aggregation and Approaches to Predict Aggregation-Prone Regions. *Annu. Rev. Chem. Biomol. Eng.* **8,** 139–159 (2017).

98. Revers, L. & Furczon, E. An Introduction to Biologics and Biosimilars. Part I: Biologics: What are They and Where Do They Come from? *Can. Pharm. J. / Rev. des Pharm. du Canada* **143,** 134–139 (2010).

99. Narhi, L. O., Schmit, J., Bechtold-Peters, K. & Sharma, D. *Classification of Protein Aggregates*. *J Pharm Sci* **101,** (2012).

100. Rosenberg, A. S. Effects of protein aggregates: An immunologic perspective. *AAPS J.* **8,** E501–E507 (2006).

101. Ratanji, K. D., Derrick, J. P., Dearman, R. J. & Kimber, I. Immunogenicity of therapeutic proteins: Influence of

aggregation. *J. Immunotoxicol.* **11,** 99–109 (2014).

102.   Moussa, E. M. *et al.* Immunogenicity of Therapeutic Protein Aggregates. *J. Pharm. Sci.* **105,** 417–430 (2016).

103.   *ICH, Q5C Quality of Biotechnological Products: Stability Testing of Biotechnological/Biological Products.* (1995).

104.   Wang, W. & Roberts, C. J. Protein Aggregation - Mechanisms, Detection, and Control. *Int. J. Pharm.* **550,** 251–268 (2018).

105.   Brader, M. L. *et al.* Examination of thermal unfolding and aggregation profiles of a series of developable therapeutic monoclonal antibodies. *Mol. Pharm.* **12,** 1005–1017 (2015).

106.   Robinson, M. J., Matejtschuk, P., Bristow, A. F. & Dalby, P. A. Tm-Values and Unfolded Fraction Can Predict Aggregation Rates for Granulocyte Colony Stimulating Factor Variant Formulations but Not under Predominantly Native Conditions. *Mol. Pharm.* **15,** 256–267 (2018).

107.   Baron, S. *et al.* The Interferons. *JAMA* **266,** 1375 (1991).

108.   Escudier, B. *et al.* Bevacizumab plus interferon alfa-2a for treatment of metastatic renal cell carcinoma: a randomised, double-blind phase III trial. *Lancet* **370,** 2103–2111 (2007).

109.   Jonasch, E. & Haluska, F. G. Interferon in oncological practice: review of interferon biology, clinical applications, and toxicities. *Oncologist* **6,** 34–55 (2001).

110.   Dragomiretskaya, N. *et al.* Use of antiviral therapy in patients with chronic hepatitis C. *Open Med. (Warsaw, Poland)* **10,** 209–215 (2015).

111.   Hochuli, E. Interferon immunogenicity: technical evaluation of interferon-alpha 2a. *J. Interferon Cytokine Res.* **17 Suppl 1,** S15-21 (1997).

112.   Braun, A., Kwee, L., Labow, M. A. & Alsenz, J. Protein Aggregates Seem to Play a Key Role Among the Parameters Influencing the Antigenicity of Interferon Alpha (IFN-α) in Normal and Transgenic Mice. *Pharm. Res.* **14,** 1472–1478 (1997).

113.   US5762923A - Stabilized interferon alpha solutions - Google Patents. Available at: https://patents.google.com/patent/US5762923A/en?q=interferon&q=alpha. (Accessed: 7th August 2018)

114.   Bessa, J. *et al.* The Immunogenicity of Antibody Aggregates in a Novel Transgenic Mouse Model. *Pharm. Res.* **32,** 2344–2359 (2015).

115.   Boll, B. *et al.* Extensive Chemical Modifications in the Primary Protein Structure of IgG1 Subvisible Particles Are Necessary for Breaking Immune Tolerance. *Mol. Pharm.* **14,** 1292–1299 (2017).

116.   Wanner, R., Breitsprecher, D., Duhr, S., Baaske, P. & Winter, G. Thermo-Optical Protein Characterization for Straightforward Preformulation Development. *J. Pharm. Sci.* **106,** 2955–2958 (2017).

117.   Linke, P. *et al.* An Automated Microscale Thermophoresis Screening Approach for Fragment-Based Lead Discovery. *J. Biomol. Screen.* **21,** 414–21 (2016).

118.   Söltl, F., Derix, J., Blech, M. & Breitsprecher, D. Analysis of formulation-dependent colloidal and conformational stability of monoclonal antibodies. *Appl. Note NT-PR-005* **1,** (2015).

119.   Savitzky, A. & E, M. J. Smoothing and Differentiation of Data by Simplified Least Squares Procedures. *Anal. Chem.* **36,** 1627–1639 (1951).

120.   Towsend, R., Kumosisski, T. F. & Timasheff, S. N. The Circular Dichroism of Variants of P-Lactoglobulin. *J. Biol. Chem.* **242,** 4538–4545 (1967).

121.   Diress, A. *et al.* Study of aggregation, denaturation and reduction of interferon alpha-2 products by size-exclusion high-performance liquid chromatography with fluorescence detection and biological assays. *J. Chromatogr. A* **1217,**

3297–3306 (2010).

122.   Sharma, V. K. & Kalonia, D. S. Polyethylene glycol-induced precipitation of interferon alpha-2a followed by vacuum drying: Development of a novel process for obtaining a dry, stable powder. *AAPS J.* **6,** 31–44 (2004).

123.   Kantardjieff, K. A. & Rupp, B. Protein isoelectric point as a predictor for increased crystallization screening efficiency. *Bioinforma. Discov. NOTE* **20,** 2162–2168 (2004).

124.   Sharma, V. K. & Kalonia, D. S. Temperature- and pH-Induced Multiple Partially Unfolded States of Recombinant Human Interferon- 2a: Possible Implications in Protein Stability. *Pharm. Res.* **20,** 1721–1729 (2003).

125.   Bis, R. L., Singh, S. M., Cabello-Villegas, J. & Mallela, K. M. G. Role of benzyl alcohol in the unfolding and aggregation of interferon α-2a. *J. Pharm. Sci.* **104,** 407–415 (2015).

126.   van de Weert, M. & Jørgensen, L. *0 Infrared Spectroscopy to Characterize Protein Aggregates*. *Analysis of Aggregates and Particles in Protein Pharmaceuticals* (John Wiley & Sons, Inc., 2012). doi:10.1002/9781118150573.ch10

127.   Johnson, W. C. Protein secondary structure and circular dichroism: A practical guide. *Proteins Struct. Funct. Genet.* **7,** 205–214 (1990).

128.   Panjwani, N., Hodgson, D. J., Sauvé, S. & Aubin, Y. Assessment of the Effects of pH, Formulation and Deformulation on the Conformation of Interferon Alpha-2 by NMR. *J. Pharm. Sci.* **99,** 3334–3342 (2010).

129.   Mohl, S. & Winter, G. Continuous Release of rh-Interferon α-2a from Triglyceride Implants: Storage Stability of the Dosage Forms. *Pharm. Dev. Technol.* **11,** 103–110 (2006).

130.   Hermeling, S. *et al.* Structural characterization and immunogenicity in wildtype and immune tolerant mice of degraded recombinant human interferon alpha2b. *Pharm. Res.* **22,** 1997–2006 (2005).

131.   Dimitrov, D. S. *Therapeutic Proteins*. (Humana Press, Totowa, NJ, 2012). doi:10.1007/978-1-61779-921-1_1

132.   Dimitrov, D. S. Therapeutic antibodies, vaccines and antibodyomes. *MAbs* **2,** 347–356 (2010).

133.   Elvin, J. G., Couston, R. G. & Van Der Walle, C. F. Therapeutic antibodies: Market considerations, disease targets and bioprocessing. *Int. J. Pharm.* **440,** 83–98 (2013).

134.   DeFrancesco, L. Drug pipeline Q4 2015. *Nat Biotech* **34,** 128 (2016).

135.   Wang, W. & Kelner, D. N. Correlation of rFVIII inactivation with aggregation in solution. *Pharm. Res.* **20,** 693–700 (2003).

136.   Runkel, L. *et al.* Structural and Functional Differences Between Glycosylated and Non-glycosylated Forms of Human Interferon-β (IFN-β). *Pharm. Res.* **15,** 641–649 (1998).

137.   Sethu, S. *et al.* Immunogenicity to Biologics: Mechanisms, Prediction and Reduction. *Arch. Immunol. Ther. Exp. (Warsz).* **60,** 331–344 (2012).

138.   *ICH , Q6B Specifications: Test Procedures and Acceptance Criteria for Biotechnological/Biological Products*. (1999).

139.   Capelle, M. A. H., Gurny, R. & Arvinte, T. High throughput screening of protein formulation stability: Practical considerations. *Eur. J. Pharm. Biopharm.* **65,** 131–148 (2007).

140.   He, F., Hogan, S., Latypov, R. F., Narhi, L. O. & Razinkov, V. I. High throughput thermostability screening of monoclonal antibody formulations. *J. Pharm. Sci.* **99,** 1707–1720 (2010).

141.   Chaudhuri, R., Cheng, Y., Middaugh, C. R. & Volkin, D. B. High-throughput biophysical analysis of protein therapeutics to examine interrelationships between aggregate formation and conformational stability. *AAPS J.* **16,** 48–64 (2014).

167

142. Roberts, C. J. Therapeutic protein aggregation: mechanisms, design, and control. *Trends Biotechnol.* **32,** 372–380 (2014).

143. Burton, L., Gandhi, R., Duke, G. & Paborji, M. Use of Microcalorimetry and Its Correlation with Size Exclusion Chromatography for Rapid Screening of the Physical Stability of Large Pharmaceutical Proteins in Solution. *Pharm. Dev. Technol.* **12,** 265–273 (2007).

144. Kumar, V., Dixit, N., Zhou, L. & Fraunhofer, W. Impact of short range hydrophobic interactions and long range electrostatic forces on the aggregation kinetics of a monoclonal antibody and a dual-variable domain immunoglobulin at low and high concentrations. *Int. J. Pharm.* **421,** 82–93 (2011).

145. Ericsson, U. B., Hallberg, B. M., DeTitta, G. T., Dekker, N. & Nordlund, P. Thermofluor-based high-throughput stability optimization of proteins for structural studies. *Anal. Biochem.* **357,** 289–298 (2006).

146. Menzen, T. A. Temperature-Induced Unfolding, Aggregation, and Interaction of Therapeutic Monoclonal Antibodies. *PhD Thesis, LMU Munich* (2014).

147. King, A. C. *et al.* High-throughput measurement, correlation analysis, and machine-learning predictions for pH and thermal stabilities of Pfizer-generated antibodies. *Protein Science* **20,** 1546–1557 (2011).

148. Breitsprecher, D., Glücklich, N., Hawe, A. & Menzen, T. Thermal Unfolding of Antibodies Comparison of nanoDSF and μDSC for thermal stability assessment during biopharmaceutical formulation development. *Appl. Note NT-PR-006, NanoTemper Technol. GmbH* (2016).

149. Sanchez-Ruiz, J. M. Theoretical analysis of Lumry-Eyring models in differential scanning calorimetry. *Biophys. J.* **61,** 921–935 (1992).

150. Nagai, H., Kuwabara, K. & Carta, G. Temperature dependence of the dissociation constants of several amino acids. *J. Chem. Eng. Data* **53,** 619–627 (2008).

151. Reijenga, J. C., Gagliardi, L. G. & Kenndler, E. Temperature dependence of acidity constants, a tool to affect separation selectivity in capillary electrophoresis. *J. Chromatogr. A* **1155,** 142–145 (2007).

152. Zbacnik, T. J. *et al.* Role of Buffers in Protein Formulations. *J. Pharm. Sci.* **106,** 713–733 (2017).

153. Lazar, K. L., Patapoff, T. W. & Sharma, V. K. Cold denaturation of monoclonal antibodies. *MAbs* **2,** 42–52 (2010).

154. Schön, A. *et al.* Denatured state aggregation parameters derived from concentration dependence of protein stability. *Anal. Biochem.* **488,** 45–50 (2015).

155. Rizzo, J. M. *et al.* Application of a high-throughput relative chemical stability assay to screen therapeutic protein formulations by assessment of conformational stability and correlation to aggregation propensity. *J. Pharm. Sci.* **104,** 1632–1640 (2015).

156. Menzen, T. I. M. & Friess, W. Temperature-Ramped Studies on the Aggregation , Unfolding , and Interaction of a Therapeutic Monoclonal Antibody. 445–455 (2014). doi:10.1002/jps.23827

157. Menzen, Tim, Wolfgang, F. High-Throughput Melting-Temperature Analysis of a Monoclonal Antibody by Differential Scanning Fluorimetry in the Presence of Surfactants. *Int. J. Drug Dev. Res.* **3,** 26–33 (2011).

158. Fukada, H. & Takahashi, K. Enthalpy and heat capacity changes for the proton dissociation of various buffer components in 0.1 M potassium chloride. *Proteins Struct. Funct. Genet.* **33,** 159–166 (1998).

159. Goldberg, R. N., Kishore, N. & Lennen, R. M. Thermodynamic quantities for the ionization reaction of buffers. *J. Phys. Chem. Ref. Data* **31,** 231–370 (2002).

160. Liu, H., Chumsae, C., Gaza-Bulseco, G. & Goedken, E. R. Domain-level stability of an antibody monitored by reduction, differential alkylation, and mass spectrometry analysis. *Anal. Biochem.* **400,** 244–250 (2010).

168

161. Vlasak, J. & Ionescu, R. Fragmentation of monoclonal antibodies. *MAbs* **3,** (2017).

162. Perez-Riba, A. & Itzhaki, L. S. A method for rapid high-throughput biophysical analysis of proteins. *Sci. Rep.* **7,** 1–6 (2017).

163. Ross, P. *et al.* Isothermal chemical denaturation to determine binding affinity of small molecules to G-protein coupled receptors. *Anal. Biochem.* **473,** 41–45 (2015).

164. Freire, B. U.S. Patent Application No. 16/080,271. (2013). doi:10.1016/j.(73)

165. Temel, D. B., Landsman, P. & Brader, M. L. *Orthogonal Methods for Characterizing the Unfolding of Therapeutic Monoclonal Antibodies: Differential Scanning Calorimetry, Isothermal Chemical Denaturation, and Intrinsic Fluorescence with Concomitant Static Light Scattering. Methods in Enzymology* **567,** (Elsevier Inc., 2016).

166. Yasuda, M., Murakami, Y., Sowa, A., Ogino, H. & Ishikawa, H. Effect of additives on refolding of a denatured protein. *Biotechnol. Prog.* **14,** 601–606 (1998).

167. Arora, D. & Khanna, N. Method for increasing the yield of properly folded recombinant human gamma interferon from inclusion bodies. *J. Biotechnol.* **52,** 127–133 (1996).

168. De Bernardez Clark, E. Refolding of recombinant proteins. *Curr. Opin. Biotechnol.* **9,** 157–163 (1998).

169. Ho, J. G. S. & Middelberg, A. P. J. Estimating the potential refolding yield of recombinant proteins expressed as inclusion bodies. *Biotechnol. Bioeng.* **87,** 584–592 (2004).

170. Lee, S.-H., Carpenter, J. F., Chang, B. S., Randolph, T. W. & Kim, Y. Effects of solutes on solubilization and refolding of proteins from inclusion bodies with high hydrostatic pressure. *Protein Sci.* **15,** 304–313 (2006).

171. Austin, P. C. & Hux, J. E. A brief note on overlapping confidence intervals. *J. Vasc. Surg.* **36,** 194–195 (2002).

172. Zhang, J. & Liu, X. Y. Effect of protein – protein interactions on protein aggregation kinetics. **119,** 10972–10976 (2003).

173. Pace, C. N. *et al.* Denaturation of Proteins by Urea and Guanidine Hydrochloride. in *Protein Folding Handbook* **1,** 45–69 (Wiley-VCH Verlag GmbH & Co. KGaA, 2008).

174. Ahmad, F. & Bigelow, C. C. Estimation of the Free Energy of Stabilization of Ribonuclease A, Lysozyme, a-Lactalbumin, and Myoglobin. *J. Biol. Chem.* **257,** 12935–12938 (1982).

175. Kumar, S., Sharma, D. & Kumar, R. Effect of urea and alkylureas on the stability and structural fluctuation of the M80-containing Ω-loop of horse cytochrome c. *Biochim. Biophys. Acta - Proteins Proteomics* **1844,** 641–655 (2014).

176. Poklar, N., Vesnaver, G. & Lapanje, S. Studies by UV spectroscopy of thermal denaturation of β-lactoglobulin in urea and alkylurea solutions. *Biophys. Chem.* **47,** 143–151 (1993).

177. Poklar, N., Vesnaver, G. & Lapanje, S. Denaturation behavior of α-chymotrypsinogen A in urea and alkylurea solutions: Fluorescence studies. *J. Protein Chem.* **13,** 323–331 (1994).

178. Warren, J. R. & Gordon, J. A. The nature of alkylurea and urea denaturation of α-chymotrypsinogen. *Biochim. Biophys. Acta - Protein Struct.* **420,** 397–405 (1976).

179. Gordon, J. A. Denaturation of globular proteins. Interaction of guanidinium salts with three proteins. *Biochemistry* **11,** 1862–1870 (1972).

180. Ibarra-Molero, B. & Sanchez-Ruiz, J. M. Are There Equilibrium Intermediate States in the Urea-Induced Unfolding of Hen Egg-White Lysozyme? *Biochemistry* **36,** 9616–9624 (1997).

181. Semisotnov, G. V. *et al.* Protein Globularization During Folding. A Study by Synchrotron Small-angle X-ray Scattering. *J. Mol. Biol.* **262,** 559–574 (1996).

182. Svilenov, H. & Winter, G. The ReFOLD assay for protein formulation studies and prediction of protein aggregation

during long-term storage. *Eur. J. Pharm. Biopharm.* **137,** 131–139 (2019).

183. Mason, P. E. *et al.* The hydration structure of guanidinium and thiocyanate ions: Implications for protein stability in aqueous solution. *Proc. Natl. Acad. Sci.* **100,** 4557–4561 (2003).

184. Poklar, N., Petrovc, N., Oblak, M. & Vesnaver, G. Thermodynamic stablity of Ribonuclease A in alkylurea solutions and preferential solvation: A calorimetric and spectroscopic study. *Biophys. Chem.* 832–840 (1999).

185. Monera, O. D., Kay, C. M. & Hodges, R. S. Protein denaturation with guanidine hydrochloride or urea provides a different estimate of stability depending on the contributions of electrostatic interactions. *Protein Sci.* **3,** 1984–91 (1994).

186. De Young, L. R. *et al.* Aggregation and Denaturation of Apomyoglobin in Aqueous Urea Solutions. *Biochemistry* **32,** 3877–3886 (1993).

187. Mehta, S. B., Bee, J. S., Randolph, T. W. & Carpenter, J. F. Partial unfolding of a monoclonal antibody: Role of a single domain in driving protein aggregation. *Biochemistry* **53,** 3367–3377 (2014).

188. Andrews, J. M. & Roberts, C. J. A Lumry−Eyring Nucleated Polymerization Model of Protein Aggregation Kinetics: 1. Aggregation with Pre-Equilibrated Unfolding. *J. Phys. Chem. B* **111,** 7897–7913 (2007).

189. Roberts, C. J. Kinetics of irreversible protein aggregation: Analysis of extended Lumry-Eyring models and implications for predicting protein shelf life. *J. Phys. Chem. B* **107,** 1194–1207 (2003).

190. Arosio, P., Rima, S. & Morbidelli, M. Aggregation mechanism of an IgG2 and two IgG1 monoclonal antibodies at low pH: From oligomers to larger aggregates. *Pharm. Res.* **30,** 641–654 (2013).

191. Polumuri, S. K., Haile, L. A., Ireland, D. D. C. & Verthelyi, D. Aggregates of IVIG or Avastin, but not HSA, modify the response to model innate immune response modulating impurities. *Sci. Rep.* **8,** 11477 (2018).

192. Kijanka, G. *et al.* Submicron Size Particles of a Murine Monoclonal Antibody Are More Immunogenic Than Soluble Oligomers or Micron Size Particles Upon Subcutaneous Administration in Mice. *J. Pharm. Sci.* **107,** 2847–2859 (2018).

193. Spasoff, A. *et al.* A Risk- and Science-Based Approach to the Acceptance Sampling Plan Inspection of Protein Parenteral Products. *J. Pharm. Sci.* **107,** 2306–2309 (2018).

194. Capelle, M. A. H., Gurny, R. & Arvinte, T. A high throughput protein formulation platform: Case study of salmon calcitonin. *Pharm. Res.* **26,** 118–128 (2009).

195. Razinkov, V. I., Treuheit, M. J. & Becker, G. W. Accelerated formulation development of monoclonal antibodies (MABS) and mab-based modalities: Review of methods and tools. *J. Biomol. Screen.* **20,** 468–483 (2015).

196. McClure, S. M., Ahl, P. L. & Blue, J. T. High Throughput Differential Scanning Fluorimetry (DSF) Formulation Screening with Complementary Dyes to Assess Protein Unfolding and Aggregation in Presence of Surfactants. *Pharm. Res.* **35,** 81 (2018).

197. Alsenaidy, M. A. *et al.* High-throughput biophysical analysis and data visualization of conformational stability of an igg1 monoclonal antibody after deglycosylation. *J. Pharm. Sci.* **102,** 3942–3956 (2013).

198. Austerberry, J. I. *et al.* The effect of charge mutations on the stability and aggregation of a human single chain Fv fragment. *Eur. J. Pharm. Biopharm.* **115,** 18–30 (2017).

199. Kheddo, P. *et al.* The effect of arginine glutamate on the stability of monoclonal antibodies in solution. *Int. J. Pharm.* **473,** 126–133 (2014).

200. Chakroun, N., Hilton, D., Ahmad, S. S., Platt, G. W. & Dalby, P. A. Mapping the Aggregation Kinetics of a Therapeutic Antibody Fragment. *Mol. Pharm.* **13,** 307–319 (2016).

201. Greene, R. F. & Pace, C. N. Urea and Guanidine Hydrochloride Denaturation of Ribonuclease. *J. Biol. Chem.* **249,** 5388–5393 (1974).

202. Nick Pace, C., Laurents, D. V & Thomson, J. A. pH dependence of the urea and guanidine hydrochloride denaturation of ribonuclease A and ribonuclease T1. *Biochemistry* **29,** 2564–2572 (1990).

203. Guo, J. *et al.* Characterization and Higher-Order Structure Assessment of an Interchain Cysteine-Based ADC: Impact of Drug Loading and Distribution on the Mechanism of Aggregation. *Bioconjug. Chem.* **27,** 604–615 (2016).

204. Yamaguchi, S., Yamamoto, E., Mannen, T. & Nagamune, T. Protein refolding using chemical refolding additives. *Biotechnol. J.* **8,** 17–31 (2013).

205. Arakawa, T. & Ejima, D. Refolding Technologies for Antibody Fragments. *Antibodies* **3,** 232–241 (2014).

206. Pramanick, S., Singodia, D. & Chandel, V. *Excipient Selection In Parenteral Formulation Development. Pharma Times* **45,** (2013).

207. Breitsprecher, D. *et al.* Automated nanoDSF for High-Throughput Thermal , Colloidal and Chemical stability screenings. *Prometh. NT.Plex Prod. information, NanoTemper Technol. GmbH*

208. Nemergut, M. *et al.* Analysis of IgG kinetic stability by differential scanning calorimetry, probe fluorescence and light scattering. *Protein Sci.* **26,** 2229–2239 (2017).

209. Freskgard, P.-O., Martensson, L.-G., Jonasson, P., Jonsson, B.-H. & Carlsson, U. Assignment of the Contribution of the Tryptophan Residues to the Circular Dichroism Spectrum of Human Carbonic Anhydrase II. *Biochemistry* **33,** 14281–14288 (1994).

210. Woody, A.-Y. M. & Woody, R. W. Individual tyrosine side-chain contributions to circular dichroism of ribonuclease. *Biopolymers* **72,** 500–513 (2003).

211. Sreerama, N. *et al.* Tyrosine, Phenylalanine, and Disulfide Contributions to the Circular Dichroism of Proteins: Circular Dichroism Spectra of Wild-Type and Mutant Bovine Pancreatic Trypsin Inhibitor †. *Biochemistry* **38,** 10814–10822 (1999).

212. Hawe, A., Kasper, J. C., Friess, W. & Jiskoot, W. Structural properties of monoclonal antibody aggregates induced by freeze–thawing and thermal stress. *Eur. J. Pharm. Sci.* **38,** 79–87 (2009).

213. Franey, H., Brych, S. R., Kolvenbach, C. G. & Rajan, R. S. Increased aggregation propensity of IgG2 subclass over IgG1: Role of conformational changes and covalent character in isolated aggregates. *Protein Sci.* **19,** 1601–1615 (2010).

214. Apicella, A. *et al.* A Hydrophobic Gold Surface Triggers Misfolding and Aggregation of the Amyloidogenic Josephin Domain in Monomeric Form, While Leaving the Oligomers Unaffected. *PLoS One* **8,** e58794 (2013).

215. Telikepalli, S. N. *et al.* Structural Characterization of IgG1 mAb Aggregates and Particles Generated Under Various Stress Conditions. *J. Pharm. Sci.* **103,** 796–809 (2014).

216. Weiss, W. F., Hodgdon, T. K., Kaler, E. W., Lenhoff, A. M. & Roberts, C. J. Nonnative Protein Polymers: Structure, Morphology, and Relation to Nucleation and Growth. *Biophys. J.* **93,** 4392–4403 (2007).

217. Arosio, P., Barolo, G., Müller-Späth, T., Wu, H. & Morbidelli, M. Aggregation Stability of a Monoclonal Antibody During Downstream Processing. *Pharm. Res.* **28,** 1884–1894 (2011).

218. Eisenberg, D. *et al.* The Structural Biology of Protein Aggregation Diseases: Fundamental Questions and Some Answers. *Acc. Chem. Res.* **39,** 568–575 (2006).

219. Wlodarczyk, S. R., Custódio, D., Jr, A. P. & Monteiro, G. Influence and effect of osmolytes in biopharmaceutical formulations. *Eur. J. Pharm. Biopharm.* **131,** 92–98 (2018).

220. Hamada, H., Arakawa, T. & Shiraki, K. Effect of additives on protein aggregation. *Curr. Pharm. Biotechnol.* **10,** 400–407 (2009).

221. Inoue, N., Takai, E., Arakawa, T. & Shiraki, K. Specific Decrease in Solution Viscosity of Antibodies by Arginine for Therapeutic Formulations. *Mol. Pharm.* **11,** 1889–1896 (2014).

222. Dear, B. J. *et al.* Enhancing Stability and Reducing Viscosity of a Monoclonal Antibody with Co-solutes by Weakening Protein-Protein Interactions. *J. Pharm. Sci.* (2019). doi:10.1016/J.XPHS.2019.03.008

223. Golovanov, A. P. *et al.* A simple method for improving protein solubility and long-term stability. *J. Am. Chem. Soc.* **126,** 8933–8939 (2004).

224. Zhang, J., Frey, V., Corcoran, M., Zhang-Van Enk, J. & Subramony, J. A. Influence of Arginine Salts on the Thermal Stability and Aggregation Kinetics of Monoclonal Antibody: Dominant Role of Anions. *Mol. Pharm.* **13,** 3362–3369 (2016).

225. Arakawa, T. & Maluf, N. K. The effects of allantoin, arginine and NaCl on thermal melting and aggregation of ribonuclease, bovine serum albumin and lysozyme. *Int. J. Biol. Macromol.* **107,** 1692–1696 (2018).

226. Platts, L. & Falconer, R. J. Controlling protein stability: Mechanisms revealed using formulations of arginine, glycine and guanidinium HCl with three globular proteins. *Int. J. Pharm.* **486,** 131–135 (2015).

227. Baynes, B. M., Wang, D. I. C. & Trout, B. L. Role of Arginine in the Stabilization of Proteins against Aggregation. *Biochemistry* **44,** 4919–4925 (2005).

228. Arakawa, T., Kita, Y., Ejima, D., Tsumoto, K. & Fukada, H. Aggregation Suppression of Proteins by Arginine During Thermal Unfolding. *Protein Pept. Lett.* **13,** 921–927 (2006).

229. Yoshizawa, S., Arakawa, T. & Shiraki, K. Thermal aggregation of human immunoglobulin G in arginine solutions: Contrasting effects of stabilizers and destabilizers. *Int. J. Biol. Macromol.* **104,** 650–655 (2017).

230. Setnikar, I. & Paterlini, M. R. Osmotic pressure and tolerance of injectable solutions. *J. Am. Pharm. Assoc. Am. Pharm. Assoc. (Baltim).* **49,** 5–7 (1960).

231. Krishnan, S. *et al.* Aggregation of granulocyte colony stimulating factor under physiological conditions: Characterization and thermodynamic inhibition. *Biochemistry* **41,** 6422–6431 (2002).

232. Soenderkaer, S. *et al.* Effects of sucrose on rFVIIa aggregation and methionine oxidation. *Eur. J. Pharm. Sci.* **21,** 597–606 (2004).

233. Alekseychyk, L., Su, C., Becker, G. W., Treuheit, M. J. & Razinkov, V. I. High-Throughput Screening and Stability Optimization of Anti-Streptavidin IgG1 and IgG2 Formulations. *J. Biomol. Screen.* **19,** 1290–1301 (2014).

234. Feeney, J. *et al. Stabilization of Protein Structure by Sugars. NMR in Biological Research·. Peptides and Proteins* **21,** (Elsevier, 1982).

235. Barnett, G. V. *et al.* Osmolyte Effects on Monoclonal Antibody Stability and Concentration-Dependent Protein Interactions with Water and Common Osmolytes. *J. Phys. Chem. B* **120,** 3318–3330 (2016).

236. Kim, N. A., Thapa, R. & Jeong, S. H. Preferential exclusion mechanism by carbohydrates on protein stabilization using thermodynamic evaluation. *Int. J. Biol. Macromol.* **109,** 311–322 (2018).

237. Thakkar, S. V. *et al.* Excipients Differentially Influence the Conformational Stability and Pretransition Dynamics of Two IgG1 Monoclonal Antibodies. *J. Pharm. Sci.* **101,** 3062–3077 (2012).

238. Courtenay, E. S., Capp, M. W., Anderson, C. F. & Record, M. T. Vapor Pressure Osmometry Studies of Osmolyte-Protein Interactions: Implications for the Action of Osmoprotectants in Vivo and for the Interpretation of 'Osmotic Stress' Experiments in Vitro. *Biochemistry* **39,** 4455–4471 (2000).

239.	Tsumoto, Kouhei Umetsu, Mitsuo Kumagai, Izumi Ejima, Daisuki Philo, John Arakawa, T. Role of Arginine in Protein Refolding , Solubilization , and Purification. *Biotechnol. Prog.* **20,** 1301–1308 (2004).

240.	Ho, J. G. S., Middelberg, A. P. J., Ramage, P. & Kocher, H. P. The likelihood of aggregation during protein renaturation can be assessed using the second virial coefficient. *Protein Sci.* **12,** 708–716 (2003).

Appendix

A.1 List of publications associated with this thesis

<u>Svilenov, H.</u> and Winter, G., **2019**. Rapid sample-saving biophysical characterisation and long-term storage stability of liquid interferon alpha2a formulations: Is there a correlation? *International Journal of Pharmaceutics*, 562, pp. 42-50

<u>Svilenov, H</u>. and Winter, G., **2019**. The ReFOLD assay for protein formulation studies and prediction of protein aggregation during long-term storage. *European Journal of Pharmaceutics and Biopharmaceutics*, 137, pp. 131-139

<u>Svilenov, H</u>., Gentiluomo, L., Friess, W., Roessner, D. and Winter, G., **2018**. A New Approach to Study the Physical Stability of Monoclonal Antibody Formulations - Dilution from a Denaturant. *Journal of pharmaceutical sciences*, 107(12), pp.3007-3013.

<u>Svilenov, H</u>.*, Markoja, U.[+] and Winter, G.*, **2018**. Isothermal chemical denaturation as a complementary tool to overcome limitations of thermal differential scanning fluorimetry in predicting physical stability of protein formulations. *European Journal of Pharmaceutics and Biopharmaceutics*, 125, pp.106-113.

A.2 List of presentations associated with this thesis

Oral presentations:

<u>Svilenov H.</u>, Winter G. Formulation of therapeutic proteins - Protein unfolding, refolding, aggregation and long-term storage stability. International Research Conference on Protein Stability and Interactions, **2019**, Heidelberg, Germany

*<u>Svilenov H.</u>, Markoja U., Winter G. Isothermal Chemical Denaturation for Formulation Studies of a mAb: Effect of Formulation pH, Denaturant Choice and Incubation Time 11th PBP World Meeting, **2018**, Granada, Spain

Poster presentations:

<u>Svilenov H.</u>, Winter G. The ReFOLD assay for selection of protein formulations for long-term stability studies. International Research Conference on Protein Stability and Interactions, **2019**, Heidelberg, Germany

<u>Svilenov H.</u>, Winter G. The ReFOLD assay for protein formulation studies and prediction of protein aggregation during long-term storage. Gordon Research Conference on Biotherapeutics and Vaccines Development. **2019**. Galveston, USA.

<u>Svilenov H.</u>, Winter G. Typical Pitfalls of High Throughput Thermal Denaturation Studies to Predict Protein Conformational Stability in Different Formulations: Overlooking Buffer pH shifts 11th PBP World Meeting, **2018**, Granada, Spain

<u>Svilenov H.</u>, Winter G. Concentration Dependence of the Apparent Gibbs Free Energy of Unfolding and its Relation to Protein Aggregation Rates. 11th PBP World Meeting, **2018**, Granada, Spain

<u>Svilenov H.</u>, Markoja U., Winter G.What is the Role of Chemical Denaturation in the Assessment of Protein Conformational Stability in Different Formulation Conditions? - A Case Study with a Monoclonal Antibody. Colorado Protein Stability Conference, **2017, Breckenridge, USA

*Selected by peer review process.
**Second poster prize in the Timasheff Award competition.

A.3 Curriculum vitae

Personal data:

Name: Hristo Lyubomirov Svilenov

Date of birth: 18 February 1988

Place of birth: Sofia, Bulgaria

Nationality: Bulgarian

Languages: Bulgarian, English, German

Education:

03.2016 – 05.2019	PhD Studies
	Ludwig-Maximilians-Universität, Munich, Germany
	Department of Pharmacy, Chair of Pharmaceutical Technology and Biopharmaceutics
	Supervisor: Professor Dr. Gerhard Winter
09.2006 – 02.2012	Pharmacy, Master, State exams
	Medical University of Sofia, Sofia, Bulgaria

Professional experience:

05.2018 - 06.2018	Visiting Researcher
	Manchester Institute of Biotechnology, University of Manchester, United Kingdom
	Hosts: Dr. Robin Curtis and Dr. Alexander Golovanov
03.2016 – 05.2019	Marie Curie Fellow
	Ludwig-Maximilians-Universität, Munich, Germany
	Department of Pharmacy, Chair of Pharmaceutical Technology and Biopharmaceutics
07.2015 – 05.2019	Researcher
	Bioskinco GmbH (now QRSkin GmbH), Munich, Germany
04.2014 – 07.2015	Assistant (pre-doc), Faculty member, Faculty of Chemistry and Pharmacy
	Sofia University, Sofia, Bulgaria
02.2012 – 04.2014	Assistant (pre-doc), Faculty member, Faculty of Pharmacy
	Medical University of Sofia, Sofia, Bulgaria